CHARACTERISATION OF NANOFILTRATION MEMBRANES FOR SULPHATE REJECTION

THESIS

Submitted in Partial Fulfilment of the Requirements for the Degree of Doctor of Philosophy in the School of Engineering at the University of Glasgow

By

Tariq Nabil Nada

University of Glasgow

May 2014

Nanofiltration Membranes Characterisation for Sulphate Rejection

Declaration

This thesis contains no material which has been accepted for the award of any other degree or diploma, except where due reference is made in the text of the thesis. To the best of my knowledge, this thesis contains no material previously published or written by another person, except where due reference is made in the text of the thesis.

Tariq Nabil Nada Glasgow, May 2014

Acknowledgments

I would like to express my gratitude first and foremost to my supervisor Dr Trevor Hodgkiess for his guidance, effort, time, support and good-humoured advice throughout my studies. I am absolutely grateful for his unique suggestions on my attitude towards my research.

I would like also to express my many thanks to my employer Saline Water Conversion Corporation (SWCC) of Saudi Arabia for their continuous cooperation and support. A special gratitude goes to my sponsor the Ministry of Higher Education, represented by the Royal Embassy of Saudi Arabia – Cultural Bureau in London.

I would also like to express my thanks to the Faculty of Engineering and the Department of Mechanical Engineering for having granted me the opportunity to carry out this research. Many thanks go to the wonderful people in the workshop in the James Watt south building for their technical support and friendly personalities.

This work would not have been possible without the unlimited, unconditional and unending continuous support and encouragement of my family. My father makes me strong, my mother makes me optimistic even with the most difficult circumstances, my brothers makes me hopeful and my sister makes me happy.

Finally, I am immensely grateful for my wife, and I wish to express my appreciations for her patience and love (I do love you so much).

to Omar and Abdullah

ABSTRACT

Nanofiltration (NF) membranes are used for a range of industrial applications one of which is for the removal of the sulphate constituent in seawater. This is a mature activity for the treatment of seawater that is to be injected into oil reservoirs in the offshore oil/gas industry. Such sulphate removals have also been the subject of much interest, as a pretreatment strategy, in seawater desalination plants that is either utilising thermal technology or reverse osmosis. Nevertheless, there is a need for robust criteria, such as the comparative permeate flux and sulphate rejection, of selecting the optimum NF membrane.

There is a major difficulty in the assessment of the comparative filtration performance and the role of membrane structure because the data from manufacturers and also the information from the scientific literature emanates from different testing protocols. This can result in an enigmatical situation for obtaining the optimum NF membrane for a particular application.

Against the above background this PhD project has focused on undertaking a fundamental study of different commercially available NF membranes in order to facilitate improved assessment of their filtration performance for sulphate rejection applications in relevant standardised testing conditions. Moreover, on the basis that those variations in membranes' functioning are attributed to membrane structure and characteristics, a major segment of the research was focused on correlating filtration performance and membrane features.

The research comprised two main phases; the first phase involved determining the comparative filtration performance of eight commercially available NF membranes supplied from four manufacturers. The second main phase was to undertake detailed characterisation studies on the NF membranes in order to obtain a clear understanding of their sulphate separation mechanism and permeate flux.

The first phase involved assessments of the permeate flux and selectivity of the eight membranes. The experimental protocol in the second, characterisation part of the work was directed to the identification and evaluation of NF active surface layer characteristics:

- Pore characterisation by porosity factor calculations,
- Hydrophilicity/Hydrophobicity nature by contact angle measurements,
- Surface Free Energy calculations,

- Surface roughness measurements by AFM,
- Membrane potential measurements and average charge density calculations.

This approach is an acknowledged strategy for NF membrane scientific research assessment and, in the current work provided key data of membrane features that facilitated a systematic understanding of membrane functioning. These characterisation features were also linked successfully to the membrane performance parameters to yield a characterisation/performance envelope which represents a useful basis for NF membrane selection and utilisation to optimise membrane usage and consequent economic advantage.

The general discussion includes a summary of the interface between the role of NF and the operational and economic features of the two main types of desalination processes. It includes an outline of a process scheme for the incorporation of NF pretreatment into an MSF plant from the conceptual design stage as opposed to the application employed hitherto where the emphasis has been on attaching NF pretreatment equipment on to an existing unit.

As a result, it is expected that NF usage should increase performance ratio, reduce energy consumption, hence the running cost, and increase recovery.

Scientific contributions arising from this PhD work:

1. Paper at International Desalination Association IDA World Congress – Perth Convention and Exhibition Centre (PCEC), Perth, Western Australia September 4-9, 2011. Titled: "Comparison of the Performance of NF Membranes for Sulphate Rejection", REF: IDAWC/PER11-003

2. Poster exhibited at the Euromembrane meeting in London, 23rd – 27th September 2012. Titled: "NF membranes characterisation: relating performance (flux and rejection) with surface properties (contact angle and surface free energy)".

Table of contents

List of Tables:

List of Figures:

Nomenclature:

Atomic Force Microscopy	AFM
American Society for Testing and Materials	ASTM
Bottom Brine Temperature	BBT
Contact Angle	CA
Charge Density	CD
Dead End Flow	DEF
De-Ionised Water	DI
Electrodialysis	ED
Electrodialysis Reversal	EDR
Fiber Reinforced Plastic	FRP
Filtration Streaming Potential	FSP
Hollow Fine Fiber	HFF
Homogenous Solution Diffusion	HSD
International Desalination Association	IDA
Ion-Exchange Capacity	IEC
Iso-Electrical Point	IEP
Kingdom of Saudi Arabia	KSA
Liquid–Liquid Displacement Porosimetry	LLDP
Multi Effect Boiling	MEB
Multi Effect Distillation	MED
Million Gallon per Day (= 3,785 m^3/d)	MGD
Million Imperial Gallon per Day (= 4,546 m^3/d)	MIGD
Multi Stage Flush	MSF
Make Up Ratio	MUR
Molecular Weight Cut-Off	MWCO
Nanofiltration	NF

Natural Organic Matter	NOM
Part Per Million	PPM
Performance Ratio	PR
Product Water	PW
Point of Zero Charge	PZC
Reverse Osmosis	RO
Recovery Ratio	RR
Scanning Electron Microscopy	SEM
Sulphate Removal Process	SRP
Saline Water Conversion Corporation	SWCC
Sea Water Reverse Osmosis	SWRO
Top Brine Temperature	TBT
Total Dissolved Solids	TDS
Thin Film Composite	TFC
Trihalomethanes	THM
Trans-Membrane Streaming Potential	TMS
Tangential Streaming Potential	TSP
Thermal Vapour Compression	TVC
Ultrafiltration	UF
United Nation	UN
Vapour Compression Distillation	VCD
World Health Organisation	WHO

Chapter 1: INTRODUCTION

1. Background

With ever increasing population and rise in their living standards and needs, together with the expansion of industrial and agricultural activities, there is always an increase in demand for good quality water throughout the world. Moreover, throughout the world, water scarcity is being recognised as a present and future threat to human activity. To meet this rise in demand, water treatment, in all its forms, is also on the rise. This tends to be the case also for the seawater desalination market on the global scale of which 609 new plants were added with total production of 4.079 million m^3/day during the period from mid-2012 to August 2013 [1]. However, one of the major impediments in the wide spread application of seawater desalination technology, whether thermal or membrane, is the relatively high cost associated with it. Recently many advances have been made in seawater desalination technology which leads to substantial decline in water production cost. One advance is the breakthrough application of nanofiltration (NF) membrane pretreatment technique for both thermal and membrane processes as that targets the removal of scale formation agents mainly sulphate. Sulphate scaling represents an inherent problem to all forms of desalination processes (either thermal or membrane type) as it could lead to their precipitation on the desalination equipment, e.g., tubes or membranes. This will increase the production cost and energy consumption of desalination processes and, in the worst scenario, it may ruin the plant leaving only one alternative for the plant operator; re-tubing for thermal plants or changing the membranes for membrane type of desalination.

On the same reflection, sulphate scaling is also an issue in operations involving seawater injection in the oil/gas extraction industry. It's considered that, oilfield applications of desalination technology, represented by the usage of nanofiltration membranes, are increasing almost as dramatically as the price of oil [1]. A growing trend to develop unconventional oil resources means many wells now require the use of water to increase oil production by flushing heavy oil from underground reservoirs. These operations requires large amount of relatively high quality water almost free of sulphate.

Hence, the continued development of NF membranes technology in the view of sulphate rejection from seawater for desalination plants pretreatment and water injection in the offshore oil/gas industry is a promising technique that could offer significant benefits by

optimum elimination of sulphate ions. This would indeed; help in minimising sulphate scale formation on equipment involved in both desalination processes and oilfield operations.

2. Nanofiltration applications for sulphate removals from seawater

"Membrane Softening" Membrane softening is a term applied to a water treatment process that uses nanofiltration membrane technology to reduce hardness and remove organics, colour, bacteria, and other impurities from the raw water supply.

NF membrane is a type of pressure driven membrane that has properties in between those of ultrafiltration (UF) and reverse osmosis (RO) membranes. NF membranes are generally characterised by charge density and pore size in the range of nanometers. The charge is most often negative (in seawater environments) and has an effect on the selective passage nature of these membranes. The separation performance of NF membranes depends mainly on two effects. The sieving effect, which is important for neutral components, and the electrostatic effect as a result of charge interactions between the pore surface and the ions in the water. Moreover, the degree of rejection by the NF membrane is lesser for monovalent ions, such as Cl^-, Na^+, than that for the divalent SO_4^{2-} and Ca^{2+}. The said ion selectivity allowed for the use of NF in the removal of hardness from saline water. The NF process benefits from ease of operation, reliability and comparatively low energy consumption (in comparison to RO membranes) as well as high efficiency of divalent ion removal.

NF membrane has been applied in softening of brackish water and drinking water; removal of colour, turbidity, removal of dissolved organic substances which are precursors to disinfection by-products Trihalomethanes (THM), and removal of sulphate from seawater. In this regard, NF membranes based on their membrane polymer structure and fabrication method provides unique permeate quality having negligible sulphate content suitable for pre-treating seawater prior to its feed to reverse osmosis and/or thermal desalination processes as well as oil/gas industry applications to overcome the problem of sulphate scale in both fields.

Nevertheless, nanofiltration to remove sulphate from seawater is a relatively new established technique having considerable interest in both desalination industry as well as operations involving seawater injection in the oil/gas extraction industry, but the separation processes are not well understood.

3. The relevance of the research topic

In seawater desalination, the thermal distillation technologies are now relatively mature. However, there is room for development of scale prevention techniques to allow high temperature operation of brine temperatures without the problems of sulphate scaling. Because of the unavailability of satisfactory treatment against calcium sulphate scale, the method utilised in practice to avoid calcium sulphate scale precipitation depends upon maintaining the operation parameters of the desalination plant below the solubility limits. The limitation is the top brine temperature (TBT) which is generally kept less than about 112 ^{0}C in multi stage flash (MSF) distillers, and, for multi effect distillation (MED), lower than this figure due to the mechanism of the heat transfer. Therefore, there are research efforts being undertaken into the use of NF membrane softening as a possible pretreatment for distillation processes. This would, technically, allow operation with top brine temperatures well in excess of the calcium sulphate limit of 120 °C for MSF units as a result of sulphate removal from seawater feed to the plant.

On the same reflection for seawater reverse osmosis (SWRO) plant the limitation is that the brine concentration should not exceed 2.5 – 3.5 times the feed sea water (depending on feed water sulphate content). Pretreatment by the use of NF is believed that such implementation probably holds out the greatest prospect for improved SWRO reliability and extension of membrane lives.

The potential breakthrough in the productivity and economics of seawater desalination by the usage of NF membrane as a pretreatment for sulphate ion removal (and all other scale-forming ions) can be confirmed to be very promising. As it would lead to a significant increase in the productivity and energy efficiency of future desalination plants not least by facilitating an extension of current operational limits (e.g. TBT in thermal desalination units).

During the last few years' interest in the research and development of NF membrane application as a pretreatment for desalination plants has been increasing due to superior filtrate quality compared to the conventional filtration pretreatment (critical discussion of such usage is available in chapter 4).

However, more intensive and critical investigations in such NF application are required for improving and optimising the effectiveness of hybrid plants operation. In addition, continued NF membrane research will provide a vital role in the development of future seawater

desalination industry and operation by providing an optimum feed water quality allowing for plants performance to reach higher operating standards than the currently achievable leading to increases in productivity associated with cost reduction per unit volume of product fresh water.

For the application of nanofiltration membranes for de-sulphating the seawater prior to down-hole injection for enhanced oil recovery in offshore oil production it is considered to be standalone technology, hence its implementation becomes routine.

Associated with these applications, nowadays, there are several manufacturers and suppliers for the commercial nanofiltration membranes for the target purpose of application. Manufacturers and suppliers usually quote operational performance according to certain experimental parameters set by them. Therefore, there is no universal reference to compare the performance of the available NF membranes in the market under constant operational conditions.

Moreover, different NF membranes have different properties and not all of the NF membranes could be used to reach the demand for optimum sulphate rejection for both applications of desalination pretreatment or offshore oil/gas production. NF operations should be designed properly based on optimum membrane selectivity and permeability. It has been acknowledged, that achieving optimum performance is a function of carefully choosing the NF membrane.

This highlights the objective of this research study, which comprises an intensive detailed characterisation for commercial NF membranes to assess and compare them under uniform testing environments. Accordingly, this research will provide a framework for direct comparison of the physical and chemical characteristic of nanofiltration membranes. It has been concluded that the key to utilising the most appropriate NF membrane for the particular application of sulphate rejection is the selection of a membrane with the optimum sulphate rejection and permeate flow rate characteristics under certain operating parameters.

4. Scope of the PhD

The selectivity of NF membranes' to separate sulphate ions from seawater is influenced by operating conditions (more particularly feed water temperature and pressure), seawater chemistry and NF membrane morphology. Therefore, to understand differences among various commercial NF membranes behaviour, this PhD project objective to examine and characterise eight commercial nanofiltration membranes for sulphate rejection under various operating conditions in order to determine the most appropriate membrane for the target purposes. Furthermore, a focused thermodynamic analysis on the potential for the use of nanofiltration NF as a pretreatment for MSF desalination process showing the benefits obtainable from the use of NF as a pretreatment system for chosen commercial desalination plant.

An approach to characterise the NF membranes are set to be:

I. Phase one: laboratory experimental examination for the potential of different commercial nanofiltration NF membranes for sulphate rejection under:
    i. ASTM standards. Involving investigations of the important influences of varying operational parameters - in particular feed water pressure and temperature.
    ii. Simulated seawater. As for mixed electrolytes solutions, some questions still exist to evaluate the separation performance of NF membranes since rejection to ions by NF membrane is different from that in the single salt solution as a result of the attractive and repulsive forces among ions.

II. Phase two: involve assessing the sulphate separation process of the measured flux and ion rejection during phase one. Using NF characterisation techniques of: porosity factor, contact angle, surface free energy, Atomic Force Microscopy (AFM), membrane potential and charge density calculations.

Based on the findings of the two phases, this work aims to provide fundamental knowledge and clearer understanding of NF membranes performance more particularly for sulphate rejection applications. Allowing a systematic way of NF membrane selection and optimising its operating conditions for a proposed particular application to enhance both the NF membrane and the industry (whether desalination or oil/gas separation) longevity and consequent economic benefit for water production by undertaking a study of the benefits obtainable from the use of NF as a pretreatment system for a chosen MSF seawater desalination plant, showing the contribution of this research to the industry.

5. Thesis organisation

The following chapter 2: looks at the crucial need for seawater desalination, followed by an overview of the desalination methods that are commercially available. These can be classified in two main categories, thermal processes and membrane processes, with sub-categories for each and its economics. There follows an illustration of the most common problem to all forms of desalination processes; scale formation and more particularly sulphate scale and how NF implementation can contribute to solve such problem.

Chapter 3: is mainly defining NF membrane technology, the way they work and what they are.

The thesis then goes on to critical review of the current utilisation of NF membranes to overcome the sulphate scale problem by elimination of the ions from the feed water inlet to the desalination plants and oil and gas applications, in chapter 4. Including an assessment of two desalination plants (one thermal and one SWRO) using NF as a pretreatment.

Chapter 5: critical literature review linking to the stated problem over previous work for NF characterisation. Summarising what is known and the gap that this thesis is aiming to fill, for a better understanding of optimum NF selection and usage as pretreatment for desalination plants.

- Note: the detailed procedure and the critical review of each individual characterisation technique are provided at the introduction of each chapter of the named characteristic technique.

There follows, in chapter 6: a description of the NF membranes used in this research and the experimental protocols (research procedure) that have been adopted.

The main series of experimental findings, results and discussions are then presented as follow.

Chapter 7: NF membranes filtration performance evaluation in ASTM, simulated seawater and pure water flux. Including the determination of effects of feed water pressure and temperature on the performance of the NF membranes in terms of product water flow and sulphate rejection.

Chapters 8 – 11: is reporting the main findings and observations of each characterisation technique of the commercial NF membranes subjected to tests and their relevance to

performance aspects of NF membranes. Those characterisation parameters are: porosity factor (chapter 8), assessment of membrane hydrophilicity through contact angle measurements followed by surface free energy calculations (chapter 9), AFM studies to quantify and visualise membranes surface roughness (chapter 10) and NF membranes charge density calculations from the membrane potential measurements (chapter 11).

Chapter 12: discusses overall results (findings) to critically characterise the NF membrane's optimum selection for the target process.
In addition, based on the contribution impact of this research in terms of desalination industry, fundamental thermodynamic analysis has been undertaken to demonstrate the benefits obtainable from the use of NF as a pretreatment system for a chosen MSF desalination plant in Saudi Arabia.

Chapter 13: summarise the overall conclusions, followed by recommendations for future research studies.

Thesis references and appendices are then presented at the end of the thesis.

Chapter 2: SEA WATER DESALINATION FOR WATER SECURITY

1. Overview:

All aspects related to water are becoming more and more important, and so is desalination [1]. Today, desalination is an essential part of the world water management strategies. It is practiced in 150 countries with 300 million people around the world relying on desalinated water for all or some of their daily needs. However, the UN estimates that 1.2 billion people now live in regions facing water scarcity, and a further 600 million will encounter water scarcity by 2025 [1].

Seawater desalination is a realistic option to create water. The International Desalination Association (IDA) at its World Congress in Perth – Australia in September 2011 announced an increase of 8.8% in global desalination capacity [2].

The total worldwide capacity of all desalination plants, including plants in operation and plants under commissioning is 86 million m^3/day from over 16,000 plants in August 2013, and it is expected to reach about 100 million m^3/day by 2015 [3].

On a global scale, fresh water resources are limited. During the second half of the past century the use of industrial water desalination processes has been adopted by a large number of countries. In some situations (e.g. China), the use of desalination is necessary to provide additional water to sustain industrial and urban activities. In other cases, seawater desalination is the only means to provide a sustainable source of fresh water for all forms of human activities such as in the Kingdom of Saudi Arabia and other Arabian Gulf states.

2. How much water is there?

If all the Earth's water – including its rivers, lakes, groundwater, seawater and glacial icecaps – were contained in a bubble, that bubble would measure 1,385 km in diameter. The volume of all this water is $\left[\frac{4}{3}\pi\left(\frac{1385}{2}\right)^3\right]$ = 1,391 million km^3. The picture on Figure 2.1(a) [3], by Jack Cook of the Woods Hole Oceanographic Institution, illustrates the relative size of that water-filled sphere compared to the size of Earth. About 97% of the available water is represented by salty water often with a salinity level > 35,000 mg/l (3.5 wt %) as shown in Figure 2.1(b) [4]. Therefore, the largest potential source of alternative water supply requires and will continue to require saline water desalination.

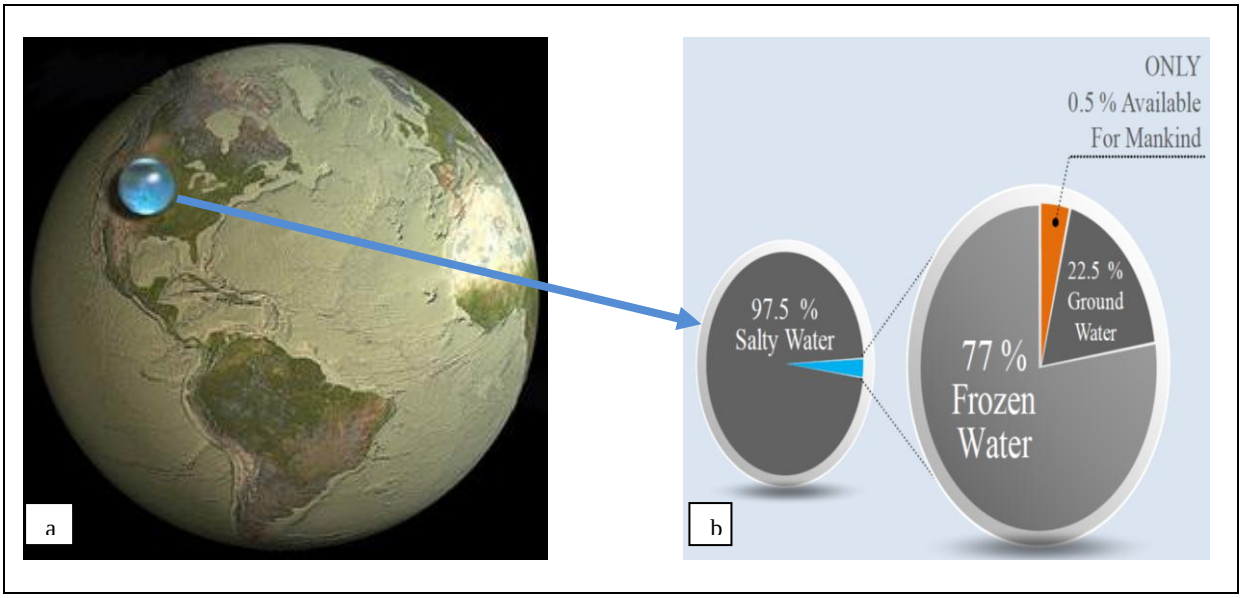

Figure 2.1 (a) Comparison of all earth available water to the size of the planet [3], (b) Abundance of water on earth [4].

3. Review of Desalination processes:

A desalination process essentially separates saline water into two parts - one that has a low concentration of salt; named as treated water or product water or permeate, and the other with a much higher concentration than the original feed water, usually referred to as brine reject or simply as 'concentrate'. The two main methods of water desalination are; membrane and thermal techniques. Within those two broad types, there are sub-categories (processes) using different techniques. The oldest sea water desalination methods are thermal technologies, based on evaporating water and collecting the condensate. The most applicable thermal technologies are:

1) Multi Stage Flash (MSF).
2) Multi-Effect Distillation (MED).
3) Vapour Compression Distillation (VCD).

On the other hand, the major membrane processes for saline water desalination are:

1) Reverse Osmosis (RO).
2) Electrodialysis (ED) and Electrodialysis reversal (EDR)

The account of desalination capacity by technology on a worldwide basis is shown in Figure 2.2, which has been produced upon Global Water Intelligence 2013 statistics of Media Analytics [10].

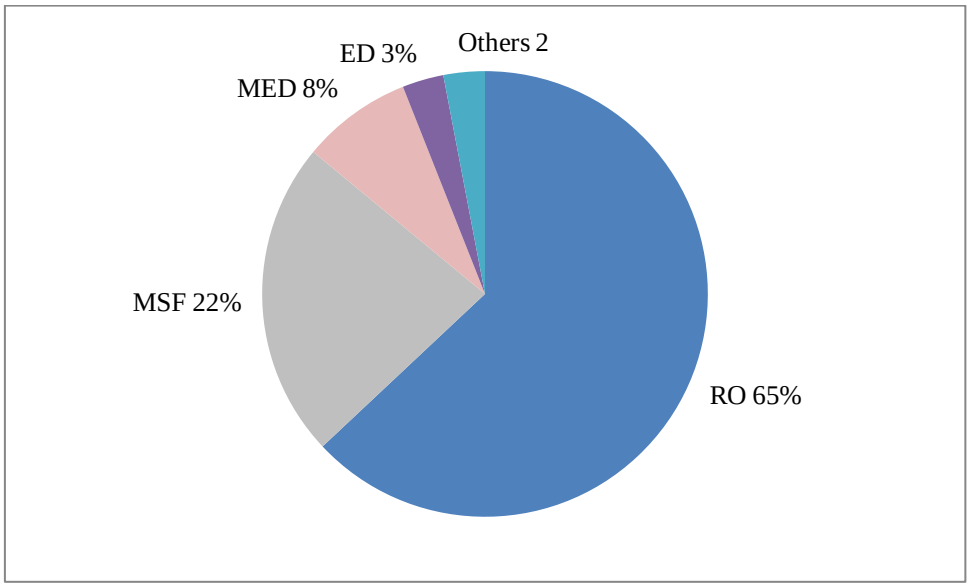

Figure 2.2 Capacity percentage of each desalination technology out of the world total production 2013 [10].

3.1 Thermal Technologies:

Thermal technologies, as the name implies, generally involve the heating of saline water and collecting the condensed vapour (distillate) to produce pure water.

3.1.1 Multi Stage Flash (MSF):

This process involves the use of distillation through several (multi-stage) chambers. In the MSF process, each successive stage of the plant operates at progressively lower pressures created by a vacuum system. The feed water is first heated by pressurised steam, and is led into the first 'flash chamber', where the pressure is released, causing the water to boil rapidly resulting in sudden evaporation or 'flashing'. This 'flashing' of a portion of the feed continues in each successive stage, because the pressure at each stage is lower than in the previous stage as a result of the vacuum system action. The vapour generated by the flashing is converted into fresh water by being condensed on heat exchanger tubing that runs through each stage. The tubes are cooled by the incoming cooler feed water (brine recycle). Generally, only a small percentage of the feed water is converted into vapour and condensed. Multi-stage flash distillation plants have been built since the late 1950s. Some MSF plants can contain from 15 to 25 stages. MSF distillation plants can involve either a 'once-through'

or ‘recycled’ process. In the ‘once-through’ design, the feed water is passed through the brine-heater and flash chambers just once and disposed of, while in the recycled design, the feed water for cooling is recycled. However, the once through type has only limited application for economical reasons related to the amount of chemical treatment for the feed water, and the need for a larger vacuum system.

Each of these processes can be structured as a ‘long tube’ or ‘cross tube’ design. In the long tube design, tubing is parallel to the concentrate flow, while in the cross tube design, tubing is perpendicular to the concentrate flow. MSF plants are subject to corrosion and scale formation. Those are the major concerns of the designers and developers to minimise such effects on the process in order to raise the process efficiency [5].

3.1.2 Multi-Effect Distillation (MED):

The MED process has been used since the late 1950s and early 1960s. Multi-effect distillation (note that; in some texts it may be referred to as multi effect boiling MEB), occurs in a series of vessels (effects) and uses the principles of evaporation and condensation at reduced ambient pressure. In MED, a series of evaporator effects produce water at progressively lower pressures. Water boils at lower temperatures as pressure decreases, so the water vapour of the first vessel or effect serves as the heating medium for the second, and so on. In fact, that two types of distillation mechanism take place in MED plant, first is by boiling, and also by flushing. Although boiling produces almost 80% of the plant total production, nevertheless, flushing is taking place. This is the reason it may be more accurate to call it MED instead of MEB.

The more vessels or effects there are, the higher the performance ratio and hence reduced energy consumption. Depending upon the arrangement of the heat exchanger tubing, MED units could be classified as horizontal tube, vertical tube or vertically stacked tube bundles. There have been several MED plants built in the Middle East. Although MED plants are employed less extensively than the MSF types in terms of plants numbers and production, nevertheless, this technique is receiving the attention of researchers and designers to overcome the limitations of this type in operation of which the main limitation is due to the scale formation. This feature restricts the first effect temperature (i.e. the brine highest temperature) hence the available temperature range. Scale deposition is more of a problem in MED plants than in MSF units because, in the former, evaporation – condensation processes take place at the same location [6].

3.1.3 Vapour Compression Distillation (VCD):

The vapour compression distillation (VCD) process is used either in combination with other processes such as the MED, or by itself, as they share the same operating principle. The heat for evaporating the water comes from the compression of vapour, rather than the direct exchange of heat from steam produced in a boiler. Vapour compression (VC) units have been built in a variety of configurations. In some cases, a mechanical compressor is used to generate the heat for evaporation. However, due to the mechanical mal-operations of the mechanical compressors, thermal compressors such as steam ejectors are more likely to be used. The VC units are generally small in capacity, and are often used at hotels, resorts, palaces and in industrial applications [6,7].

3.1.4 Comments on thermal technologies:

Distillation processes produce about 26 million cubic meters of distilled water per day globally, which is about 30 percent of the worldwide desalination capacity. MSF plants provide about 75 percent of that capacity. Most of those plants have been built in the Middle East, where energy resources have been plentiful and relatively inexpensive. A powerful reason for selecting the thermal type of seawater desalination plants is its ability to utilise the waste heat of a power plant. In such type of plant with cogeneration of power and water (dual purpose station), part or all of the steam that has done its work in the steam turbine will be extracted to the distillation unit(s). This will increase the plant overall efficiency and reduce the fuel : products cost. The types of combination and the thermodynamic assessment of each are beyond the objective of this thesis.

3.2 Membrane Technologies:

Sea water membrane technologies can be subdivided into two broad categories: Electrodialysis/Electrodialysis Reversal (ED/EDR), and Reverse Osmosis (RO).

3.2.1 Electrodialysis (ED) and Electrodialysis Reversal (EDR):

Electrodialysis (ED) is a voltage-driven membrane process. An electrical potential is used to move salts through a membrane, leaving fresh water behind as product water. ED was commercially introduced in the 1950's, about 10 years before reverse osmosis (RO).

ED depends on the following general principles:

a) Salts dissolved in water are ions, either positively charged (cations), or negatively charged (anions).
b) Since like charges repel each other and unlike charges attract, the ions migrate toward the electrodes with an opposite electric charge
c) Suitable membranes can be constructed to permit selective passage of either anions or cations.

In a saline solution, dissolved ions such as sodium (Na^+) and chloride (Cl^-) migrate to the opposite electrodes passing through selected membranes that either allow cations or anions to pass through (not both). Membranes are usually arranged in an alternate pattern, with anion-selective membrane followed by a cation-selective membrane. During this process, the salt content of the alternate water channels is diluted, while concentrated solutions are formed in adjacent channels and at the electrodes. Concentrated and diluted solutions are created in the spaces between the alternating membranes, and these spaces bound by two membranes are called cells. An ED unit consists of several hundred cells bound together with electrodes, and is referred to as a stack. Feed water passes through all the cells simultaneously to provide a continuous flow of desalinated water and a steady stream of concentrate (brine) from the stack.

In the early 1970's, the Electrodialysis Reversal (EDR) process was introduced. An EDR unit operates on the same general principle as an ED unit, except that both the product and concentrate channels are identical in construction. At intervals of several times an hour, the polarity of the electrodes is reversed, causing ions to be attracted in the opposite direction across the membranes. Immediately following reversal, the product water is removed until the lines are flushed out and desired water quality restored. The flush takes just a few minutes

before resuming water production. The reversal process is useful in preventing the membranes from fouling [7].

3.2.2 Reverse Osmosis (RO):

In relation to thermal processes**,** Reverse Osmosis (RO) is a relatively new process that was commercialised in the 1970's. Currently, RO can be considered as the solution for quick and economic way for sea water desalination. As a result, RO plants number is growing rapidly in terms of construction and capacity.

The RO process uses pressure as the driving force to push saline water through a semi-permeable membrane into a product water stream and a concentrated brine stream is left behind to be rejected.

The process is explained as; osmosis is a natural phenomenon by which H_2O from a low salt concentration passes into a more concentrated solution through a semi-permeable membrane. When pressure is applied to the solution with the higher salt concentration solution, the H_2O will flow in a reverse direction through the semi-permeable membrane, leaving the salt behind. This is known as the Reverse Osmosis process or RO process.

In addition to seawater desalination, RO technology is used to purify water for a wide range of applications, including semiconductors, food processing, biotechnology, pharmaceuticals, power generation, brackish water desalting, and municipal drinking water.

In Europe, reverse osmosis, due to its lower energy consumption, has gained much wider acceptance than its thermal alternatives [9].

4. Critical issues of seawater desalination related to the research topic:

4.1 Desalination cost (Economics):

Desalination processes are very energy intensive. However, desalination cost involves significant scatter due to so many factors and special conditions related to each individual case. Even though seawater desalination cost has decreased over the last years, the cost of water produced from desalination systems is very much site specific and the variability of cost per cubic metre exists because it depends upon many factors, unique in each case, most important of which are the desalination technology, feed water chemistry, energy source, capacity of the plant, and other site related factors [10-15], which is beyond the objective of this research work.

The increase of desalination capacity is caused primarily not only by increases in water demand but also by the significant reduction in desalination cost as a result of significant technological advances that result in making desalinated water cost promising. The cost of desalinated seawater has reduced to around \$0.50/m^3 for large scale plants.

The table below shows the cost of 1 m^3 at selected seawater desalination plants:

Plant	Capacity, m^3/day	Technology	Cost in \$/m^3 [11]
Shuaiba Phase 3 (Saudi Arabia)	721,185	MSF	0.46
Perth (Australia)	143,700	SWRO	1.2

Table 2.1 Cost of 1 m^3 product water at selected seawater desalination plants

These figures are constantly changing because the desalination market is growing very rapidly worldwide. Moreover, the economic analysis is based on a number of determining factors such as capital, energy, labour, chemicals, materials, and consumables cost. This varies tremendously upon a serious of complex integrated factors. This imposes a difficulty for the assessment of desalination competing technologies and its associated economics.
As a matter of fact, desalination is considered still to be expensive to solve all the world water shortage, therefore reducing the cost of water production is one of the greatest challenges that faces the desalination industry.

The progress in, and development of, desalination technology has resulted from substantial research efforts to lower the cost of desalinated water. One of the several opportunities for improvements in desalination practices is the introduction of nanofiltration membranes as a pretreatment ahead of desalination plants of either reverse osmosis or thermal units [13]. Such special conditions hybrid systems can offer an increase and more stable production (processes evaluation and studies are detailed in chapter 4).

4.2 Scale deposition in Desalination plants:

"The history of desalination is the history of the control of scale formation"
Professor R.S. Silver, University of Glasgow, circa 1970.

4.2.1 Scale and its effect on desalination processes:

Most people working in seawater desalination recognise that scale formation problems are facts of their practical life. Scale deposition is the most undesirable yet unavoidable problem in desalination plants. It can be considered as one of the most critical aspects in desalination design considerations and in plant operation [16]. Scaling can lead to serious reductions in the performance and efficiency of the plant and, in the worst scenarios total ruination, especially in the high temperature zones in thermal distillation and on the membrane surfaces for SWRO plants as shown in Figure 2.3.
Both the high degree of hardness and high TDS in the seawater place limits on product water recovery.

Scale deposition on the outside surface of a HTFF-MED plant tube taken from the 1st effect

Scaled SWRO membrane surface

Figure 2.3 Photos of scale deposition in seawater desalination plants [Information department of SWCC, Kingdom of Saudi Arabia, Riyadh]

Depending on the desalination plant operating conditions and the location (section) in the plant, two types of scale can form. An alkaline scale made of $CaCO_3$ and/or $Mg(OH)_2$ and non-alkaline scale such as calcium sulphate $CaSO_4$. Although there is a possibility for other kinds of scale formation depending on the plant location and the feed water chemistry, those mentioned above are the most probable scale formations that takes place especially for the seawater desalination plants [19]. One particular extreme difficulty with $CaSO_4$ is that it is extremely hard and therefore difficult to remove once it formed. And if it has the chance to form and precipitate, the only method to remove it often is by shutting down the desalination plant and attempt either to remove the scale layer by dissociation using pure water (very slow) or by mechanical removal which will need manpower. For both cases of removal the plant production will be lost.

To prevent and avoid alkaline scale formation certain techniques are applied, however the most common in the industry is injecting:

- For thermal plants;
  - either anti-scalent into the brine recirculation stream,
  - or (strong) acid – usually sulphuric acid – into the feed water inlet.
- While for membrane the injection of either acid or/and anti-scalent will be at the feed stream.

Use of anti-scalants has proved effective in preventing alkaline scale formation but has failed to increase significantly water recovery, for example, from Arabian Gulf seawater beyond 35% in both the membrane and the thermal processes.

On the other hand acid treatment for scale control in thermal plants can lead to high corrosion rates over long operation periods. This has been attributed to:

1. Low brine recycle pH.
2. The difficulty of controlling the brine pH which needs accurate pH meters and acid dosing control.

Moreover, there are the extreme operational risks encountered using acid dosing system in terms of staff safety and equipment deterioration.

However, the use of NF membranes (as part of combined NF-seawater desalination) to pretreat feed to the plant in order to remove hardness (eliminating both anti-scalent and acid dosing, or at very minor dosing rate), is a promising approach mainly for economic reasons

related to the plant overall performance ratio and product water quality and quantity (processes evaluation and studies are detailed in chapter 4).

4.2.2 Sulphate behaviour and its effect in desalination plants by means of Calcium Sulphate formation:

Sulphate ion as (SO_4^{2-} ppm) varies in the range of 2640 to 3100 ppm for normal seawater [18]. In order to understand the effects of sulphate scale on the performance of a desalination plant and its limitations and restrictions on the processes, it is useful to consider the behaviour of calcium sulphate in seawater under a range of temperatures and concentrations.

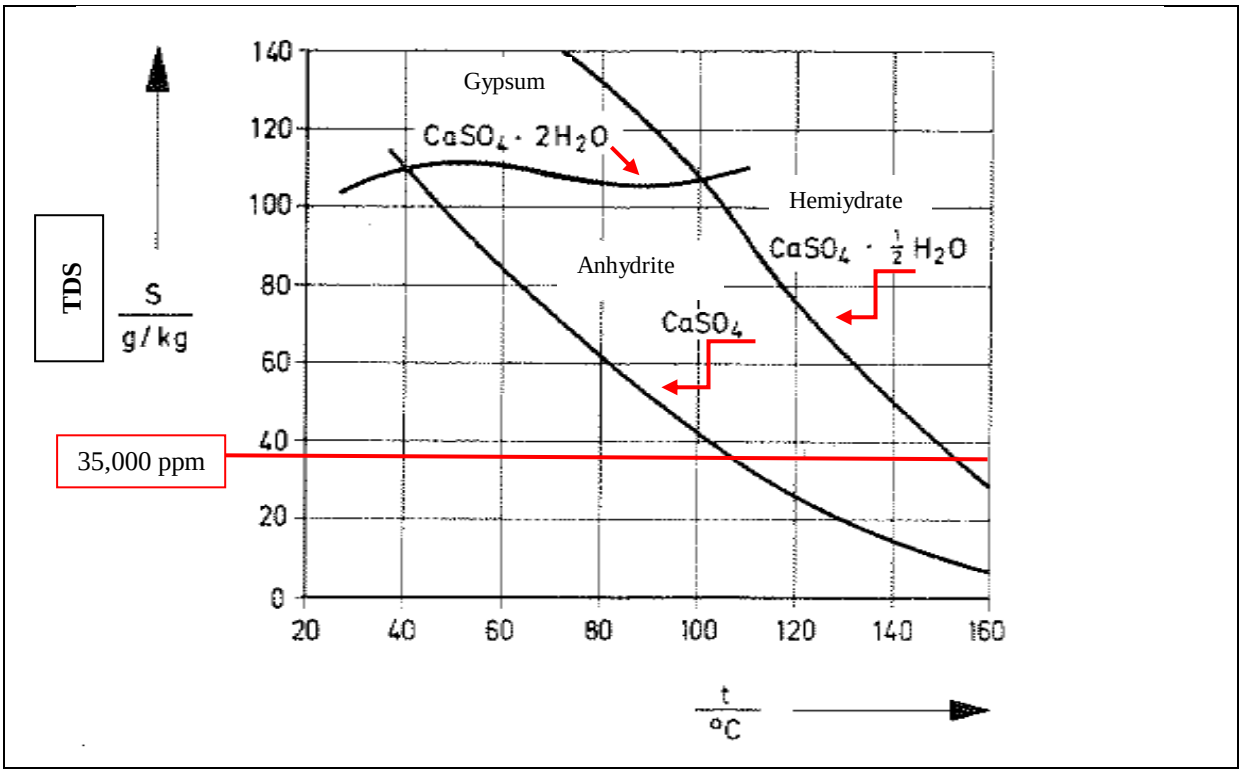

Figure 2.4 Solubility limits for the three forms of calcium sulphate in seawater concentrates [21].

Figure 2.4 shows the solubility limits of the three forms of calcium sulphate for standard seawater concentrations as a function of the temperature. Calcium sulphate precipitates in three different solid phases: $CaSO_4.2H_2O$ dihydrate (so-called gypsum), $CaSO_4.{}^1/_2H_2O$ hemiyhdrate and $CaSO_4$ anhydrite, although at ambient temperatures (about 20 °C), gypsum is the most common one. The other phases are the products of gypsum dehydration at relatively higher temperatures. In general gypsum is the stable form at low temperatures while anhydrite is formed at higher temperature. Even though, anhydrite would be expected

above 40 °C due to its lower solubility while gypsum can be found at temperatures up to 100 °C.

Calcium sulphate scale in desalination processes occurs when the concentration of the calcium sulphate exceeds the saturation point (solubility limit) at which, after a certain time, scale nucleation starts followed by the precipitation of scale.

For thermal desalination plants, where temperature will be the major factor to consider in order to avoid the formation of calcium sulphate scale, operation on the left hand side of the hemiydrate form is essential. This indicates a limitation of the plant top operating temperature, so called top brine temperature (TBT), to be (in an ideal situation) 120 ^{o}C for a brine salinity concentration not more than (60 – 70 g/kg). However, such operational conditions are considered to be very critical and do need a very close monitoring to avoid exceeding the solubility limits of hemihydrate as if it had the chance to form (in relatively short period of time) it will precipitate as well acting as a catalyst to the anhydrite form. Therefore, desalination manufacturers and operators are recommending a maximum TBT of 117 ^{o}C and 103 ^{o}C for 2 and 2.5 brine concentration times feed seawater, respectively.

Operating on the right hand side of the anhydrite form (i.e. less than 120 ^{o}C) can be carried out without precipitation because its mechanism of formations of scale involves a relatively long time to nucleate in relation to the brine resident time in the tubes (for MSF) and as it fall in MED distillers. For membrane type of desalination plants, deposition of calcium sulphate may take place if the brine concentration exceeds 100 g/kg, i.e. exceeding the gypsum form solubility limits.

It should be emphasised that this type of information is based on the equilibrium studies and does not indicate the rates at which the precipitation occurs. The kinetics of $CaSO_4$, precipitation also strongly depends upon water quality and other ions present in the sea water. Thus, each plant is influenced by its own operational parameters and the feed water quality.

5. Conclusion:

Desalination is an appropriate solution for the future sustainable water supply, providing hope to the world community that it can provide water, the essence of life, at a reasonable cost, solving the scarcity of existing water supplies, avoiding regional and territorial conflicts, and providing the water resource for sustainable development. Accordingly, as President John F. Kennedy said five decades ago, "*If we could produce fresh water from salt water at a low cost that would indeed be a great service to humanity, and would dwarf any other scientific accomplishment."*

If an appropriate reliable approach can be achieved to eliminate the sulphate ion from the feed water, this would allow operating the desalination plants at a higher degree of efficiency and performance ratio. The use of NF as feed pretreatment to MSF for sulphate removal (operating at temperatures above the conventional – theoretical – maximum of around 120 ^{o}C) has been demonstrated on a pilot plants and few limited number of commercial plants (see chapter 4), its application has not as yet seen extensive adaptation in the desalination industry as more research and developments are required to advance the knowledge hence the confidence.

This fact is the driving motivator of this research work, by optimising the utilisation and selection of nanofiltration membranes for sulphate rejection from feed water ahead of desalination plants.

Chapter 3: NANOFILTRATION MEMBRANE (NF)

This part of the thesis reviews NF membrane science and technology, particularly in the field of seawater related separation processes.

1. Introduction:

Five membrane processes commonly used in water treatments are, reverse osmosis (RO), nanofiltration (NF), ultrafiltration (UF), microfiltration (MF), and Electrodialysis/Electrodialysis reversal (ED/EDR). However, the first four processes have the same separation mechanism for removal by pressure difference across the membrane, while the fifth type (ED/EDR) uses a charge driven membrane [5].

The potential of each type of the pressure driven membranes in removing certain water constituent is illustrated in the following chart (Figure 3.1).

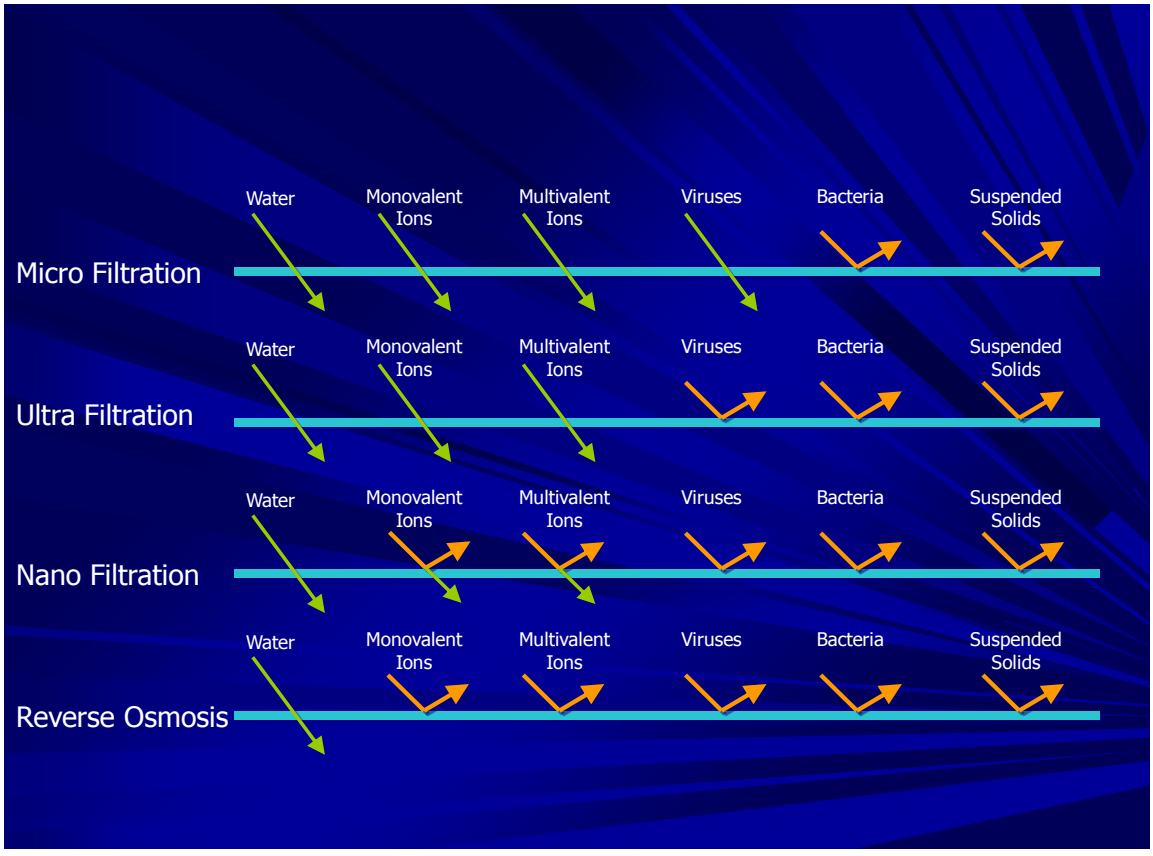

Figure 3.1 Pressures driven membranes rejection capability chart [35].

In general, NF is considered to be a process intermediate between UF and RO (as shown in Figure 3.1) as a result, having rejection characteristics that range from “loose” RO to “tight” UF.

From a practical point of view, the applied pressure in NF is generally a higher order of magnitude than in UF, but lowers than in RO. NF differs from UF and RO also in the separation mechanism, basically determined by two distinct properties [22,35]:

1. The pore size of the membrane ranging from 0.5 and 2 nm (in diameter), that corresponds to a molecular weight cut off value of approximately 50-500 g/mol. Therefore, the separation of components with these molecular weights from higher molecular weight components can be accomplished.

2. NF membranes have a slightly charged surface. Because the dimensions of the pores are less than one order of magnitude larger than the size of ions, charge interaction plays a role. This effect can be used to separate ions with different valences (mainly bivalent ions).

As the nanofiltration process lies between reverse osmosis and ultrafiltration, the transfer which separate H_2O and salts can be convective and/or diffusive. The first mechanism, of diffusion type similar to that of reverse osmosis, is independent of the flux of solvent and of the pressure; it depends only on the salts gradient of concentration on both sides of the membrane. The second mechanism corresponds to a selective drive of the aqueous solutions by solvent through the membrane: the convection [35].
A more recently proposed separation phenomenon is the partial or full dehydration of hydrated solutes during transport [112]. Simply defined as; the energy required to allow an ion to reduce the number of water molecules in their hydration shells, hence higher likelihood to permeate [103]. In other words, highly hydrated species are better rejected than less hydrated ones.

However, in comparison with ultrafiltration and reverse osmosis, nanofiltration has always been a difficult process to define and to describe [22]. Moreover, despite benefiting from a fast technological development, these mechanisms of transport and separation are not completely cleared up yet [23].

2. Historical background:

In the late 1970's (between 1976 to 1977) a membrane manufacturer located in California USA, formulated a special pressure driven membrane with a rejection rate of 47% for monovalent ions in order to reduce the TDS of a particular water having a feed water TDS of

930 ppm [24]. After that, this type of membranes become known as nanofiltration membranes and have been utilised in a various types of industries (see section 5 of this chapter). However, the usage of such type of membranes for seawater treatments was mainly for water softening (and organic removal).

Nanofiltration membranes were commercialised in 1984 when a membrane was introduced that separated divalent ions from monovalent ions in water solutions. The membrane caught the attention of an oil company, which used seawater to drive oil in offshore formations containing high concentrations of divalent cations. In 1988, the oil company used NF membranes to remove most of the sulphate from seawater before injecting it into oil-containing formations. Using seawater NF is now standard in offshore oil production in oil-containing formations with high hardness concentration [25].

By the late 1990's (till now) there is some work being undertaken into the use of NF membrane softening as a possible pretreatment for desalination (SWRO and/or thermal) plant. However, although, it is safe to say that NF implementation in desalination practice has shown many advantages, nonetheless, it is well believed that the evolution and characterisation of NF is needed for the optimisation of NF applications in the seawater desalination industry [26].

3. NF membrane materials:

The present design and manufacturing of nanofiltration membranes is based mostly on the design of reverse osmosis membranes including such aspects as materials of construction and the membrane configurations [5,6].
The traditional materials used for NF membranes are organic polymers. The polymer which has most commonly been used for manufacturing nanofiltration membranes is aromatic polyamide [29].

Currently, for desalination applications thin film composite (TFC) NF membranes dominate the market [30]. A brief summary of NF TFC membranes fabrications can be described as follows.
Conventional NF thin film composite TFC membranes are made of (Figure 3.2):

1. Thin active surface layer in the order of 1 µm thickness, acting as the main barrier to the permeation of water and solutes, therefore, separation and water passage takes place at this top ultra-thin selective layer fabricated of (either fully or semi) aromatic polyamides.

   The repeating units of the polymer are held together by amide group – $CONH_2$ with asymmetrical link structure of:

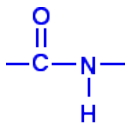

   Typically, this active layer is negatively charged in a seawater environment (which has been confirmed during membrane potential measurements – see chapter 11).

2. Middle micro-porous (polysulfone) support layer generally prepared by phase inversion process, which has pore sizes ranging from 5 to 50 nm. It not only plays a pivotal role to support the active top layer formation, but also influences the ability to achieve the high flux performance.

3. Bottom 100 to 150 µm thick backing polyester non-woven, widely used to support porous layer of NF membrane for its high strength, hence, mechanically robust.

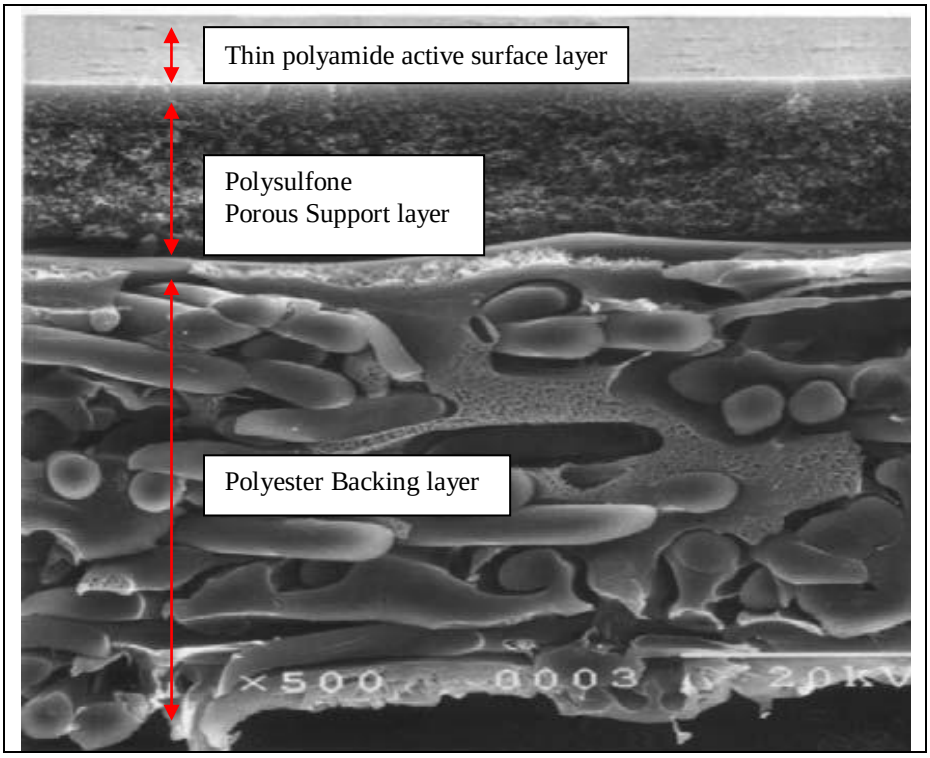

Figure 3.2 Magnified cross-section of a typical composite polyamide NF membrane [32]

Generally, interfacial polymerisation technique is widely used to prepare the top polyamide layer, in which, a poly functional amine in aqueous phase and poly functional acid chloride in organic solvents are brought into contact, both of the reactants condense to form a thin highly cross linked and network-structured polymer at the interface. Various parameters such as reactant concentration, reactivity of reactants, diffusion rate of reactants, addition of bases such as NaOH, tri-ethylamine to remove the by product formed, pretreatment conditions of the support and post treatment conditions determine the performance (mechanical strength, solvent flux and solute rejection) of TFC membranes. Apart from the pre- and post-treatment conditions, the top layer thickness has to be in the optimal range, even a slight increase in thickness resulted in increased hydraulic resistance by several folds [29].
The middle micro-porous (polysulfone) layer is generally prepared by phase inversion process. Generally, its materials are selected in such a way as to provide the necessary mechanical strength and minimal resistance to permeate flow [29].

The final resulting architecture of NF product is strongly dependent on fabrication methods of interfacial polymerisation technique followed by phase inversion process which is widely used for NF membranes manufacturing [28]. As a result, different parameters potentially affect the performance and morphology of fabricated membranes including:

1. The concentration of polymers.
2. Presence and concentrations of additives.
3. The temperature of the polymer (solution) during fabrications.

It must be mentioned that each layer of NF TFC membrane can be independently controlled and optimised to achieve desired selectivity and permeability.

The next table summarises the merits, demerits and areas of development of TFC as a material for NF membrane fabrication:

Merits	Demerits	Areas for developments
TFC gives flexibility during fabrication process, more particularly through the phase inversion stage to: 1. Produce varying thicknesses of thin top layer and support layers for different NF applications, 2. Optimisation layers with respect to structure, stability and performance to improve water flux and rejection.	This can be mainly attributed to its vulnerability to fouling and scale formation under certain applications and operational environments.	1. To increase water permeability and selectivity, 2. Less energy consumption, 3. To be more fouling resistance. 4. Recently, nano-fibers have been introduced to enhance the properties and performance of the membranes derived from conventional polymeric membrane materials [30].

Table 3.1 Merits, demerits and areas of developments of NF TFC

- Ceramic NF membranes

In addition to the available nanofiltration membranes in the markets, many companies and research institutes have been working on the development of ceramic membranes for several years [33]. Such membranes will give a wider range of nanofiltration applications beyond the standard mechanical and thermal limitations of the polymer types. It could be possible to produce a ceramic membrane with separation properties in the nanofiltration range and with permeability rates superior to that of polymer nanofiltration membranes for industries with aggressive environments. However, ceramic nanofiltration membranes are generally more expensive than standard commercial polymer membranes, and the pore size of most ceramic NF is still relatively high [22]. Therefore, their use should focus on fields of application which demand greater thermal or chemical resistance.

4. NF membrane module configurations:

There are two major membrane module configurations, those are hollow fine fiber (HFF) and spiral wound. However, for nanofiltration membranes in seawater desalination applications, the spiral wound is most widely used and available.

In a spiral wound configuration (Figure 3.3) two flat sheets of membrane are separated with a permeate collector channel material to form a leaf. This assembly is sealed on three sides with the fourth side left open for permeate to exit. A feed/brine spacer material sheet is added to the leaf assembly. A number of these assemblies (leaves) are wound around a central plastic permeate tube. This tube is perforated to collect the permeate from the multiple leaf assemblies. This unit is then placed in a cylindrical pressure vessel often glass fiber (FRP) as shown in Figure 3.3.
The typical industrial spiral wound membrane element is approximately 100 or 150 cm (40 or 60 inches) long and 10 or 20 cm (4 or 8) inches in diameter. Recently, some suppliers are producing 16 inches OD membranes for the reason to optimise the design area.

Manufacturers specify brine flow requirements to control concentration polarisation by limiting recovery (or conversion). Therefore, recovery is a function of the feed-brine path length. In order to operate at acceptable recoveries, spiral systems are usually staged with three to six membrane elements connected in series in a pressure tube. The brine stream from the first element becomes the feed to the following element, and so on for each element within the pressure tube. The brine stream from the last element exits the pressure tube to waste. The permeate from each element enters the permeate collector tube and exits the vessel as a common permeate stream. A single pressure vessel with four to six membrane elements connected in series can be operated at up to 50-percent recovery under normal design conditions. The brine seal on the element feed end seal carrier prevents the feed/brine stream from bypassing the following element [34].

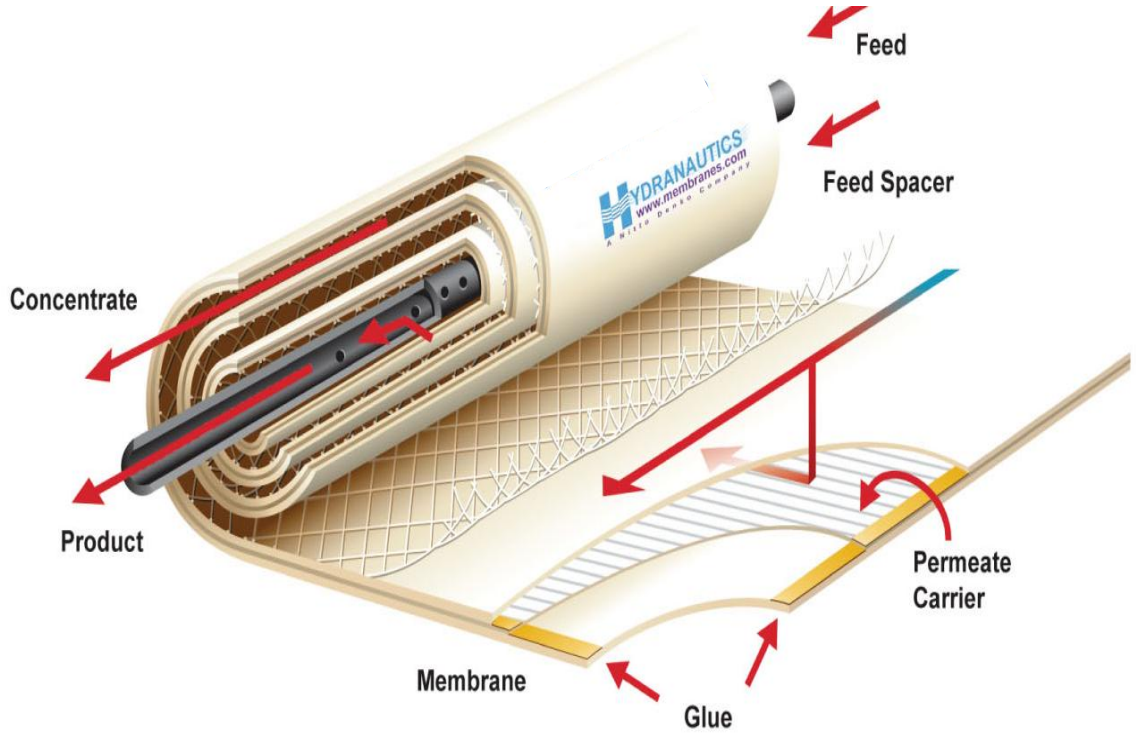

Figure 3.3 Spiral wound membrane configuration [Hydranautics, RO membrane elements brochure, 1/10].

5. NF membranes applications:

It is worth mentioning that, today, NF membranes have several applications in industry in addition to water treatments. Such industries that utilise NF membranes are: food, textile, clothing and leather, paper and graphical, chemical, metal plating and product /electronic and optical, agriculture, demineralisation of whey, demineralisation of sugar solutions, recycle of nutrients in fermentation processes, separation of sunflower oil from solvent [23].

Its wide range of application for water treatments makes it one of the most applicable membrane types over others under certain circumstances for its ability to remove the following [35]; removal of metal sulphates from waste water, removal of nickel, removal of degreasing agents from water, removal of precursors of disinfection by products, hardness removal, removal of natural organic matter (colour), removal of pesticides, removal of heavy metals and silica, removal of phosphate, sulphate (another area for this particular application is offshore oil/gas operation [36]), nitrate and fluoride, removal of algal toxins, removal of selenium from drainage water.

Thus, the most important application areas can be defined as:

- Removal of divalent ions from saline water.

- Separation between ions with different valences.
- Separation of low- and high-molecular weight components (depending on the application).

6. Nanofiltration—market size [30]:

Nafigate website forecasts that the nanofiltration market is expected to grow into US $3.0 billion in 2014. They anticipate that apart from water, food and beverages and bio-pharmacy, significant application of NF in electronics industry as well.

7. NF membranes process performance Theory and Equations [35]:

In order to understand the behaviour of NF membranes, it is appropriate to refer to the reverse osmotic concept which is typically applicable to NF with the only difference on the value of the pressure required to drive the water as a result of the pore size.

The natural osmotic phenomena takes place through a semi permeable membrane as the less concentrated water will flow to the more concentrated until reaching an equal state between both solutions. The driving force for the water flow is the difference in chemical potential between the two solutions. The flow of water across the membrane exerts a pressure called the osmotic pressure.

Reversing the natural path by applying an external pressure on the salty solution which is separated from the fresh solution by a semi permeable membrane allows the flow to go forward the fresh side (Figure 3.4). The pressure to be applied should be higher than the solution (equilibrium) osmotic pressure to achieve a reverse flow.

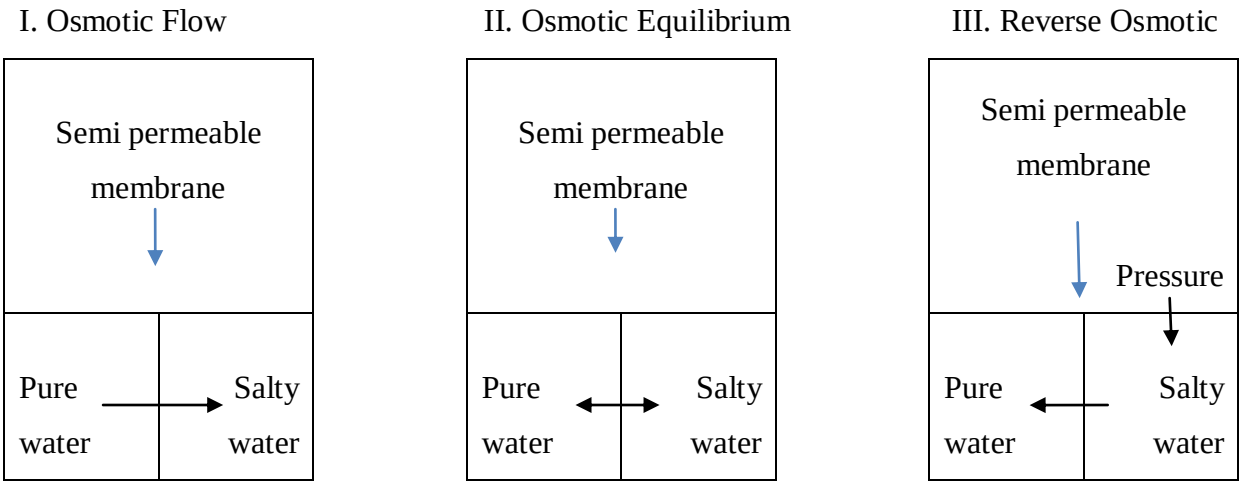

Figure 3.4 Explanation schematic of osmotic phenomena

The term semi-permeable membrane refers to a membrane that selectively allows certain species to pass through it while retaining others. In actuality, many species will pass through the membrane, but at significantly different rates. In NF, the solvent (water) passes through the membrane at a much faster rate than the dissolved solids (salts). The net effect is that a solute-solvent separation occurs, with water being the product and with a strong total retention for salts with weaker retention of the monovalent ions than the bivalent ions. The interactions between water, salts, and the membrane are the most important factors in the separation mechanism. However, the exact phenomena behaviour which occurs actually in the membrane is not well understood. Many mechanistic and mathematical models have been proposed to describe reverse osmosis and nanofiltration membranes [35, 37 – 42]. Some of these descriptions rely on relatively simple concepts while others are far more complex and require sophisticated solution techniques. Each of the major models available for transport mechanisms description in membranes and the basic equations for determining the solute and solvent fluxes, has been established for specific conditions and none is valid for wide range applications.

However, in order to understand the process, certain assumptions are made to approximate the system and describe the flow (flux). The standard model to describe the membranes processes behaviour for the separation process is the homogenous solution diffusion (HSD) model. HSD; relates the permeate quantity (flow rate) and quality (TDS) to four main factors, feed concentration, membrane characteristics (material of construction, pore size, configuration, surface parameters; such as morphology and charge), water recovery and applied pressure.

The following schematic diagram (Figure 3.5) and equations are the most commonly used for NF membrane process to determine the system characteristics.

Those equations are the one to be used for the calculations set by the ASTM D 4194 – 03 [42] thorough this research study.

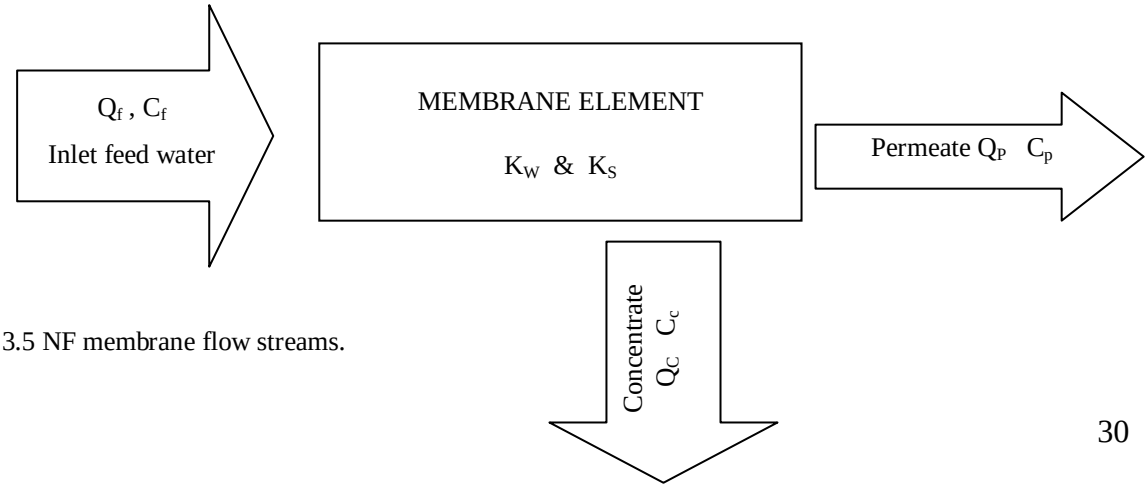

Figure 3.5 NF membrane flow streams.

1. Mass Balance for Water Flow:

$$Q_f = Q_p + Q_C \quad \text{where;}$$

Q_f = feed water flow rate

Q_p = permeate flow rate

Q_c = concentrate (brine) flow rate

2. Mass Balance for salt:

$$Q_f C_f = Q_p C_p + Q_C C_c \quad \text{where;}$$

C_f = feed water flow salt concentration

C_p = permeate salt concentration

C_c = concentrate (brine) salt concentration

3. Amount of salt passage:

$$\text{S.Passage \%} = (C_p / C_f) \times 100 = (1 - (((C_f + C_c) / 2) / C_f) \times 100$$

4. Rejection%: This is the ability of the membrane not to permit the salts to pass through.

$$\text{Rej.\%} = (1 - (C_p / C_f)) \times 100$$

5. Water flux:

$$F_w = K_w (\Delta P - \Delta\pi) = Q_p / A \quad \text{where;}$$

F_w = water flux through membrane, units of flow rate per area.

K_W = water mass transfer coefficient, units of water flux per pressure.

ΔP = applied pressure difference.

$\Delta\pi$ = salt osmotic pressure difference.

A = membrane (effective area).

$(\Delta P - \Delta\pi)$ = net applied pressure, (NAP).

8. Factors affecting the performance of NF membranes:

Four main factors influence the performance of NF membranes, those are;

1. Feed water salinity (TDS),
2. Applied pressure,
3. Recovery ratio,
4. Water temperature.

Those four factors are directly related to the membrane permeate quantity in terms of flow rate, and quality in terms of salt rejection. The following comments describes each factor effect individually on the permeate flux and the amount of salt could be rejected.

Before commencing the illustration of those factors and their effect and related limitations, it is significant to mention that each one of them has complex relations with the other three factors as well as other factors related to the membrane technology and operation. The next points are an attempt to summarise the effect of each one on the permeate flux and salt rejection.

1. **Applied Pressure**; this can be considered as one of the most critical aspects in the membrane performance and operation (see chapter 7 results discussions for detailed analysis regarding this particular factor). As the feed water pressure is increased the flow of the water through the membrane increases. The flow of the salt (salt passage) will remain (relatively) constant however; it will depend on the salt concentration difference. The upper limitation on the applied pressure will be the restrictions of the energy consumption and the compaction phenomena which are also related to other factors such as the membrane material.

2. **Recovery %;** this factor can be generally summarised as following: the higher the recovery rate the higher the product water yield from the feed water. Nevertheless, the limitations on the recovery are related to the applied pressure and the potential of scale formation as a result of the feed water salts saturation degree.

3. **Feed Water Salinity**; relating the TDS to the membrane performance, as salts concentration in the water increase this will increase its osmotic pressure thus the permeate flux will decrease and the salt passage will increase at a constant pressure.

4. **Water Temperature;** increasing the temperature of the feed increases both permeate flux and salt passage (see chapter 7 results discussions for detailed analysis regarding

this particular factor). A critical aspect to consider related to the optimum temperature to be applied is the membrane life "deterioration rate" as at certain temperature the effective life of the membrane may be affected. This is normally informed by the supplier or the manufacturer.

From an operational point of view, only the feed water TDS is the factor that could not be controlled which will depend on the source of the water, while the other three remaining factors are controlled by the plant operation conditions. Thus, in order to optimise the permeate quality and quantity those three factors (temperature, pressure and recovery) could be manipulated in a manner to satisfy the water quality needed (either for drinking or for further treatment) and the plant total energy consumption in terms of kWh/m^3, in addition, the plant equipments capacity and ability as well the manufacturer(s) recommendations for optimum conditions regard the plant operating parameters.

What has been illustrated above, for the effect of the four main factors on NF filtration performance, is a general description to cover all NF membranes. However, as proved in this research work each individual NF membrane has its own behaviour, in terms of the influence on the permeate quality and quantity, of the feed water pressure and/or temperature (see chapter 7 and research main discussion in chapter 12).

Chapter 4: REVIEWS OF NF APPLICATIONS IN DESALINATION INDUSTRY

1. NF as a pretreatment to desalination technology:

1.1 Overview:

Nanofiltration membranes can achieve typically a rejection of divalent ions (e.g. SO_4^{2-}) in a range of 75 – 99% and for monovalent ions (e.g. Na^+, Cl^-) up to 30 – 50 % [35], depending on operational conditions and inlet feed water chemistry. For this reason, NF cannot be applied alone for seawater desalination targeting product water for human consumption because the permeate (product water) would contain too high total dissolved solids TDS which according to world health organisation WHO standards should be less than 500 ppm. Nevertheless, an important aspect of this achievable rejection is that osmotic pressure (hence energy consumption) in NF is much less than in the conventional seawater desalination by reverse osmosis (SWRO).

Thus, in order to optimise the rejection ability with the energy consumption factor, a (relatively) new trend in the desalination industry emerges to integrate NF with other desalination applications. Such combination involve combining the NF membrane process with one (or more) of the conventional seawater desalination processes in one fully integrated process system to form: NF-SWRO, NF-MSF, NF-MED, and NF-SWRO-reject-MSF/or MED [13,25,26, 43 – 61].

The main advantages for these combinations by utilising NF as a pretreatment for the desalinating seawater plants gives the following:

1. Reduction of the inlet sea water TDS by up to 20 – 40 %.
2. Reduction of (SO_4^{2-}, Mg^{2+}, Ca^{2+}) – main scale forming substances – by nearly (70 – 98%) depending on the NF membrane type and the operating conditions.
3. Reduction of turbidity and microorganisms nearly approaching up to 95% (depending on the operating conditions)

The second point mentioned above of the advantages of introducing the saline water to a NF membrane prior to its feed to the desalination plant is considered, by the desalination community, to be the main potential reason for favouring NF rather than any other method for pretreatment and/or scale forming agent reduction.

The utilisation of NF membrane for pretreatment can overcome the major problems encountered by the various conventional seawater desalination processes (membrane or thermal), since it:

I. prevents fouling by the removal of turbidity and bacteria,
II. prevents plants scaling by removal of scale forming hardness ions,
III. Significantly lowers required pressure and energy to operate SWRO plant by reducing TDS of seawater feed.

Therefore, NF membranes targeting water treatment applications (in general) and seawater desalination pretreatment can be sub-categorised into two main divisions according to their implementations and marketing:

1. NF membranes for scale preventions targeting rejection of multivalent ions.
2. NF membranes that have been developed (particularly) for the removal of natural organic matter (NOM) responsible for imparting colour, taste and odor to potable water.

This NF pretreatment changes the seawater feed chemistry with the net effect of increasing SWRO, MSF and other thermal desalination plants potable water yield and product recovery ratio. Likewise, it allows for their operation without the addition of anti-scalent (or at very minor dosing rate amounts).

The combination of NF with thermal processes, such as multi stage flash (MSF), should make it possible to operate MSF plants on the NF-permeate at high distillation temperatures (TBT) of (> 120 ^{0}C) with high distillate recovery, higher flash range increases production, reduced MSF capital costs, reduced MSF operating costs and without chemical additions [26,43,44,47,50,55,57].

Furthermore, NF membrane technology could significantly improve operation and reduce the cost of the MED process, with horizontal tube evaporators or specifically when applied to MED processes using advanced heat transfer surfaces like double fluted tubes, by eliminating the risk of scaling and fouling. NF technology will permit an increase in the top temperature resulting in significant increase in output and performance ratio.

Recently, it has been shown that a design of tri-hybrid NF/SWRO/MED desalination (as shown in Figure 4.1) has been developed to enable operation of MED/TVC distiller at top brine temperature TBT of 125 ^{0}C and with significantly improved energy efficiency [49,53].

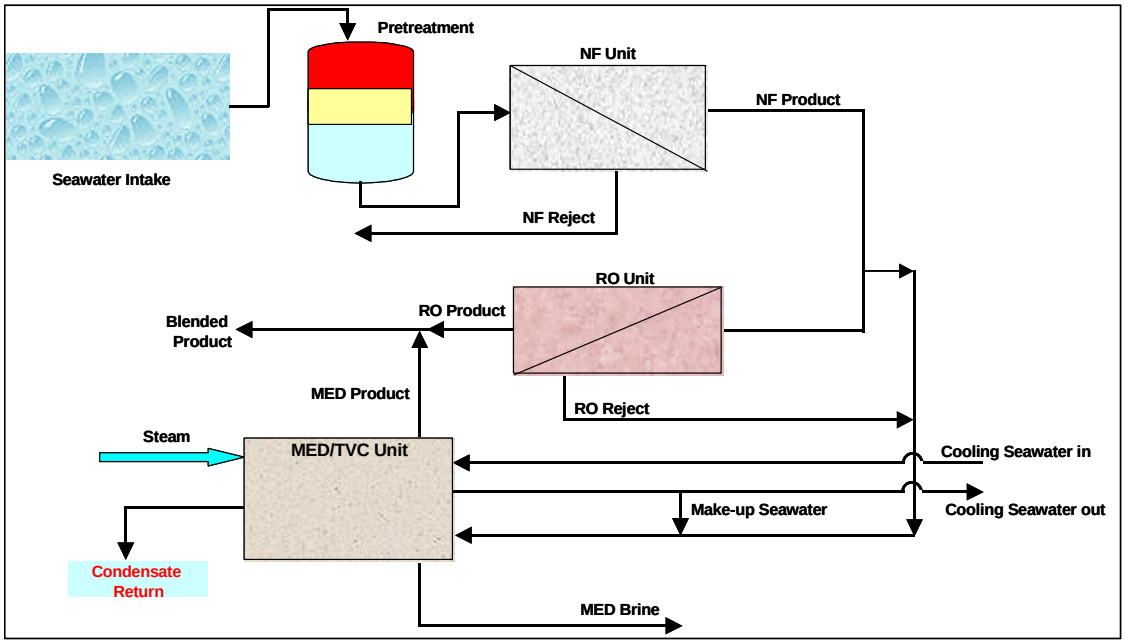

Figure 4.1 Schematic diagram of the tri-hybrid NF/RO/MED desalination system [53].

Exploratory experimental work was carried out on an MED/TVC pilot plant with a capacity of 24 m^3/d. The TBT of the MED/TVC was successfully increased in a stepwise manner from 65 ^{o}C to 125 ^{o}C using a make-up of NF permeate, without any scaling problems in a total operating period of 721 hours [53]. This study demonstrates the operation of the MED/TVC plant at elevated top brine temperature without concern for sulphate scaling on pilot plant.

Similarly, the NF–RO process makes it feasible to produce high purity permeate from a single-stage RO process without the need for a second desalination stage. This process significantly improves the quality of permeate without the need for a second stage with brackish water RO membranes [45,46,52,54,56,59].

The idea of using nanofiltration as a pretreatment process for seawater desalination is under active development by two main groups: the Saline Water Conversion Corporation (SWCC) of Saudi Arabia and the Leading Edge Technologies Ltd (LET).

For the last 15 years research and development centre (R&DC) of the Saline Water Conversion Corporation (SWCC) – the Saudi government agency delegated to desalinate seawater for civic consumption recognised as the world largest single desalination

organisation over the last three decades – has been actively involved in developing the application of nanofiltration membranes in the desalination industry. Research work is done in order to examine the reliability of NF as a pretreatment for SWRO and thermal (MSF & MED) desalination units. This includes (only) filtration performance analysis of the most commercial NF membranes available (at that time).

In view of the positive and encouraging results obtained from a pilot plant, the dual NF-SWRO desalination system was utilised to convert an existing commercial two pass SWRO plant. This has been carried out at Umm-Lujj SWRO plant (west cost of KSA) in September 2000. The plant performance after the integration shows an increase in the total production by 42% while reduces the energy consumption (in terms of kWh/m^3) by 39% [46,58]. Plant assessment is provided in next section.

On the other side, the first commercial LET Nanofiltration System to increase capacity of existing (i.e. retrofitting) MSF plant from nominal 5 MIGD to 7.2 MIGD takes place at Layyah Power and Water Station (Emirate of Sharjah – UAE). This, over-40% increase in production capacity of MSF unit was a result of a two year demonstration and simulation program developed jointly with Sharjah Electricity and Water Authority (SEWA) [50]. Plant assessment is provided in next section.

1.2 Assessment of current NF application as a pretreatment for selected plants:

- **Umm-Lujj SWRO plant:**

As a result of Umm-Lujj plant modification, it is reasonable to acknowledge that a NF–RO process combination makes it feasible to produce drinkable high quality permeates from a single-stage RO process without the need for a second RO desalination stage.

A comparison between plant original and modified design is demonstrated as follows:

Umm-Lujj plant original 2 pass RO system design set as:

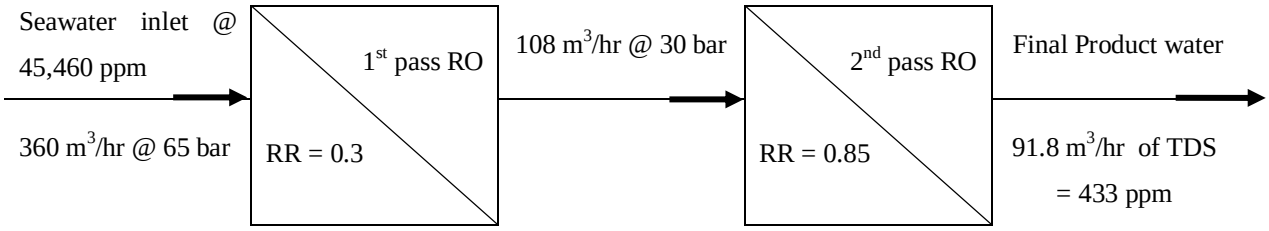

Plant RR = (1^{ST} pass RR) x (2^{ND} pass RR) = 0.3 x 0.85 = 0.255

Umm-Lujj SWRO plant modified (NF – RO) design set as:

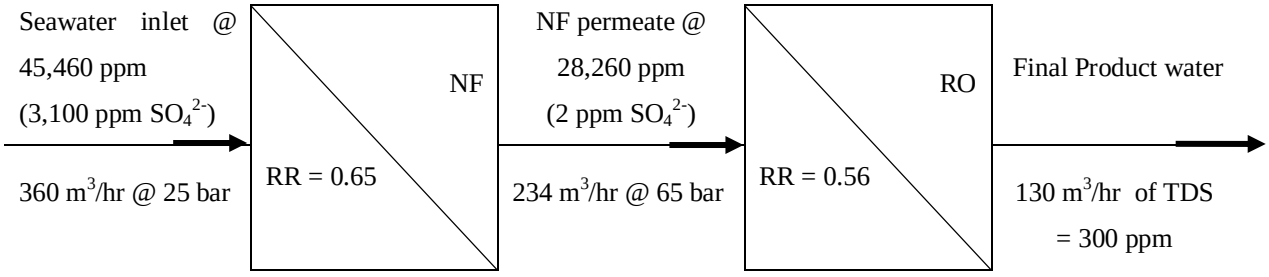

Plant RR = (NF – RR) x (RO – RR) = 0.65 x 0.56 = 0.364

The process improvements, because of introducing the NF pretreatment to Umm-Lujj SWRO plant (NF–RO) in comparison to the original design of two pass RO system operating with high seawater TDS and less than 35 percent recovery ratio and without energy recovery (the influence of energy recovery device is discussed in next page), are summarised as follows:

Comparison parameter	Original design (2 pass RO)	Modified design (NF-RO)	% of improvement
Product water quantity, m^3/hr	91.8	130	42%
Product water quality (TDS), ppm	433	300	30%
Energy consumption, kWh/m^3	9.59	5.85	39%
Plant overall recovery ratio RR	0.255	0.364	42%
Make up ratio MUR = RR^{-1} (ratio of raw seawater feed to be treated for each unit mass of final product water)	3.921	2.747	30%

Implementation of NF in Umm-Lujj SWRO plant improved the overall plant recovery ratio (RR) from 0.255 to 0.364, hence plant production has been increased by (0.364/0.255 = 1.427) 42.7%.

To this end, it has been shown from the (before and after) comparison, that when a nanofiltration unit was installed as a pretreatment for an existing reverse osmosis unit, it reflects significant improvements on the plant performance.

From an economic prospect, Umm-Lujj RO plant represents a case for which the operating costs were lower for NF-RO systems than for the original two pass RO system operating on the high TDS seawater with below 35 percent permeate recovery of the RO 1^{st} pass, and without energy recovery device.
As for any given product recovery, more energy is recovered (through energy recovery device) in a double pass RO system than in a NF-RO system [59].

In contrast with more modern single pass SWRO membranes available in the market a single pass RO can reach 45% recovery, equivalent to a MUR of 2.2. Hence, to this researcher's

knowledge, so far the economic feasibility of NF pretreatment for SWRO is debatable and only recommended in circumstances of higher recoveries to make the product water cost for a combined NF-RO plant compatible or more attractive. Such critical detailed economic feasibility study is provided elsewhere [59].

Moreover; a complication from the plant running cost as well as operation and maintenance point of view; as a result of dealing with two kinds of membranes (NF and RO), the consideration of the following aspects is necessary for both types of membranes: fouling treatments, cleaning, suppliers, membranes replacements and chemicals treatments.

In conclusion (as related to Umm-Lujj SWRO plant experience):

- It has been suggested [59] that NF as pretreatment for seawater RO systems is economical for cases where the RO unit encounter excessive membrane fouling (in particular hollow-fine-fiber RO elements) and gives a high permeate TDS.

- Recently, seawater desalination operators have realised that another way of making a benefit of the usage of NF as a pretreatment to SWRO is through NF–retrofitting. As NF–retrofitting pretreatment is cost effective compared to improving an existing pretreatment and/or adding a 2^{nd} pass RO unit for existing RO systems (that have fouling problem and a too-high product TDS).

- **Layyah MSF plant:**

As a result of upgrading MSF unit 9 of Layyah power plant in Sharjah UAE, by NF – retrofitting as a pretreatment, the output of the plant was increased from the designed capacity of 1010.5 t/hr at TBT of 105 ºC to an output of 1253 t/hr achieved when the TBT was increased to 117 ºC with conductivity of product at 454 μS /cm [50]. This is equivalent to 24% increase in plant output without any major modifications having been made to the plant. The use of NF membrane to soften the seawater feed to the MSF unit allows the increase in the top brine temperature TBT as a result of sulphate reduction from the feed from 2,650 to 48 ppm (i.e. 98% rejection) [13,50].

Although this particular practice of introducing NF to the existing MSF unit showed (at the early stage of the trial) promising results (see above paragraph) of increasing the plant production, the following problem has arise over time.

NF pretreatment require addition of acid to prevent alkaline scale ($CaCO_3$) formation on NF membrane. As a result of acid injection to the feed water, large quantity of CO_2 is being released. It is a must to remove the CO_2 produced as a result of acid addition to the seawater through a decarbonator before the feed is introduced to the MSF unit. Otherwise, the venting system will be overloaded by CO_2 and will not work efficiently as a result of CO_2 release in the high temperature stages and cause irreversible damage and corrosion in the stages.
In this particular plant, as its original design to be operated on chemical additives as a pretreatment to feed water, it has been switched to acid injection as a result of increasing the TBT because of the introduction of NF. This is due to the fact that the available chemicals for seawater pretreatment for alkaline scale prevention (e.g. $Mg(OH)_2$), is not technically capable to be operated at higher than 112 ^{0}C.

This has been done without the consideration of introducing decarbonator to get rid of the CO_2 as a consequence;

- Plant vacuum system has been overloaded.
- A gas blanket form on the condenser tubes affecting heat transfer mechanism.
- Corrosion at the vapour side of the early stages has taken place.

1.3 Conclusion:

This conclusion is based on the usage of NF as a pretreatment for sulphate rejection to prevent scale formation for opportunities and scopes for improvements in RO and thermal desalination technologies.

It can be concluded, from the present review, that the NF membranes performance as a pretreatment, especially its high ability for sulphate rejection, has been reflected in the improved performance of desalination units which received feed from NF permeate prior to sending it to either membrane or thermal desalination system.

Thus it appears that the use of a nanofiltration system has significant promise in a scale prevention technique. It can guarantees that the plants operating on such type of treated feed water by NF will not suffer (assuming optimum operating conditions) from the risk of calcium sulphate scaling.

This membrane if applied in thermal plants will allow operation at high operating temperature, with the benefits of increased production, and savings being potentially gained from such an operating mode.

On the other hand, NF pretreatment of seawater upstream of RO plants would improve the productivity of the desalination units by decreasing the scaling potential. Nonetheless, from an operational point of view, it is recommended that in order to make the NF pretreatment process very attractive, the entire process should be able to operate at the highest possible flux rate and recovery as well as lowest possible energy. Hence, an optimum flux and operating conditions are to be selected based on the input feed water quality.

It is a fact that the potential breakthrough in the productivity and economics of seawater desalination came with the realisation that the NF membrane application for sea water desalination pretreatment can remove almost all the feed water sulphate content which is the critical hard-scale forming agent. However, there are many different types of nanofiltration membranes available in the market for the target purpose. Moreover, the rejection of sulphate ion and permeate flux differs from one membrane to another (as proven in this research). This variation, especially in NF membranes filtration performance, is directly related to their properties, features and morphology (also proven in this work).

Finally, there appear to be real benefits obtained by utilising NF as pretreatment to conventional desalination technologies (whether SWRO or thermal type) for scale (more particularly – sulphate scale) control. Whereas, it is expected that the evolution and/or evaluation of NF, through critical characterisation research and analysis leading to better development; will continue to make the ultimate advantages of their usage in seawater desalination practices.

2. NF applications in oil and gas industry:

2.1 Overview:

Application of NF, for sulphate reduction from seawater prior to down-hole injection for enhanced oil recovery in offshore oil production, is nowadays a common practice [36]. This technique has been adopted to produce low sulphate seawater for water flooding in offshore oil fields. Sulphate in seawater is problematic due to its low solubility when coupled with barium and strontium salts in some oil reservoirs and due to the potential for bacteria to reduce sulphate to hydrogen sulphide within the reservoir. If sulphate scale takes place in the oil reservoir, productivity declines as a result, causing economic related expenses [62-65].

2.2 NF application assessments:

Seawater is widely used as an offshore injection fluid for pressure maintenance despite being recognised as having potentially value-eroding properties. The most widely recognised problem is scale formation from chemical incompatibility of the injected seawater (high sulphate) and the original formation brine (barium, strontium) [67]. In reservoirs which contain a substantial barium or strontium content, seawater injection will cause the naturally-occurring sulphate contained in the seawater to precipitate with the barium and/or strontium, and can eventually diminish the output of the production wells. Also, sulphate reducing bacteria in some reservoirs can feed on sulphate in seawater, thereby producing hydrogen sulphite and ‘souring’ the well or reservoir [68]. Due to the issues resulting from seawater injection, a mitigating trend in water flooding is the removal of sulphates from seawater to prevent souring and scaling, referred to as the sulphate removal process (SRP). This process involves de-sulphating the seawater using nanofiltration membranes while maintaining a high salinity [68-70] (as NF is not capable to separate monovalent ions – e.g. Na^+ – at high rejection rates). Both polymeric TFC and ceramic NF have been used, however, a very limited number of operators have used the ceramic type of NF due to its high price in comparison to the TFC membranes [69,70].

It has been reported by mid 2013 [71], that there are over 60 NF SRP systems in operation on offshore production facilities around the world. Thus the offshore industry is familiar with NF membrane usage for sulphate rejection application as its application is considered as routine.

However, a major challenge with offshore SRP systems utilising NF is the significant capital investment for platform space and weight which are required for installation. Moreover, recently, a study [70] concluded that not all the NF membranes could be used for such application (as a result of NF membranes performance variation in terms of water flux and sulphate rejection) to reach the demand for offshore oil production.

In a four-part article series [62-65], highlights sulphate scale problems in oil fields water injection operations, it was suggested that NF operations in such applications should be designed properly based on optimum membrane selectivity.

A number of previous investigations [62-70] have considered critical NF characterisation for the target application. The results showed that although the SO_4^{2-} rejection of all the NF membranes tested are always higher than 95%, however, different NF membranes have different properties (as proven in the current research work) and not all the NF membranes are suited for producing softened water for oilfield applications. Moreover;

- Each study has been designed (examining) water sample based on the local site seawater chemistry.
- It has been acknowledged, that achieving optimum oil recovery is a function of carefully choosing NF membrane.

Therefore, providing clear universal reference for NF membranes selection for optimum permeate flux and sulphate rejection (which has been devolved in this research work – check chapter 12) can customise water quality cost-effectively, thereby expanding the operator ability to enhance recovery.

2.3 Conclusion:

NF membranes have selective separation characteristic of divalent ions (more particularly sulphate content in seawater), therefore it is suitable for softening of seawater and providing permeate with excellent quality for oilfield water injection, in order to reduce the risk of sulphate scaling significantly. Furthermore, NF softening seawater has been used successfully in oil industry over years. However, there is a need for robust criteria, such as comparative flux and sulphate rejection, of selecting the optimum NF membrane.

Recently, it has been reported that manufacturers and suppliers companies of NF membranes pursue marketing strategies to the huge potential market of oil industry [72].

This imposes a need for NF characterisation and, to this researcher's knowledge not much research work has been reported extensively on the subject of optimum NF selection in oil fields based on critical NF characterisation for sulphate rejection.

Chapter 5: REVIEW OF NF CHARACTERISATION

1. Background:

Satisfying the growing demand for water in a sustainable way is a major challenge – and opportunity – for desalination community. This growth is not only driven by increased demand for desalinated water, but also due to technological developments that improved the reliability and decreased the cost of desalination.

Such technology is introducing NF to pretreat seawater and using its permeate as the feed inlet to the desalination plant and also, to partially desalinate seawater for oil and gas industry applications (see chapter 4).

However, this (relatively) new technology currently is under significant development. From desalination prospect as stated by R.S.Silver (1988) [73], "*when something new and useful begins, its initial rate of growth is like the results of seeding, proportional to the number sown*". Accordingly, since the second half of the 1990s, characterisation research on the general and wide range of applications of nanofiltration membranes was increased as shown in Figure 5.1.

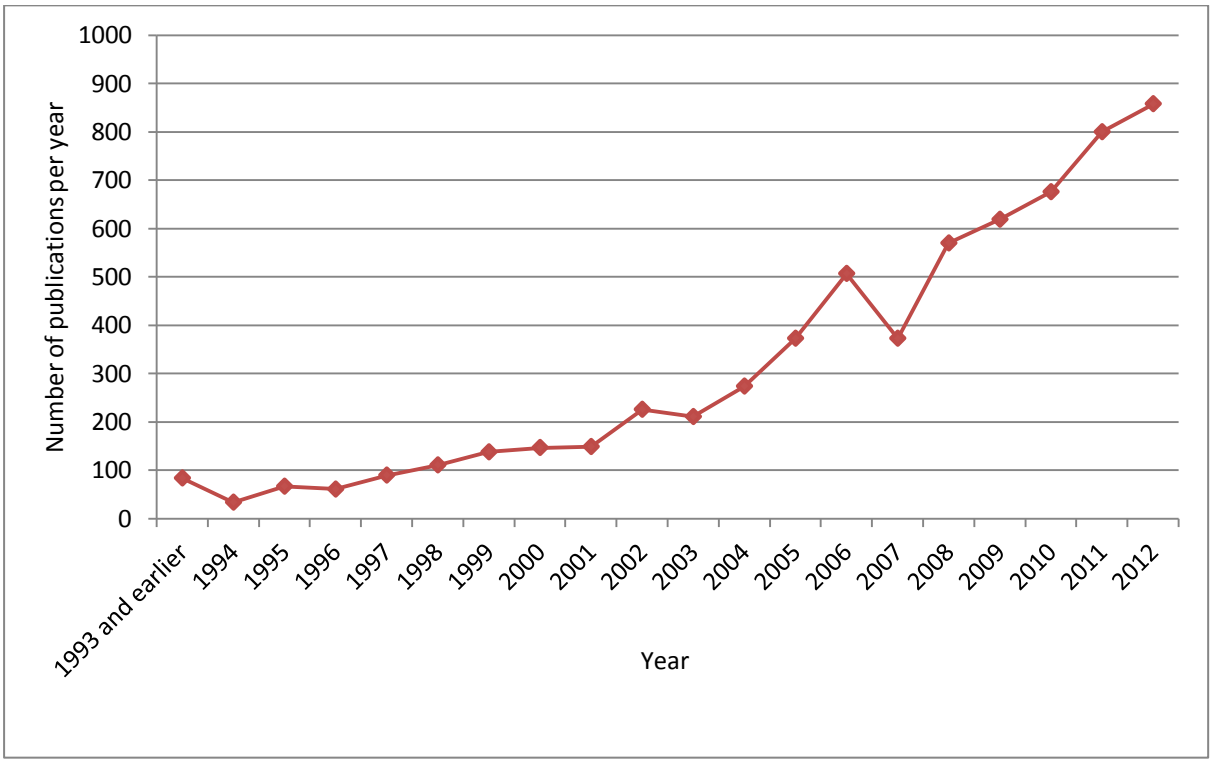

Figure 5.1 Research publications on NF membrane science and technology from mid 1990's until 2012 [sciencedirect.com & isiknowledge.com]

As a consequence, much is now known about the nature and performance of nanofiltration membranes in their range of applications. Nonetheless, it is to be expected that the evolution of NF (for desalination implementations in particular) will continue with research and development in the following areas:

1) Critically understanding NF performance, either by:

    I. Pilot testing (experimental data collection), or
    II. Modelling.
    III. Critical characterisation covering all physical and chemical aspects of NF to correlate such findings with performance behaviour.

2) NF membranes with controlled pore size.

3) Possibility of NF in hollow-fiber configuration.

4) Prediction and control of fouling.

5) Development of NF membrane material to achieve a specific application.

6) And for sea water desalination usage of NF as pretreatment, the major area of research and development is NF characterisation for optimum hybrid with thermal and/or RO processes.

2. NF characterisation:

2.1 Introduction:

NF membrane characterisation is obviously important in order to the critical understanding of transport mechanisms and performance. This aspect is illustrated by the extensive and continuous studies and proposals within the last 10 – 15 years [23,25,26,28,40,48,51,74-106,109]. This can be classified in two major directions according to approaches, namely: experimental methodology or modelling work.

2.2 NF characterisation by modelling:

An overview of the development of reliable predictive modelling technique, for NF characterisation can be summarised as follows.

Some researchers [40,74-84] have been trying to develop modelling techniques that might result in a smaller number of experiments and subsequently save time and money in the development stage of a process. This has been based on assuming that a good predictive model will allow improved correlation between NF membrane characteristics and process performance in order to optimise the usage of NF.

Most of the models have been established for specific conditions for a target purpose of NF application and validated using; simple salts solutions and assuming the permeate flux as an independent variable. Which contradict with the primary fact that NF permeate is dependent on the osmotic pressure at the membrane surface.

Moreover, most of the modelling works:

I. Did not consider the surface morphology for NF characterisation, which is agreed to be essential information.
II. Are based on uniform properties across NF membrane, whereas experimental work usually indicates some scatter in between samples of the same membrane.
III. Has shown to be limited in terms of correlating NF membrane filtration performance to membrane characteristics parameters.
IV. Membrane charges based on modelling are in contradiction with values from the literature obtained by measurements.
V. Researchers would suggest laboratory experiments to be carried out to confirm and validate the findings of the proposed model.

As a consequence, none of the existing models is valid for wide range of NF applications [81]. Therefore, it is concluded that NF membrane cannot be fully characterised by a number of controlling equations through modelling studies. Nevertheless, such research direction is important for the purpose of developing a suitable predictive model.

On the other hand, from an operation point of view for NF facilities, to develop a high level of confidence in order to provide feasibility of NF technological advances for seawater desalination, laboratory and pilot testing for NF filtration performance evaluation followed by critical characterisation analysis to correlate outcomes of such research work, is a crucial stages for several reasons:

I. To confirm technological viability.
II. Provide acceptable background information to optimise:
    - design criteria
    - operation parameters
III. Ensure a successful utilisation.

In addition, it has been reported, "because of the complex rejection behavior of NF membranes, it is difficult to accurately project performance of NF plants operating on natural waters. Therefore, pilot-plant testing is commonly used before building full-scale NF plants" [25]. Moreover, nanofiltration membrane performance in seawater desalination is an extremely difficult process to describe theoretically.

Finally, to this researcher's knowledge, the current scientific knowledge based only on computerised software modelling for NF membrane filtration performance in desalination applications is not sufficient to fulfil the industrial requirements for optimum integration with other desalination technologies, such as MSF.

2.3 NF characterisation by experimental methodology:

A reasonable volume of literature on NF characterisation is available through experimental procedures to explain and control membranes performance for a process and/or in membrane enhancement studies [23,28,48,51,85-106] targeting interpretation of NF membrane characteristic(s) to its performance towards water productivity and rejection ability. This involves the study of the physical and/or chemical interactions between the solutes and the membrane interface.

Contact angle measurements leading to surface free energy calculations, surface roughness quantifications, and NF charge determinations are three characterisation methods that appear to be recommended as the physics behind the equations describing these techniques consider relatively understandable.

A review over the focus of these research and studies can be outlined as follows.

The separation mechanisms of NF membranes can be attributed to:

1. The transport mechanisms.
2. Pore size.
3. Surface morphology.
4. Charge effects

Identifying and relating the membrane performance with the characteristics of the above mentioned parameters has shown [102,106] that they are complex and not completely understood, in terms of selecting a membrane for a particular application.

At present, NF membranes are commonly characterised in terms of:

1. Primary characterisation of NF filtration performance for the evaluation of flux and rejection data for model water.
2. Contact angle that is formed when a droplet of either water or air (depending on the technique used) is placed on the membrane surface is used to identify the wettability criteria and to quantify the hydrophobicity/hydrophilicity of the membrane surface.
3. Calculations of NF surface free energy (SFE) values as a consequence of contact angle measurements made using three distinctive measuring liquids.
4. Atomic force microscopy is used to both quantify and visualise the roughness of membrane surfaces.
5. Streaming potential measurements are used as an indicator of NF effective charge.

While other characteristics may be measured for membrane surfaces this list is the most adopted approach for NF membranes researchers and manufacturers.

It is worth mentioning that each of those characterisation protocols has more than a single approach. Moreover, recently it has been reported that despite the wealth of information that may be derived from the aforementioned surface characterisation techniques a standard method for applying these techniques to membrane surfaces is lacking [104].

In this section of the thesis, a general demonstration of the usefulness and development of those techniques, in order to obtain more accurate characteristics of NF membrane, is provided. However, for the techniques used in this research study, the justification and detailed features will be presented at the introduction of the dedicated chapters devoted of each method.

2.4 Correlation between membrane properties and membrane filtration performance:

Whilst membrane properties have a great influence on its corresponding performance, those property characteristics should be capable of describing the observed behaviour of the different membranes under uniform testing conditions. However, more data are required to improve the confidence in correlations in order to state whether relying on NF permeation and rejection information can be used as quantitative methods in order to state the reliability of NF choice.

In term of the correlation of the membrane performance and its characteristics, it would be useful to construct an envelope of the variance in NF membrane filtration performance (permeate flux and sulphate rejection) data, to the membrane properties. This is a core objective of the current study work (which has been achieved – please check chapter 12).

2.5 Development of NF membrane surfaces characterisation techniques [91,99,100,101,104]:

The following comments are made regarding the development and application of standard techniques for characterising NF surfaces:

1) Contact angle measurements that enable the calculation of membrane surface free energy and all its constituents.

   A reasonable amount of past research works have evaluated contact angle measurements for characterising interfacial properties of NF membranes. Such measurements are usually followed by the calculations of membrane surface energy properties such as the apolar (van der Waals) and polar (acid–base) components, as a result of contact angle measurements using polar and apolar liquids.

   Using captive bubble method produces reliable contact angle results for NF membrane surfaces.

In other words, the procedure involves measurement of the contact angle (e.g. by captive bubble technique) followed by calculation of the surface free energy and all its constituents. To assess the membrane wettability behaviour and its hydrophilicity nature.

2) Surface roughness

Surface roughness measurements using the AFM technique is justified for membrane surface morphology, however, it very dependent on the standard technique to be utilised. NF average surface roughness measured by AFM is commonly used for drawing correlation between membrane surface morphology and membrane performance. Although AFM is widely used to characterise NF membranes, it is very difficult to compare different measurements. In the literature one finds roughness values obtained by several modes of AFM (mentioned or not), determined for different scan areas (mentioned or not) [156].

3) Charge density

The standard method for determining the zeta potential of NF surfaces using streaming potential measurements by electro-kinetic analyser produces measurements of NF charge along the surface. This method is more relevant to NF characterisations towards scale tendency studies. Moreover, considerable deviations can occur in the final results from the differences in samples treatments and equipment operation conditions. To better understand the influence of NF charge on rejection studies and the findings, it is preferable to consider the charge through the membrane by measuring the membrane potential, hence, calculating the charge density (which is the method used in this work).

As stated earlier, it is difficult to compare the obtained results of the NF characterisation in the literature because the membrane characteristics have not been established in the same comparable testing conditions. This disparity does not allow for equal comparison of relative assessments of NF surfaces.

- An example of the variations on the reported values in the literature of the contact angle results of the same membrane (DOW NF 270) is illustrated in Table 5.1 below.

Contact angle (^{o})	22	27	39	43
Reference work	107	95	102	66

Table 5.1 Reported values of (DOW NF 270) contact angle

- An example of the variations on the reported values in the literature of NF surface roughness measured using AFM of the same membrane (DOW NF 90) is illustrated in Table 5.2 below.

AFM Surface roughness result	57.6 (average surface roughness, nm)	69.9 (mean roughness, nm)	90.0 (Root-mean-square roughness, nm)	129.5 ±23.4 (Root-mean-square roughness, nm)
Reference work	97	108	51	66

Table 5.2 Reported values of (DOW NF 90) surface roughness

Tables 5.(2 and 3) indicates clearly how inconsistent such results for NF characteristics in the literature.

Moreover, membrane manufacturers sometimes give information about the membrane sign of charge without evidence. This results in contradictions in the literature, where some researchers base the charge on some experimental results which seem to disagree with manufacturers (private) data. NF (UTC-20) membrane is an example where the manufacturer (Toray Industries) declares that the membrane carries a positive charge at a working pH in the range of 6–8 (for continuous use) without further specifications. However, in the literature, the charge of the UTC-20 NF membrane has been reported to be negatively charged, having a zeta potential (= - 9.5 mV) at (pH = 7) in 0.01 M KCl [168].

Hence, it is very difficult to derive usable information from such studies and researches for the purpose of NF selection for a target application. It is therefore of a paramount importance to standardise characterisation methods of contact angle, AFM measurements and membrane charge quantification for a range of commercially NF membranes for sulphate rejection applications.

2.6 NF characterisation for sulphate rejection:

Seawater is characterised by having high sulphate content (see chapter 2). This property gives rise to a major problem of sulphate scaling in seawater desalination plants and offshore oil/gas operations. NF is one way of solving this problem (see chapter 4)

In the literature, most of the studies that have been undertaken to characterise NF for such application focuses on the determination of NF filtration performance, i.e. permeation and rejection.

The problem is that these previous researches have been carried out in a number of different solutions, i.e. there is no universal reference for the comparison of the differences in their properties and their relation to membrane characteristics.

Another crucial aspect is the need, when comparing different filtration performance from various membranes, to correlate such performance data with membrane characteristics.

For example, two investigations [80,109] featured the same nanofiltration membrane (DOW NF 90) however, the reported performance values varied as a result of different feed water chemistry and testing conditions, as follow:

Reference work	Experimental Protocol	Filtration Performance
80	Cross flow filtration set up, for feed water of 5000 ppm $NaSO_4$, at 9 bar and ambient temperature	98 % rejection, water permeability = 20 $L/m^2.hr$
109	Dead end module filtration, for feed water of 20 ppm $NaSO_4$, at 20 bar and ambient temperature	93 % rejection, water permeability = 2.8 $L/m^2.hr.bar$

Moreover, these two studies [80,109] did not employ a comprehensive examination of NF surface characteristics, although, one of the studies [109] evaluated membrane porosity, however, separation performance for NF membranes does not depend solely on pore size.

Thus, information obtained from studies based on permeation and rejection data only, is of limited use without the means of relating such data to membrane characterisation

In this regard, to this researcher's knowledge, no studies exist on the characterisation of a series of commercial NF membranes of different manufactures/suppliers to be used for the pretreatment of seawater in desalination processes and offshore oil/gas applications for sulphate rejection.

3. Conclusions:

Despite benefiting from the technological development in NF research towards desalination implementations, optimisation of nanofiltration membranes to achieve a specified performance remains a challenging research goal for membrane technology.
Commercially available NF membranes have various filtration performances (see next chapter 6). Moreover, as a consequence in the differences of their manufacture, they have different characteristics. Previous studies [25,26,48,51] have shown that for the specific application of NF in desalination pretreatment, a proper selection of NF membrane properties can result in improved performance and a lowering of operating cost.

Accordingly, a thorough understanding of the interrelation between NF membrane filtration performance and its characteristics is of paramount importance in membrane research.
Laboratory experimental data for water flux and rejection ability in conjunction with advanced scientific characterisation techniques over a range of commercially NF membranes can be used to establish optimum membrane properties, best performance in terms of retention and permeation, optimise NF application process, and also assess the economic viability of the process.
In other words, a critical characterisation of NF membranes should make a significant contribution towards more efficient implementation of the membrane in terms of filtration performance and economics of nanofiltration technology as a seawater desalination pretreatment step for RO and thermal processes.

The overall objective of this project is to use a comprehensive approach for standardising NF characterisation and to quantitatively evaluate the combined effects of membrane properties on filtration performance. The surface properties of NF membranes that can have an enormous affect on its filtration performance are: porosity, wettability, hydrophobicity/hydrophilicity, surface roughness and NF charge.
Therefore, it will be important to investigate all aspects of membrane active surface characterisation, including contact angle, surface roughness and streaming potential with regard to sulphate rejection applications in desalination practices.

By developing the most appropriate techniques for assessment of NF for the target purpose with a major aspect of this being the development of appropriate envelope for membrane selection database.

Chapter 6: MATERIALS AND METHODOLOGY

1. Materials:

Eight commercially available nanofiltration membranes were used in this study. Identified simply as: A, B, C, D, E, F, G and H (for the reason of signing a non disclosure agreement NDA) supplied by the membrane manufacturers. All are:

- Typical nanofiltration membrane with applications in the drinking water production.
- Made via the process of interfacial polymerisation.
- Negatively charged (at typical seawater environments).
- Of cross linked Thin-Film Composite TFC NF type. This is a composite membrane since it is manufactured with two layers of different polymers. Its active layer has an asymmetrical structure made out of:

A	Polyamide Composite
B	Polyamide Composite
C	Polyamide Composite
D	Polyamide Composite
E	Polyamide Composite
F	Semi aromatic Polyamide Composite
G	Polypiperazine amide Composite
H	Polyamide Composite

- The thin film membrane of very low thickness is deposited on a macro-porous support by means of a polysulfone flexible layer to confer a mechanical resistance.
- Of spiral wound configuration module type.

NF (B – G) membranes have been delivered as a flat sheet form as shown in Figure 6.1, bagged and sealed in a robust plastic bag. They have been kept in their sealed bag until they were used.

Figure 6.1 NF membrane sheet.

While NF A membrane was supplied in the final product form (see Figure 6.2), i.e. in the form of spiral wound assembly.

Figure 6.2 NF A membrane as delivered, covered by FRP

Table 6.1 lists all NF membranes recommended areas of applications and performance specifications according to the brochures provided by the manufacturer.

NF membrane	Information parameters						
	Area of applications	Performance specifications					
		Salt rejection %	Permeate flux	Testing conditions			
				Pressure, bar	Temperature, ^{O}C	Feed chemistry	Recovery
A	High hardness rejection for brackish and seawater softening applications.	55 % NaCl	4.5 m^3/day per single 8 inches element of 75 ft^2	3.5	25	500 mg/l NaCl	Brine flow rate 20 l/min
B	Provides optimum hardness rejection for softening applications.	84.0 – 95.7 % $CaCl_2$	6.59 m^3/day per single 8 inches element of 400 ft^2	5.2	25	500 mg/l $CaCl_2$	15%
C	High rejection of natural organic materials and moderate rejection of total hardness.	73.0 – 92.0 % $CaCl_2$	39.70 m^3/day per single 8 inches element of 400 ft^2				
D	Provides optimum hardness rejection for softening applications.	84.0 – 95.7 % $CaCl_2$	31.04 m^3/day per single 8 inches element of 400 ft^2				

E	Designed to remove a high percentage of salts, nitrate, iron and organic compounds.	85% NaCl	28.4 m^3/day per single 8 inches element of 400 ft^2	4.8	25	2000 mg/l NaCl	15%
F	Designed to remove a high percentage of TOC and THM precursors and hardness ions, while having a medium univalent salts passage.	97% $MgSO_4$	47.3 m^3/day per single 8 inches element of 400 ft^2	4.8	25	2000 mg/l $MgSO_4$	15%
G	Designed to reject multivalent salts, passing monovalent salts. Used in a variety of applications such as desalting hardness ions.	98% $MgSO_4$	51.9 m^3/day per single 8 inches element of 400 ft^2	8.9	25	2000 mg/l $MgSO_4$	15%
H	Separation of higher molecular weight components (>200 dalton) and multivalent ions from various feed solutions.	99.3% $MgSO_4$	5.6 m^3/day per single 4 inches of 85 ft^2	6.5	25	5000 mg/l $MgSO_4$	15%

- **Comments:**

1. Although all eight membranes are designed for water treatment applications, more particularly for seawater hardness contents rejection such as sulphate, however, NF C is mainly designed for organic materials rejection. It has been introduced to this study to investigate the differences in performance as a result of different manufacturing, processing, area of applications and characteristics conditions.

2. NF A and E are characterised in terms of salt rejection on a univalent solution, whereas all other NF membranes are characterised (perhaps more appropriately) in divalent ions.

3. Noting the difference in testing standards, this illustrates the difficulty in assessing much of the data especially permeability and rejection as different membrane manufacturers tend to quote the performance of their product(s) under different test conditions. Therefore no clear comparison can be done.

4. All membrane producers typically declare two points:

    - The permeability of modules with a tolerance of ± 15–20% of the nominal reported value in the data sheet.

    - For the same manufacturer of more than one commercial NF membranes product, they usually quote "Although the membranes are made via the process of interfacial polymerisation, they differ in performance because of different processing conditions".

Table 6.1 Specifications of the NF membranes under study

2. Research protocol:

The adopted approach of this research has been designed to meet the research main goal to describe NF membranes performance and mechanisms in seawater desalination practices for sulphate rejection applications. The intention is to represent a correlation between membrane filtration performance and all related physical and chemical features parameters of the membrane, to develop a fundamental understanding and a quantification of these important phenomena on membrane functioning.

Two main phases to evaluate the NF membranes are set to be:

1. Phase one: assessing the eight different commercial NF membranes filtration performance in terms of permeation and sulphate rejection under uniform testing environments features to tolerate the ASTM D4194-03 Standard Test Methods for Operating Characteristics of Reverse Osmosis and Nanofiltration Devices [42] with some forethought differences in further experiments to formalise the objectives of this particular project (this is detailed in the next chapter 7).

2. Phase two: assessing the mechanism of sulphate separation process in relation to the measured NF membrane flux and (SO_4^{2-}) ion rejection (evaluated in phase one) using NF characterisation methods.

Therefore, the outcomes of this work are expected to provide a firm fundamental knowledge and clearer understanding of NF membranes performance, a systematic process for membrane selection of the target application and the optimum operating parameters (for long-term membrane operation) and thereby to provide a basis for the optimum usage of NF membrane for the sulphate removal in desalination plants and oil/gas applications to increase productivity.

3. **Techniques:** (the following list provides the used techniques, however, the detailed experimental and calculation procedures and the critical review of each are provided at the introduction of each chapter of the named technique).

In this research work, the use of multi characteristic techniques, measurement protocols and testing methods have been adopted in order to achieve the research objectives summarised in chapter 1.

The following techniques are used for the purpose of this research:

1. Uniform experimental examination for the potential of the eight different commercial nanofiltration (NF) membranes for SO_4^{2-} separation, through measuring permeation and rejection ability.

   Three sets of experiments carried out for each membrane.

   1.1. First set of experiments examined the membranes rejection and product flow under typical ASTM testing standards, simulated seawater environment and measuring the flux for pure water.

   1.2. Second and third set of experiments involved investigations of the important influences of varying operational parameters - in particular feed water pressure and temperature. This has been done by keeping all the operational parameters constant and varying only one parameter: either the pressure or the temperature at typical ASTM solution.
2. Contact angle measurement investigated to accurately characterise NF membranes surface hydrophilicity and leading to surface free energy calculations as determined from the contact angle data. The surface free energy component of three liquids (water, ethylene glycol and diiodomethane) was studied.
3. Atomic Force Microscopy AFM studies for surface roughness determinations.
4. Membrane potential measurement, leading to charge density calculations of the NF membrane.
5. All the data obtained from these techniques is used to correlate and understand variations in flux and sulphate rejection among tested membranes.

It is considered [99,100,104] that NF characterisation results of contact angle measurements (leading to surface energy calculations), surface roughness quantifications using AFM, and membrane potential measurements (leading to membrane charge density calculations), from

the perspective of utilities (operation), are of greatest use during the membrane selection phase of a project since their influence on plant performance can be overcome by operational factors such as membrane fouling. In this regard membrane characteristics parameters determination has been carried out on virgin membrane samples.

The following Table 6.2 summarise the characterisation methods that have been adopted to meet the research objectives for NF membranes in this study in order to provide the desired correlation between filtration performance data of phase one with characterisation parameters obtained from phase two.

Work phase number	Investigated NF Membrane parameters		Characteristic method	*Measuring technique*
One	1. Filtration performance		Permeate flux and sulphate rejection measurements	Laboratory bench-scale dead-end flow experimental rig.
Two	2. NF characteristics:	2.1. Porosity	Porosity Factor	Calculated from pure water permeation data
		2.2 NF active surface morphology: ➢ Wettability and hydrophilicity/hydrophobicity nature	I. Contact Angle II. Total Surface Free Energy	Captive bubble Calculated of contact angle measurements
		➢ Roughness	Quantitative and imaging NF surface average roughness	Atomic Force Microscopy AFM
		2.3. NF Charge	Averaged charge density	Calculated from Trans Membrane Streaming potential TMS measurements

Table 6.2 Summary of the research adopted approaches and techniques

Chapter 7: NF MEMBRANES FILTRATION PERFORMANCE EVALUATION

1. Introduction:

1.1 Overview:

The aim of this part of the research is to measure the sulphate separation performance of the membranes under study for seawater desalination and oil/gas industry assessments. Covering two main categories;

I. The parameters which characterise the performance of a membrane are the water permeability (water flux) and the solute permeability (sulphate rejection).
II. Pore characteristics (chapter 8).

The key to utilising the most appropriate NF membrane for particular application is the selection of a membrane with the optimum sulphate rejection and permeate flow rate characteristics under certain uniform operating parameters. These factors are directly related to the membrane permeate quantity in terms of flow rate, and quality in terms of sulphate rejection.

Therefore, the major point of interest at this stage of this research is targeting an intensive detailed characterisation for the NF membranes under study. To assess and compare all under uniform testing environments for sulphate rejection for the prevention of sulphate scale formation in sea water desalination plants. The examination of the eight commercial nanofiltration membranes supplied by the membrane manufacturers used a laboratory scale membrane rig – at Glasgow University; Mechanical Engineering Department – according to ASTM D4194-03 Standard Test Methods for Operating Characteristics of Reverse Osmosis and Nanofiltration Devices [42].

Additional investigations involved the important practical effect of the feed water temperature and pressure increases on the membrane behaviour in terms of permeate quantity and its sulphate content (i.e. rejection).

1.2 Review of the development of NF membrane filtration performance testing protocols [99,104]:

Membrane flux and rejection are measured in a laboratory environment using either:

- Dead End Flow (DEF) cell(s),
- or a cross flow unit.

In cross flow filtration, feed moves parallel to the membrane to generate shear stress to scour the surface. This operational mode is particularly effective when feed water carries high level of foulants such as suspended solids and macromolecules.

In dead-end filtration, no cross flow exits and feed moves toward the membrane. All the particles that can be filtered by the membrane settle on its surface. This mode of operation is particularly effective when feed water carries low level of suspended solids. Many surface water filtrations, pretreatment for SWRO, and tertiary filtrations are adapting dead-end modes.

In comparison, the benefits of DEF are relatively quick processing times, minimal equipment and feed water requirements and potential for longer membrane usage. While, the benefit of using cross flow filtration is better control of concentration polarisation.
However, the cross flow technique requires significantly more ancillary equipment as well as larger amounts of feed water compared to the DEF technique.
For NF membranes performance evaluation in terms of permeate flow and ions rejection, it has been reported [99], there is no difference in permeate quality or flux decline between the cross flow and DEF experiments. Also, for cross flow filtration, some reports and comments from practitioners [110], suggest that test results are subject to measurement errors attributed to different test conditions in test cells and modules, such as much higher or lower Reynolds numbers for cross flow filtration.

The filtration performance of the NF membranes under current investigation is determined using the dead end flow approach because:

1. It complies with the objective of this research to standardise select NF membrane based on characterisation methods and to quantitatively evaluate the combined effects of select membrane properties on membrane performance.
2. The available membrane test unit is adopting this mode of operation.

2. Experimental procedure:

2.1 Testing solutions:

In order to critically compare NF membrane performance towards permeate and sulphate rejection ability, a range of testing solutions have been chosen to meet the objective of building up information on a number of binary and multiple ion systems. This primary characterisation includes the evaluation of permeate flux and sulphate rejection in the following environments:

1. ASTM solution (2 gm/l $MgSO_4$) [42]. To provide universal reference to compare the performance of the available NF membranes under constant operational conditions.
2. Simulated seawater (35 gm/l NaCl + 2 gm/l $MgSO_4$). As for mixed electrolytes solutions, some questions still exist for traditional models to evaluate the separation performance of NF membranes since rejection to ions is different from that in the single salt solution as a result of the attractive and repulsive forces among ions [99,100].
3. Pure distilled water. This was employed in order to assess membrane flux which is controlled by hydraulic permeability, the thickness of the membrane layer, available membrane surface area and the trans-membrane pressure. Moreover, enabled the calculation of the porosity factor of each NF membrane.

2.2 The Test Rig:

As shown in Figure 7.1, the experimental rig consists of six identical test cells (Figure 7.3), each hosting a single nanofiltration membrane sample of 5 cm in diameter. The cells are supplied with the pressurised testing solution from the main temperature-regulated reservoir via a low pressure (LP) and high pressure (HP) pumps in series. The three-way manual control valve, on the output of the HP pump, regulates the inlet flow and thereby the inlet pressure to the HP manifold. The HP manifold pressure is regulated to the individual test cell via adjustment of their individual associated manual inlet and outlet valves. The rejected concentrate (brine) from the NF modules flows back into the reservoir tank via each NF modules' associated outlet valves and brine flow meters. The filtered permeate is collected from each individual test cell in pre-calibrated burettes.

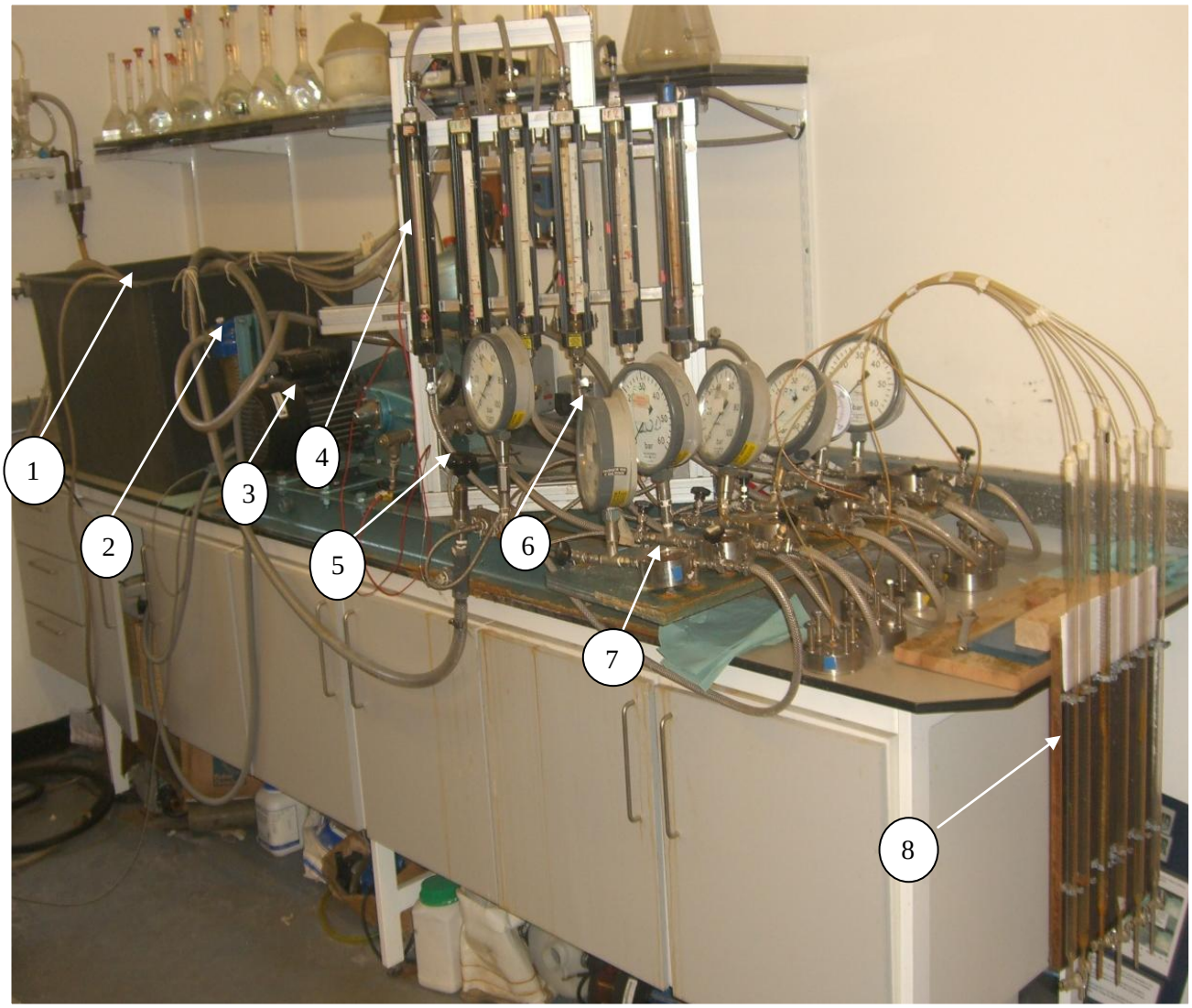

1	Main reservoir	5	Inlet feed pressure regulator
2	5-micron-suction filter	6	Cell inlet feed pressure gage
3	High pressure pump (HP)	7	Cell
4	Brine reject flow meter	8	Permeate burette

Figure 7.1 Experimental rig main components.

2.2.1 Process flow and control:

As shown in Figure 7.1 the system starts with the main tank (reservoir) made of fibre glass with a maximum capacity of 250 litres. Two temperature control devices are available, cooling coils supplied by tap water and an electrical heating element. Both are provided to adjust the feed water temperature according to the desirable set point. A temperature sensor is provided to measure the water temperature.

The suction hose, pressure regulator return hose and the brine reject lines are collected in the tank. Thus, it can be said that the system is a close circuit.

Water will be sucked by the low pressure (LP) centrifugal pump through the 5 micron suction filter to ensure a clean (free of any suspended particles) water. Then water will be discharged from the (LP) pump to be sucked by the high pressure reciprocating positive-displacement pump (HP) pump, driven by a 2.2 kW motor. The HP pump is capable to produce a pressure up to 85 bar.

The desirable pressure can be adjusted by the pressure regulator (as shown on the left hand side of Figure 7.2) setting in between the HP pump discharge line and the cells inlet isolating valves. Water will pass to a distribution chamber (as shown in the right hand side of Figure 7.2) to be introduced to each cell individually by the inlet hose.

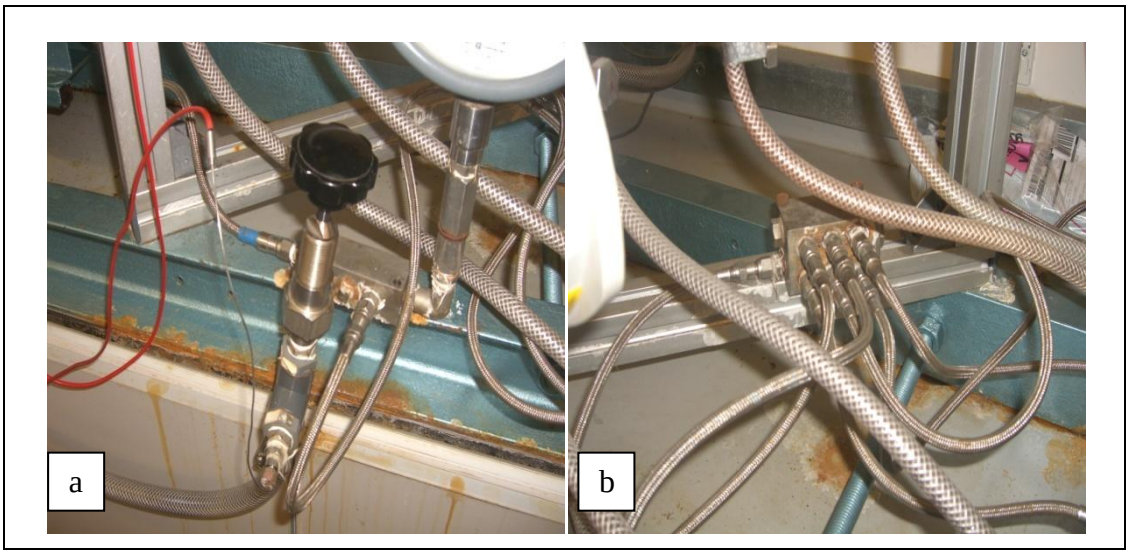

Figure 7.2 a) Inlet feed pressure regulator , b) Cells inlet feed water distributor.

2.2.2 Cells section:

Six identical cells each consisting of: inlet isolating valve, inlet feed water pressure gauge, lower and upper blocks tightened together by four screws, baffled rubber base, two o-rings, ceramic plate, permeate outlet hose, brine reject hose, outlet isolating valve and permeate burette are shown in Figure 7.3.

Feed water will pass the inlet valve which will be throttled to maintain the experiment pressure set point as the pressure after the pressure regulator is usually kept slightly higher than the experiment main pressure set point to overcome the losses in the system.

Water will enter the cell going upwards to the baffled rubber base facing the active side of the membrane. Thus, it is important to ensure that the membrane is set properly in the cell to avoid any experimental errors.

Part of the feed water will pass through the membrane flowing upwards through the ceramic support plate to leave the cell upper block going into the outlet hose (permeate). The remaining portion will leave the lower block through the outlet isolating valve which is used to control the brine flow according to the experiment set point. This brine will be discharged back to the main reservoir.

Permeate will be collected in the burette to be measured when the reading time is set.

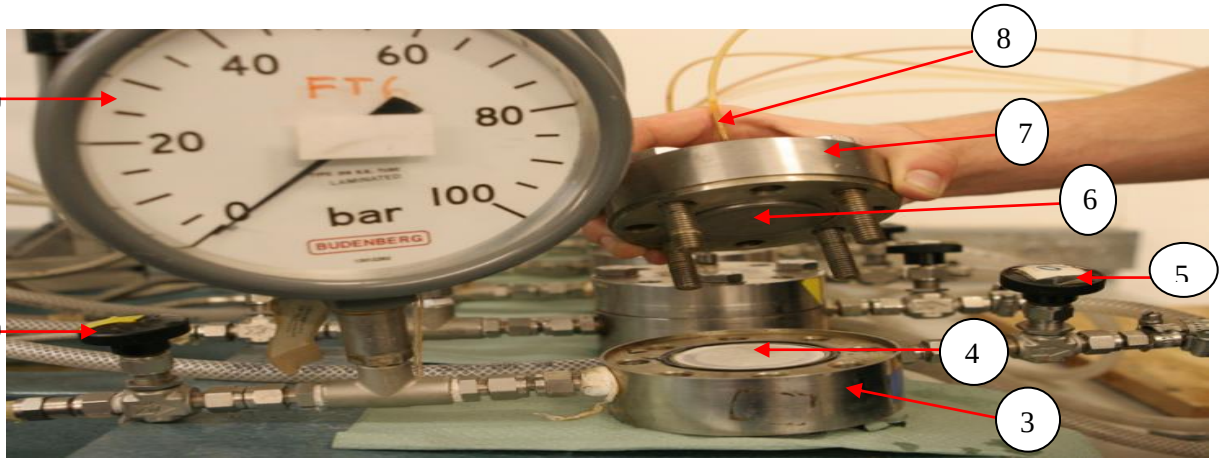

1	Inlet feed water pressure gauge meter	5	Brine reject isolating valve
2	Inlet feed water isolating valve	6	Permeable ceramic support plate
3	Cell lower block	7	Cell upper block
4	NF membrane sample	8	Permeate outlet hose

Figure 7.3 Individual cell main components.

2.3 Experiments main features:

2.3.1 ASTM experiments:

Each NF membrane was subjected to three main categories of ASTM experiments. Those three main experiments are designed to apply the ASTM standards with some differences during experiments II and III to formalise the objectives of this particular project. The details of the operational parameters of each are as follow:

- ASTM Experiment I, (Exp.I) – steady state:

This experiment is a typical ASTM test method. I.e. all the parameters are constant during the full running hours of the experimental work. Its main objective is to study the membrane performance; water flux and its sulphate rejection ability under steady state conditions.

Main features of Exp.I are:

Feed water concentration	= 2000 ppm $MgSO_4$
Feed water temperature	= 25 ^{0}C (±1)
Feed water pressure	= 9 bar
Brine rejection flow rate	= 1 litre/min.

- ASTM Experiment II, (Exp.II) –temperature factor-:

This experiment is designed to test the performance of the membrane permeability and sulphate rejection ability under various feed water temperatures. Thus, the inlet water temperature was not held constant but was allowed to rise as much as the system allows without exceeding the maximum allowable operating temperature of 45 ^{0}C recommended by manufacturers. All other factors were kept constant according to ASTM standards.

Main features of Exp.II are:

Feed water concentration	= 2000 ppm $MgSO_4$
Feed water temperature	= 19 – 35 ^{0}C
Feed water pressure	= 9 bar
Brine rejection flow rate	= 1 litre/min.

- ASTM Experiment III, (Exp.III) – pressure factor-:

This experiment is designed to test the effect of the increase in inlet feed water pressure on the membrane performance i.e. the permeate flow and sulphate rejection.
As Exp.I was carried out at 9 bar, thus, the first pressure set value for Exp.III was 15, followed by 20, then 25 bar.
So it can be divided into three sub-experiments as; Exp. III/1, Exp. III/2 and Exp. III/3, defined as experiment number three – pressure factor – at 15, 20 and 25 bar respectively.

Main features of Exp.III are:

Feed water concentration	= 2000 ppm $MgSO_4$
Feed water temperature	= 25 ^{0}C (±1)
Feed water pressure	= 9, 15, 20 & 25 bar
Brine rejection flow rate	= 1 litre/min.

2.3.2 Simulated seawater (SW) experiment:

In order to critically evaluate the water flux and sulphate rejection of NF membranes for an optimum characterisation when implemented in seawater desalination, it is of a paramount need to test them in similar water chemistry environment to determine:

1. How does the presence of sodium chloride affect NF sulphate rejection?
2. Whether the membrane will attain the same retention in comparison to ASTM test (where the solution compose of single salt of magnesium sulphate).

This experiment has been developed to simulate salinity concentrations level similar to those of seawater and at the same given operational parameters of ASTM.

Main features of SW Exp. are:

Feed water chemistry	= 2000 ppm $MgSO_4$ + 35,000 ppm NaCl
Feed water temperature	= 25 ^{0}C (±1)
Feed water pressure	= 9 bar
Brine rejection flow rate	= 1 litre/min.

2.3.3 Pure water (Distilled) experiment:

The membranes were characterised in terms of pure water permeability by measuring the pure water permeate flux as a function of feed pressure, to enable the calculation of:

- Pure water permeability constant (also known as; hydraulic permeability of pure water). Both parameters are often used in the literature to describe NF performance [95,102,109].
- Porosity factor as a representation of NF pore characteristics.

Main features of PW Exp. are:

Feed water chemistry	= Distilled water
Feed water temperature	= 25 ^{0}C (±1)
Feed water pressure	= 9 bar
Brine rejection flow rate	= 1 litre/min.

2.4 Experimental procedure:

Each experiment was conducted over 10 to 16 continuous operating hours depending on the experimental objective, and the settling time to reach desirable operating parameters.
Following the ASTM standards, the first reading took place after an hour when the entire experimental conditions had attained steady state i.e. the feed water temperature and pressure.

2.5 Measurements procedure:

2.5.1 Water flux:

The permeate (PW) was collected and measured in burettes marking scale in (ml/hr/cell), however, to match the standard dimensions in expressing NF performance, during results analysis, flux will be reported in L/hr.m^2 using the conversion equation of:

PW in:	mL	1 L		100^2 cm^2
	hr	1000 mL	NF sample area = 3.14 x $(5/2)^2$ cm^2	m^2

Therefore, the conversion factor is: PW in ($L/hr.m^2$) = PW in (mL/hr) x (0.509 $L/mL.m^2$).

2.5.2 Sulphate rejection determination:

The performance of NF membranes for sulphate retention characteristic is one of the most critical parameters in the current research phase. The ability of the NF membrane not to permit the sulphate ions to pass through has been calculated using the following equation:

$$\left(1 - \frac{amount\ of\ sulphate\ in\ the\ permeate\ (ppm)}{amount\ of\ sulphate\ in\ the\ feed\ (ppm)}\right) x\ 100$$

The amount of sulphate ions in feed water of both ASTM and SW tests is:

- feed water has 2000 ppm $MgSO_4$,having a molecular weight of (24.3 as Mg^{2+} + 96.1 as SO_4^{2-}) = 120.42,
- percentage of SO_4^{2-} = 96.1/120.42 = 0.798 = 79.8 % of the feed salt concentration,
- Thus, the amount of sulphate in the feed is 2000 x 0.798 = 1596 ppm,

Sulphate rejection percentage can be calculated as:

$$SO_4^{2-}Rej\ \% = \left(1 - \frac{amount\ of\ sulphate\ in\ the\ permeate\ (ppm)}{1596\ ppm}\right) x\ 100\%$$

The determination of sulphate content in the permeate has been measured as follows:

2.5.2.1 ASTM test:

Permeate conductivity measured using Hanna [HI-8633N] multi-range conductivity meter (0.1 to 199900 µS/cm), utilises four ring potentiometric probes that offer greater versatility along with temperature compensation. Then conductivity reading were converted to sulphate content using a calibration graphs produced from a series of standard solutions made up using magnesium sulphate salt $MgSO_4$ (detailed in Appendix 1).

2.5.2.2 Simulated seawater test:

Sulphate content in the permeate has been measured directly as ppm using Hanna Instruments [HI 96751] – sulphate portable photometer. That measures the sulphate content in water samples in the 0 to 150 mg/L (ppm) range, by sulphate precipitation with barium chloride crystals.

2.6 Sample preparation:

As detailed earlier in chapter 6, all tested NF membranes are of thin film composite TFC type of spiral wound configuration enclosed in a sealed plastic bag or fibre-reinforced plastic (FRP) containing a storage preservative solution. Hence, prior to performing experimental measurements on membranes as recommended by ASTM standards, the following steps were followed:

1. All membranes have been protected from direct sunlight and stored in a cool, dry laboratory with an ambient temperature range of 17 to 21 °C.
2. Two days before conducting experiments on a membrane. Samples from different parts of the NF membrane under study have been cut according to the cell fitting diameter of 5 cm. A hollow circular sharp punch (cutter) having an outside diameter of 5 cm was used to stamp out samples of the membrane. A mechanical press was used to provide equally distributed impact to produce a clean cut.
3. Followed by samples rinsing with distilled water, then stored completely immersed in distilled water 48 hours prior to experiment.

3. Results:

This part will provide the six cells average (in both permeate flow and sulphate rejection) of each experiment for each NF membrane, i.e. for each reading; the number illustrated in the tables shows the average of the six cells at the time of recording the data.

3.1 ASTM experiments results:

3.1.1 ASTM Exp.I (steady state test at 25 ^{0}C, 9 bar) results:

- NF membrane A

Reading number	Product water flow (L/hr.m^2)	SO_4^{2-} content in permeate (ppm)	SO_4^{2-} rejection %
1 (after 1 hr of reaching steady state)	34.10	29.68	98.14
2 (4 hrs after reading #1)	34.10	26.81	98.32
3 (4 hrs after reading #2)	34.10	27.29	98.29
AVG.	34.10	27.93	98.25

Table 7.1: NF membrane A data at ASTM Exp.I

- NF membrane B

Reading number	Product water flow (L/hr.m^2)	SO_4^{2-} content in permeate (ppm)	SO_4^{2-} rejection %
1 (after 1 hr of reaching steady state)	20.43	5.58	99.65
2 (4 hrs after reading #1)	20.40	5.58	99.65
3 (4 hrs after reading #2)	20.36	5.58	99.65
AVG.	20.40	5.58	99.65

Table 7.2: NF membrane B data at ASTM Exp.I

- NF membrane C

Reading number	Product water flow ($L/hr.m^2$)	SO_4^{2-} content in permeate (ppm)	SO_4^{2-} rejection %
1 (after 1 hr of reaching steady state)	26.48	103.74	93.50
2 (4 hrs after reading #1)	26.45	103.74	93.50
3 (4 hrs after reading #2)	26.55	102.14	93.60
AVG.	26.49	103.26	93.53

Table 7.3 NF membrane C data at ASTM Exp.I

- NF membrane D

Reading number	Product water flow ($L/hr.m^2$)	SO_4^{2-} content in permeate (ppm)	SO_4^{2-} rejection %
1 (after 1 hr of reaching steady state)	31.60	9.57	99.40
2 (4 hrs after reading #1)	31.60	9.89	99.38
3 (4 hrs after reading #2)	31.60	9.25	99.42
AVG.	31.60	9.57	99.40

Table 7.4: NF membrane D data at ASTM Exp.I

- NF membrane E

Reading number	Product water flow ($L/hr.m^2$)	SO_4^{2-} content in permeate (ppm)	SO_4^{2-} rejection %
1 (after 1 hr of reaching steady state)	18.30	5.10	99.68
2 (4 hrs after reading #1)	18.50	7.66	99.52
3 (4 hrs after reading #2)	18.30	6.38	99.60
AVG.	18.36	6.38	99.60

Table 7.5 NF membrane E data at ASTM Exp.I

- NF membrane F

Reading number	Product water flow ($L/hr.m^2$)	SO_4^{2-} content in permeate (ppm)	SO_4^{2-} rejection %
1 (after 1 hr of reaching steady state)	61.08	13.40	99.16
2 (4 hrs after reading #1)	60.97	13.24	99.17
3 (4 hrs after reading #2)	61.23	14.04	99.12
AVG.	61.09	13.56	99.15

Table 7.6 NF membrane F data at ASTM Exp.I

- NF membrane G

Reading number	Product water flow ($L/hr.m^2$)	SO_4^{2-} content in permeate (ppm)	SO_4^{2-} rejection %
1 (after 1 hr of reaching steady state)	29.40	14.50	99.09
2 (4 hrs after reading #1)	29.57	13.93	99.12
3 (4 hrs after reading #2)	29.53	13.69	99.14
AVG.	29.50	14.04	99.12

Table 7.7 NF membrane G data at ASTM Exp.I

- NF membrane H

Reading number	Product water flow ($L/hr.m^2$)	SO_4^{2-} content in permeate (ppm)	SO_4^{2-} rejection %
1 (after 1 hr of reaching steady state)	26.01	29.56	98.14
2 (4 hrs after reading #1)	25.58	31.11	98.05
3 (4 hrs after reading #2)	26.11	29.34	98.16
AVG.	25.90	30.0	98.12

Table 7.8 NF membrane H data at ASTM Exp.I

Statistical analysis:

Each experiment was performed on six cells of a commercial NF membrane. Each cell hosted a sample of 5 cm in diameter and had identical operating conditions. A set of readings were taken from the six cells after 1 hour of reaching experimental steady state (temperature and pressure). Then the second and third readings were taken after 4 and 8 hours of operation,

therefore 18 sets of readings could be attributed to each membrane. Sample standard deviations (for both measured parameters) were then calculated over each of the 18 values (detailed in Appendix 2). Table 7.9 lists the average permeate flux and sulphate rejection percentage with the standard deviation (*S*).

NF	Average Product water flow ($L/hr.m^2$)	Product water flow, standard deviation, *(S)*	Average SO_4^{2-} rejection %	SO_4^{2-} rejection %, standard deviation, *(S)*
A	34.10	0.4592	98.25	0.5383
B	20.40	0.4252	99.65	0.0377
C	26.49	0.7393	93.53	0.4443
D	31.60	0.0594	99.4	0.0801
E	18.36	0.2836	99.6	0.1312
F	61.09	0.7574	99.15	0.1147
G	29.50	0.8693	99.12	0.2089
H	25.90	0.8024	98.12	0.4996

Table 7.9 Standard deviation of flux and rejection of the NF membranes at ASTM test

Figure 7.4 shows plots of these results, error bars relate to two standard deviations, which correspond to a confidence limit of 95.45%.

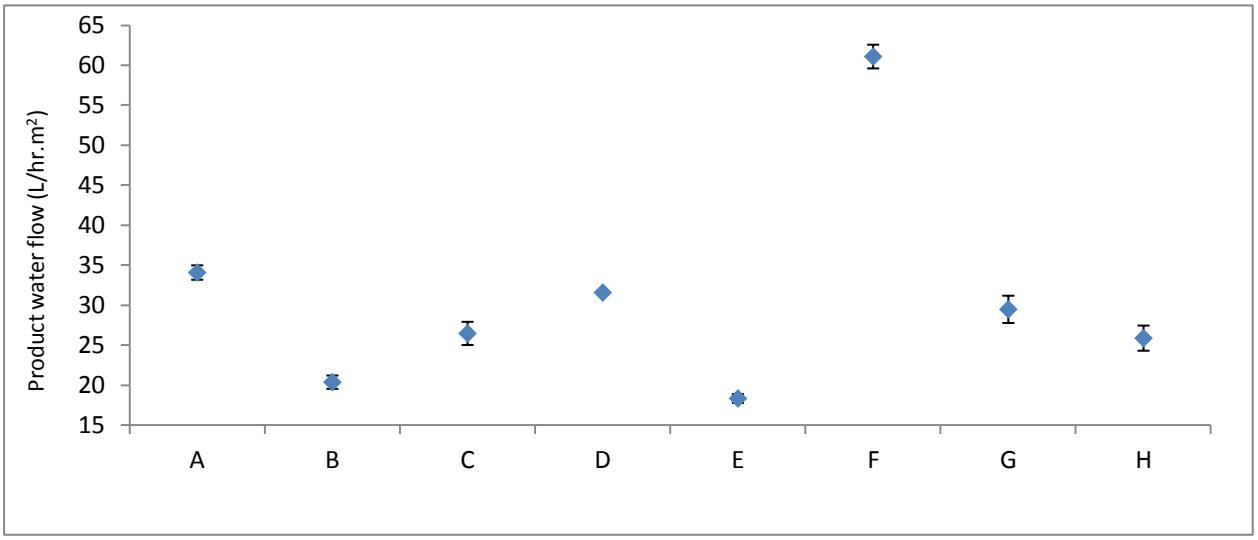

Water flux of the NF membranes in ASTM Exp.I

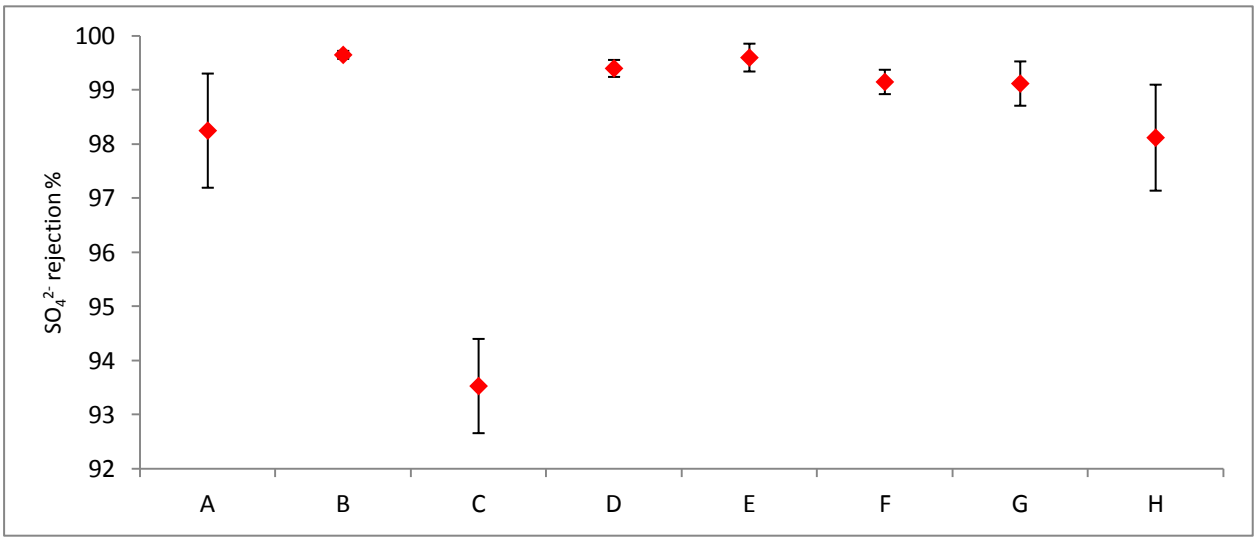

Sulphate rejection of the NF membranes in ASTM Exp.I

Figure 7.4 Permeate and sulphate rejection performance of the NF membranes in ASTM Exp.I (steady state test at 25 ^{0}C, 9 bar)

As can be seen membrane F demonstrates the highest product flow, followed by NF A, D, G, C and H, which fall in the same range. NF B and E show the least permeate flux in comparison to the rest of the tested membranes.

The analysis reveals that no differences can be ascribed to the sulphate rejection of seven of the membranes. The clearly low sulphate rejection of membrane C is understandable in terms of its market application.

3.1.2 ASTM Experiment II, (Exp.II) – temperature factor – results:

The trends of sulphate rejection and permeate behaviour with increasing feed water temperature of all tested NF membranes are shown in the following charts from Figure 7.5 to Figure 7.12.

- NF membrane A

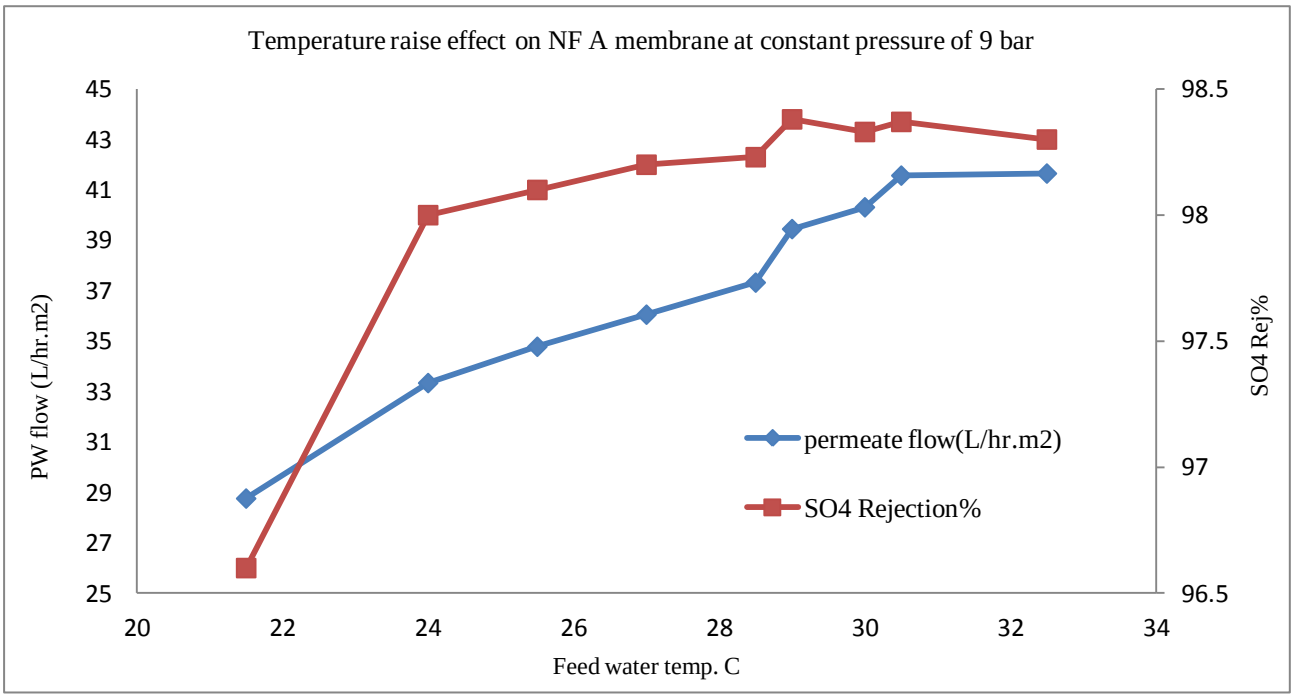

Figure 7.5 SO_4^{2-} rejection% and permeate flow behaviour of NF (A) membrane against feed water temperature increase at constant pressure of 9 bar.

- NF membrane B

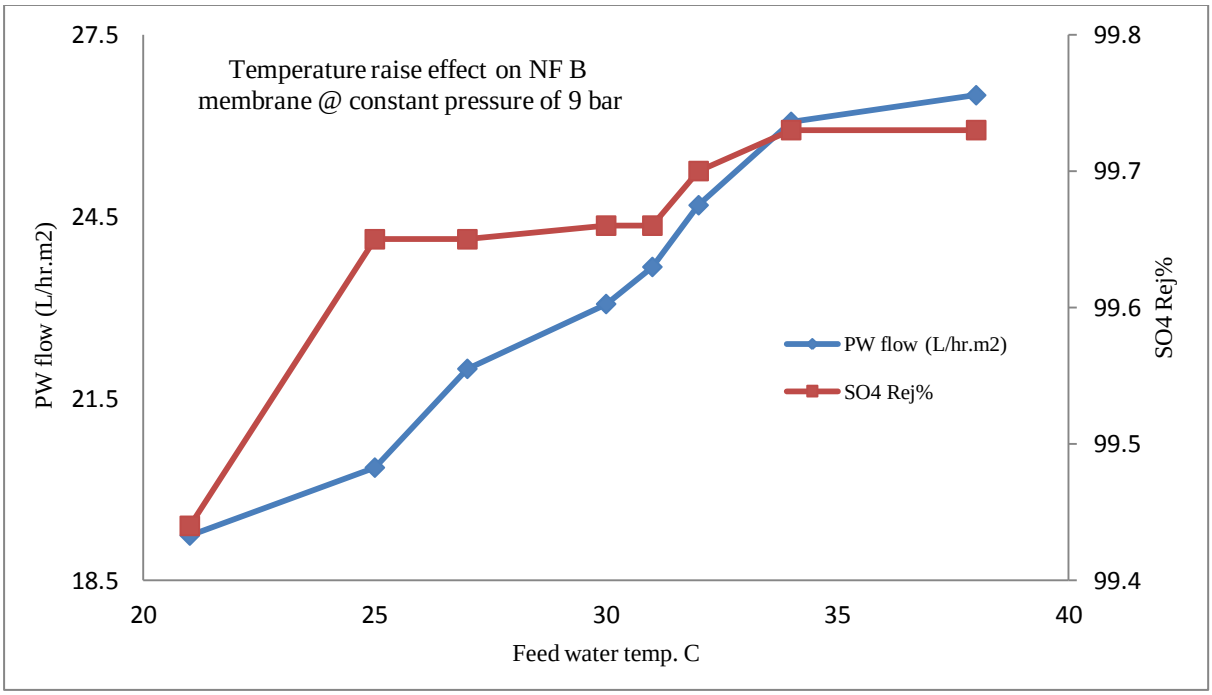

Figure 7.6 SO_4^{2-} rejection% and permeate flow behaviour of NF (B) membrane against feed water temperature increase at constant pressure of 9 bar.

- NF membrane C

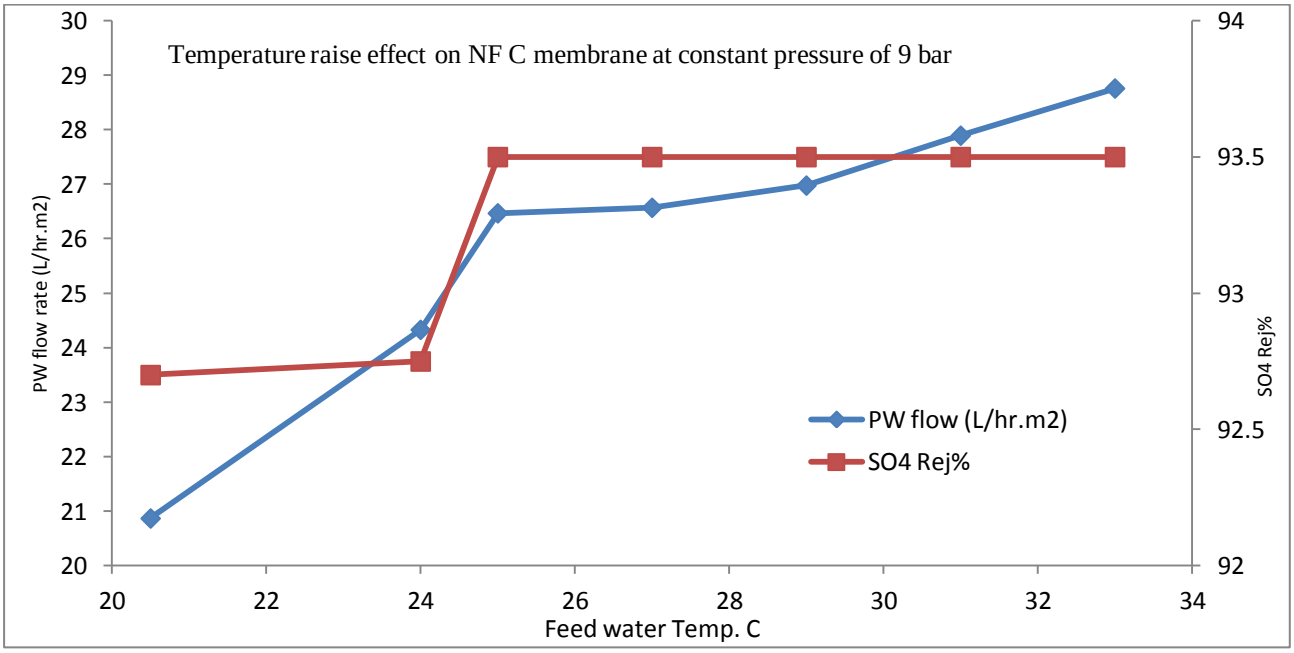

Figure 7.7 SO_4^{2-} rejection% and permeate flow behaviour of NF (C) membrane against feed water temperature increase at constant pressure of 9 bar.

- NF membrane D

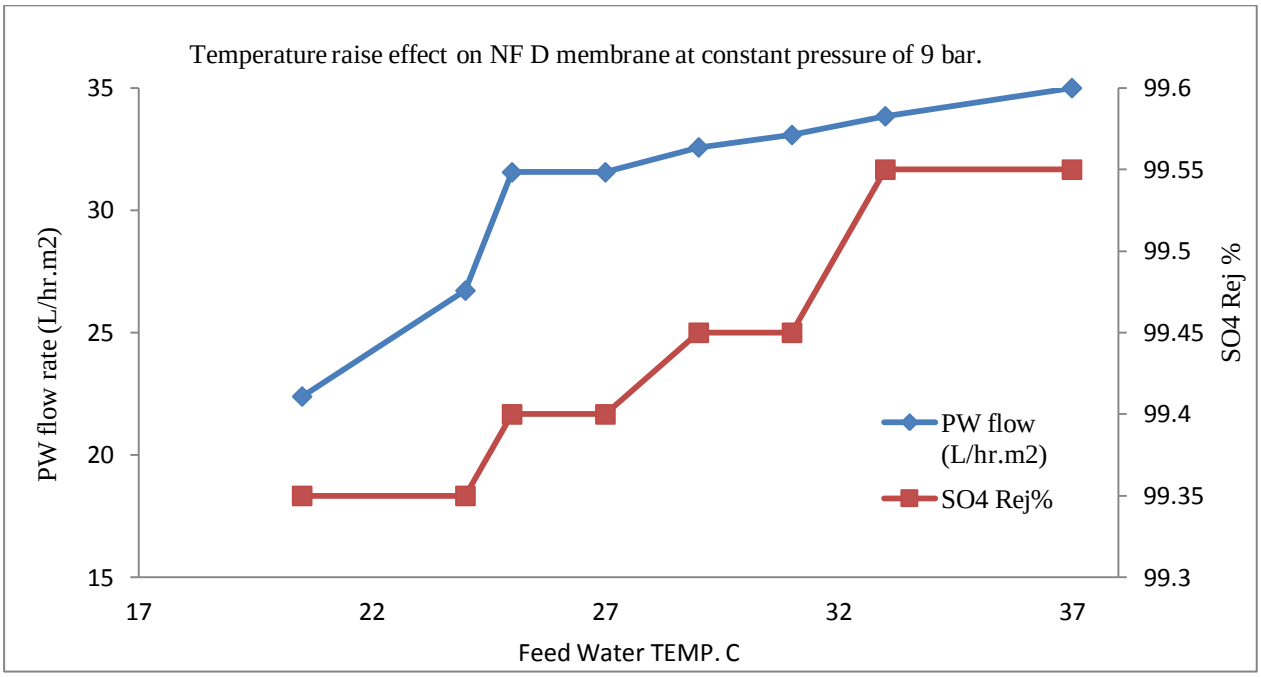

Figure 7.8 SO_4^{2-} rejection% and permeate flow behaviour of NF (D) membrane against feed water temperature increase at constant pressure of 9 bar.

- NF membrane E

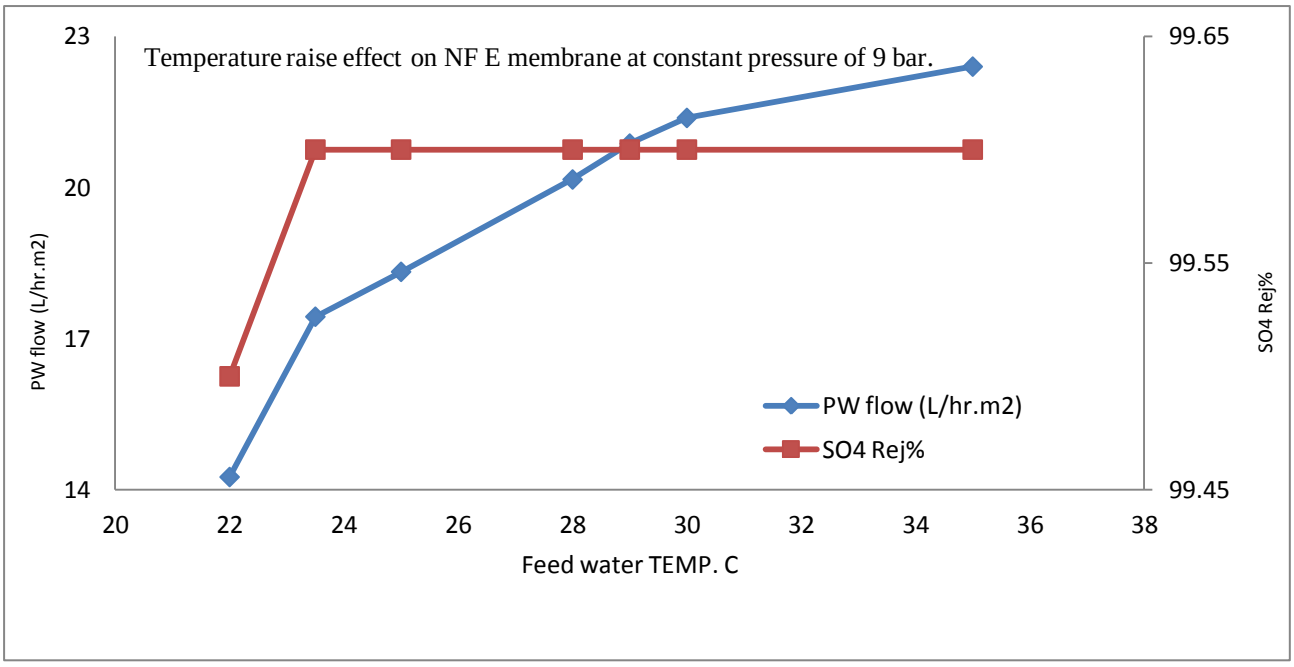

Figure 7.9 SO_4^{2-} rejection% and permeate flow behaviour of NF (E) membrane against feed water temperature increase at constant pressure of 9 bar.

- NF membrane F

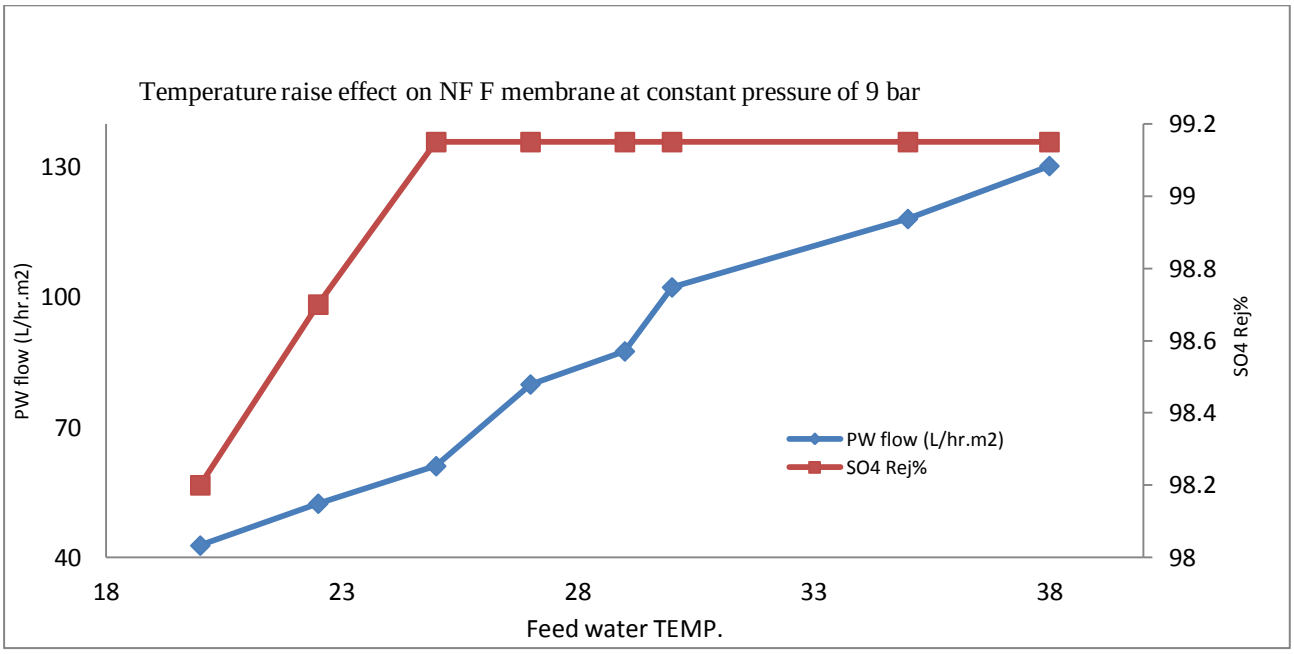

Figure 7.10 SO_4^{2-} rejection% and permeate flow behaviour of NF (F) membrane against feed water temperature increase at constant pressure of 9 bar.

- NF membrane G

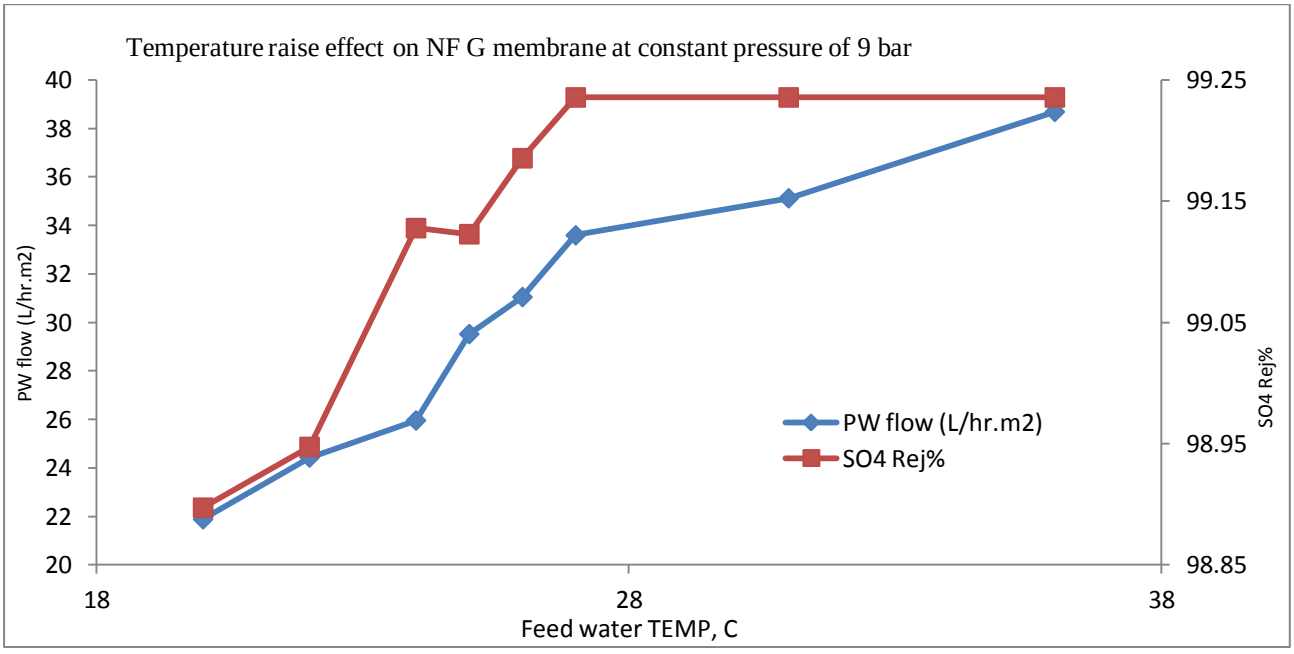

Figure 7.11 SO_4^{2-} rejection% and permeate flow behaviour of NF (G) membrane against feed water temperature increase at constant pressure of 9 bar.

- NF membrane H

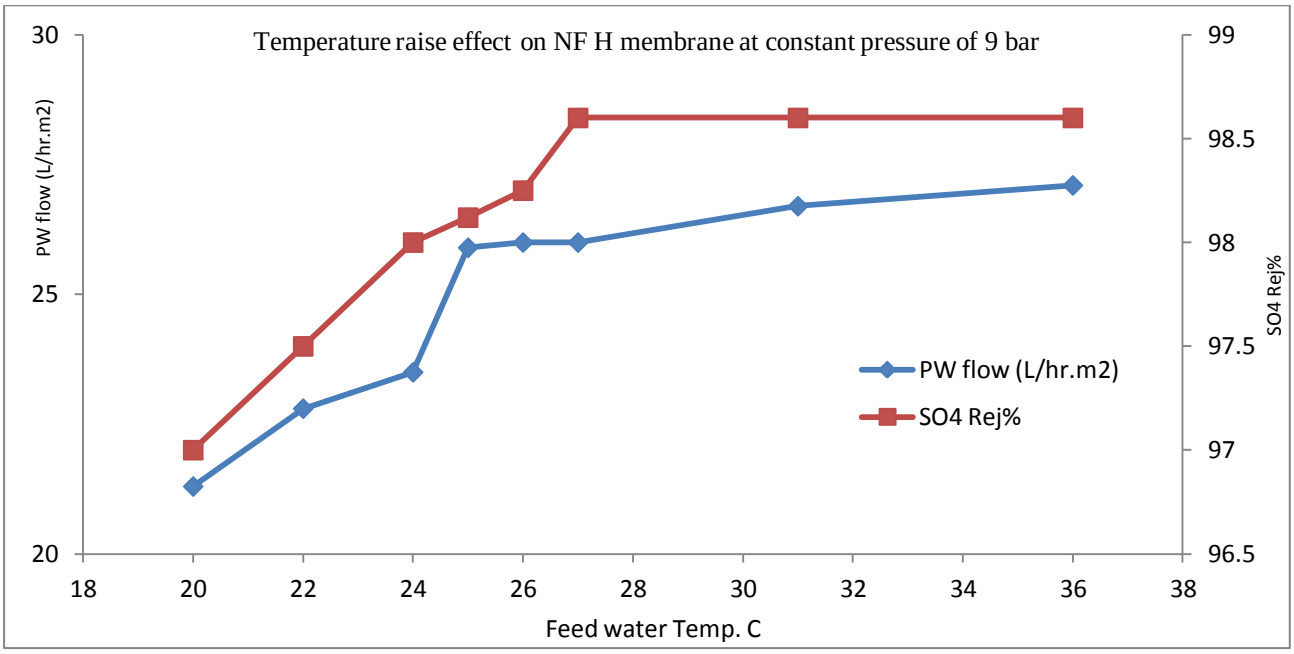

Figure 7.12 SO_4^{2-} rejection% and permeate flow behaviour of NF (H) membrane against feed water temperature increase at constant pressure of 9 bar.

In general, increasing feed flow temperature had an obvious effect on the NF performance. An increase in feed temperature resulted in an increase in permeate flow; however, NF product quality (in terms of sulphate rejection percentage) reached a plateau, where after the increase in feed temperature did not affect the membrane rejection ability.

3.1.3 ASTM Experiment III, (Exp.III) – pressure factor – results:

The following Tables (7.10 – 7.17) and charts (7.13 – 7.20) show the results of NF membranes performance in terms of permeability and SO_4^{2-} rejection ability at different set of inlet feed water pressure. Reported results were built on the average of the six cells on three different readings on two days of continuous 12 hours ruining.

- NF membrane A

Feed water pressure (bar)	Permeate Flow (L/hr.m^2)	SO_4^{2-} content in permeate (ppm)	SO_4^{2-} Rejection %
9	34.10	27.93	98.25
15	48.35	26.65	98.33
20	62.09	25.85	98.38
25	91.87	39.10	97.55

Table 7.10 Membrane A data at ASTM Exp.III

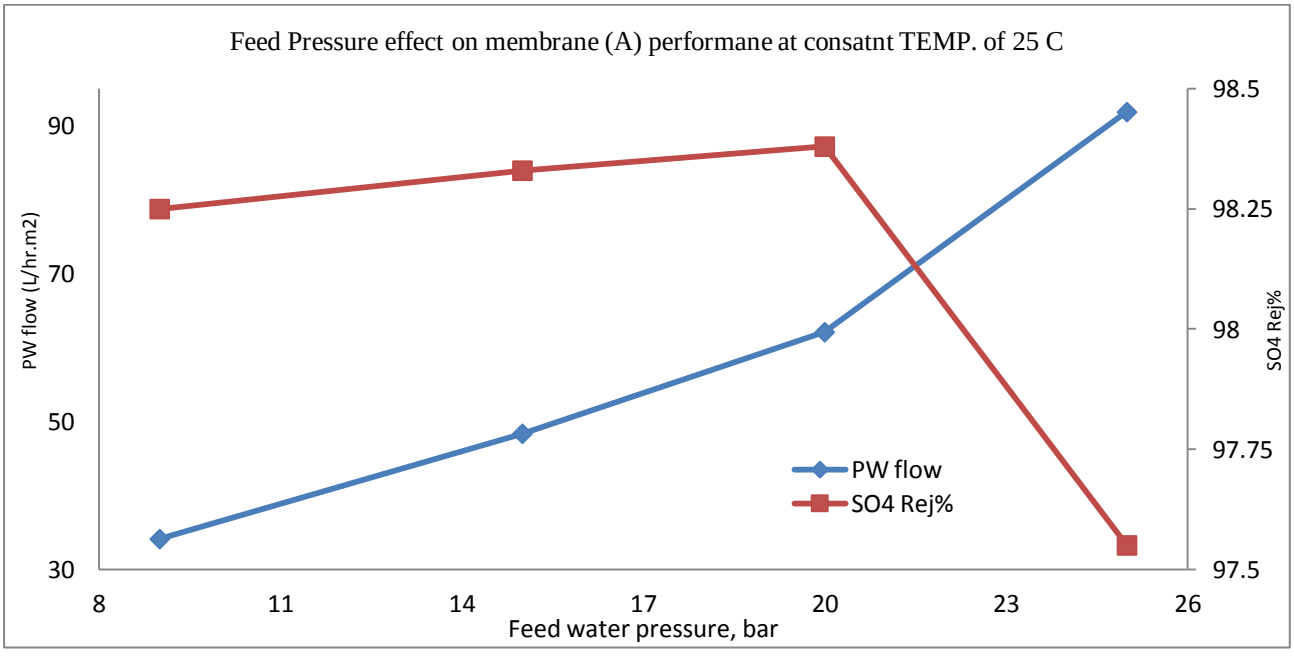

Figure 7.13 Effect of feed water pressure rise on SO_4^{2-} rejection percentage and the permeate flow rate of NF membrane (A).

- NF membrane B

Feed water pressure (bar)	Permeate Flow ($L/hr.m^2$)	SO_4^{2-} content in permeate (ppm)	SO_4^{2-} Rejection %
9	20.40	5.58	99.65
15	35.78	5.58	99.65
20	44.79	5.10	99.68
25	52.93	5.10	99.68

Table 7.11 Membrane B data at ASTM Exp.III

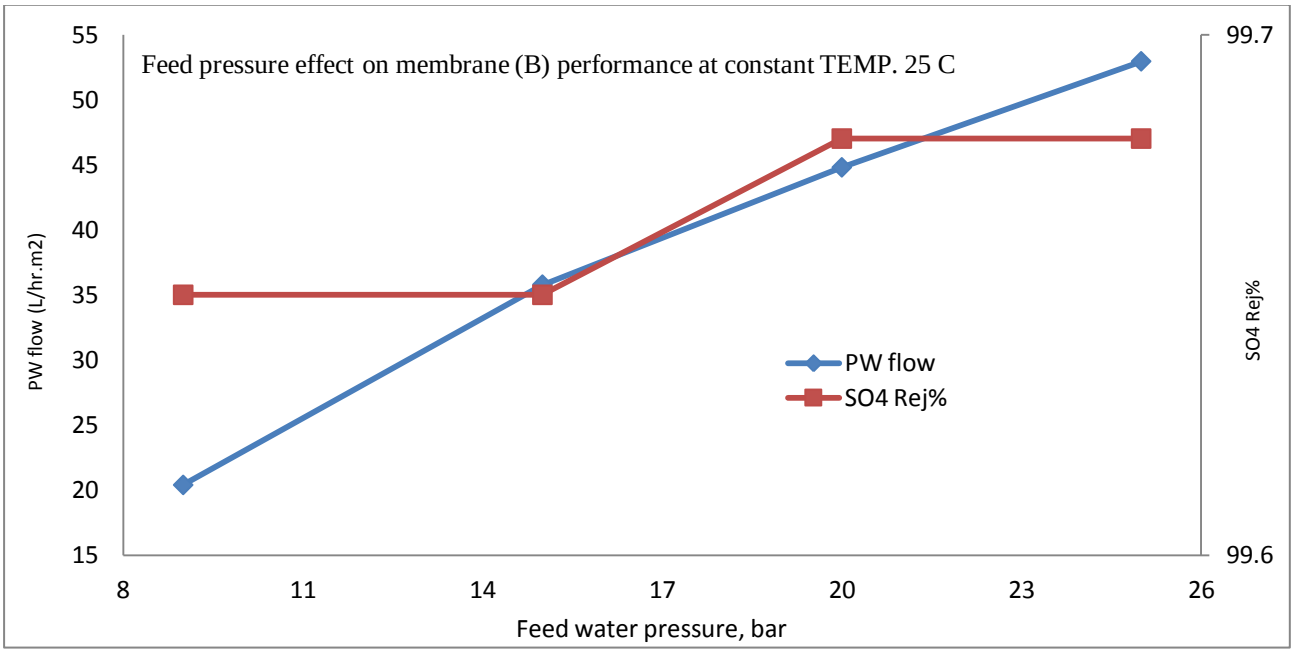

Figure 7.14 Effect of feed water pressure rise on SO_4^{2-} rejection percentage and the permeate flow rate of NF membrane (B).

- NF membrane C

Feed water pressure (bar)	Permeate Flow ($L/hr.m^2$)	SO_4^{2-} content in permeate (ppm)	SO_4^{2-} Rejection %
9	26.49	103.26	93.53
15	39.19	100.54	93.70
20	45.81	88.57	94.45
25	54.46	79.80	95.0

Table 7.12 Membrane C data at ASTM Exp.III

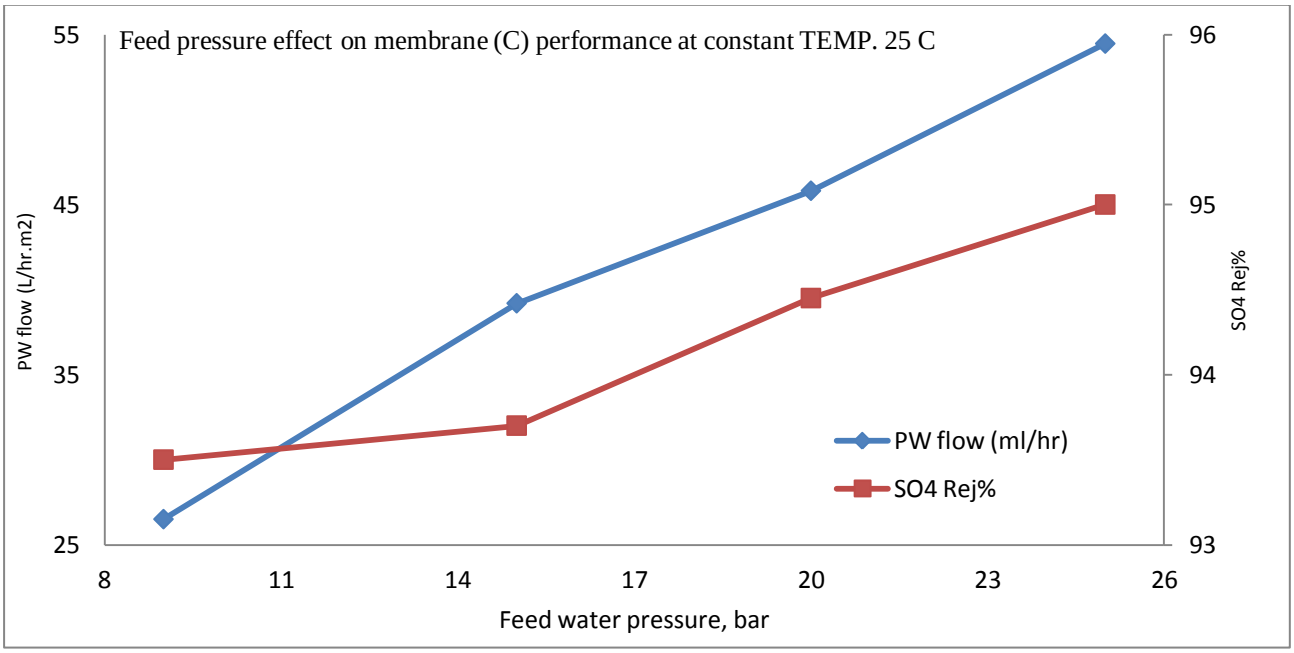

Figure 7.15 Effect of feed water pressure rise on SO_4^{2-} rejection percentage and the permeate flow rate of NF membrane (C).

- NF membrane D

Feed water pressure (bar)	Permeate Flow ($L/hr.m^2$)	SO_4^{2-} content in permeate (ppm)	SO_4^{2-} Rejection %
9	31.60	9.57	99.40
15	53.40	8.45	99.47
20	60.67	8.29	99.48
25	71.90	7.82	99.51

Table 7.13 Membrane D data at ASTM Exp.III

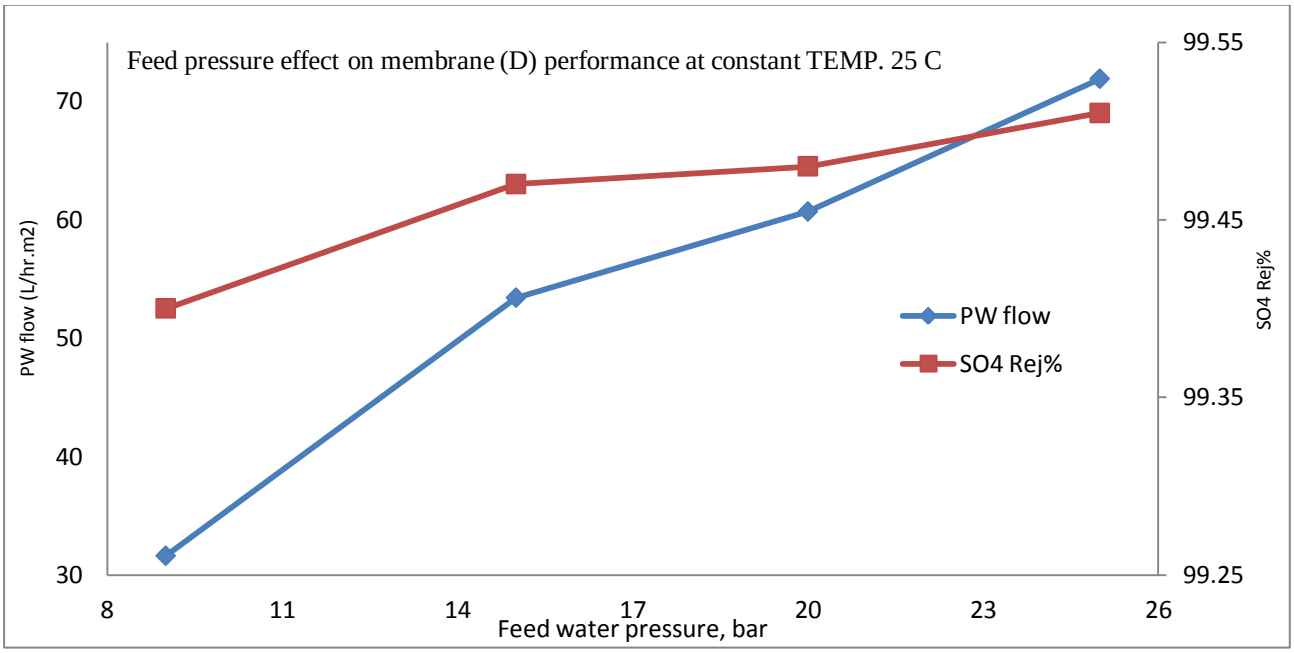

Figure 7.16 Effect of feed water pressure rise on SO_4^{2-} rejection percentage and the permeate flow rate of NF membrane (D).

- NF membrane E

Feed water pressure (bar)	Permeate Flow ($L/hr.m^2$)	SO_4^{2-} content in permeate (ppm)	SO_4^{2-} Rejection %
9	18.36	6.38	99.60
15	34.10	6.38	99.60
20	41.22	6.38	99.60
25	44.28	5.58	99.65

Table 7.14 Membrane E data at ASTM Exp.III

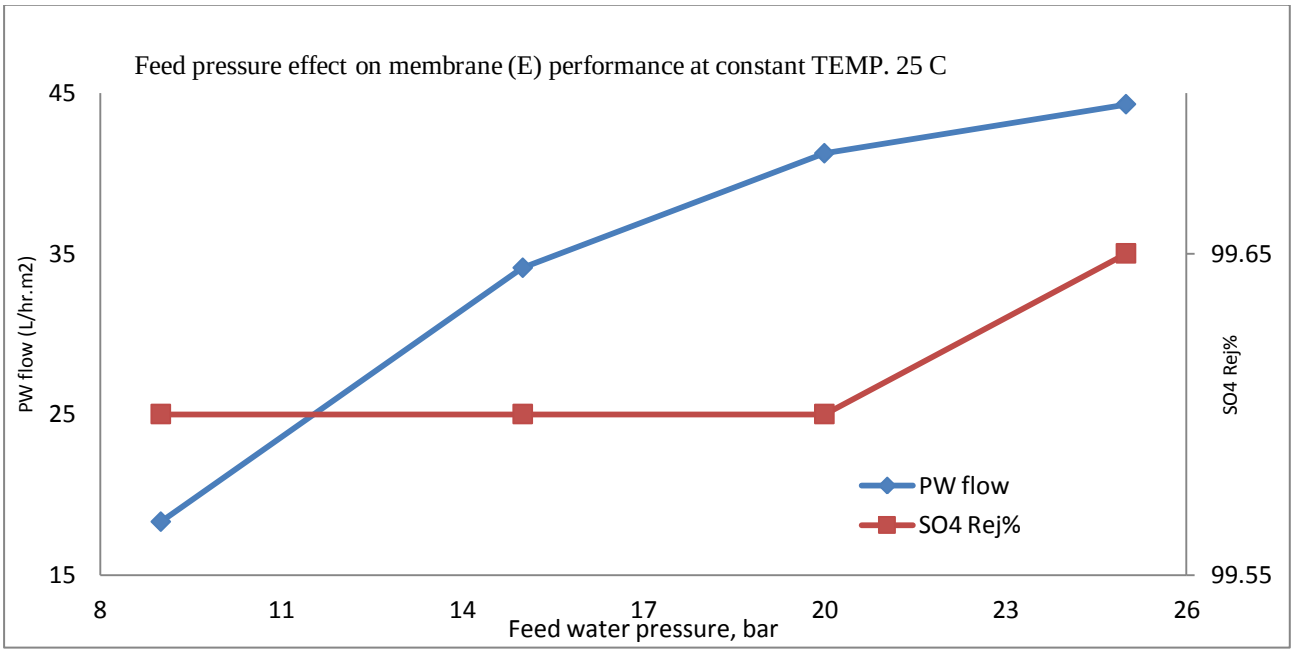

Figure 7.17 Effect of feed water pressure rise on SO_4^{2-} rejection percentage and the permeate flow rate of NF membrane (E).

- NF membrane F

Feed water pressure (bar)	Permeate Flow ($L/hr.m^2$)	SO_4^{2-} content in permeate (ppm)	SO_4^{2-} Rejection %
9	61.09	13.56	99.15
15	86.53	12.92	99.19
20	96.71	12.28	99.23
25	100.81	11.33	99.29

Table 7.15 Membrane F data at ASTM Exp.III

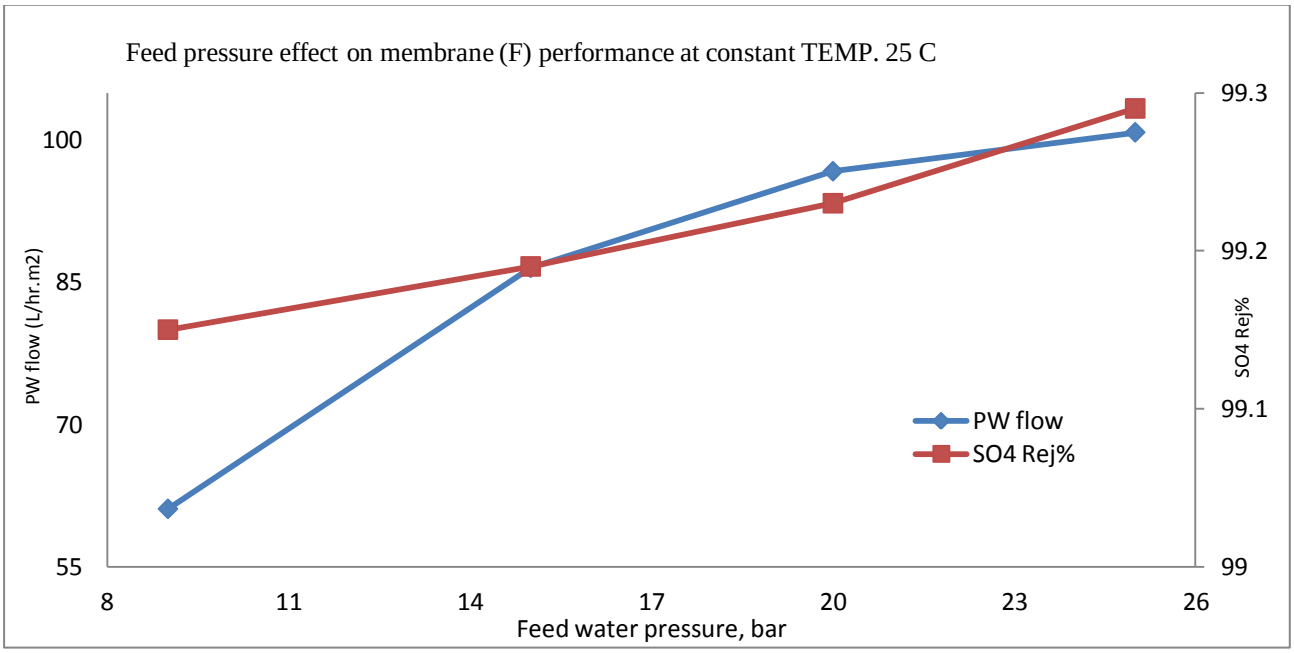

Figure 7.18 Effect of feed water pressure rise on SO_4^{2-} rejection percentage and the permeate flow rate of NF membrane (F).

- NF membrane G

Feed water pressure (bar)	Permeate Flow ($L/hr.m^2$)	SO_4^{2-} content in permeate (ppm)	SO_4^{2-} Rejection %
9	29.50	14.04	99.12
15	49.88	13.24	99.17
20	61.26	13.24	99.17
25	76.53	12.76	99.20

Table 7.16 Membrane G data at ASTM Exp.III

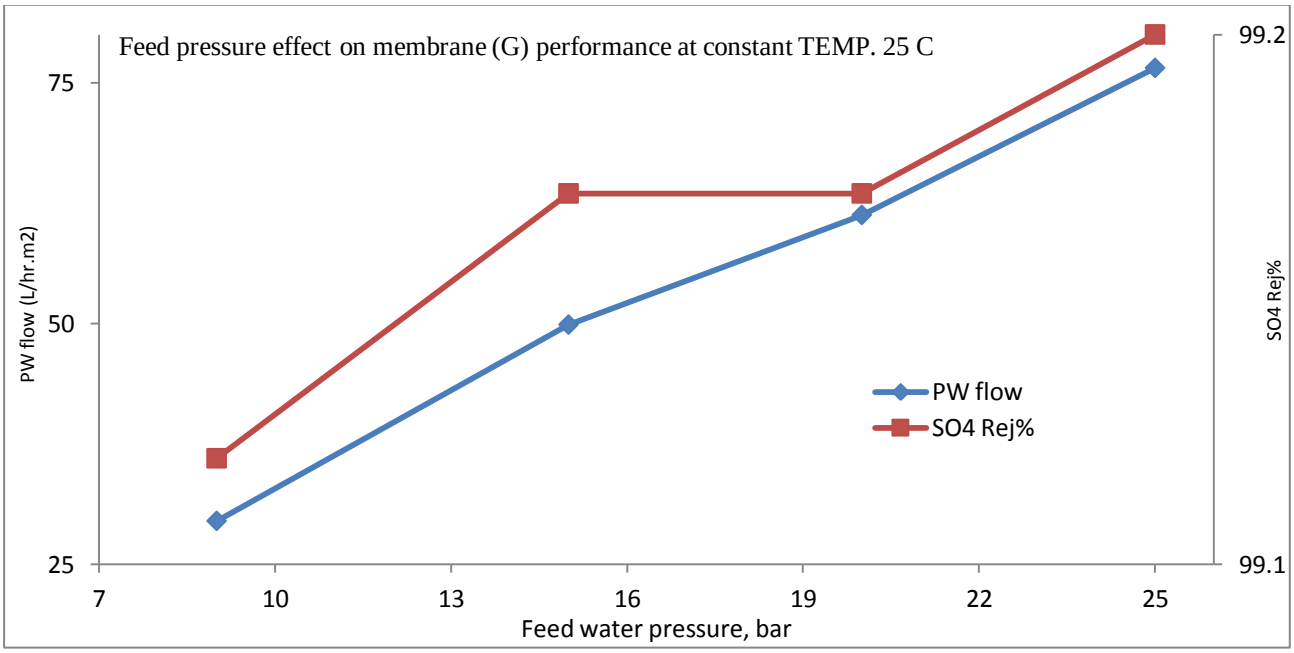

Figure 7.19 Effect of feed water pressure rise on SO_4^{-2} rejection percentage and the permeate flow rate of NF membrane (G).

- NF membrane H

Feed water pressure (bar)	Permeate Flow ($L/hr.m^2$)	SO_4^{2-} content in permeate (ppm)	SO_4^{2-} Rejection %
9	25.90	30.0	98.12
15	37.48	29.04	98.18
20	45.30	28.40	98.22
25	53.69	28.40	98.22

Table 7.17 Membrane H data at ASTM Exp.III

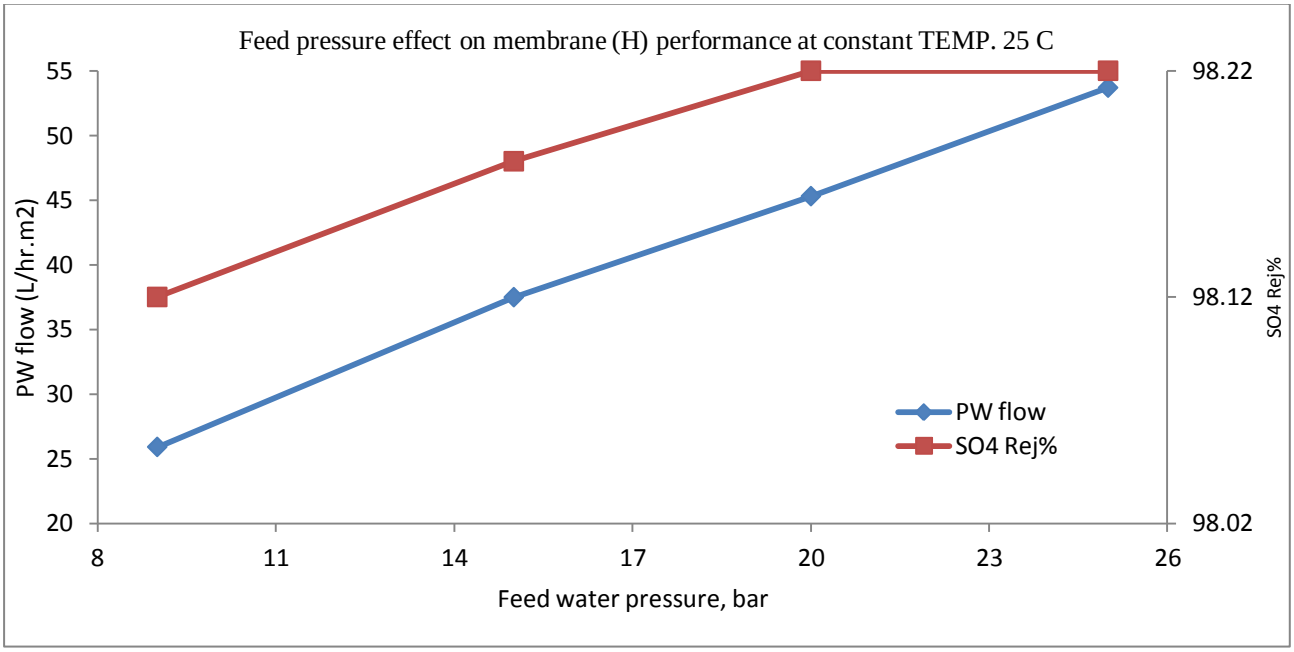

Figure 7.20 Effect of feed water pressure rise on SO_4^{-2} rejection percentage and the permeate flow rate of NF membrane (H).

In general, increasing feed water pressure had an obvious effect on the NF performance. An increase in inlet pressure resulted in an increase in permeate flow; however, NF product quality (in terms of sulphate rejection) differs from membrane to another according to the following table:

NF membrane	Effect of inlet feed water applied pressure increase, bar, on membrane sulphate rejection		
	9 – 15	15 – 20	20 – 25
A	Slight increase	Slight increase	Decrease
B	Constant	Slight increase	Constant
C	Slight increase	increase	increase
D	Slight increase	Slight increase	Slight increase
E	Constant	Constant	Slight increase
F	Slight increase	Slight increase	Slight increase
G	Slight increase	Constant	Slight increase
H	Slight increase	Slight increase	Constant

Table 7.18 The effect of increasing feed water pressure on the NF membranes performance in terms of sulphate rejection

3.2 Simulated Seawater (SW) experiment results:

The following Tables (7.19 – 7.26) list the NF membranes' performance in the simulated seawater experiment. Data are based on the six cells average (in both permeate flow and sulphate rejection) of each experiment for each NF membrane, i.e. for each reading; the number illustrated in the tables shows the average of the six cells at the time of recording the data.

- NF membrane A

Reading number	Product water flow ($L/hr.m^2$)	SO_4^{2-} content in permeate (ppm)	SO_4^{2-} rejection %
1 (after 1 hr of reaching steady state)	20.10	27	98.30
2 (4 hrs after reading #1)	19.65	30	98.12
3 (4 hrs after reading #2)	22.05	30	98.12
AVG.	20.6	29	98.18

Table 7.19 NF membrane A data at SW Exp.

- NF membrane B

Reading number	Product water flow ($L/hr.m^2$)	SO_4^{2-} content in permeate (ppm)	SO_4^{2-} rejection %
1 (after 1 hr of reaching steady state)	9.19	6	99.62
2 (4 hrs after reading #1)	9.59	5	99.68
3 (4 hrs after reading #2)	8.79	6	99.62
AVG.	9.2	5.67	99.64

Table 7.20 NF membrane B data at SW Exp.

- NF membrane C

Reading number	Product water flow ($L/hr.m^2$)	SO_4^{2-} content in permeate (ppm)	SO_4^{2-} rejection %
1 (after 1 hr of reaching steady state)	15.0	106	93.35
2 (4 hrs after reading #1)	14.9	110	93.10
3 (4 hrs after reading #2)	14.5	99	93.79
AVG.	14.8	105	93.41

Table 7.21 NF membrane C data at SW Exp.

- NF membrane D

Reading number	Product water flow ($L/hr.m^2$)	SO_4^{2-} content in permeate (ppm)	SO_4^{2-} rejection %
1 (after 1 hr of reaching steady state)	18.4	10	99.37
2 (4 hrs after reading #1)	18.6	10	99.37
3 (4 hrs after reading #2)	17.9	10	99.37
AVG.	18.3	10	99.37

Table 7.22 NF membrane D data at SW Exp.

- NF membrane E

Reading number	Product water flow ($L/hr.m^2$)	SO_4^{2-} content in permeate (ppm)	SO_4^{2-} rejection %
1 (after 1 hr of reaching steady state)	7.6	7	99.56
2 (4 hrs after reading #1)	8.0	8	99.49
3 (4 hrs after reading #2)	7.2	6	99.62
AVG.	7.6	7	99.56

Table 7.23 NF membrane E data at SW Exp.

- NF membrane F

Reading number	Product water flow ($L/hr.m^2$)	SO_4^{2-} content in permeate (ppm)	SO_4^{2-} rejection %
1 (after 1 hr of reaching steady state)	39.1	14	99.12
2 (4 hrs after reading #1)	38.7	13	99.18
3 (4 hrs after reading #2)	38.3	15	99.06
AVG.	38.7	14	99.12

Table 7.24 NF membrane F data at SW Exp.

- NF membrane G

Reading number	Product water flow ($L/hr.m^2$)	SO_4^{2-} content in permeate (ppm)	SO_4^{2-} rejection %
1 (after 1 hr of reaching steady state)	15.3	15	99.06
2 (4 hrs after reading #1)	15.6	10	99.37
3 (4 hrs after reading #2)	15.0	17	98.93
AVG.	15.3	14	99.12

Table 7.25 NF membrane G data at SW Exp.

- NF membrane H

Reading number	Product water flow ($L/hr.m^2$)	SO_4^{2-} content in permeate (ppm)	SO_4^{2-} rejection %
1 (after 1 hr of reaching steady state)	10.4	29	98.18
2 (4 hrs after reading #1)	11.0	29	98.18
3 (4 hrs after reading #2)	10.7	32	97.99
AVG.	10.7	30	98.12

Table 7.26 NF membrane H data at SW Exp.

Figure 7.21, shows a comparison of the filtration performance of the NF membranes from highest to lowest in terms of water flux and sulphate rejection in both:

1. ASTM Exp.I (steady state test at 25 ^{0}C, 9 bar) of 2000 ppm $MgSO_4$.
2. Simulated seawater experiment (25 ^{0}C, 9 bar) of 2000 ppm $MgSO_4$ and 35,000 ppm NaCl.

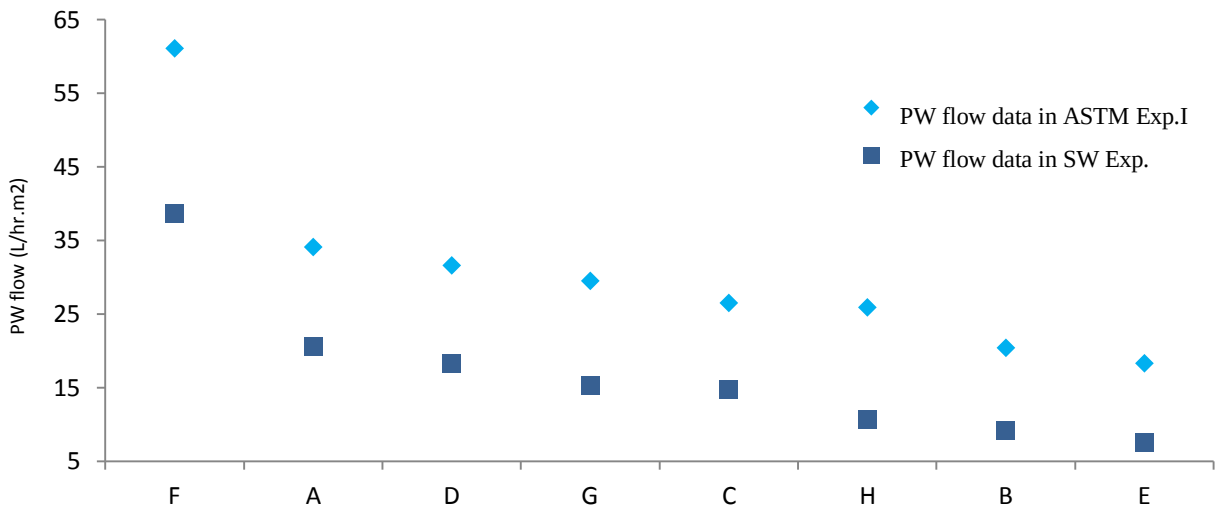

a) Water flux of the NF membranes in ASTM Exp.I and SW experiments.

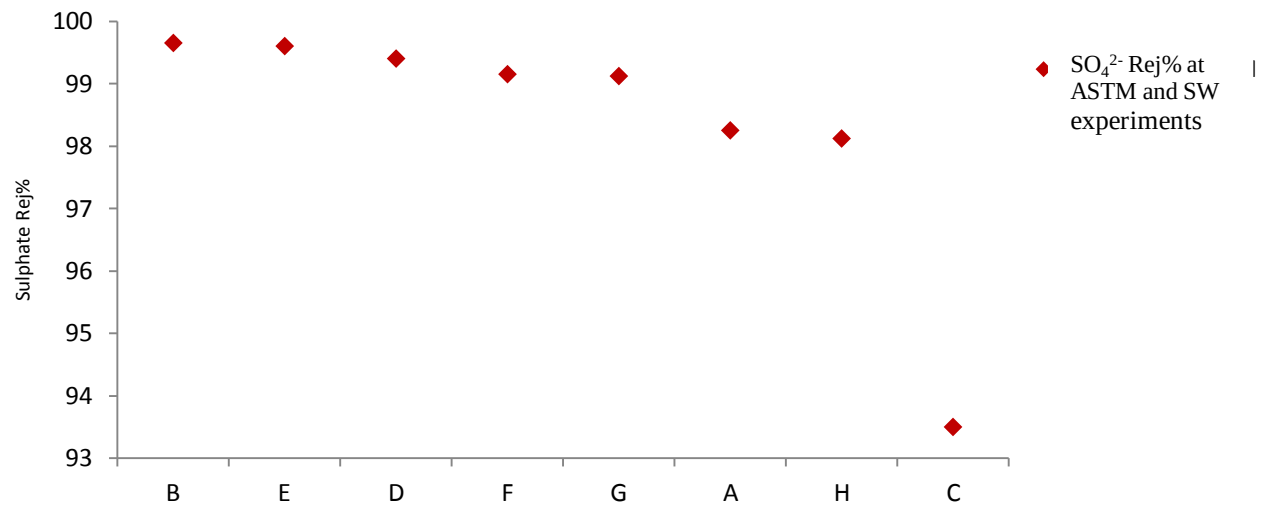

b) Sulphate rejection of the NF membranes in ASTM Exp.I and SW experiments.

Figure 7.21 Comparison of the NF membranes performance at ASTM ExpI and simulated seawater experiment in order from highest to lowest of: a) water flux and b) sulphate rejection.

Figure (7.21-b) shows that the sulphate rejection of the NF membranes is independent of the feed-water chemistry. As each membrane attain almost the same sulphate retention in both:

- ASTM solution of (2000 ppm $MgSO_4$).
- Simulated seawater solution of (2000 ppm $MgSO_4$ + 35,000 ppm NaCl).

3.3 Pure water experiment:

The permeability of pure water of the NF membranes is listed in Table 7.27. The number illustrated for each reading represents the average of the six cells at the time of recording the data.

NF	Permeability of pure water flow rate ($L/hr.m^2$) Reading number			
	1 (after 1 hr of reaching steady state)	2 (4 hrs after reading #1)	3 (4 hrs after reading #2)	AVG.
A	35.33	35.68	35.88	35.63
B	20.90	21.50	21.73	21.37
C	28.45	29.0	28.06	28.50
D	32.30	32.30	33.12	32.57
E	18.10	18.30	18.57	18.32
F	66.70	66.45	66.88	66.68
G	30.50	30.50	30.62	30.54
H	26.40	26.40	26.60	26.46

Table 7.27 Permeability of pure water results of the NF membranes.

Figure 7.22 shows a representation chart for the eight NF membranes in order from highest to lowest based on the flux flow rate data of ASTM Exp.I, simulated seawater and pure water permeability experiments all at constant operating parameters of (25 ^{0}C and 9 bar). As can be seen, the order of the membrane performance is identical in all three environments.

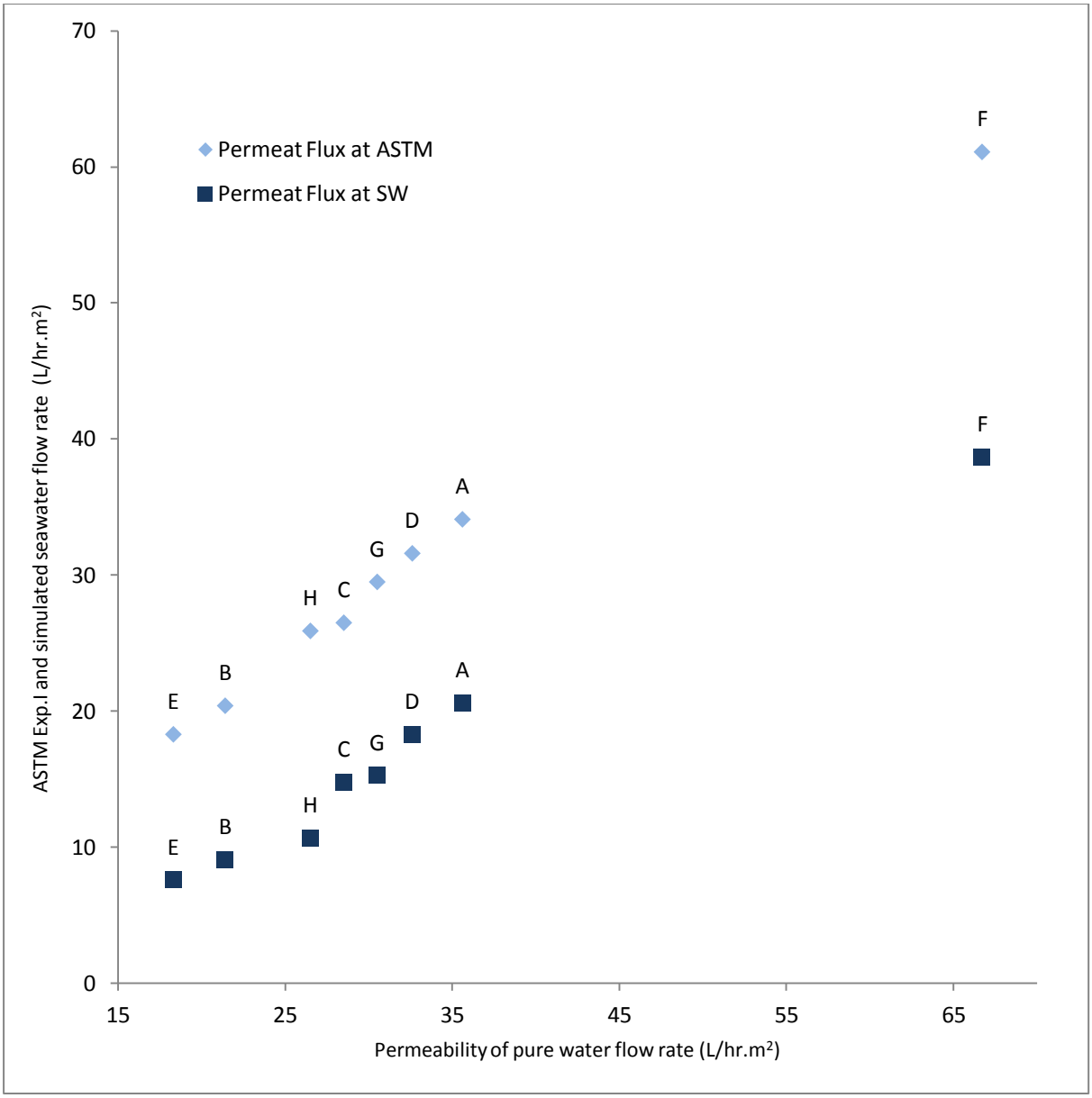

Figure 7.22 Demonstration of the water flux of the NF membranes in three experiments (pure water permeability, ASTM Exp.I and simulated seawater).

4. Comments:

4.1 Comments on the intended approach:

Membrane test cells are extensively used for quality assurance, screening tests and in many research projects. However, many practitioners will agree that test cell results may vary considerably and their accuracy can be inadequate for scale-up to larger membrane units. The reliability of test cells is, besides other factors, influenced by small-scale variations of membrane material properties. The performance of membrane modules, in contrast, depends only on the average properties of a large membrane area.

Other workers have suggested that [110]:

There are two principle possibilities to improve the reliability of test cells:

I. Either the use of larger test cells to sample a more representative membrane area,

or

II. Multiple parallel measurements (which is the case in the current research work), where the average from all the samples is a more reliable estimate than a single sample.

Moreover, this work is:

1. Testing actual NF membranes supplied by manufacturers which are available in the market for commercial sale, i.e. material found in modules not membrane material used for laboratory tests.
2. Testing six cells at the same operating environment and building the final results on the average considering the standard deviation (see Appendix 2).
3. Following ASTM standards.

4.2 Comments on experimental findings:

4.2.1 ASTM Exp.I (steady state test at 25 ^{0}C, 9 bar)

In this experiment, NF membranes have been characterised in terms of their filtration performance. The SO_4^{2-} rejection ability of all NF membranes but one (C) examined here is considered to be excellent, 98.12% – 99.65%. The remaining membrane which exhibited a rejection of 93.5%, is targeted mainly towards organic removal.

Table 7.28 lists all tested NF membranes in order from highest to lowest in terms of permeate flux and sulphate rejection ability. The number in brackets represents the slandered deviation.

One specific NF membrane (F), stood out as possessing the desirable properties of high SO_4^{2-} rejection (99%) together with higher permeate flux (61.09 L/hr.m^2) at ASTM testing conditions.

NF membranes list in order from highest to lowest flux at ASTM Exp.I	Average Permeate flux, L/hr.m^2		NF membranes list in order from highest to lowest sulphate rejection % at ASTM Exp.I	Average SO_4^{2-} rejection%
F	61.09 (± 1.48)		B	99.65 (± 0.07)
A	34.10 (± 0.90)		E	99.60 (± 0.26)
D	31.60 (± 0.12)		D	99.40 (± 0.16)
G	29.50 (± 1.70)		F	99.15 (± 0.22)
C	26.49 (± 1.45)		G	99.12 (± 0.41)
H	25.90 (± 1.57)		A	98.25 (± 1.06)
B	20.40 (± 0.83)		H	98.12 (± 0.98)
E	18.36 (± 0.56)		C	93.53 (± 0.87)

Table 7.28 List of NF membranes order from highest to lowest according to ASTM ExpI data.

4.2.2 ASTM Experiments II, (Exp.II – temperature factor) and ASTM Experiments III, (Exp.III – pressure factor):

The two operating variables examined here – feed water pressure and temperature – exert their influence on NF membrane product water quantity and quality. The entire eight commercial NF membranes exhibit the same general behaviour of more water flux (production) with increasing the inlet feed water temperature or pressure. However, the only differences are the rate of increase for each membrane demonstrates.

- **Temperature factor:**

The temperature tests were conducted to extend the performance characterisation, to investigate the effect of different climate as temperature varies over time and with seasons.
It is well known that, increasing the temperature of the feed increases both permeate flux and salt passage. As a result of changing in the transport mechanisms (convection and diffusion) due to structural changes in network pores by increasing its pore size and solution viscosity [183]. However, as shown here (for all tested NF membranes) the increase of water flux is the more dominant effect when increasing feed water temperature with the only difference between NF membranes being the rate of increase per 1 ^{0}C. While, for sulphate rejection, there is what might be called the top limit rejection ability and, after this temperature, no matter how the temperature increases, the rejection ability is generally constant.
A critical aspect to consider related to the optimum temperature to be applied is the membrane "deterioration rate" as, at a certain temperature, the effective life of the membrane may be affected. This is normally informed by the supplier or the manufacturer.

- **Pressure factor:**

The higher pressure tests were conducted for the basic reason of extending the performance characterisation, but also in the knowledge that in practice such NF membranes are likely to be used at higher pressure (up to 25 bar) than in the standard ASTM test.

Applied feed water pressure can be considered as one of the most critical aspects in the membrane performance and operation. As feed water pressure is increasing above the solution osmotic pressure (minimum requirement), the flow of the water through NF membrane increases. The flow of the salt (salt passage) remains (relatively) constant however; it depends on the salt concentration difference. The upper limitation on the applied pressure will be the restrictions of the energy consumption and the compaction phenomena which are also related to other factors such as the membrane material. And again, the difference between all the commercial NF membranes subjected to experiments is the value of flux increase per one bar increase.

It has been shown that the percentage of water flux increase, per one bar increase in the feed water pressure, is almost three times the percentage of water flux increase per one degree celsius increase on the feed water temperature. The percentage of permeate flow rate increase per one degree celsius **(**temperature coefficient) of the eight membranes was (2.2% for A,

1.3% for B, 1.2% for C, 1.5% for D, 1.2% for E, 5.0% for F, 2.2% for G and 1.7% for H). It has been reported by other workers [111] to be 2% for a commercial NF membrane (Osmonics DK8040). Although the types of equipments and experiments main features are not identical as their work was on pilot plant with actual seawater, the results show a close values representing an excellent correlation between laboratory results on multi-small membrane samples and industrial elements.

4.2.3 Simulated seawater experiment:

This test has been examining the sulphate separation performance of the NF membrane in saline water for further investigation on NF characterisation for seawater desalination. Figure 7.21 shows steady sulphate rejections and flux decrease in comparison to ASTM experiment results. The flux decrease is caused by osmotic pressure gradient as a result of NaCl presence in addition to the $MgSO_4$ salt (in comparison to ASTM solution containing $MgSO_4$ only).
For sulphate rejection behaviour, the results provide a strong indication that reflects NF ability to separate sulphate ions is totally independent of solution chemistry in regard salts components.

4.2.4 Pure water experiment:

The study of permeability of pure water in the NF membranes representing the flow per unit of pressure has facilitated the determination of (available in chapter 8):

1. NF water permeability constant (A_W) in L/m^2.hr. bar.
2. Calculations of membrane porosity factor. Where, the difference in permeability among the eight membranes was directly related to their different porosity factor.

Water permeability and porosity factor calculations are detailed in next chapter (chapter 8).

5. Conclusions:

To this end of the experimental work; assessing the filtration performance of eight commercial NF membranes (under uniform operational parameters) in terms of permeate flux and sulphate rejection, it can be concluded that the membranes have excellent performance, especially their ability to separate sulphate ions. Notwithstanding the general similarities in performance summarised, some differences have been observed. These differences can be attributed to the differences of types (polymers properties and fabrication methods) of NF membranes available in the market, resulting in differences in their properties which will be investigated in detail in the next chapters (8–11) of NF characterisation. Therefore, based on current findings, in order to make the NF pretreatment process very attractive for sulphate rejection applications, the entire process should be able to operate at highest possible flux rate combined with optimum sulphate rejection as well as lowest possible energy. Hence, optimum operating conditions (pressure and temperature) should be selected based on the input feed water quality in addition to NF membrane manufacturer recommendations. It has to be understood that commercial NF membranes do have some differences in rejection properties.

Therefore, in order to meet the main objectives of this research study and to address the issues of NF applications for sulphate rejection, further work of the project involves the use of surface characterisation techniques of porosity factor calculations, contact angle measurements, surface free energy calculations, Atomic Force Microscopy studies, membrane potential measurements and charge density calculations. The objective has been to correlate these features and parameters with the measured NF membranes filtration performance data obtained from this phase to critically understand the differences in their performance. By then, such findings will cover the three main NF characterisation categories: transport properties, pore characteristics and surface features. This would enable the development of a complete standardised suite for universal characterisation of the most known commercial NF membranes for sulphate rejection implementations.

Chapter 8: NF MEMBRANES PORE CHARACTERISATION

1. Overview:

The determination of pore characteristics is an important aspect of NF membrane assessment, especially when used in conjunction with other characterisation techniques to develop a full envelope towards better understanding of NF filtration performance.

To a large extent, NF performance is related to the pore characteristics of the membrane both on the surface and throughout the thickness of the membrane. The pore characteristic of NF membrane includes pore size distribution, surface porosity and pore shape. However, two membranes with essentially the same pore size can display markedly different water permeability and solute rejection. This can be because of variations in pore tortuosity and surface chemistry [99]. It is worth mentioning now; however, that separation performance for NF membranes does not depend solely on pore size alone (as will be demonstrated later in this thesis – see chapter 12).

In the literature, there are three main approaches to NF pore characterisation; these can be classified in terms of techniques as; visualization, flow and fluid intrusion and solute rejection methods. An assessment of thee three techniques is illustrated next.

2. Assessment of NF pore determination methods:

I. Visualization:

Atomic Force Microscopy (AFM) (and Scanning Electron Microscopy (SEM) to a certain degree) both can be used as tools in the analysis of surface pore characteristics. However, these techniques are limited in that they are only able to measure the properties of the membrane surface.

AFM in particular has been adopted to provide evidence of a porous structure of NF, some researchers have found pore size to be of ~1 nm in diameter were present [88,149] (please refer to AFM chapter 10).

More recently, the use of fractured carbon nano-tubes as high resolution AFM tips to interrogate the NF active layer and concluded that pores are present. The authors also filled the active layer with a suspension of osmium dioxide and imaged the membrane using transmission electron microscopy. This technique also indicated that the active layer is indeed porous and pore size distributions were calculated for several membranes [88,106,114].

II. Flow and fluid intrusion:

Fluid intrusion methods measure porosity but suffer from problems because of membrane swelling, pore imperfections or lack of information on internal pore structure, requiring assumptions to be made that cannot necessarily be confirmed by experiment [115]. Nitrogen adsorption–desorption technique [116] and Liquid–Liquid Displacement Porosimetry (LLDP) are based on the same principles of the gas–liquid displacement used to measure pore size distribution [117]. Both methods are based on the correlation between the applied pressure and the pore radius open to flux. Concerning the outcomes of such techniques (more particularly of LLDP) it is worth noting that its application on nanofiltration membranes to determine the pore size and distribution have been analysed by a very limited number of research studies [117].

III. Solute rejection method; also known as molecular weight cut-off (MWCO). This can be sub-classified into two themes; rejection of charged and uncharged solutes.

MWCO is a measure for the size of the pores and is defined as the molecular weight of a component that is retained for 90% by the membrane. MWCO values strongly depend on experimental conditions, such as the nature of the feed solution and the type of the membrane. This hampers a comparison of the results of the different values available in literature as well as information provided by NF membranes manufacturers [89,118,119].

For the rejection of:

- Uncharged solutes:

This seems to be a function of both solute (size and polarity), as well as membrane properties (pore size, membrane material and membrane charge) [109,120,121]. Although the mechanism of uncharged solute rejection is not yet clearly understood, it has, for example, been shown that rejection usually remains constant and/or drops slightly with increasing feed concentration [109,128].

- Charged solutes:

Also, is determined by both the solute and the membrane properties. Moreover, there is the added effect of the charged solute and its interaction with the charged surface of the membrane, since it is well known that the surface charge of NF membranes is also influenced by the solution (solutes) in contact with the membrane [86,122].

Therefore, solute rejection methods for pore size characterisation suffer from the assumption that rejection is based on size alone, and that parameters such as particle morphology and surface charge are unimportant [99]. Clearly this is not the case as many researchers have found that the surface chemistry of membranes, as well as pH, ionic strength [98,123] and feed-water temperature (as has been proved during phase one of the current work) all play a role in solute rejection.

Overall, those techniques are acceptable to certain degree for the purpose of fundamental evaluation of pore size. However, a considerable number of assumptions are involved; such as:

1. Ideal solution behaviour.
2. Ion concentration is the same in the nano-pore as in the bulk solution.
3. Pore radius is representative of constant size.
4. All pores are in uniform cylindrical shape.
5. Ion rejection is due to pore size only.

Despite this, MWCO remains a popular method for membrane manufacturers to describe the characteristics of their products.

In comparison of determining NF membranes pore size by three different methods (AFM, steric pore flow model to obtain the effective pore size by several organic uncharged solutes and a liquid–liquid displacement technique) a study [117] suggested that basic information of pore size obtained by any technique to have similar results. Nevertheless, it is important to point out that the pore identification obtained from pure water permeability experiments refers to effective, active or open, pores; while other methods give information on the pore openings present at the membrane surface [117].

To this end, and for the purpose of further proceeding in NF characterisation for the target purpose of this work, it is safe to acknowledge that there is sufficient evidence to prove that NF porous active layer is indeed present having pores in scale range of 1 nm in diameter.

In this study, the use of the hydraulic permeability method of pure water for NF active layer porosity determination has been chosen for porosity factor calculations.
Whilst the limitation of the hydraulic permeability technique is that pore tortuosity must be assumed or measured using other characterisation methods and it is unable to identify pore

geometry (which is considered to be a desirable area of improvement for all available techniques), such choice can be justified as follow [99,117]:

1. It is the most reliable of the fluid intrusion methods and has the benefit that it can be performed as part of normal membrane flux experiments.
2. It tests the membrane in the wet state, so can give information very close to the normal operating conditions of the membrane.
3. It evaluates only the open pores, not any closed or blocked ended ones.

3. Porosity factor calculations:

Membrane porosity is defined as the portion of a membrane filter volume which is open to fluid flow, also known as void volume.

NF membrane porosity factor is an essential representation for two aspects in relation to the pores. Those are: pore size and quantity of pores (active membrane surface) [109,124].
Based on the capillary pore diffusion model and the Hagan-Poiseuille equation, porosity factor is calculated as a function of pure water flux (permeability), water viscosity and NF membrane active layer thickness.

Consequently, by taking the advantage of pure water permeability data obtained from phase one (chapter 7, section 3.3 – pure water experiment results) of this research work, the NF membrane porosity factor can be determined using the following equation:

$$(\varepsilon.r)^2 = A_W * 8 * \eta * \Delta x \qquad \text{(Equation 8.1) [109]}$$

Where;

$(\varepsilon.r)$ Porosity factor, nm

ε Membrane porosity

r Pore radius

A_W Water permeability constant, L/m^2.hr. bar (see Table 8.1)

η Pure water viscosity = 0.001 Pa.s

Δx NF membrane active layer thickness = 1.0 μm

Taking the NF membrane active layer thickness = 1.0 μm, can be justified as follows:

1. This active layer thickness has been measured [109] for three commercial NF membranes and found to be 1.0 μm.
2. 1.0 μm ± 0.05 is the value quoted in the literature relating to some of the membranes studied in this work.
3. Some researchers [112] have referred to this value (1.0 μm ± 0.05) based on analysis of rejection data [85].

Water permeability constant is directly calculated from permeability of pure water data at 9 bar as show in the following table;

NF membrane	permeate flux of pure water experiment at 9 bar ($L/m^2.hr$) (see table 7.27)	A_W Water permeability constant $L/m^2.hr.\ bar$
F	66.68	8.33
A	35.63	4.45
D	32.57	4.07
G	30.54	3.81
C	28.50	3.56
H	26.46	3.31
B	21.37	2.67
E	18.32	2.28

Table 8.1 Water permeability constant of the NF membranes in order from highest to lowest.

It has been reported that the typical water permeability range for NF membranes is between 1.4 and 12 $L/m^2.hr.bar$ [109]. Accordingly, the eight NF membranes tested here are in agreement with such values.

Fitting (A_W) values (in equation 8.1) can directly evaluate NF porosity factor. A demonstration of the calculation procedure (considering units conversion) is as follows:

For NF F membrane:

$$(\varepsilon.r)^2 = \frac{8.33\ \text{L} \mid 8 \mid 0.001\ \text{pa. s} \mid 1\text{x}10^{-6}\ \text{m} \mid 1\ \text{hr} \mid 1\text{x}10^{-5}\ \text{bar} \mid 1\ \text{m}^3}{\text{m}^2\text{. hr. Bar} \mid \mid \mid \mid 3600\ \text{sec} \mid 1\ \text{pa} \mid 1000\ \text{L}}$$

$= 1.85 \times 10^{-19}\ \text{m}^2$

Therefore, $(\varepsilon.r)$ = porosity factor = $\sqrt{1.85 \times 10^{-19}\text{m}^2}$ = 4.3×10^{-10} m = 0.43 nm.

4. Results and discussion:

Table 8.2 and Figure 8.1 show the results of the calculated porosity factor $(\varepsilon.r)$ from pure water flux data using equation (8.1)

NF membranes, in order from highest to lowest in terms of H_2O flux	Porosity factor, nm
F	0.43
A	0.31
D	0.30
G	0.29
C	0.28
H	0.27
B	0.24
E	0.22

Table 8.2 Porosity factor of NF membranes under investigation

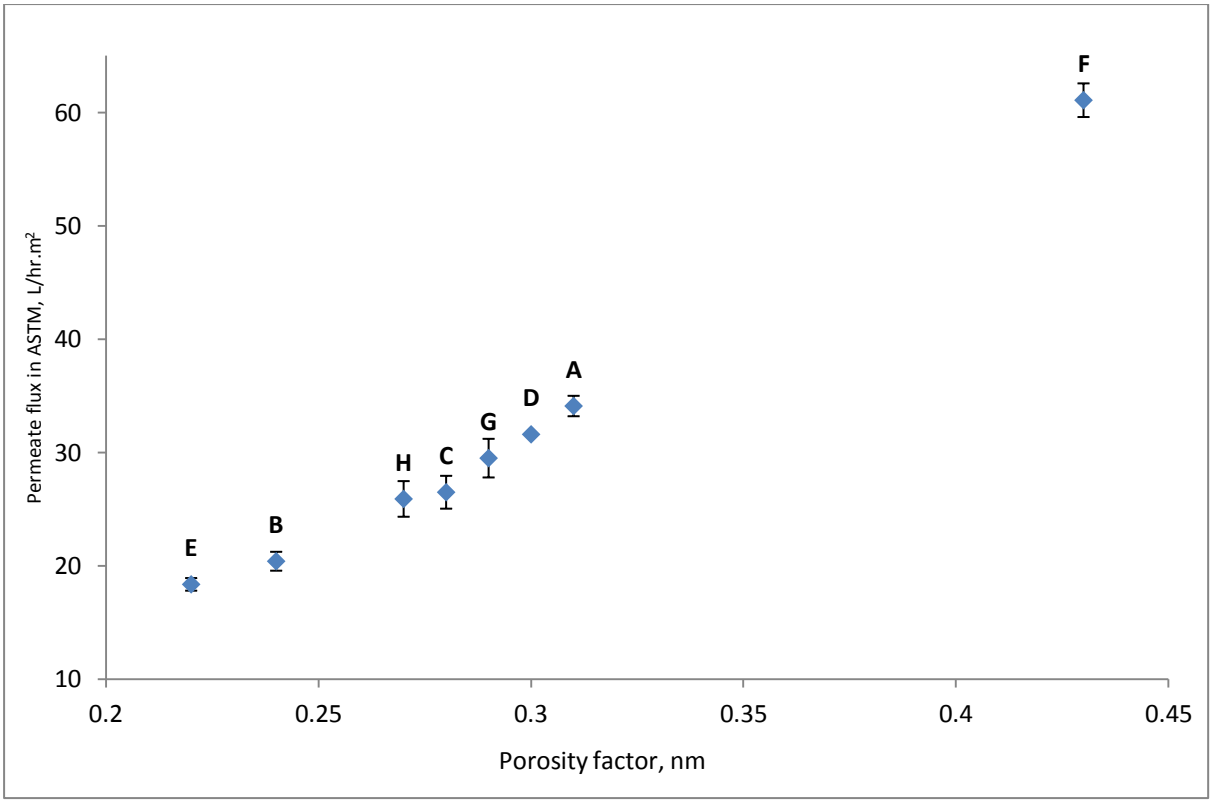

Figure 8.1The relation between the permeate flux of the NF membranes and porosity factor

It's clear that NF membrane flux is related to the porosity factor in a way that the smaller the porosity factor, the lower the flux is and vice versa. There are two possible explanations:

1. Smaller porosity factor indicate that the NF membrane surface structure is more impermeable with narrower pores, thus lower flow rates are expected.

2. High porosity factor corresponds to a relatively wide pores opening, thus water mass transfer through the membrane surface is very likely to permeate.

Porosity factor is a representation of NF membranes pores size and its effect on NF performance is in terms of flux permeation ability. With NF F membrane having a porosity factor of 0.43 nm (which has been recently reported in the literature to have the same porosity factor [182]) coming at the top of the list of the eight tested membranes with the highest water permeability constant of (8.33 L/m^2.hr.bar) in comparison to other tested membranes. While NF E the one with the lowest water permeability constant of (2.28 L/m^2.hr.bar) having a porosity factor of (0.22 nm). This information can be read as a reduction of pore size by (almost) half (from 0.43 to 0.22 nm) that corresponds to a substantial reduction in water flux by three and a half times (from 8.33 to 2.28 L/m^2.hr.bar).

Therefore, a conclusion can be drawn that; a NF membrane having higher porosity is highly beneficial to provide higher fluxes. However, other researchers have shown that pore size of the same NF membrane can vary depending on operational environment [99,125,126,129]. It has been shown that NF pores size (or volume) can either shrink or expand. This can be explained as; pore size of the membrane changes with inlet feed pH because of the presence of cross-linked polymer network which has both carboxyl and amine functional groups (see NF materials section for details – chapter 3, section 3). The pore size of the membrane would be reduced at both high and low pH. At high pH, the carboxyl groups would be de-protonated ($\equiv COO^-$), and at low pH, the amino groups would be protonated ($\equiv NH3^+$) [126].

5. Conclusions:

In order to characterise NF membranes pore, the porosity factor calculation method based on the capillary pore diffusion model and the Hagan-Poiseuille equation, calculated as a function of pure water flux (permeability) has been adopted. Such method is acknowledged to be reliable in order for evaluating NF membrane porosity as an essential representation for pore size. Results obtained can be considered acceptable in terms of NF characterisation for the target research interests.

It is important to emphasise that NF exact pore size and geometry evaluation is still debatable because of the fact that the dimensions of the pores in the NF active layer are in the nano scale and this imposes limitations on their accurate measurement using available techniques.
For that reason, a new technique of using positron annihilation spectroscopy [99,127] are emerging in order to tackle such obstacles for more accurately determining the internal three-dimensional porous structure of NF membranes. Moreover, the pore size of NF membrane can change depending on operating parameters. At high pH values pore size can be reduced because the negatively charged groups on the membrane pore surface adopt an extended conformation due to electrostatic repulsion between them. This expanded conformation reduces the pore size (or pore volume) of the membrane [128].

To sum up in the view of NF characterisation for sulphate rejection applications (in desalination pretreatment and oil/gas industry) with a prospect of pore size; over a range of available NF membranes for such application; the one with highest porosity factor (i.e. the one with wider pores opening) produces the highest permeate flux.

Chapter 9: CONTACT ANGLE MEASUREMENTS AND SURFACE FREE ENERGY CALCULATIONS

1. Introduction:

1.1 Overview:

As discussed earlier during the design process of the experimental protocol of this research work (chapter 6), it is important to investigate the importance of surface properties of NF membranes on its filtration performance in seawater desalination pretreatment. One important characteristic is NF surface hydrophilicity/hydrophobicity nature.

Typically a membrane can be characterised as hydrophilic or hydrophobic according to a contact angle measurement. In other words, the index of membrane surface hydrophilicity/hydrophobicity is the contact angle [99,130,131].

Its basic fundamental is based on; when a drop of liquid is brought into contact with a membrane surface (or, alternatively, an air bubble on a wetted membrane surface as the membrane is immersed in a liquid) the final shape taken up by the drop (or the bubble) depends on the relative magnitudes of the molecular forces that exist within the liquid itself and between liquid and membrane surface [104]. Membrane surface hydrophilicity is higher while its contact angle is smaller or higher contact angle indicates higher hydrophobicity of the membrane surface.

In here, contact angle measurements made by the captive bubble technique where the contact angle is measured between an air bubble and a membrane in a solution environment.

1.2 Contact Angle, Wettability and Surface Free Energy definitions [132]:

Contact angle (made by captive bubble technique) can be defined in terms of geometry as the angle formed by an air bubble at the three phase boundary where a liquid, gas (air) and solid (NF membrane) intersect. The contact angle between NF membrane surface and liquid in contact is a quantitative measure of the wettability. In membranes polymer science, for water filtration, wettability (as the name implies) is defined as the actual process by which water spreads on (wets) a membrane surface. The wettability of a membrane is tied to the chemical properties of the membrane surface. The material composition of the membrane and its corresponding surface chemistry determine the interaction with water, thus affecting its wettability. Membranes in an aqueous environment have an attractive or repulsive response

to water. In addition, the distinction between hydrophobic and hydrophilic relates to the amount of surface free energy of the membrane surface polymer.

Surface free energy phenomenon is due to the unbalance between:

- equal attraction forces of liquid (water) molecules and membrane surface, and
- liquid (water) molecules at the air phase, therefore they have larger attraction forces towards the liquid/membrane surface than air.

This leads to a situation where the interface has excess free energy. Such surface free energy can be calculated in mJ/m^2 by measuring the contact angle of a series known properties liquids.

2. Experimental Procedure:

2.1 Contact angle measurement technique:

There are three methods to measure contact angle of membrane surface [133,134], those are; the Wilhelmy plate technique, sessile drop and the captive bubble. The captive bubble which has been used in this work, can be described briefly as an air bubble is introduced into liquid reservoir beneath a submerged sample of NF membrane.
Technically, the air bubble released from a syringe needle travels upward to the wet NF membrane surface where it settles to form at contact angle.

Contact angle measurements were obtained using a contact angle kit (Figure 9.1) equipped with a compact canon power shot EOS digital still camera with built-in flash zoom, optical image stabilizer and total 15 megapixel high sensitivity sensor combined with image processor to enhanced image quality.

Three contact angles were measured for each virgin NF membrane in every testing solution. Each contact angle was the average of the left and right contact angles analysed using software and the reported value (result) is the average of three measured contact angles (of scatter less than 5%).

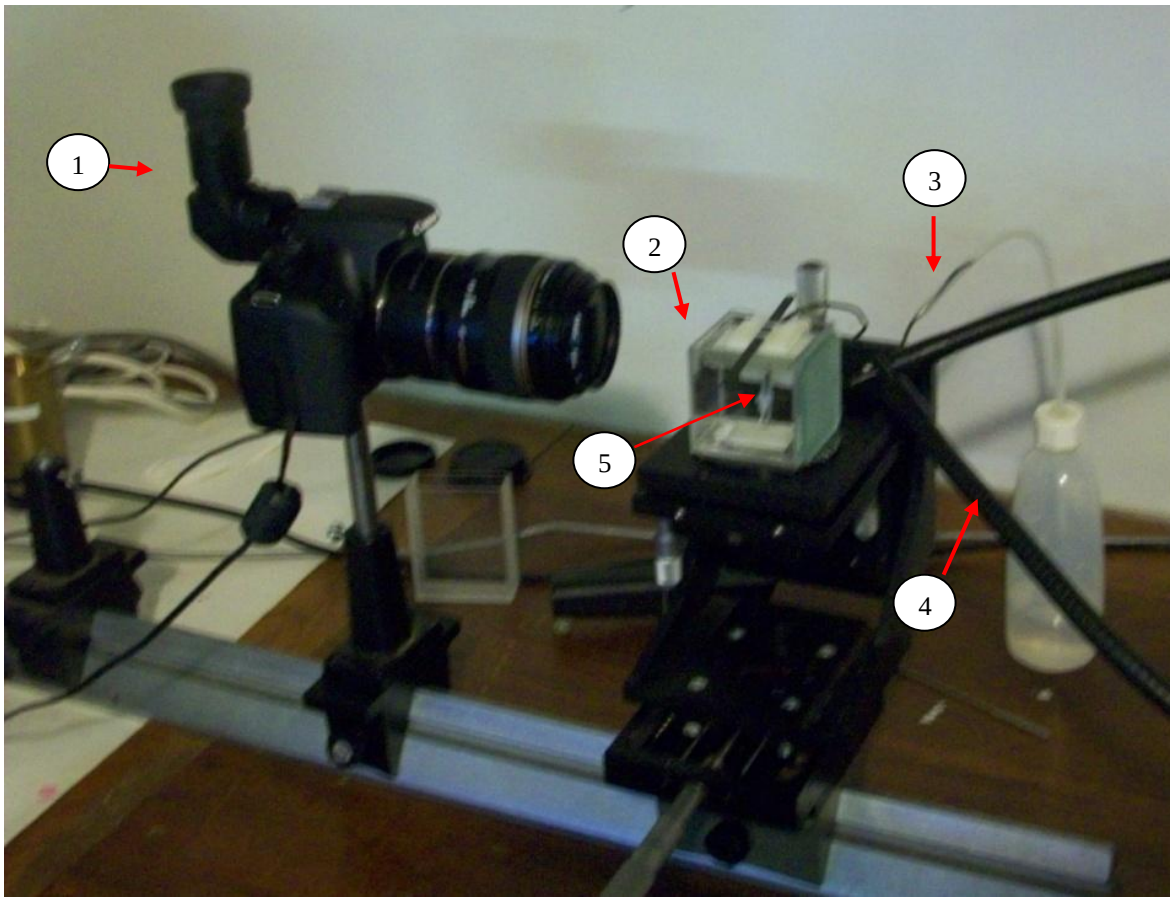

Figure 9.1 Contact angle measuring kit equipments, 1. digital camera, 2. NF membrane holder, 3. air hose, 4. adjustable light beam, 5. syringe needle.

2.2 Sample preparation:

Each NF membrane sample before exposure to any testing solution was dipped in ethanol for 20 minutes followed by distilled water rinsing. This treatment is recommended by membrane manufacturers to open the pores of the material.

A glass plate was used to clamp the sample, and then submerged into the testing solution for 5 minutes at room temperature before introducing the air bubble. Individual air bubble was introduced to the samples and measured.

2.3 Software:

Contact angle images have been processed as ImageJ file (a general purpose free image-processing package - [http://imagej.en.softonic.com/]). Then, each image has been computationally analysed using the snake analysis plugin option called DropSnake.

Snake analysis for contact angle measurement is widely used in computer assisted tools. It provides a way to ensure the smoothness constraint of the curve without assumptions by adapting segmentation fashion with minimum curvature property, obtained by a piecewise polynomial fit allowing a good description of the air bubble [135].

The best fitting line for each photo based on (almost) equal right and left contact angles has been recorded as shown in Figure 9.2.

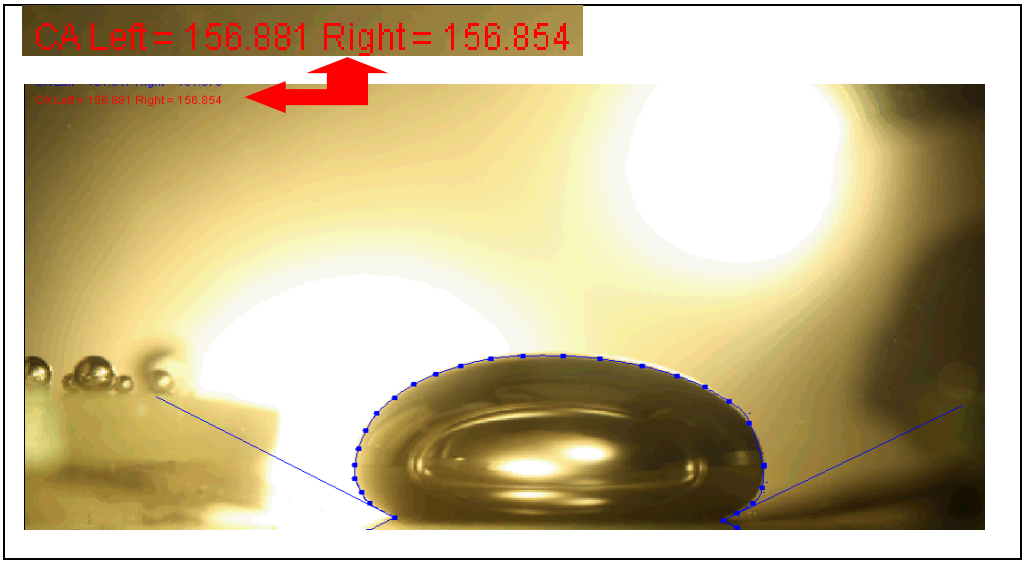

Figure 9.2 Example of snake analysis data output for contact angle measurements. (Photo of NF D membrane in ethylene-glycol).

In order to understand the numerical value of the measured contact angle provided by the software as shown in Figure 9.2, a close-up focus on the right hand side of the air bubble (Figure 9.3) is as follows;

The measured contact angle represents the angle between the air bubble and the membrane surface (θ_{NF-air}). This numerical value should be subtracted from (180^{o}) to represent the contact angle between the liquid and NF surface (θ_{NF-l}), to comply with the accordance of captive bubble technique.

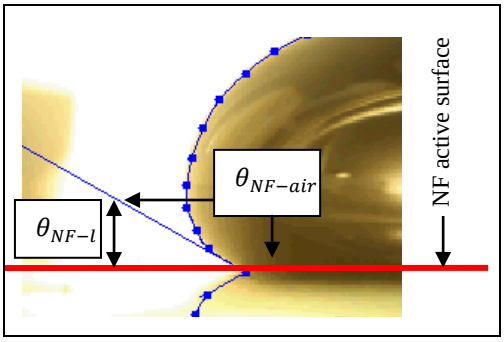

Figure 9.3 Digital image of an air bubble on a wetted NF

2.4 Testing solutions used for contact angle determination for:

2.4.1 NF membranes hydrophilicity/hydrophobicity characterisation:

As the aim of this work is to characterise NF membranes for sulphate rejection in seawater desalination applications, therefore, it is important to investigate the influence of water salinity on their contact angles. Although the contact angles are usually evaluated using pure water, in here, the contact angles of the NF membranes have been measured in; distilled water, ASTM solution of (2000 ppm $MgSO_4$) and simulated seawater of (35,000 ppm NaCl + 2000 ppm $MgSO_4$) to investigate the changes of the NF membrane hydrophilicity/hydrophobicity with the presence of salts.

2.4.2 Surface free energy calculations:

Three reference liquids used to measure the contact angle for the purpose of NF membranes surface energy calculations. Those are; simulated seawater, ethylene-glycol and diiodomethane. Such liquids have been chosen on a basis of discriminating between polar and dispersive components as suggested by one of the most common methods (Van Oss) for the calculation of the surface free energy of polymers, utilising the results of the contact angle measurements [136].

2.5 Converting contact angle measurements into surface free energy:

2.5.1 Theory:

The surface free energy of a solid polymer (NF membranes) is typically characterised through the analysis of series of contact angles of distinguished liquids. The contact angle is related to the key thermodynamic parameters of NF surface by the well known Young equation [136]. Writing Young equation parameters to represent the case of the current research, as follows:

$$\cos\theta_{NF-l} = \frac{\gamma_{NF-air} - \gamma_{NF-l}}{\gamma_{l-air}}$$

Where, θ_{NF-l} is the contact angle between NF surface and the liquid, γ_{NF-air} is the NF-air interfacial energy, γ_{NF-l} is the NF-liquid interfacial energy and γ_{l-air} is the liquid-air interfacial energy, as demonstrated in Figure 9.4.

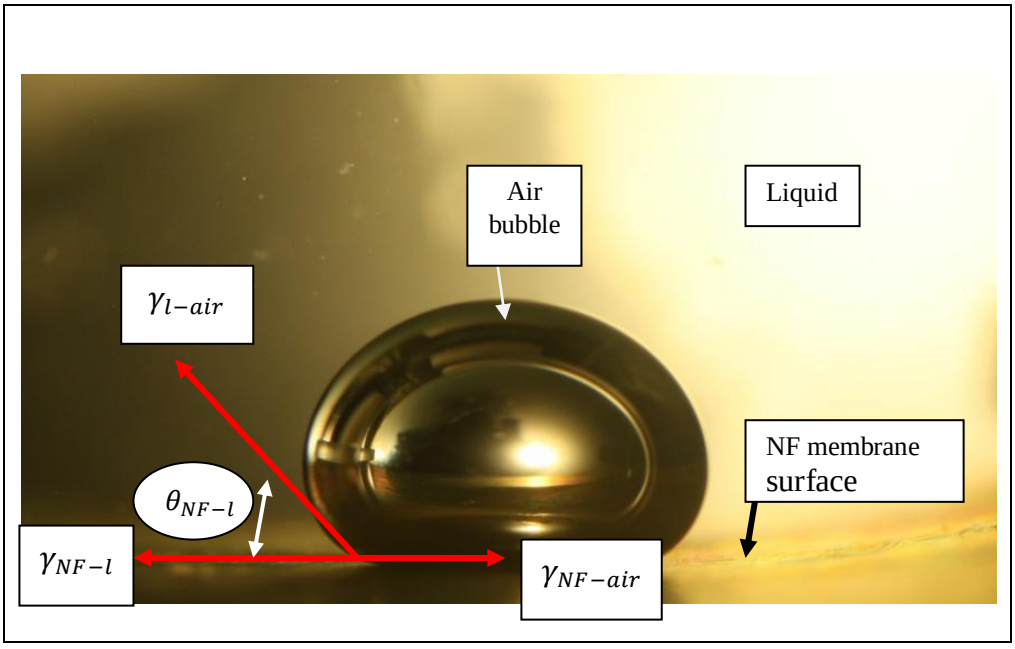

Figure 9.4 Surface free energies components

The surface energies related to the NF membrane are based on the splitting of surface free energy into two components [137]:

$$\gamma = \gamma^{LW} + \gamma^{P}$$

Where, γ^{LW} is the dispersive component and is associated with the Van Der Waals electro-dynamic long-range interactions forces [138].

The second parameter of the equation $\gamma^{p}$is the polar component. The polar component is defined as a function of an acid-base model or electron-acceptor/electron-donor as it represents polar forces based on short-range interactions (acid-base) such as hydrogen bonds constitute. The polar component is considered to equal:

$$\gamma^{P} = 2\sqrt{\gamma^{P+}}\sqrt{\gamma^{P-}}$$

Where the basic component, γ^{P-}, and the acidic component, γ^{P+}, are associated with the acid-base interactions.

Consequently, the surface free energy components along with the measured contact angle can be written using the Young equation as [136,139]:

$$\frac{1}{2}\,\gamma_l(1+\cos\theta_{NF-l}) = \sqrt{\gamma_l^{LW}\gamma_{NF}^{LW}} + \sqrt{\gamma_l^{p+}\gamma_{NF}^{p-}} + \sqrt{\gamma_l^{p-}\gamma_{NF}^{p+}}$$

Where θ_{NF-l} is the static contact angle on the NF formed at the three-phase interface between membrane active surface, liquid, and air phases (Figures 9.3 and 9.4), γ_l is the liquid total surface energy, and $\gamma_l^{LW}, \gamma_l^{p-}, \gamma_l^{p+}, \gamma_{NF}^{LW}, \gamma_{NF}^{p-}\gamma_{NF}^{p+}$ are the dispersive, basic and acidic surface energy components of the liquid and of the NF membrane respectively. To calculate the three components of the surface free energy of the NF membrane, this can be numerically analysed through set of three known polar and apolar liquids whose properties are known and well characterised and commonly used in the literature. From the measurement of their contact angle, a set of three non-linear equations with three unknowns is derived.

2.5.2 Calculation approach:

In order to improve the quality and reliability of the calculation, three distinctive fluids, one primary dispersive, one acidic and one with basic nature are used. In this work, the three liquids have been chosen to compromise the satisfaction of liquids differences and to meet the research target (Table 9.1) are simulated-seawater (SW), ethylene-glycol (EG) and diiodomethane (D), having the following properties:

Liquid	γ_l (liquid surface energy)	γ_l^{LW} (dispersive component)	γ_l^{P} (polar component)	γ_l^{P+} (polar-acidic component)	γ_l^{P-} (polar-basic component)
simulated-seawater	72.8	21.8	51	25.5	25.5
ethylene-glycol	48	29	19	1.92	47
diiodomethane	50.8	50.8	0	0	0

Table 9.1 Total, polar and dispersive components of the three liquids used for surface energy calculations all in mJ/m^2 [139].

Thus, as the three known properties liquids for measuring the contact angle to calculate the surface free energy of the NF membranes under study was selected, a set of three equations can be solved for each NF membrane from the measured contact angles. The following analysis has been undertaken to enable the solution of the three equations for each NF surface free energy as follows.

I. Seawater equation:

$$36.4\ (1+\cos\theta_{SW,NF}) = \sqrt{21.8\ \gamma_{NF}^{LW}} + \sqrt{25.5\ \gamma_{NF}^{p-}} + \sqrt{25.5\ \gamma_{NF}^{p+}}$$

II. Ethylene-Glycol equation:

$$24\ (1+\cos\theta_{EG,NF}) = \sqrt{29\ \gamma_{NF}^{LW}} + \sqrt{1.92\ \gamma_{NF}^{p-}} + \sqrt{47\ \gamma_{NF}^{p+}}$$

III. Di-Iodomethane equation:

$$25.4\ (1+\cos\theta_{D,NF}) = \sqrt{50.8\ \gamma_{NF}^{LW}}$$

2.5.3 Solving procedure:

1. From Di-Iodomethane equation:

$$25.4\ (1+\cos\theta_{D,NF}) = \sqrt{50.8\ \gamma_{NF}^{LW}}$$

γ_{NF}^{LW} can be calculated directly by rearranging the parameters in the equation as follow:

$$\gamma_{NF}^{LW} = \left(\frac{25.4\ (1+\cos\theta_{D,NF})}{\sqrt{50.8}}\right)^2$$

2. Then, both Seawater and Ethylene-Glycol equations can be solved simultaneously for γ_{NF}^{p-} and γ_{NF}^{p+} as follow:

2.1. From Seawater equation:

$$\sqrt{25.5\ \gamma_{NF}^{p-}} + \sqrt{25.5\ \gamma_{NF}^{p+}} = 36.4\ (1+\cos\theta_{sw,NF}) - \sqrt{21.8\ \gamma_{NF}^{LW}}$$

$$\div \sqrt{25.5}$$

$$\sqrt{\gamma_{NF}^{p-}} + \sqrt{\gamma_{NF}^{p+}} = \frac{36.4\ (1+\cos\theta_{sw,NF}) - \sqrt{21.8\ \gamma_{NF}^{LW}}}{\sqrt{25.5}}$$

2.2. And from Ethylene-Glycol equation:

$$\sqrt{1.92\ \gamma_{NF}^{p-}} + \sqrt{47\ \gamma_{NF}^{p+}} = 24\ (1+\cos\theta_{EG,NF}) - \sqrt{29\ \gamma_{NF}^{LW}}$$

$$1.38\sqrt{\gamma_{NF}^{p-}} + 6.85\sqrt{\gamma_{NF}^{p+}} = 24\ (1+\cos\theta_{EG,NF}) - \sqrt{29\ \gamma_{sNF}^{LW}}$$

$$\div 1.38$$

$$\sqrt{\gamma_{NF}^{p-}} + 4.96\sqrt{\gamma_{NF}^{p+}} = \frac{24\ (1+\cos\theta_{EG,NF}) - \sqrt{29\ \gamma_{NF}^{LW}}}{1.38}$$

2.3. Hence, to solve for γ_{NF}^{p+}:

(Ethylene-Glycol equation) – (Seawater equation) =

$$\left(\sqrt{\gamma_{NF}^{p-}} + 4.96\sqrt{\gamma_{NF}^{p+}} = \frac{24\,(1+\cos\theta_{EG,NF}) - \sqrt{29\,\gamma_{NF}^{LW}}}{1.38}\right)$$

$$-\left(\sqrt{\gamma_{NF}^{p-}} + \sqrt{\gamma_{NF}^{p+}} = \frac{36.4\,(1+\cos\theta_{sw,NF}) - \sqrt{21.8\,\gamma_{NF}^{LW}}}{\sqrt{25.5}}\right)$$

$$\xrightarrow{yields} 3.96\sqrt{\gamma_{NF}^{p+}} = \frac{24\,(1+\cos\theta_{EG,NF}) - \sqrt{29\,\gamma_{NF}^{LW}}}{1.38} - \frac{36.4\,(1+\cos\theta_{sw,NF}) - \sqrt{21.8\,\gamma_{NF}^{LW}}}{5.05}$$

$$\gamma_{NF}^{p+} = \left(\left[\frac{24\,(1+\cos\theta_{EG,NF}) - \sqrt{29\,\gamma_{NF}^{LW}}}{1.38} - \frac{36.4\,(1+\cos\theta_{sw,NF}) - \sqrt{21.8\,\gamma_{NF}^{LW}}}{5.05}\right] \Big/ 3.96\right)^2$$

2.4. And to solve for γ_{NF}^{p-}:

From seawater equation:

$$\gamma_{NF}^{p-} = \left(\frac{36.4\,(1+\cos\theta_{sw,NF}) - \sqrt{21.8\,\gamma_{NF}^{LW}}}{5.05} - \sqrt{\gamma_{NF}^{p+}}\right)^2$$

3. Then, finding γ_{NF}^{p} using the equation:

$$\gamma_{NF}^{p} = 2\sqrt{\gamma_{NF}^{p-}}\sqrt{\gamma_{NF}^{p+}}.$$

4. Finally, NF total surface free energy calculated as:

$$\gamma_{NF} = \gamma_{NF}^{LW} + \gamma_{NF}^{p}$$

Summarising the procedure for NF surface free energy calculations, the sequence for equations to be solved are as follow:

$$1)\quad \gamma_{NF}^{LW} = \left(\frac{25.4\,(1+\cos\theta_{D,NF})}{7.127}\right)^2$$

$$2)\quad \gamma_{NF}^{p+} = \left(\frac{24\,(1+\cos\theta_{EG,NF}) - \sqrt{29\,\gamma_{NF}^{LW}}}{1.38} - \frac{36.4\,(1+\cos\theta_{sw,NF}) - \sqrt{21.8\,\gamma_{NF}^{LW}}}{5.05} \Big/ 3.96\right)^2$$

$$3)\quad \gamma_{NF}^{p-} = \left(\frac{36.4\,(1+\cos\theta_{sw,NF}) - \sqrt{21.8\,\gamma_{NF}^{LW}}}{5.05} - \sqrt{\gamma_{NF}^{p+}}\right)^2$$

$$4)\quad \gamma_{NF}^{p} = 2\sqrt{\gamma_{NF}^{p-}}\sqrt{\gamma_{NF}^{p+}}$$

$$5)\quad \gamma_{NF} = \gamma_{NF}^{LW} + \gamma_{NF}^{p}$$

3. Results and discussion:

3.1 Contact angle results in distilled water, ASTM solution and simulated-seawater SW:

The following Table 9.2 lists the contact angle (CA) results of the NF membranes.

NF membrane	CA (^{o}) in distilled water	CA (^{o}) in ASTM	CA (^{o}) in SW
A	34.0	33.2	33.0
B	53.2	51.0	50.2
C	40.5	38.8	38.0
D	36.6	35.3	34.0
E	56.0	54.7	53.6
F	33.1	31.9	31.3
G	39.4	37.3	37.0
H	45.8	42.4	42.1

Table 9.2 Contact angle results of NF membranes in different salinity solutions

The data on Table 9.2 is illustrated for clarity in bar chart in Figure 9.5 displays the reduction in contact angle values of the NF membranes. As shown, for all the membranes, the corresponding contact angle has gradually decreased from distilled water to ASTM solution to simulated seawater. Reflecting the moderate enhancement in NF hydrophilicity influenced by the presence of salts.

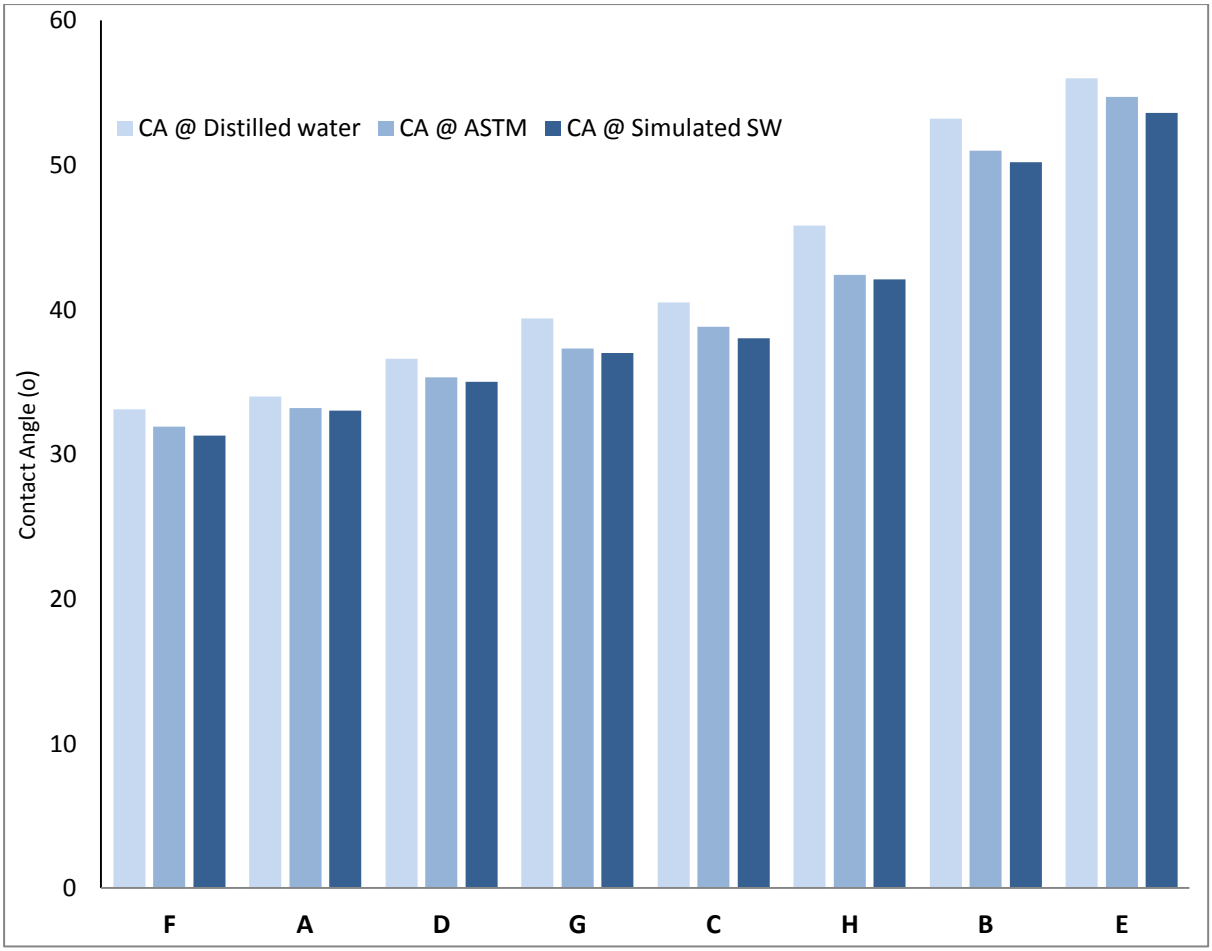

Figure 9.5 Contact angle results of the eight NF membranes in distilled water, ASTM and simulated seawater (note: NF membranes are in order from highest to lowest flux according to ASTM test)

A large contact angle corresponds to a hydrophobic surface, where less wettability occurs on the membrane surface. Whereas, small contact angle indicates more hydrophilic surface, i.e. more wettability takes place. Figure 9.6 shows an example of contact angle shape on hydrophilic and hydrophobic NF membranes tested here. Those photos clearly demonstrate the wettability behaviour of different NF membranes (in terms of surface hydrophilicity). As more hydrophilic NF membrane (identified by low contact angle) will allow more water to spread on its surface, hence, expecting to make it easier for water molecules to penetrate NF pores. On the other hand, hydrophobic NF membrane is less wetted; therefore, water permeability will decrease in comparison to hydrophilic membrane.

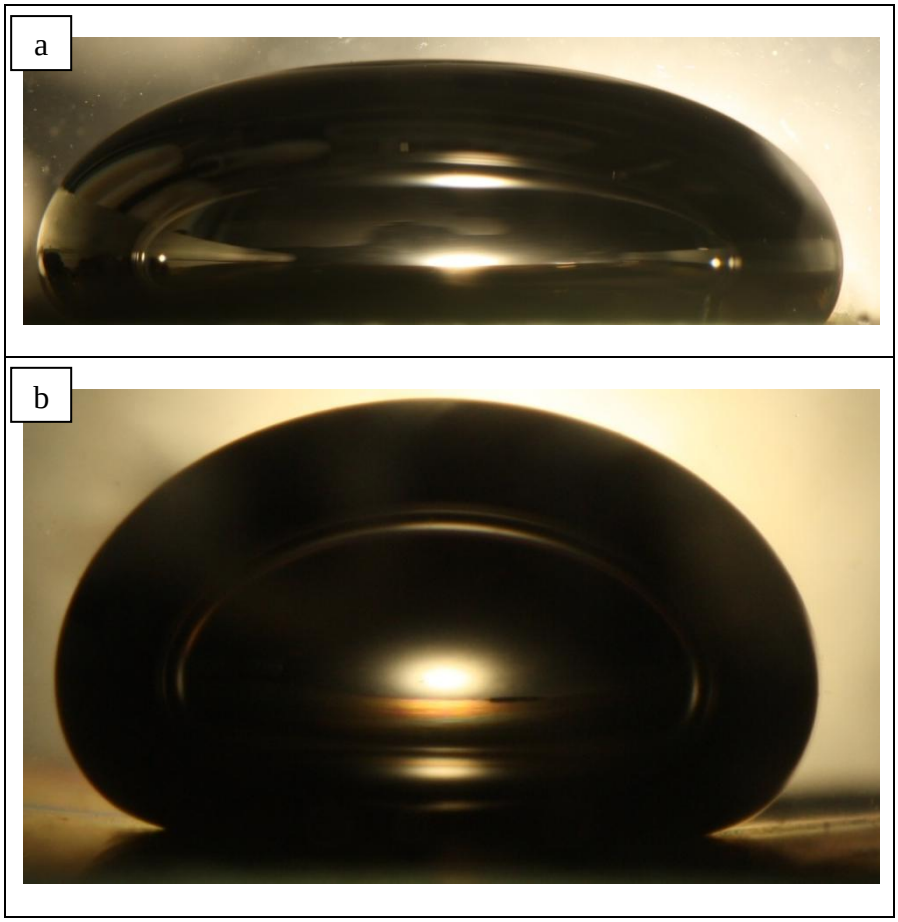

Figure 9.6 Contact angle shape on: (a) hydrophilic NF, (b) hydrophobic NF.

Over the entire NF membranes under study, contact angle experimental results show that introducing salts to pure water (either by adding $MgSO_4$ for ASTM solution or $MgSO_4$ and NaCl for simulated seawater solution) slightly decreases the contact angle (i.e. more wettability takes place on NF membrane surface). It suggests that the hydrophilicity of NF membranes slightly increases in saline water. This behaviour is in agreement with recent research results, characterising three commercial RO membranes [140].

The possible explanations for this phenomenon are:

1. Due to the surface nature of NF membranes, having negative charge (confirmed by charge density calculations based on membrane potential measurements – please refer to chapter 11) and the high ability to reject divalent anions (confirmed during phase one of experimental work – please refer to chapter 7). For saline water having salt(s) of NaCl and/or $MgSO_4$, some cations are adsorbed and enriched on the membrane surface. These adsorbed cations can orient surrounding water molecules. Thereby, the interactions between the interfacial water molecules and NF surface are strengthened

because of the formation of a layer of adsorbed cations on membrane surface [140]. As a result, more wettability occurs, suggesting the slight improvement of NF surface hydrophilicity in saline water.

2. Thermodynamically, this can be explicated as the increased ordering of the interfacial water molecules with NF membrane surface decreases interfacial entropy (assuming no change in interfacial enthalpy) as a result, increases free energy [101,141], which again can justify the slight development in NF membrane surface hydrophilicity.

3.2 Contact angle results in ethylene-glycol and diiodomethane:

Utilising contact angles of three different liquids with known dispersive and polar components has been adopted in order to calculate the surface free energy of the NF membranes.

The contact angles of the three chosen liquids (seawater, diiodomethane and ethylene-glycol) as described in section 2.4.2 of this chapter are listed in Table 9.3.

NF	θ_{SW}	θ_D	θ_{EG}
A	33.0	28.9	22.4
B	50.2	36.1	31.8
C	38.0	33.5	26.0
D	34.0	29.3	23.2
E	53.6	39.9	32.3
F	31.3	25.7	18.9
G	37.0	32.2	25.6
H	42.1	34.6	28.1

Table 9.3 Contact angle measurements of NF membranes in seawater, diiodomethane and ethylene-glycol

As shown, for all the NF membranes, the higher contact angle values were obtained for seawater, followed by diiodomethane and finally ethylene-glycol with the same relative trends between the membranes in the three solutions.

The variation in the contact angle values of the NF membranes was the highest in seawater, with a range between 31.3^{o} for NF F (being most hydrophilic) and 53.6^{o} for NF E (being most hydrophobic). The lowest contact angle range between the membranes was in ethylene-glycol, with a range between 18.9^{o} – 32.3^{o} for NF F and E respectively.

3.3 Correlation between NF membrane filtration performance and its corresponding contact angle:

Contact angle measurements indicate that NF E is the most hydrophobic membrane having the largest contact angle in all solutions. In contrast, NF F is the most hydrophilic, having the smallest contact angle in all solutions. While the rest of the tested NF membranes fall in-between.

In order to correlate the hydrophilicity/hydrophobicity represented by the contact angle of the NF membranes to its filtration performance for the purpose of critical characterisation, Figure 9.7 shows a relation between NF membrane permeability and its contact angle. Figure 9.7 is based on data of permeability results in ASTM testing environment (see chapter 7, section 3.1.1 for details) and the contact angle values in ASTM solution (Table 9.2).
This can explain the difference in permeability among the tested NF membranes. The highest contact angle was measured for NF E at 54.7^{o}, therefore, it is the most hydrophobic among the tested membranes having the lowest flux of 18.30 L/hr.m^{2}. Then, it is apparent that as the measured contact angle value decreases, indicating advancement in NF membranes hydrophilicity, the corresponding NF flux increases. The lowest contact angle of 31.9^{o} has been measured for NF F membrane; therefore, it is the most hydrophilic with the highest flux of 61.09 L/hr.m^{2}.

NF A is the second most hydrophilic (and of permeability order) among the eight NF membranes. Having a contact angle of 34.1^{o}, which is less than 7% increase to the measured contact angle of NF F membrane. However, the difference in permeate flux between NF F (of 61.09 L/hr.m^{2}) and NF A (of 34.10 L/hr.m^{2}) is of substantial magnitude. Indicating that, although, NF hydrophilicity/hydrophobicity is affecting membrane permeability;

nevertheless, it counts as one of many factors influencing NF permeability. This will be investigated in further phases of this research.

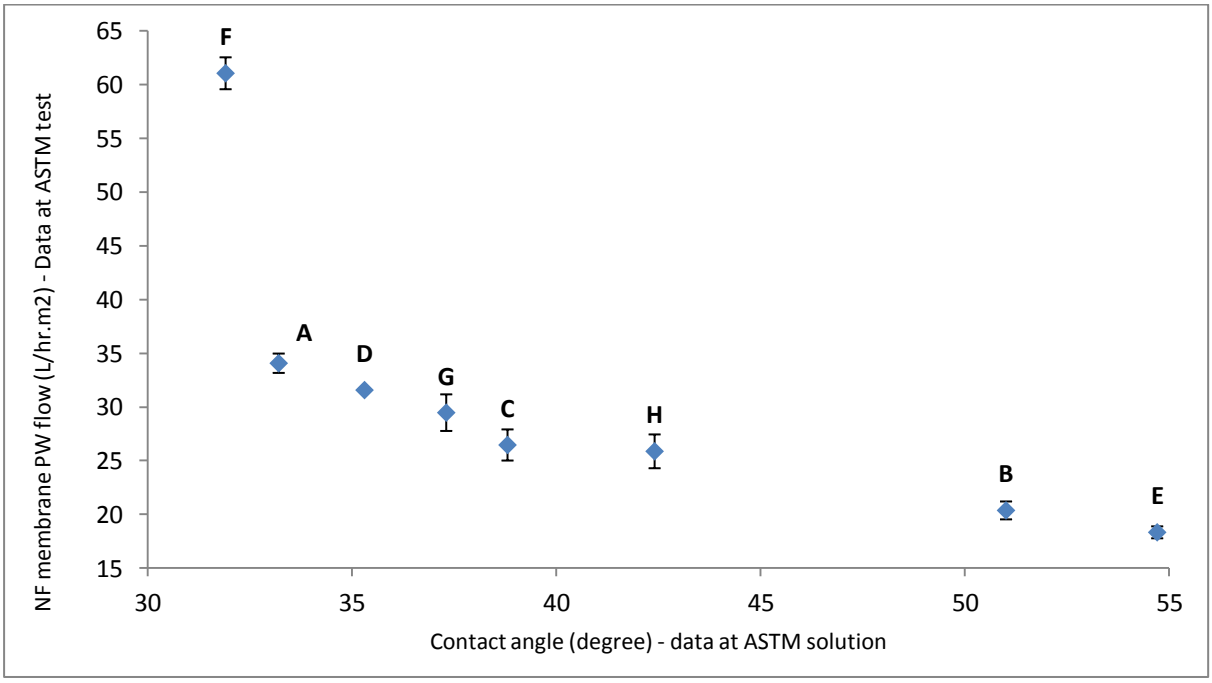

Figure 9.7 The relation between NF flux and its contact angle.

Such correlation between NF membrane hydrophilicity represented by contact angle and its permeation ability can be (generally) interpreted as follows: as the NF membrane surface is more hydrophilic and wettable, the contact angle drops and therefore, more water passage takes place.

Expanding this explanation sequentially as:

1. High hydrophilic NF membrane surface (indicating by low contact angle), provides more wettability to water molecules.
2. Hence, the ionic interaction between water molecules and the negatively charged NF surface (confirmed in charge density calculations part of this work – chapter 11) increase.
3. Therefore, NF flux increases in comparison with less hydrophilic (i.e. hydrophobic) membrane.

In comparison, no clear relationship between NF membrane sulphate rejection ability with being either hydrophilic or hydrophobic was found, as shown in Figure 9.8.

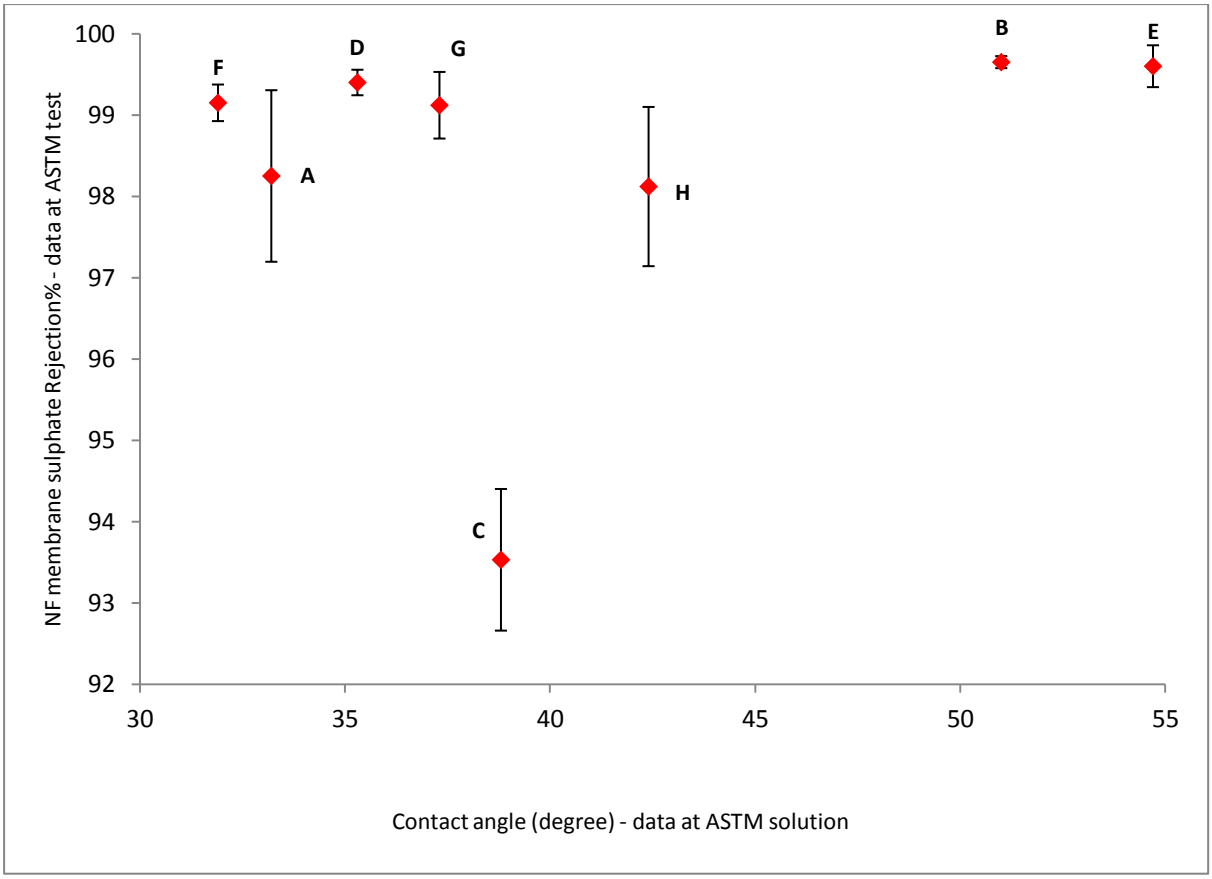

Figure 9.8 NF membrane sulphate rejection percentages and its Contact angle in ASTM

3.4 Surface free energy of the NF membranes:

Extending the characterisation process for the surface hydrophilicity/hydrophobicity of the tested NF membranes towards optimum utilisation for sulphate rejection applications in seawater desalination (and oil/gas separation applications), a further step in this research is undertaken by undertaking surface free energy calculations based on contact angle measurements.

As explained in section 2.5, for the purpose of calculating surface free energy, this involved measuring the contact angle on three distinctive fluids. Those are: simulated seawater, ethylene-glycol and diiodomethane (results are listed in Table 9.3). This comprised using a set of three non-linear equations with three unknowns. As solving the set of equations will lead to the total surface energy of the NF membranes. Moreover, it will yield its constituents components (dispersive, polar-acidic and polar-basic).

For the purpose of demonstrating the calculation scheme, NF A membrane surface free energy calculations are detailed.

From Table 9.3, the contact angle measurements for NF A membrane are; 33.0°, 28.9° and 22.4° in seawater, diiodomethane and ethylene-glycol respectively.

Hence, calculations are carried out in the following sequence (please refer to section 2.5.3 for equations derivative):

1. $\gamma_{NF}^{LW} = \left(\frac{25.4\,(1+\cos\theta_{D,NF})}{7.127}\right)^2 = \left(\frac{25.4\,(1+\cos 28.9)}{7.127}\right)^2 = 44.67\ mJ/m^2$

2. $\gamma_{NF}^{p+} = \left(\frac{24\,(1+\cos\theta_{EG,NF}) - \sqrt{29\,\gamma_{NF}^{LW}}}{1.38} - \frac{36.4\,(1+\cos\theta_{sw,NF}) - \sqrt{21.8\,\gamma_{NF}^{LW}}}{5.05} \Big/ 3.96\right)^2 =$

$$\left(\frac{24\,(1+\cos 22.4) - \sqrt{29*(44.67)}}{1.38} - \frac{36.4\,(1+\cos 33.0) - \sqrt{21.8(44.67)}}{5.05} \Big/ 3.96\right)^2 = 0.006\ mJ/m^2$$

3. $\gamma_{NF}^{p-} = \left(\frac{36.4\,(1+\cos\theta_{sw,NF}) - \sqrt{21.8\,\gamma_{NF}^{LW}}}{5.05} - \sqrt{\gamma_{NF}^{p+}}\right)^2$

$$= \left(\frac{36.4\,(1+\cos 33.0) - \sqrt{21.8*(44.67)}}{5.05} - \sqrt{0.006}\right)^2 = 48.91\ mJ/m^2$$

4. $\gamma_{NF}^{p} = 2\sqrt{\gamma_{NF}^{p-}}\sqrt{\gamma_{NF}^{p+}} = 2\sqrt{48.91}\sqrt{0.006} = 1.108\ mJ/m^2$

5. $\gamma_{NF} = \gamma_{NF}^{LW} + \gamma_{NF}^{p} = 44.67 + 1.108 = 45.78\ mJ/m^2$

The exact same procedure has been followed to calculate the total surface free energy and its constituents of the NF membranes (detailed in Appendix 3). Results are shown in Table 9.4.

NF	γ_{NF}^{LW} dispersive component (mJ/m^2)	γ_{NF}^{P+} polar-acidic component (mJ/m^2)	γ_{NF}^{P-} polar-basic component (mJ/m^2)	γ_{NF}^{P} polar component (mJ/m^2)	γ_{NF} NF membrane total surface free energy (mJ/m^2)
A	44.67	0.006	48.91	1.10	45.78
B	41.52	0.086	31.04	3.27	44.79
C	42.71	0.028	44.56	2.26	44.98
D	44.51	0.006	48.06	1.13	45.65
E	39.66	0.218	26.99	4.85	44.52
F	45.90	0.005	49.37	1.07	46.98
G	43.29	0.017	45.57	1.76	45.06
H	42.22	0.043	40.19	2.65	44.87

Table 9.4 Calculated surface free energy components of all tested NF membranes

The calculated surface energy components evaluated in mJ/m^2 of all NF membranes under study varied from; (44.52 – 46.98) for the total surface free energy, (39.66 – 45.90) for the dispersive component, (1.07 – 4.85) for the polar component, (0.005 – 0.218) for the polar acidic component and (26.99 – 49.37) for the polar basic component.

Such values fall in the reported range of almost all known polymer surfaces [142].

The trends in surface free energy results and its components listed in Table 9.4 are shown in Figure 9.9.

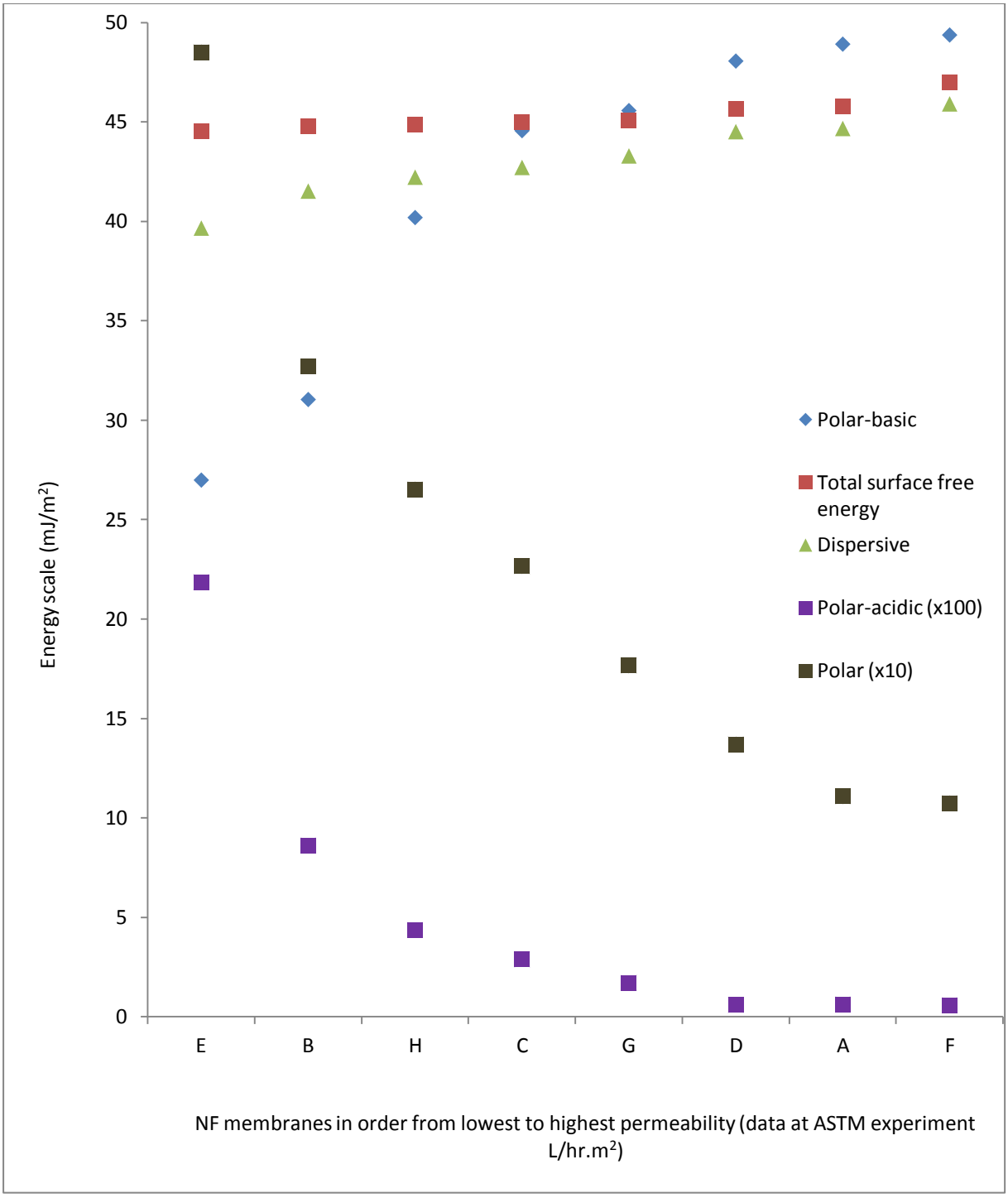

Figure 9.9 NF permeability correlation with surface free energy components.

As shown, the relation between NF membrane permeability performance and its surface energy constituents can be read as follows.

Over the range of NF membranes under investigation, an increase in total surface free energy, dispersive and polar-basic components, and a decrease in the polar and polar-acidic components are associated with an increase in NF flux.

An in-depth analysis of the role played by each surface energy component in NF performance, more particularly its water flux, is provided next.

NF membrane surface energy were characterised in terms of total surface energy (γ_{NF}) and its corresponded contributors. The dispersive component (γ_{NF}^{LW}) and the polar component also known as the acid–base component (γ_{NF}^{P}). The polar component is comprised of two complementary parameters; the acidic (electron-acceptor) (γ_{NF}^{P+}) and the basic (electron-donor) (γ_{NF}^{P-}) surface energy components.

The polar component interactions are most accurately defined as interactions resulting from the sharing of electrons (or protons) between NF surface polymer functional groups and other polar molecules [139], water molecules in this research work. The functional groups may serve as either electron acceptors or electron donors. Hence, results could be explained by considering the magnitude of each component. Figure 9.9 shows that an increase in (γ_{NF}^{P-}) and a decrease in (γ_{NF}^{P+}) are associated with an increase in water permeability of NF membranes.

Extending the illustration, NF membrane having low polar-acidic and high polar-basic, i.e. its surface tends to function as electron donor, will produce high interfacial interaction energy with water molecules, resulting of more water passage through NF surface. Alternatively, high polar-acidic and low polar-basic causes a reduction in the magnitude of interfacial interaction, hence, the amount of water molecules passage through NF will reduce.

In here, NF F membrane with the highest flux (of 61.09 L/hr.m^2 at ASTM test) among the tested NF membranes is having the lowest value of (γ_{NF}^{P+}= 0.005 mJ/m^2) and highest (γ_{NF}^{P-}= 49.37 mJ/m^2). In contrast, E membrane represents the converse behaviour.

For the dispersive component of NF surface energy, which is defined as function of dispersion forces and is attractive for most systems, hence, it will determine NF surface affinity for water (i.e., its hydrophilicity/hydrophobicity). In other words, high dispersive component value is a characteristic of a hydrophilic membrane [139], and the dispersion forces relate closely to the wetting ability for the NF membrane [142].

As the results reveal, the higher (γ_{NF}^{LW}) value is, the more water passage takes place through NF surface. This can be explained as water structuring is induced near to NF surface, as water molecules form electro-dynamic long-range interactions forces, which is a feature of the dispersive component.

Finally, considering total surface energy (γ_{NF}) influence on NF performance. Although NF membranes order from highest to lowest in terms of permeability and total surface energy are matching. However, changes in the total surface energy of the eight NF membranes are narrow (46.98 – 44.52 mJ/m^2), in comparison to the broad differences in permeate flux (61.09 – 18.30 L/hr.m^2). This implies that, NF permeability performance in saline water does not solely depend on membrane surface characteristics represented by surface energy. This observation is further supported by the next phases of the work for a better understanding of NF filtration performance in desalination practices for optimum utilisation.

4. Conclusions:

This part of the current work has expanded the previous work of the filtration performance evaluation of the eight membranes under study by relating the preceding-determined performance parameters of NF membranes to the contact angle and the calculated surface free energy. Measurements of contact angle and surface energy calculations have yielded a clear correlation between NF permeate flux and both contact angle and surface energy but no relation to sulphate rejection.

Usually, NF membranes surface (hydrophilicity/hydrophobicity) is characterised based on the contact angle of pure (distilled) water [89,90,144]. However, the present work suggests that, to meet the purpose of NF characterisation for seawater desalination, contact angle measurements have been carried out in ASTM and simulated seawater solutions. Results have revealed that presence of salts does affect the hydrophilicity of NF membranes. In a way that, membrane surface became more hydrophilic (i.e. more wettable) indicted by slight reduction in contact angle with introducing either $MgSO_4$ or NaCl and $MgSO_4$ in comparison to distilled water.

Although, NF performance (water flux) could be related to surface wettability as determined by contact angle alone, nevertheless, the specific nature of surface free energy constituents must be consider. Further testing and analysis with measurements in other distinctive fluids, followed by surface energy mathematical calculations has revealed that the ionic interaction between water molecules and NF surface increases as the hydrophilicity increases. Due to the fact that NF active surface polymer material of fabrication acts in a way of electron donor defined by an increase in polar-basic component (γ_{NF}^{P-}) and electron acceptor defined by a

decrease in polar-acidic component (γ_{NF}^{P+}). This increase in electron donor functionality and decrease in electron acceptor functionality is related to NF active surface polymer concentration [143].

Accordingly, as the NF active surface polymer concentration decreases, this results in decreasing electron acceptor functionality and increasing electron donor functionality, hence NF surface become more hydrophilic represented by low contact angle. Consequently, the ionic interactions between H_2O molecules and NF surface increases as well as wettability, explaining the increase in permeate flux over the range of NF membranes under study.

In conclusion, from desalination point of view, as contact angle measurements show that saline water causes slight improvement of NF membranes hydrophilicity. Explained by considering the calculated surface energy constituents, as for a more hydrophilic NF leading to strengthens the interactions between the interfacial water molecules and membrane surfaces (influenced by surface polymer concentration) which will increase the permeate.

Therefore, for NF membranes to be implemented in desalination applications as mean of pretreatment a suggestion based on the current findings; that NF manufacturers need to optimise membrane polymer concentration during its fabrication process to meet the target purpose.

Finally, to this end, contact angle studies followed by surface energy calculations have been able to generally characterise the hydrophilicity/hydrophobicity of the NF membranes. However, another factor that affects NF performance is the relative magnitude of surface roughness, which is not accounted for by contact angle results. Therefore, the next phase of the research work will involve the usage of Atomic Force Microscopy (AFM) in order to provide qualitative measurements of the surface roughness of the NF membranes, to perceive NF performance towards the research target.

Chapter 10: ATOMIC FORCE MICROSCOPY (AFM) STUDIES AND ANALYSIS

1. Introduction:

1.1 Overview:

It has been demonstrated in the previous chapter 9 that contact angle analysis followed by surface free energy calculations accurately characterised the general hydrophobicity/ hydrophilicity of the NF membranes surfaces. In this chapter, the consideration of NF membranes is extended by atomic force microscopy (AFM) measurements in order to critically characterise the morphology parameters and incorporate into the NF membranes' performance.

In general, AFM has received considerable attention within the membrane research community for more than a decade and is widely used and accepted as a viable tool and method to investigate and characterise membrane surface roughness and determining membrane physical morphology [85,87,88,107,146-150,153,154,159,161]. Moreover, a study [148] concluded that over a range of available scanning devices for membranes surface characterisation, AFM is the most adequate in obtaining information on membranes surface roughness and imaging three-dimensional (3-D) display of membrane surfaces.

For NF membrane in particular, recently AFM has been intensively employed to characterise the morphology of NF membranes in order to measure membrane surface roughness and to study hydrophobicity focusing on TFC membranes [85,88,149,153,156]. Also, it has been shown that AFM output data can be related to membrane formation parameters and separation performance [77,85,151,152]. In addition, a study discussed briefly some of the general issues pertaining to the use of standalone AFM for improvement in nanofiltration membrane research towards its implementations as a pretreatment for seawater desalination [154].

1.2 Brief description of AFM technology:

The atomic force microscope (AFM) is one of the family of scanning probe microscopes. The imaging technique consists of a mechanical device, which is able to measure very small forces when atoms or molecules come together, so it was named atomic force microscopy. A critical part of the device called the cantilever is a plate spring, which is fixed at one end. At

the other end it supports a pointed tip. The tip can be moved across a sample surface line by line [145]. AFM uses the flexible cantilever as a type of spring to measure the force between the tip and the sample. The basic idea of an AFM is that the local attractive or repulsive force between the tip and the sample is converted into bending, or deflection, of the cantilever. The cantilever deflection must be detected in some way and converted into an electrical signal to produce the images. Imaging quality depends on the radius and angle of the end of the cantilever tip [155]. AFM has the capability to provide both qualitative and quantitative information on many physical properties of membrane morphology, such as surface texture and roughness. Also, it can produce topographical images in 2D and 3D of membrane surface morphology from micrometer-size down to the atomic level whether in air or in liquid with the ability to scan from 1 nanometer to 8 micrometres. AFM scans are obtained by measuring changes in the magnitude of the interaction between the scanning probe and the specimen surface as the surface is scanned beneath the probe [145,155,160].

In this research work, the AFM spectra were recorded on a JPK NanoWizard® II AFM system (JPK Instruments AG) shown in Figure 10.1, with imaging mode of intermittent contact in fluid in which to be employed when oscillating the cantilever in water or any other fluid [107,155,156] (ASTM solution in here). Triangular silicon nitride cantilever with a spring constant in the range of 0.05 – 0.3 N/m are suitable for this type of AFM application [155]. Therefore, knowing that the geometry and material of the chosen cantilever contribute to the imaging mode of operation, hence, the most appropriate cantilever for usage in the intermittent contact in fluid mode has been chosen, as follow:

- Veeco, model no: MLCT
- Material: non-conductive silicon nitride
- Cantilever: T: 0.59 – 0.61 um
- Coating: front side: none, back side: top – 60 um Au/BOT – 15 um Cr
- Resonance frequency 26 -50 KHz , K (spring constant) : 0.1 N/m.

Also, an available feature in the software of fast fourier transform filtering was applied to all images to remove unwanted noise and improve resolution.

Figure 10.1 JPK NanoWizard® II AFM device

2. AFM imaging method and standards adopted to suit this research interest and objectives:

2.1 Mode of operation:

There are three common modes of AFM operation and these are contact mode, non-contact mode and tapping mode. Each can be used to scan a NF membrane surface either in liquid or air [145,155,156]. In the literature, nanofiltration membrane surfaces have been studied using both tapping and contact mode, in different scanning sizes under ambient laboratory conditions and in high purity water to determine the degree of hydrophobicity of the NF membranes under study [107,156]. The studies concluded that, although the absolute roughness values are different for noncontact and tapping mode and for different areas of scanning, nevertheless, no difference is found between the rankings of nanofiltration membranes with respect to their surface roughness. In addition, at small scanning size of 1x1 μm, when imaging with tapping mode in water a number of features were observed which were not observed with the same membrane in air or in contact mode in water [107].

Therefore, as the objective of this work is characterising NF membrane towards sulphate rejection for desalination applications, thus, imaging the samples in ASTM solution, hence, the AFM scanning carried out using tapping mode – (intermittent contact in liquid); in which the cantilever vibrates at a tip-sample distance closer to the region of contact imaging. The following Table 10.1 summarises AFM protocol with justifications as follows:

Chosen AFM parameters	Justification
• Tapping mode	❖ This technique overcomes some of the limitations of other available techniques, when scanning in liquid [155].
• In liquid	❖ As NF samples to be submerged in ASTM solution for evaluation of NF characteristics in uniform environment over the research work.
• Parameters evaluation over 1x1 μm	❖ Small scanning size of 1x1 μm when imaging with tapping mode in water, a number of features can be observed which cannot be observed using other scanning options [107,155].

Table 10.1 Main parameters of the adopted AFM mode of operation

2.2 Sample preparation:

For each of the eight NF membranes under investigation; three samples of $1cm^2$ taken from different parts of the flat sheet was placed onto a glassware test plate with special glue for polymers use (Araldite® Rapid 2K Part A & B). Then, samples were submerged in ASTM solution at room temperature over 24 hrs before imaging.

For improving the accuracy of the results, the measurements of surface roughness were carried out once for the three samples of each NF, taken from different locations of the membrane sheet.

3. AFM results:

3.1 Surface roughness analysis:

AFM can directly facilitate many parameters to quantify NF membrane surface roughness. Those are; average roughness (R_a), root-mean square RMS roughness (defined as the square root of the mean value of the squares of the distance of the points from the image mean value) (Rq) and peak-to-valley height (R_Z), as presented by the following equations [145,157]:

1. average roughness $R_a = \frac{1}{n}\sum_{i=1}^{n} Z_i$
2. root-mean square (RMS) roughness $R_q = \sqrt{\frac{1}{n}\sum_{i=1}^{n} Z_i^2}$
3. or peak-to-valley height $R_Z = Z_{max} - Z_{min}$

Where; *Zi* is height at point *i*, *n* is number of points in the image and *Zmax* and *Zmin* are the highest and the lowest Z values, respectively.

A demonstration of the surface roughness data obtained using AFM is shown in Figure 10.2:

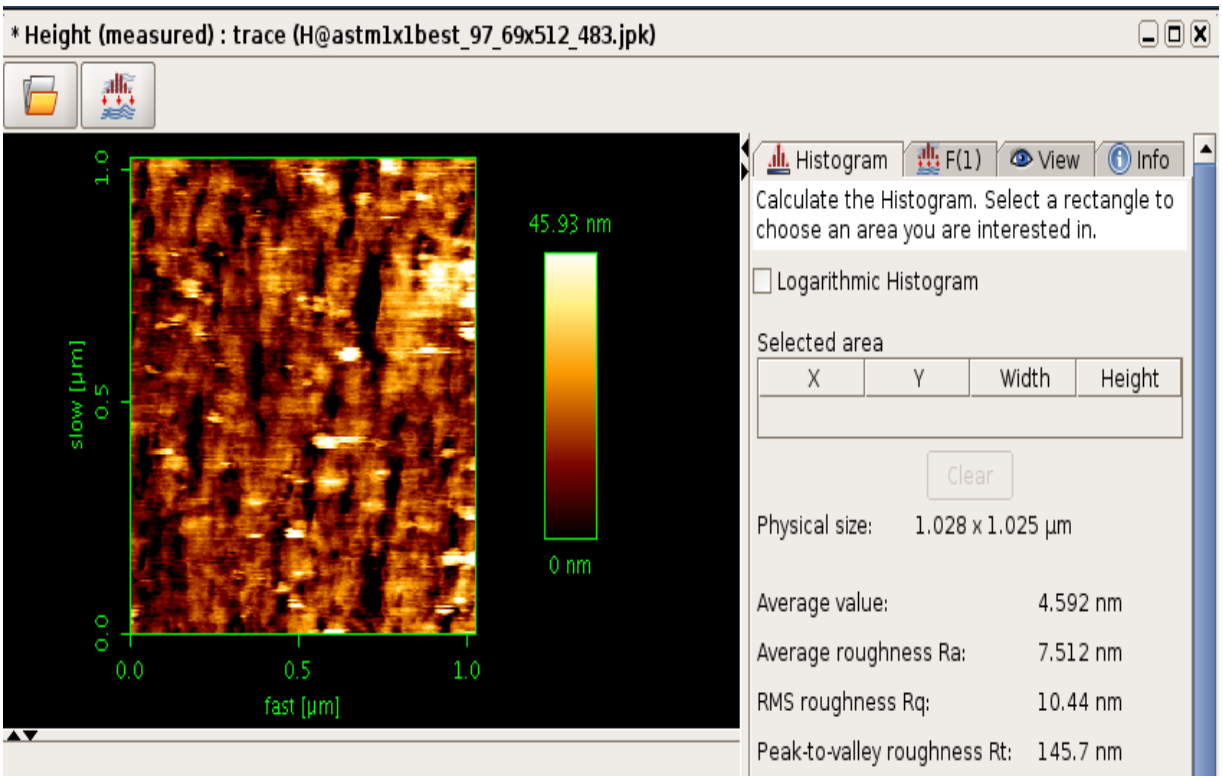

Figure 10.2 Surface roughness parameters of AFM analysis

3.2 AFM data:

AFM results and images are shown in Table 10.2 and Figures 10.3.1-8

Roughness measurements obtained by AFM with tapping mode – (intermittent contact in liquid) over 1x1 μm are given in Table 10.2. These values represent the average of three different images of each membrane, where the scatter between results is in the range of 5%. Nevertheless, no difference is found between the rankings of NF membranes in order from highest to lowest in terms of roughness value either represented using any of the three measured parameters (see discussion section).

NF	AFM Data		
	Avg. surface roughness, R_a , nm	RMS* roughness, nm	Peak to valley, nm
A	4.445	6.08	48.36
B	16.890	20.80	165.50
C	28.800	35.87	250.80
D	4.804	6.178	51.76
E	17.590	21.35	171.80
F	3.267	4.056	32.95
G	5.059	6.42	62.90
H	7.512	10.44	145.70

Table 10.2 AFM roughness measurements

Figure 10.3 (1 – 8), shows the AFM 3-D high resolution images of NF membranes zoomed in area of 1 μm^2, demonstrating actual height data with interpretation of the references to colour where the darker areas indicates depressions “valley” and the more brighter areas indicates the highest point “peaks”. NF images show that the surface roughness is not similar for the

eight NF membranes and they have different overall surface structure. Table 10.2 shows these surface roughness parameters for all studied NF membranes using AFM.

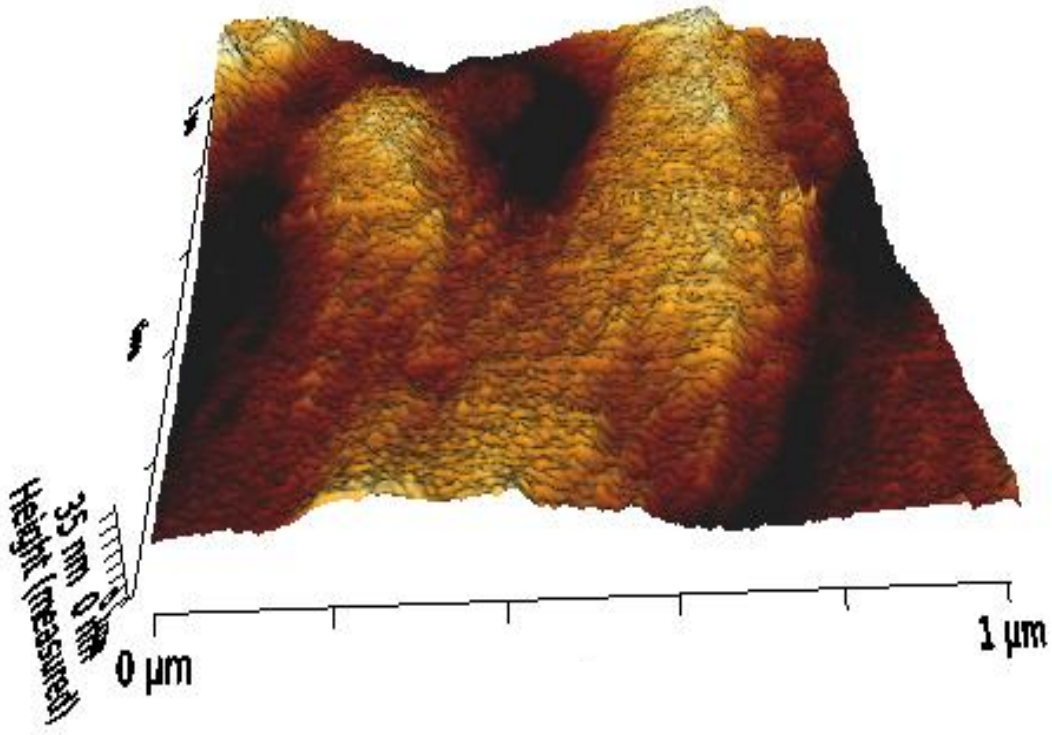

Figure 10.3.1 NF A membrane 3-D projection

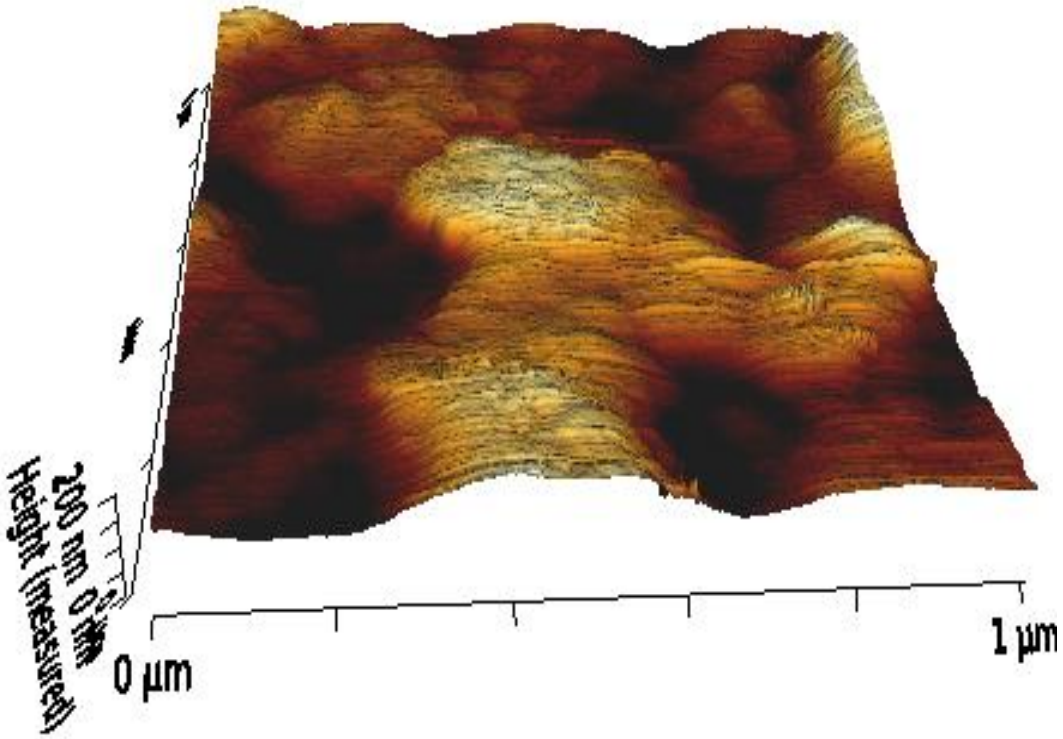

Figure 10.3.2 NF B membrane 3-D projection

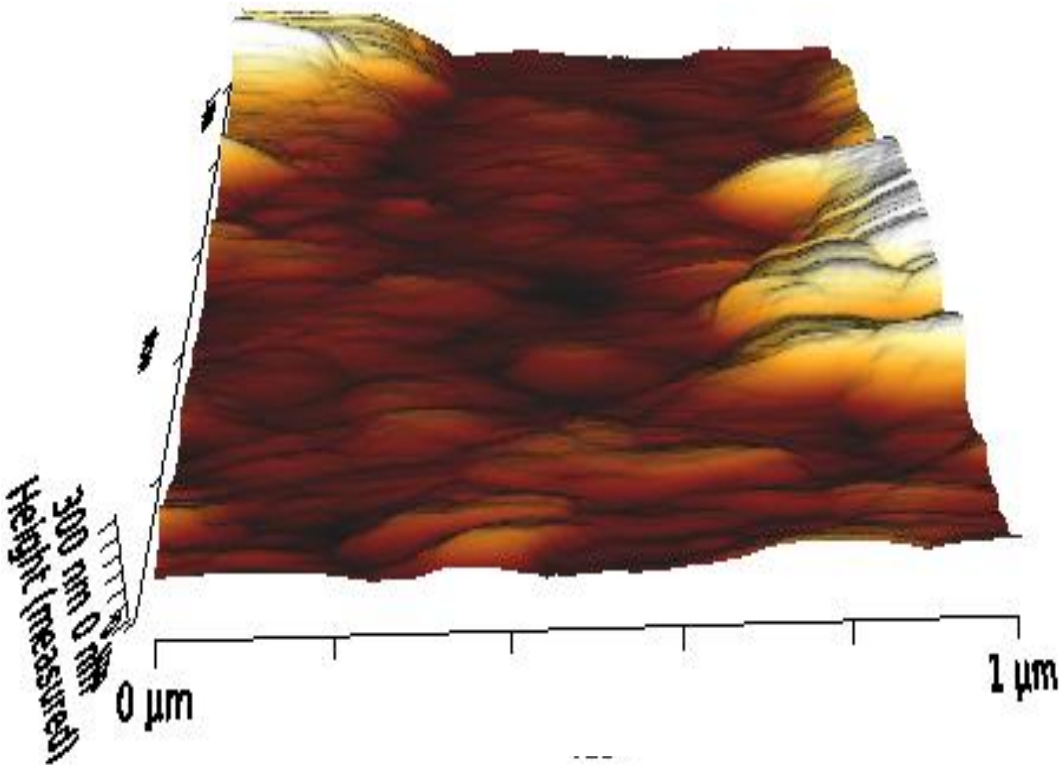

Figure 10.3.3 NF C membrane 3-D projection

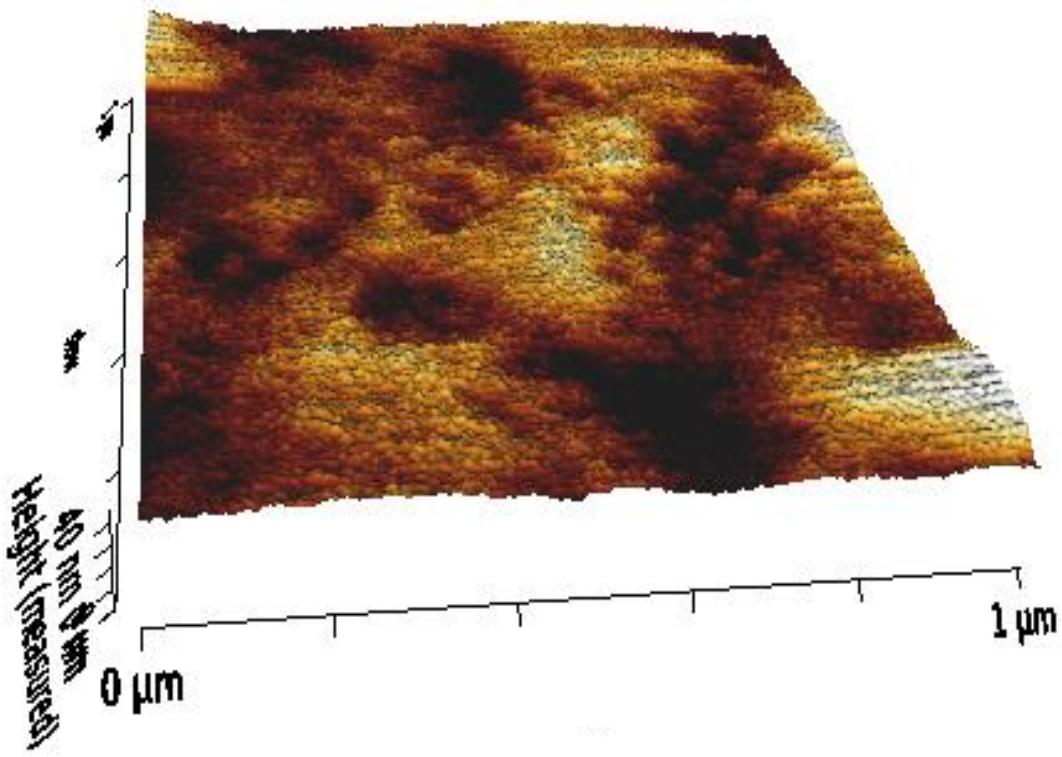

Figure 10.3.4 NF D membrane 3-D projection

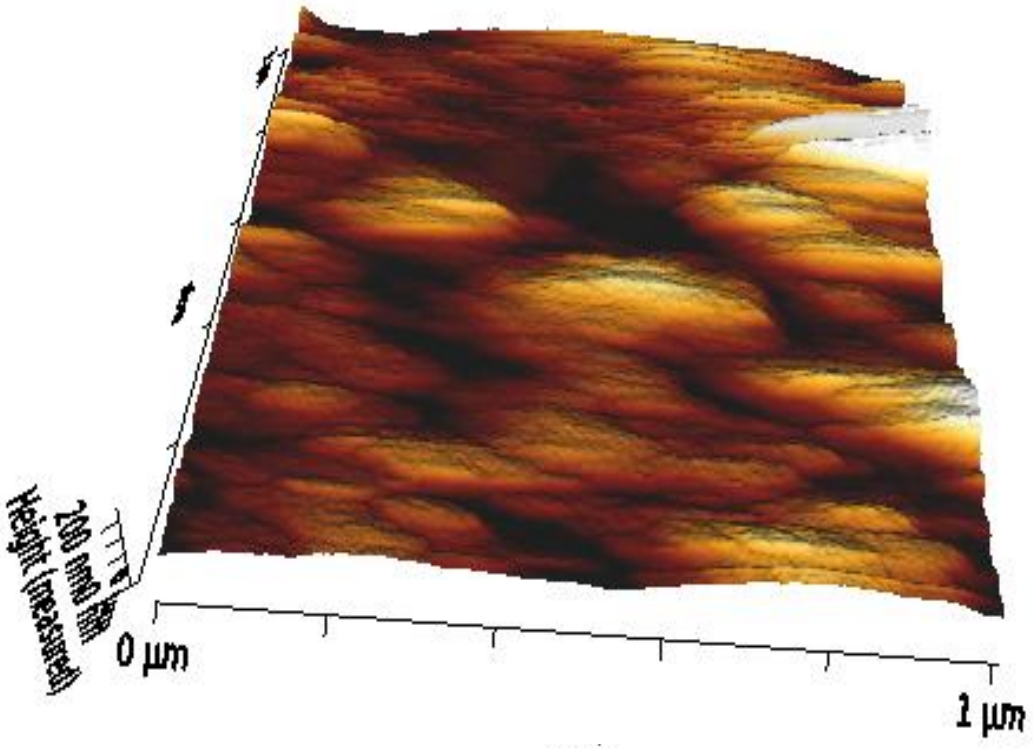

Figure 10.3.5 NF E membrane 3-D projection

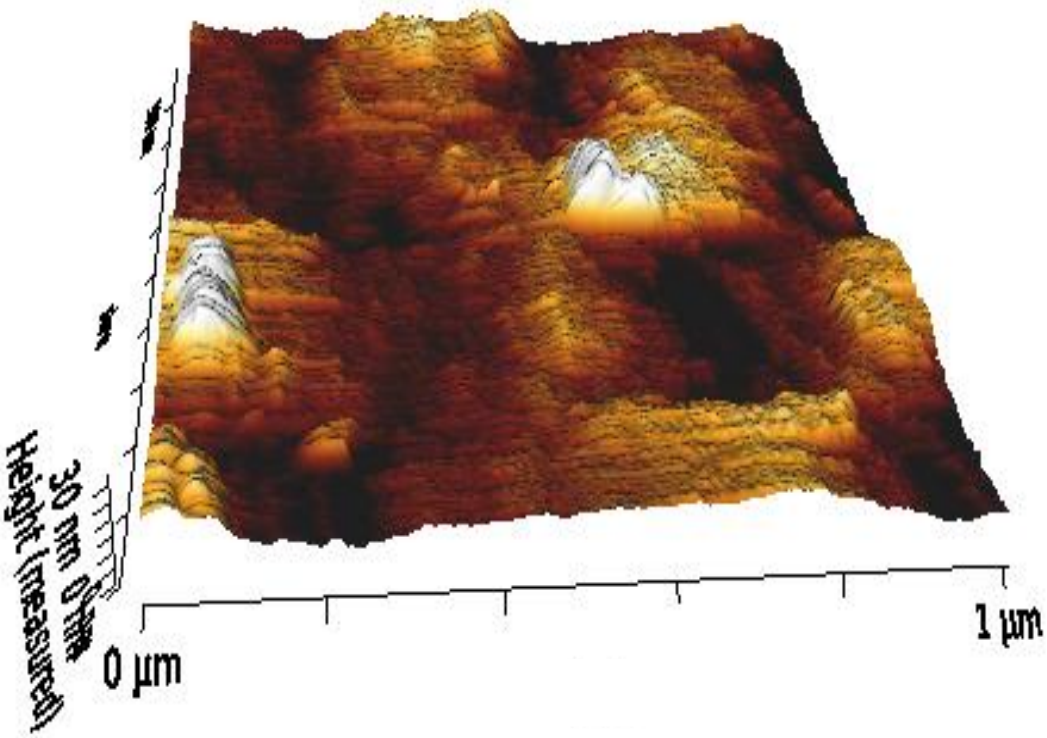

Figure 10.3.6 NF F membrane 3-D projection

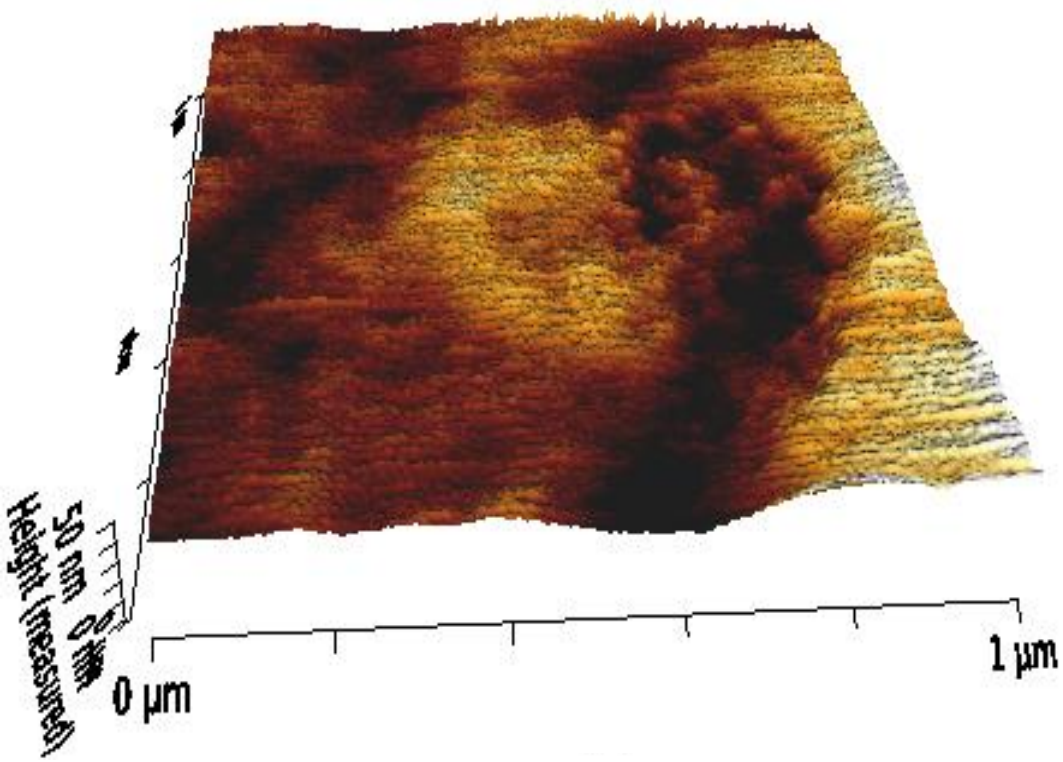

Figure 10.3.7 NF G membrane 3-D projection

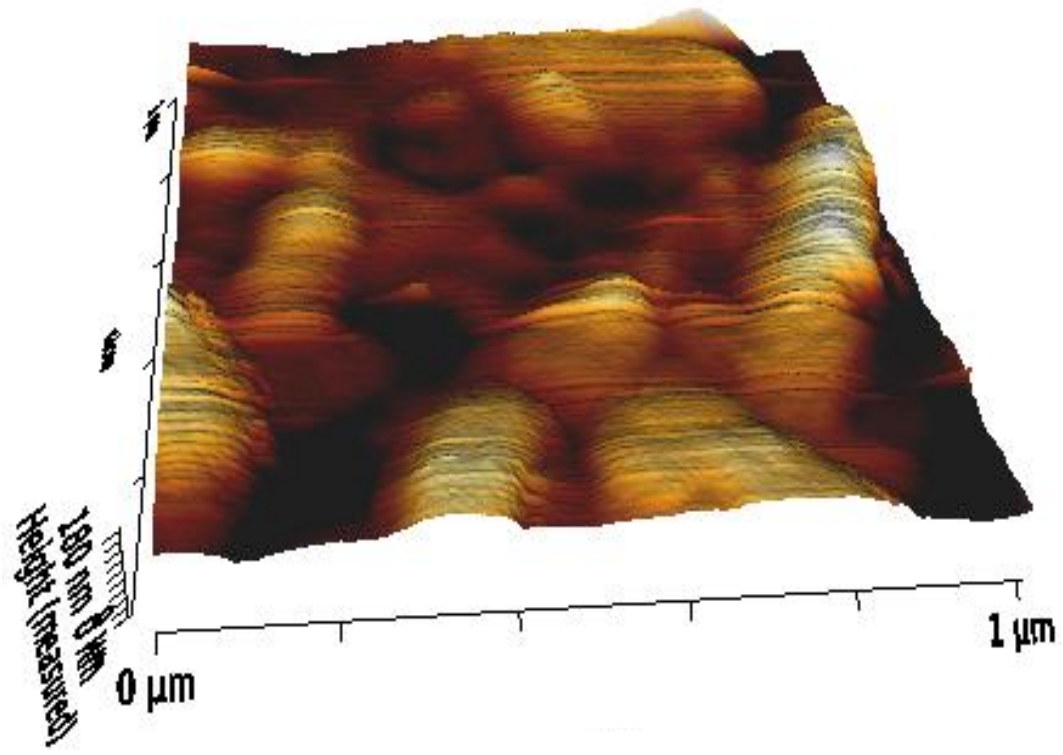

Figure 10.3.8 NF H membrane 3-D projection

AFM many raw data acquisition consider as valuable information to quantify NF membranes surface roughness. Nonetheless, in relation to NF characterisation such data requires critical evaluation to be correlated to NF membranes filtration performance and to show that the surface properties as evaluated by AFM correlate to the process behaviour.

The surface roughness of the NF membranes can be presented by three parameters as shown in Table 10.2. Since the trends shown by the three parameters (average roughness, root-mean square roughness and peak-to-valley height) are identical as shown in Figure 10.4, in the following discussion, just one parameter, the average surface roughness (R_a) will be chosen as representative for NF surface roughness data through the process of correlation with filtration performance.

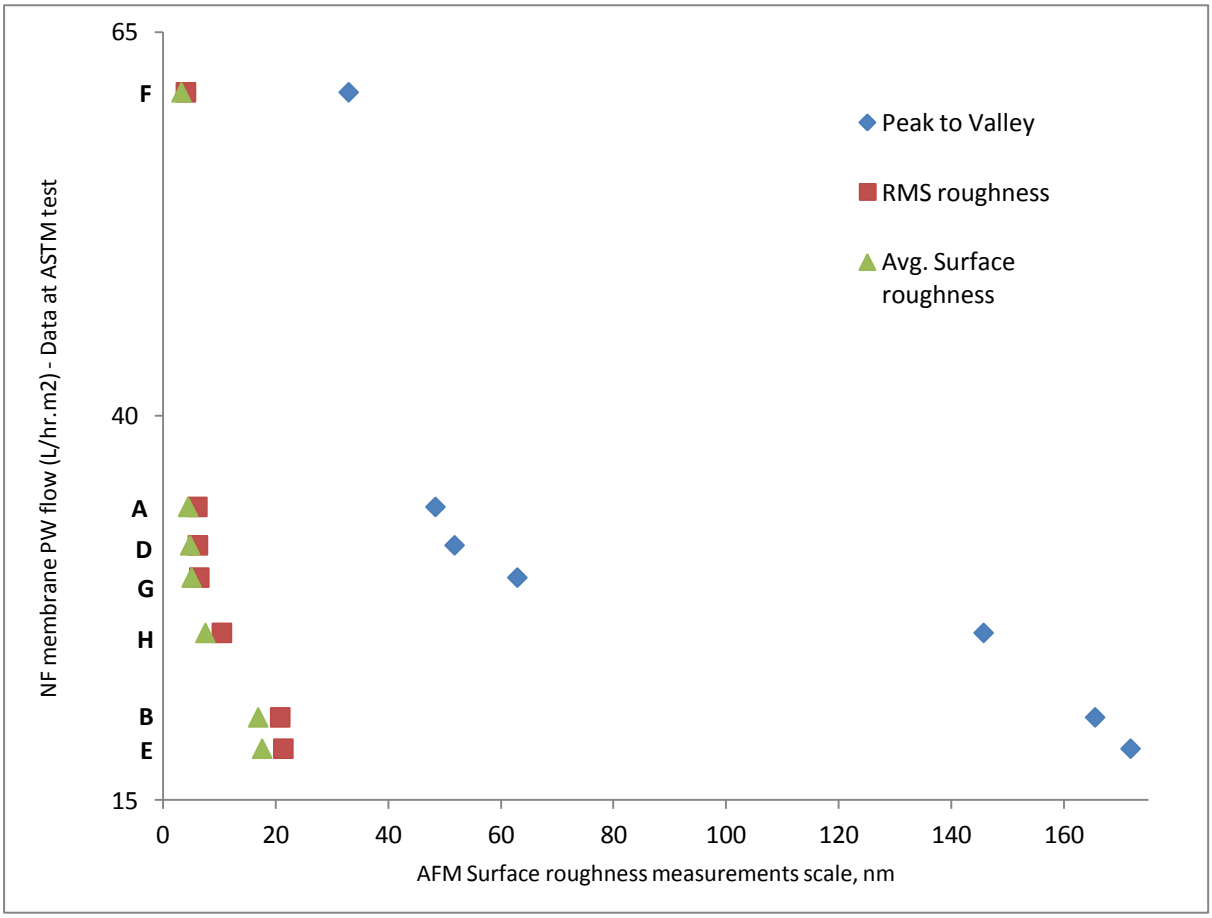

Figure 10.4 Trends of the three parameters representing NF surface roughness in relation to permeate flux

Therefore, a full explanation on the obtained AFM surface roughness data analysis is produced with relevant to data generated during previous phases of the research work.

3.3 Discussions:

As contact angle measurements (chapter 9) proves that a small contact angle represents a hydrophilic NF membrane surface and as the contact angle is increased less surface wettability occurs indicating a more hydrophobic surface. This in turn has been explained in relation to the experimental work results of phase one of this research showing that the permeate flux of the most hydrophobic membrane (NF – E) was substantially lower than the permeate flux of the most hydrophilic membrane (NF – F).

AFM data is another characterisation tool to investigate NF membranes surface morphology by providing quantifiable roughness values that can be complemented with permeation studies of test rig filtration experiments to extend the process of critical characterisation of the eight commercial nanofiltration membranes of different manufactures/suppliers used in this research for sulphate rejection applications. Hence, the aim is to assess any correlation of surface morphology of NF membranes defined by surface roughness of AFM to NF membrane functioning.

Moreover, in terms of analogy, both contact angle measurements and using AFM gives presentation of the membrane surface status, consequently, adopting both techniques in order for critical characterisation of NF membranes adds wider perspective to the research outcomes. In addition, AFM provides visualisation pictures of NF membrane surface.

As a quantitative evaluation of data extracted from the literature to support the argument, the following table shows a comparison of surface roughness parameters of NF E membrane obtained by AFM.

NF membrane	Avg. surface roughness, R_a , nm		RMS roughness, nm		Peak to valley, nm	
	This work	Reference work [88]	This work	Reference work [88]	This work	Reference work [88]
E	17.590	22.763	21.350	27.751	171.80	142.854

Table 10.3 Comparison of AFM data for NF E membrane

The differences in between the measured parameters can be attributed to the differences of the measurement protocol. As in the reference work [88], measurements have been carried

out by contact mode in air medium. While scanning in the current work has been carried out using tapping mode – (intermittent contact in liquid ASTM solution) to standardise the testing solution through the research work.

Table 10.4 lists all NF membranes under investigation (excluding NF C – which will be discussed later) in order from highest to lowest flux in correlation to membrane surface parameters of; contact angle, total surface energy and AFM average surface roughness. It is apparent that the AFM data relates well to membrane functional performance in relation to permeate flux.

NF	Avg. Permeate flux, L/hr.m^2 (in ASTM solution)	Contact angle (^{0}) in ASTM	γ_{NF} (NF membrane total surface energy, mJ/m^2)	AFM – Avg. surface roughness, R_a , nm	Surface morphology
F	61.09	31.9	46.98	3.267	Most hydrophilic and smooth
A	34.10	33.2	45.78	4.445	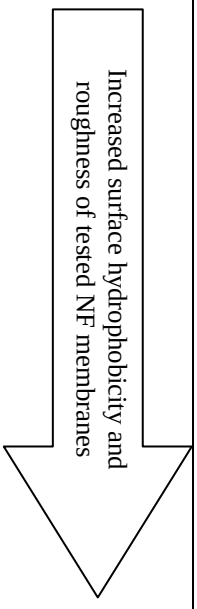
D	31.60	35.3	45.65	4.804	
G	29.50	37.3	45.06	5.059	
H	25.90	42.4	44.87	7.512	
B	20.40	51.0	44.79	16.890	
E	18.36	54.7	44.52	17.590	Hydrophobic and rough surface

Table 10.4 NF membranes in order from highest to lowest permeate flux in relation to surface characterisation data

Table 10.4 displays that the order of NF membranes surface roughness (from lower to higher values) is matching the order of permeate flux (from highest to lowest). Thus, NF membrane surface roughness can be correlated with process behaviour in a way that, with an increase in the NF membrane surface roughness, its permeated flux decreases and vies versa.

Surface roughness has a strong influence on local mass transfer [149], therefore, the possible explanation of how surface roughness affects NF membrane permeate flux is that, low surface roughness of NF membranes can induce the mass transfer of water flow rate. This is to do with both phenomena of wettability and tangential flow rate. As the NF membrane surface roughness is low (i.e. smooth) more wettability and tangential flow rate occurs therefore, more chance for water mass transfer through the pores active layer takes place.

Furthermore in respect of illustrating the effect of NF surface roughness on membrane ability to permeate water, the difference in water flux between NF F having the highest production of (61.09 L/hr.m^2) and NF E having the lowest production of (18.36 L/hr.m^2) is three times. This corresponds to an increase of surface roughness from (3.267 nm) to (17.590 nm) for NF F and E respectively; by nearly 600%.
In other words, the correlation between NF surface roughness and its performance in terms of water production is very crucial as slight increase in membrane roughness results in a dramatic decree in permeate flux. In extension to the illustration; NF A which comes second to NF F in the above list is almost half production compared to F, with an increase in surface roughness by almost 30%.
This shows to which degree NF membrane permeability is a function of its surface roughness, therefore, and in order to optimise membrane performance yielding more permeate its surface roughness should be kept as low as possible, as far as production rate is the main objective for NF membrane usage.

This relation between NF ability for pure water passage with surface structure status confirms the previous correlations provided by correlating membrane wettability measured by contact angle and surface free energy with flux (please see contact angle and surface free energy calculations – chapter 9).

There is also close correlation between surface roughnesses represented by the measured height values – on the bottom left hand side – of the 3-D projection images produced by AFM (Figures 10.3.1-8) with the flux of NF membranes. Figure 10.5 shows that NF flux

decreases as the measured height values of surface roughness depicted in AFM 3-D images increase.

In comparison, no clear relationship between NF membrane sulphate rejection ability with its surface roughness measurement represented by AFM as shown in Figure 10.6.

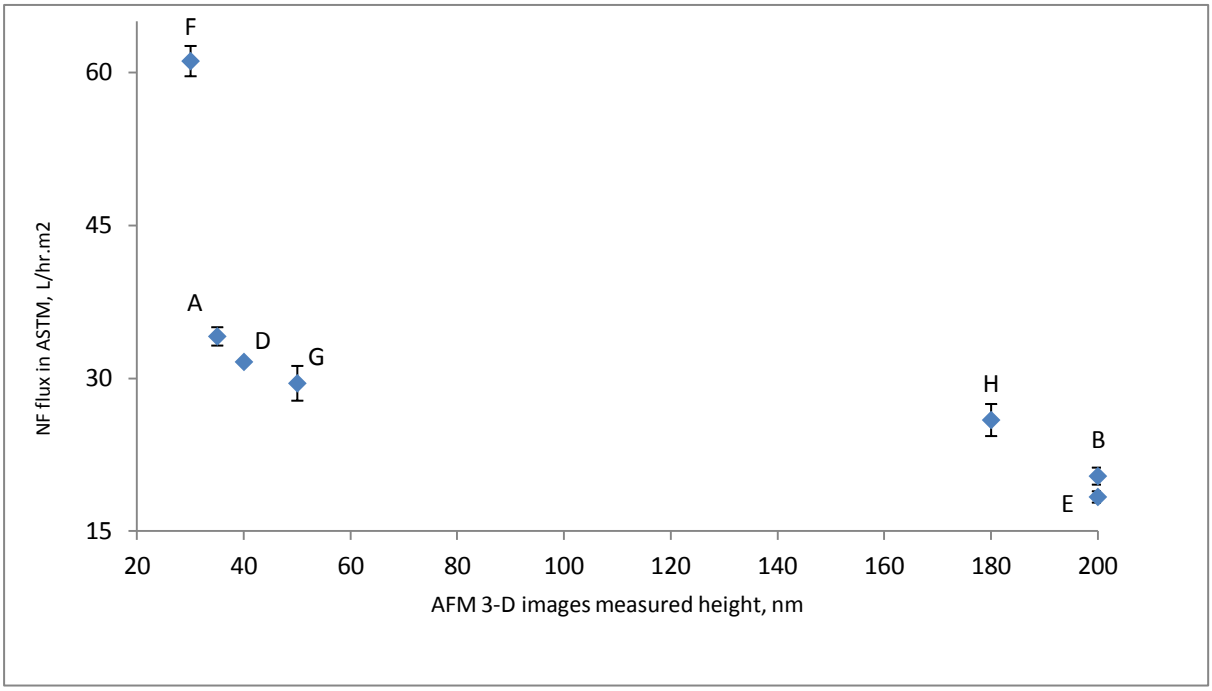

Figure 10.5 Correlation between NF flux and measured height of AFM 3-D images

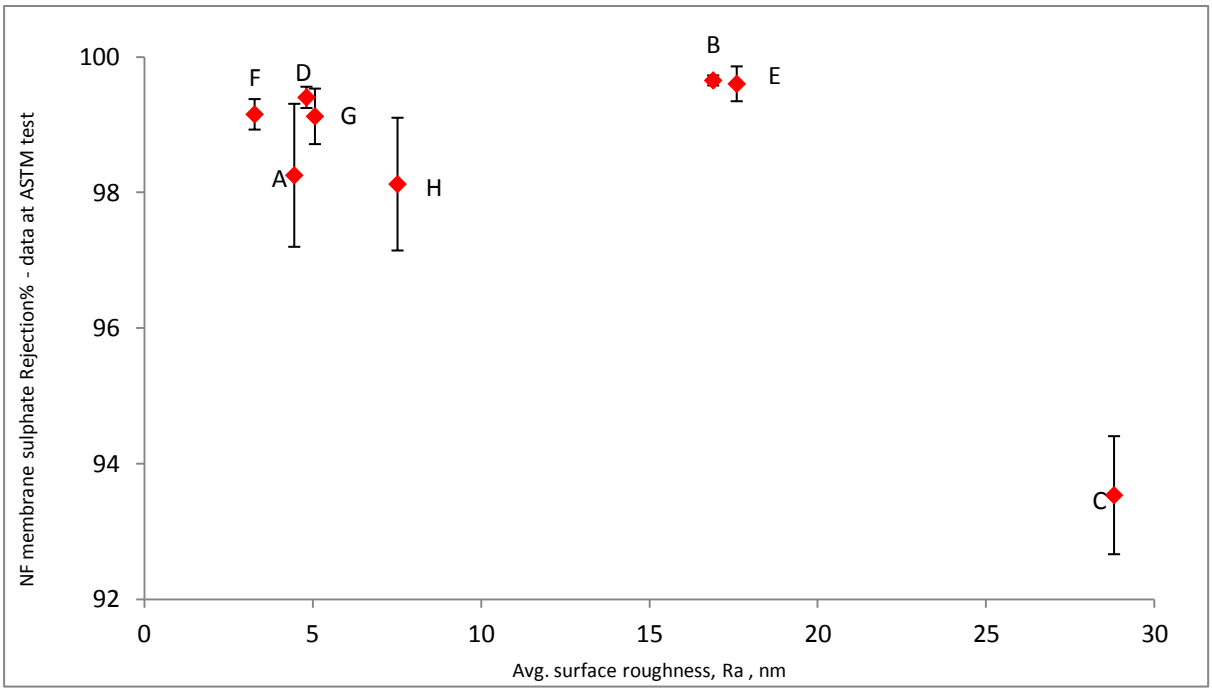

Figure 10.6 NF membrane sulphate rejection percentages and its Avg. surface roughness in ASTM

NF surface parameters affecting the filtration performance of a NF membrane in terms of permeation rate such as surface roughness is playing a role in determining the product water flux through the membrane. This has been demonstrated during this part of the work as all the data obtained using AFM together with data and information of previously adopted technique (contact angle measurements, hence, total surface free energy calculation results) to characterise NF surface morphology; indicates that NF performance (more particularly permeate flux) is a function of membrane surface morphology. In a way that for a smooth NF surface that is identified by; low surface roughness, low contact angle and high surface free energy, corresponds to high permeate flux.

It appears reasonable to propose the following;
As the NF membrane surface character is recognise as a function of both:

1. Morphology represented in this chapter by surface roughness as a result of AFM characterisation, and contact angle, wettability and surface free energy in the previous chapter 9.
2. Charge, defined by charge density – please refer to charge density calculations chapter 11.

And, as NF filtration performance defined during phase one of this research work in terms of permeate flux and sulphate rejection.

It has been clearly shown that NF permeability is correlated to its surface morphology, with no clear relation in between NF ability to reject sulphate ions and its morphology parameters. Therefore, a conclusion may be drawn that the charge density of NF membranes to impact its rejection ability. This will be investigating in next chapter of charge density determination for the NF membranes.

3.4 AFM data evaluation:

Atomic force microscopy has been successfully used to:

I. Quantify surface morphology represented in terms of surface roughness.
II. Producing high resolution 3-D images of NF surfaces.

This in turn, provides surface roughness measurements, therefore, investigating its influence on membrane performance as proven.

Although AFM is widely used to characterise NF membranes surface morphology and despite the many raw data output of AFM device, such data evaluation is as important as data acquisition, however, it is very difficult to compare the different roughness values reported in the literature because:

1. Much data published in relation to NF characterisation lacks critical data processing and evaluation to be correlated to NF membranes filtration performance [145].
2. One finds roughness values obtained by several modes of AFM (mentioned or not), determined for different scan areas (mentioned or not) [156].

Therefore, an interpretation on the obtained AFM data analysis has been produced with relevant to data generated during other phases of the research work to take NF characterisation to further advanced level in order to meet the objective of optimum NF application for sulphate rejection in seawater desalination industry (and oil/gas industry).

3.5 AFM for NF pore identification:

More indirect data can be obtained out of AFM device, such as pore size, however, there are some lacks of accuracy of determining pore dimensions using AFM, and those are listed as:

1. It will be based on mathematical modelling that involves considerable amount of assumptions resulting in an estimated value.

2. In the literature;
   I. AFM cannot directly give distributions for pores of nanometre dimensions due to convolution of the tip and pore [77].

   II. Great care must be taken when assigning pore sizes, as AFM can only give the sizes of the openings of the pores, and does not give any information about their sizes in the interior of the membranes, which is a possible reason for any discrepancies in values obtained from other methods studying flow through the membrane [107].

   III. It has been shown through comprehensive analysis and control experiments [158,159] that the measurements of the pore size using AFM are not very reliable due to AFM lateral resolution being too low to measure the pore size.

4. Conclusions of AFM studies:

4.1 Conclusions over AFM characterisation:

In order to realistically characterise NF membranes to understand its performance at desalination practices, all surface properties must be taken into account.

In this part of the work, the outcomes from using AFM as a tool for NF membranes characterisation are described and critically discussed. The surface roughness was analysed for a range of NF membranes under study, and compared with the experimentally measured separation performance. Adding AFM data to the series of characterisation methods adopted in this work for eight commercial nanofiltration membranes of different manufactures/suppliers for evaluation for seawater desalination processes, in the view of sulphate rejection applications (in which to this researcher's knowledge) has never previously been attempted and this worth contributes to widen the understanding of NF membranes characterisation. Combining the data in this manner allows a greater understanding of the membranes' performances and also the relationship between the characterisation techniques.

From the data obtained of AFM usage the following conclusions can be drawn:

1. Although, contact angle analysis accurately characterised the general hydrophobicity/ hydrophilicity of the NF membrane surfaces, however as the relative magnitude of surface roughness is highly valuable for better understanding of NF performance which is not accounted for by contact angle analysis, AFM has been able to identify and map NF surface roughness.
2. AFM as a tool for surface characterisation can be used to basically:
    I. Directly quantify NF membrane surface roughness.
    II. Produce 3-D images exhibiting surface roughness degree of the NF membranes that can be obviously observed.
    III. Correlating membrane surface characteristics with process behaviour.
3. It shows that AFM is a valuable technique for quantifying NF membranes surface roughness, with no other single technique directly providing such information.
4. Although, care must be taken in the quantitative use of AFM results, it is very satisfying that the surface roughness corresponds to the measured filtration performance (permeate flux).
5. AFM data output can widen the database for better NF membrane selection for the target purpose.

6. AFM utilisation for NF membrane pore identification still needs modifications in order to be a more robust method. Unfortunately sometimes the spectra are so flat that this technique can not accurately identify NF surface pores [117].

4.2 Conclusions of AFM studies towards research objective:

The major end result by the completion of this part of the work facilitates a demonstration of the fundamental principle of correlating NF membranes morphology with its ability to produce low salinity water (in terms of sulphate content). Over a range of NF membranes under characterisation in relation to surface morphology, the work showed that; the one with the most hydrophilic (i.e. smoothest) active layer with lowest surface roughness, lowest contact angle and highest total surface energy is definitely the one with the highest permeate flux. In here; NF F membrane is the one that fits under these criteria. While NF E membrane having the highest value of both surface roughness and contact angle along with lowest total surface energy is the one with the most hydrophobic surface, hence, lowest permeation in comparison with the rest of the tested membranes. However, it has been detected that this principle is only valid for NF membranes that are designed for divalent ions (e.g. SO_4^{2-}) rejection rather others designed for organic rejection as in the case of NF C membrane which shows different characteristics with no direct correlation in-between membrane surface roughness and permeate flux. This particular membrane is having the highest surface roughness of 28.80 nm, while producing 26.49 L/hr.m^2 under ASTM testing environment that is moderate production falling in between the rest of tested membranes. Therefore a conclusion can be drawn that NF membranes surface characterisations should be based on its specified application, and as the target of this research is to characterise NF membranes for sulphate rejection applications, such research direction is beyond the current aims. On the other hand, considering AFM data provided in this work, it showed (through comprehensive analysis) that NF surface roughness as measured using AFM is not directly correlated to the membrane ability for sulphate rejection.

Finally, it is expected that the provided information has been able to provide an insight the influence of NF membrane surface morphology properties on its permeate flux, providing a reasonable database for the selection of NF membranes for desalination applications and laying the scientific basis for optimising NF membranes ideally matched to specified objectives.

Chapter 11: NF MEMBRANE CHARGE QUANTIFICATION

1. Introduction:

The exact effect of NF charge on membrane separation characteristics (e.g. in seawater desalination practices) is not completely understood [23,106]. Therefore, there is a need to determine a suitable description of membrane charge effects on NF filtration performance in order to assist in the development and optimising of NF membrane separation processes for the usage as a pretreatment to desalination units.

Previous experimental studies on nanofiltration membranes applications for seawater desalination pretreatment have evaluated to some extent the zeta potential for five commercial NF membranes [51]. However, this investigation did not systematically study the role of NF charge characteristics on the performance of membranes for sulphate rejection.

Therefore, the objective of this part of the work is to systematically investigate the membrane charge characteristics and how it can be related to the filtration performance (i.e., water flux and sulphate rejection) of the eight NF membranes under study.

2. NF charge background:

NF separation mechanisms are basically determined by two distinct properties that are related to the production processes of the membrane [5]:

I. The pore size of the NF membrane.
II. The charge of the membrane surface, that can be positive or negative (depending on operation parameters and water chemistry), which affects the rejection properties of the membrane due to electric interactions between ions and charge.

Therefore, it should be noted that separation performance for NF membranes does not depend on pore size alone but is controlled by pore size exclusion and electrostatic interactions as a result of membrane charge and is attributed to co-ion electrostatic repulsion (exclusion).

Accordingly, in the prospect of optimum NF selection and utilisation as a pretreatment for desalination practice, NF charge (along with all membrane parameters) characteristics, is acknowledged to play a role in sulphate molecular rejection. As a result, quantification of NF charge as a step in the characterisation process of this research work can serve as a useful tool to fully understand and critically accelerate the synthesis development of NF membranes for the target process.

The NF active layer is the main barrier to the permeation of water and solutes [162], and its charge is one of the properties that determines membrane performance [129]. This charge in the polymer matrix of a NF thin film composite (TFC) active layer is the result of the ionization of carboxylic and amine groups that are the products of the incomplete cross-linking of reactants during active layer casting.

In relation to the charge sign of NF membranes, the following chemical equations illustrate the reaction of functional groups of NF active surface layer that will ionize in the working fluid. Depending on the operating environment (pH and water chemistry) NF active layer function groups may incur one of the following dissociation reactions [22]:

- For a negative charged NF; the carboxylic groups (COO^-) are weakly acidic and will not be dissociated at a low pH, therefore, at pH above 4, the following reaction will dominate:

$$R\text{-}COOH \rightarrow R\text{-}COO^- + H^+$$

- For a positive charged NF; ammonium groups can give the membrane a positive charge if in contact with solution having pH under 4, as follows:

$$R\text{-}NH_2 + H^+ \rightarrow R\text{-}NH_3^+$$

In summary, NF membranes are positively charged at low pH (less than 4) and strongly negatively charged at high pH (over 4) [90,129]. Looking over these equations, typically NF membranes would be negatively charged in a seawater environment.

3. Evaluation of NF charge characterisation techniques:

Many attempts over the last decade have been made to provide quantitative measurements of NF membrane charge [40,51,90,101,105,106,128,129,164-176]. Different techniques have been used to measure NF charge through two main procedures. These are potential measurements and/or ion-exchange capacity.

1. Potential measurements can be done in two different ways:
    I. Either by flow through membranes pores (trans-membrane streaming potential TMS), called membrane potential [164-168] based on the Teorell–Meyer–Sievers transport model. That means the flow is directed perpendicular to the active layer of NF membrane through membrane surface and support layer. This is also known

as filtration streaming potential (FSP) [175]. This is the method which is adopted in the current research (choice justification is provided on the next pages).

II. And/or, another by flow along the top surface (active layer only) of the membrane (tangential streaming potential TSP) that means the flow is horizontally directed to the membrane surface (mostly done by instruments measuring Zeta potential) – along the membrane surface [40,51,90,101,105,106,128,129,164-174].

The data obtained from the first method (TMS) gives qualitative evidence as a result (multilayer membrane: skin active top layer + support layer) while the data obtained from second method (TSP) provides direct information about the membrane skin active top layer only.

2. The ion-exchange capacity (IEC) is to be determined by titration [96,168,170]. This method is able to distinguish between positively and negatively charged functional groups on the membrane active surface. Whereas no overall charge density is to be quantitative but positively and negatively charged groups are determined separately. This fact makes it less beneficial in order to meet the current research objective.

It is worthwhile to mention that, although there are three ways to measure NF charge, it must be recognised that the different methods do not measure the same quantity. However, any adopted technique, whether, potential measurements (either measuring zeta or membrane potential) or titration method, to characterise NF charge over a range of membranes, all will rate them in the same order (with differences in quantities measured value(s) depending on technique) [168].

In terms of NF characterisation in general and for desalination applications evaluation in particular, most studies have focused on the determination of membrane electro-kinetic properties by zeta potential [51]. These electro-kinetic properties are frequently characterised in terms of zeta potential which is related to the surface effective charge.

However, it has been acknowledged in the literature that it would be expected that TMS pore streaming potential measurements (determined by membrane potential measurements that can be translated into surface charge density) are as important, if not more important, than zeta potential measurements (determined by surface streaming potential measurements) in controlling water flux and salt rejection [129]. As zeta potential measurements determine the number of functional groups (in equivalents) but only at the exterior membrane surface. This

is very useful for fouling studies but is of less use for describing ionic transport through a NF membrane [168]. Moreover, the charge density and zeta potential are related by the Grahame equation. Use of the Grahame equation for relating zeta potential to charge density is problematic for a heterogeneous material like the polyamide NF membrane because the Grahame equation describes the interaction of a mono-functional acidic surface with a non-interacting 1:1 electrolyte [101]. Moreover, another relationship between the measurable streaming potential and the zeta potential is given by the Helmholtz–Smoluchowski equation, using the Fairbrother and Mastin approach. Use of the Fairbrother–Mastin equation for relating zeta potential to measured streaming potentials corrects for surface conductance at low ionic strengths, but cannot account for the possible effects of specific ion adsorption [172].

In a study [168] the three methods of zeta potential, membrane potential and titration were all used to determine the charge of four NF membranes, as follows:

1. First the ion-exchange capacity was determined by titration, enabling to distinguish between positively and negatively charged functional groups on the membrane surface.
2. Secondly, measurements of the streaming potential gave a value for the charge density at the exterior membrane surface.
3. Finally, measurements of the membrane potential allowed evaluating the averaged membrane charge density.

There results and recommendations show that [168]:

1. Results obtained by three techniques are hard to compare quantitatively as each method has a different approach.
2. Measurements of the membrane potential are preferred for the calculation of the NF membranes charge.

Therefore, for the current research work the membrane potential method for NF membranes charge characterisation has been adopted. As the most distinctive feature of the membrane potential measurement is the ability to calculate NF membrane averaged charge density. This enables a critical investigation of the correlation between NF charge and its performance for sulphate rejection.

4. Membrane potential hypothesis:

4.1 Membrane potential definition [22]:

Membrane potential is the electrical potential difference between both sides of a membrane when it is separating two solutions of the same electrolyte but in different concentrations. In more detail, when a charged membrane separates solutions of the same electrolyte but of different concentration, the transfer of the electrolyte from the concentrated solution to the dilute solution takes place due to the concentration (or activities) gradient between those two phases. Furthermore, if one ion moves faster than another ion of the opposite charge, the separation of the charge takes place, setting up an electrical field which slows down the faster ion and accelerates the slower ion, where this mechanism maintains the electro-neutrality of the system. Even though no electrical field is imposed on the system, an electrical potential difference exists, regulating the flow of ions through the membrane, which is observed (hence can be measured) as the membrane potential. Consequently, membrane potential measurements allow calculating the membrane averaged charge density.

4.2 Membrane potential theory:

The theory used in this work is the modified TMS-model [168,176,177]. This is based on splitting NF membrane potential into the sum of three contributions, as follows:
Two potential differences find their origin at the interfaces between membrane and solution (at both sides) and are called Donnan potentials. They are present because of the existence of a fixed membrane charge, responsible for an ion distribution between the membrane phase and the bulk solution. The sum of the two Donnan potentials at the membrane solution interfaces (E_{DON}) is called the Donnan term and is given by the following equation:

$$E_{DON} = -\frac{RT}{F}\left[\ln\frac{C_2}{C_1} - \ln\frac{\sqrt{4C_2^2 + \emptyset^2 X^2} + \emptyset X}{\sqrt{4C_1^2 + \emptyset^2 X^2} + \emptyset X}\right] \quad (Eq\ 11.1)$$

Here X is the membrane charge density, expressed in units of equivalents per meter cubed. This parameter finds its origin in the electro-neutrality requirement of the membrane phase. The parameter $\emptyset$ ($0 < \emptyset < 1$) is a characteristic of the membrane–electrolyte pair considered, and represents the fraction of functional groups on the membrane surface that are dissociated and contribute to the membrane charge. $\emptyset$ might depend on the kind of electrolyte and on the

electrolyte concentration. $\emptyset X$ may be referred to as the effective charge density of the membrane. The TMS-model describes the membrane electrical properties in terms of effective charge density and electrostatic effects, assuming a uniform radial distribution of fixed charges and mobile species [81], therefore, $\emptyset$ is always equal to 1 [168].

The third contribution is the diffusion potential that finds its origin in a difference in transport velocity of anions and cations through the membrane. The occurrence of a charge deviation in the membrane is equilibrated by an electric force called the diffusion potential given by the following equation:

$$E_{DIF} = -\frac{RT}{F}(2\alpha - 1)\left[\ln\frac{\sqrt{4C_2^2 + \emptyset^2X^2} + (2\alpha - 1)\emptyset X}{\sqrt{4C_1^2 + \emptyset^2X^2} + (2\alpha - 1)\emptyset X}\right] \quad (Eq\ 11.2)$$

$$where;\ \alpha = \frac{D_+^m}{D_+^m + D_-^m},\ D^m = ionic\ diffusion\ cofficient\ through\ NF\ membrane$$

In this model; α is an adjustable parameter. As no good fit is obtained when taking α equal to α in water (i.e. $D_i^m \neq Di$) [168].

Indeed, in NF characterisation, ion retention also strongly depends on the pore size (as proven in porosity factor calculations – chapter 8), which is a possible physical explanation for the difference between D_i^m and Di. Therefore, the sum of E_{DON} (Eq 11.1) and E_{DIF} (Eq 11.2) is the membrane potential E_m given by the following equation:

$$E_m = E_{DON} + E_{DIF}$$

$$E_m = -\frac{RT}{F}\left[\left(\ln\frac{C_2}{C_1} - \ln\frac{\sqrt{4C_2^2 + \emptyset^2X^2} + \emptyset X}{\sqrt{4C_1^2 + \emptyset^2X^2} + \emptyset X}\right) + \left((2\alpha - 1)\ \ln\frac{\sqrt{4C_2^2 + \emptyset^2X^2} + (2\alpha - 1)\emptyset X}{\sqrt{4C_1^2 + \emptyset^2X^2} + (2\alpha - 1)\emptyset X}\right)\right] \quad (Eq\ 11.3)$$

Where;

E_m	experimentally measured membrane potential (V)
R	universal gas constant (8.314 J/mol.K)
T	Solution absolute temperature (295 K)
F	Faraday constant (= 96485 C/mol)
α	ion diffusion coefficient through NF membrane $= \frac{D_+^m}{D_+^m + D_-^m}$
$\ln {C_2}/{C_1}$	concentration ratio between both solutions. In this work, this has been maintained at a constant value of 2, with the solution of higher concentration (C_2) in contact with NF active side (to have the term ln (C_2/C_1) = ln 2 = 0.693

4.3 Assessment of membrane potential equation (Eq 11.3):

Membrane potential equation ($E_m = E_{DON} + E_{DIF}$) is a well-known expression to evaluate the membrane averaged charge density for 1-1 electrolyte by the TMS model utilising membrane potential measurements. In TMS model, the membrane potential is caused only by the concentration differences with no volumetric flux condition. That is, the contribution of the osmotic pressure to the volumetric flux is negligible. Therefore, it is applicable for membranes having very narrow pores in the range of 1 nm as the case of NF. Regarding other symmetric electrolytes (1-2, 2-1, 2-2), membrane potential equation is the same as 1-1 electrolyte [177].

Moreover, E_m equation is based on NF charge effects play moderate role assuming that ion diffusion is not hindered by NF charge only. This fact is in agreement with the NF rejection ability is a function of so many complex mechanisms and its charge is just one of those factors, as this research work revealed (check chapter 12).

In addition, although, the method of membrane potential measurements for NF charge density calculations using the E_m equation (Eq 11.3) might not taking into account the influence of the thick support layer. However, research works [167,176] have been able to cope with the influence of the support layer measuring transient membrane potentials. This has been done by assuming a transient concentration at the interface between NF active top layer and the support layer as shown in Figure 11.1.

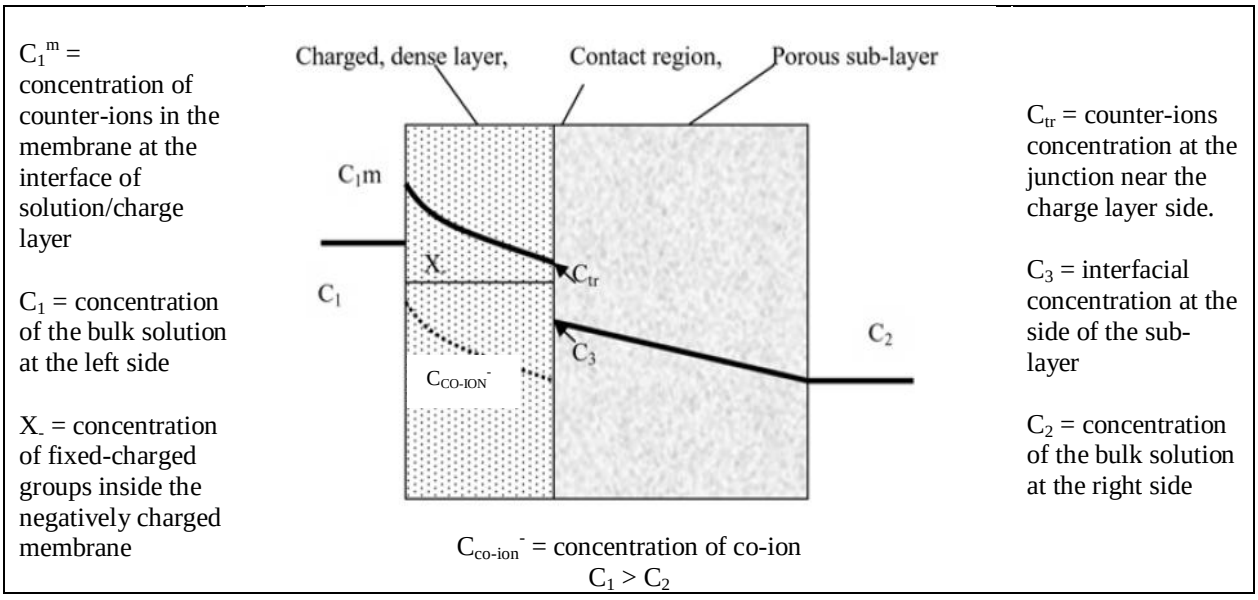

Figure 11.1 Schematic diagram of concentration profile in NF membrane considering C_{tr} [176]

This modification based on the difference in material characteristics for NF, as the top active layer is dense and negatively charged, and the sub-layer is neutral and porous. Thus, in addition to Donnan potential (equation 11.1) at the charge layer/solution interface, and diffusion potentials (equation 11.2) through both the dense layer and the sub-layer (in which E_m equation 11.3 accounts for), another contributor to the membrane potential may consists of the interfacial potential by introducing a contact factor (ξ) to E_m equation.

Even though, the role of the contact factor compensate (to certain degree) for the difference of NF materials of fabrication, nevertheless, this parameter as a correction factor to the original membrane potential equation can be negligible (for this research interests) as the differences in the calculated charge density results, whether considering interfacial potential between the top charged layer and the support layer, or not to be consider, is less than 2 % at the most [176].

Understandably, providing information on the role of the support layer of NF as additional input parameter may advance the outcome of NF separation understanding, however, for the purpose of NF characterisation (over a range of commercially available membranes – as the case in this work) and to be able to relate filtration performance to membrane potential; such detailed and complex mathematical approach will not add valuable data. Nevertheless, for those more interested in a research direction for predictive modelling towards NF as compared to the outcomes of experimental approach, will find considering the support layer role on the NF separation is to improve their work.

Accordingly, for the investigation of NF membrane electrical parameters characterisation for sulphate rejection applications, involving membrane potentials measurements in NaCl or $MgSO_4$ solutions, and calculating NF charge density, the formula to be adopted is E_m equation (Eq 11.3) defined in section 4.2

$$E_m = -\frac{RT}{F}\left[\left(\ln\frac{C_2}{C_1} - \ln\frac{\sqrt{4C_2^2+\emptyset^2X^2}+\emptyset X}{\sqrt{4C_1^2+\emptyset^2X^2}+\emptyset X}\right)+\left((2\alpha-1)\ \ln\frac{\sqrt{4C_2^2+\emptyset^2X^2}+(2\alpha-1)\emptyset X}{\sqrt{4C_1^2+\emptyset^2X^2}+(2\alpha-1)\emptyset X}\right)\right] \quad (Eq\ 11.3)$$

5. Membrane potential measurement technique:

5.1 Measurement kit:

A typical layout for membrane potential measurements, utilising the method of flow directed perpendicular to the active layer through membrane pores (trans-membrane streaming potential TMS), is shown in Figure 11.2.

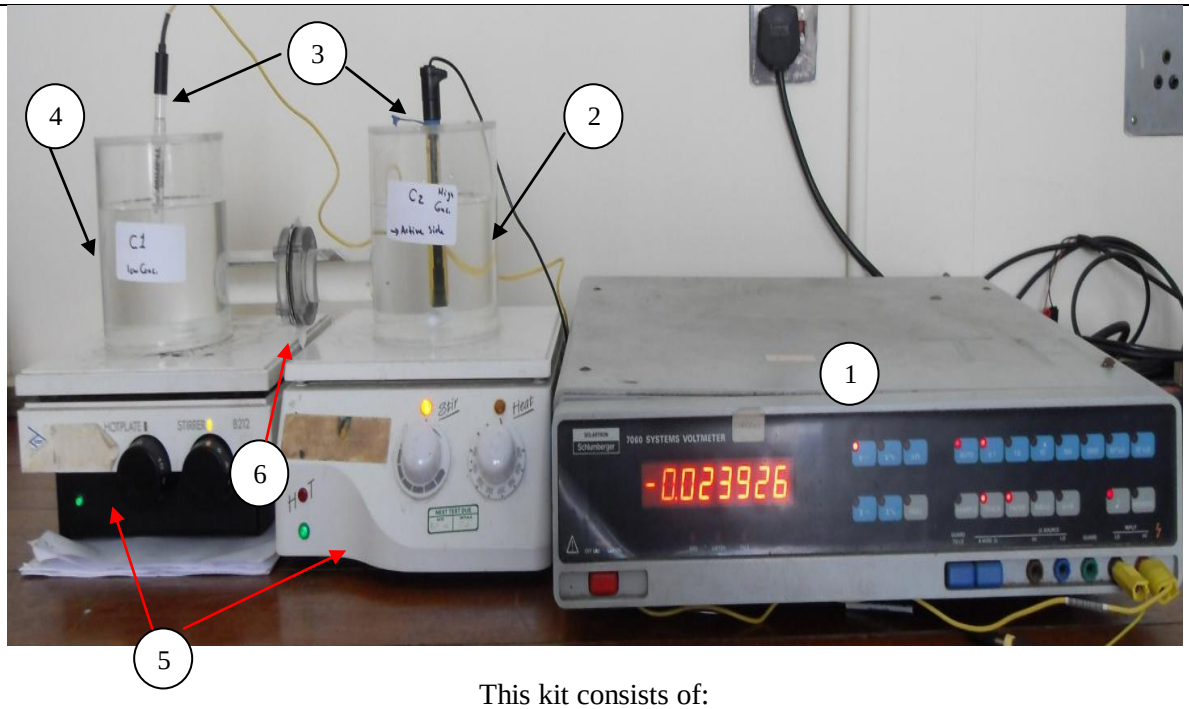

This kit consists of:

1	Voltmeter	2	High concentrated solution C_2 compartment, in contact with NF active surface
3	Ag/AgCl electrodes	4	Low concentrated solution C_1 compartment
5	magnetic stirrer	6	NF membrane sample (5 cm diameter)

A close-up photo on the compartments separating NF sample:

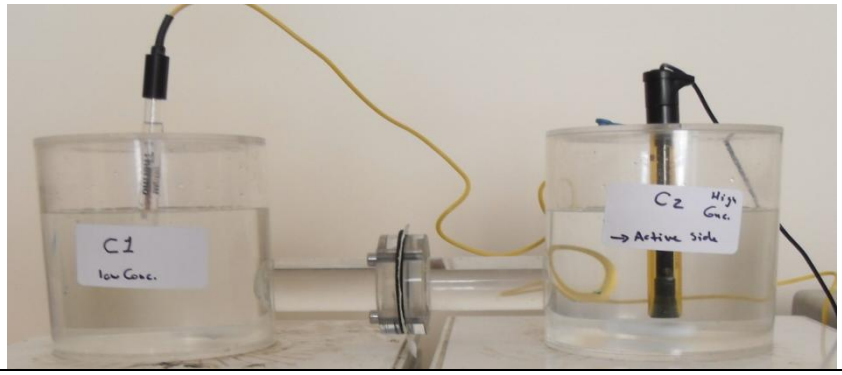

Figure 11.2 Membrane potential measurements kit.

5.2 Measurement protocol:

NF membrane potential measurements procedure is carried out as follows:

1. NF membrane under test is positioned between two half-cells.

2. Each compartment is filled with one litre of an electrolyte solution with the solution of the highest concentration C_2 in contact with the active side of the membrane (i.e. the top layer). The solutions are stirred vigorously by a magnetic stirrer. The measurements take place under ambient temperature (22 ◦C) and hydrostatic pressure.

3. Solutions at various concentrations were used but the concentration ratio between both compartments was maintained at a constant value of 2.
   To have the term $\ln (C_2/C_1) = \ln 2 = 0.693$ = constant in E_m equation 11.3.

4. In order to avoid a concentration gradient in the support layer, the membrane has been dipped in the diluted solution for 24 hrs so that the support layer is saturated with the diluted solution when the measurements are performed.

5. Ag/AgCl reference electrode is placed in each compartment and the electrodes are connected to a voltmeter as in Figure 11.2.

6. The membrane potential is directly obtained by reading the value on the display of the voltmeter. A calibration of the electrodes precedes each measurement.

7. The same procedure has been applied for three samples taken from different parts of the NF membrane under study. The three samples for each NF (of the eight membranes) show an exact membrane potential reading.

8. After measuring the membrane potential, membrane charge density has been calculated as detailed in the NF charge calculations section (section 7) of this chapter.

6. Membrane potential measurements:

6.1 Solutions preparation:

Solutions at various concentrations were used at a ratio between both compartments maintained at a constant value of 2. Concentration is reported in:

1. Equivalent per cubic meter.
2. Molarity (milli-moles per litre) = Moles per cubic meter.

The following Table 11.1 shows the specifications of the diluted solution C_1:

$MgSO_4$ solution specifications (Mol.Wt = 120.36 gm/mol)			NaCl solution specifications (Mol.Wt = 58.44 gm/mol)		
$MgSO_4$, C_1 in eq/m^3	Mass of $MgSO_4$in mg per Litre	mM/lit (mol/m^3)	NaCL, C_1 in eq/m^3	Mass of NaCl in mg per Litre	mM/lit (mol/m^3)
4.16	250	2	75	4375	75
8.33	500	4	150	8750	150
16.67	1000	8	300	17500	300
33.33	2000 (1)	16.6	600	35000 (2)	600

(1) & (2) The upper limits of $MgSO_4$ and NaCl solutions to meet ASTM and simulated seawater testing standards adopted through the whole phases of the current research work.

Table 11.1 Electrolytes concentration measurements

6.2 Membrane potential measurements results:

6.2.1 in $MgSO_4$ solution:

The membrane potentials in $MgSO_4$ solution of all NF membranes under study are listed in Table 11.2 below and represented in Figure 11.3.

$MgSO_4$, C_1 in eq/m^3	4.16	8.33	16.67
NF	NF membrane potential in milli-volts		
A	-6.54	-6.24	-5.99
B	-7.61	-7.34	-7.08
C	-3.76	-3.34	-3.10
D	-6.29	-6.01	-5.77
E	-7.27	-7.01	-6.37
F	-6.79	-6.56	-6.21
G	-6.01	-5.78	-5.42
H	-5.52	-5.05	-4.78

Table 11.2 Membrane potential of the NF membranes in $MgSO_4$ solution

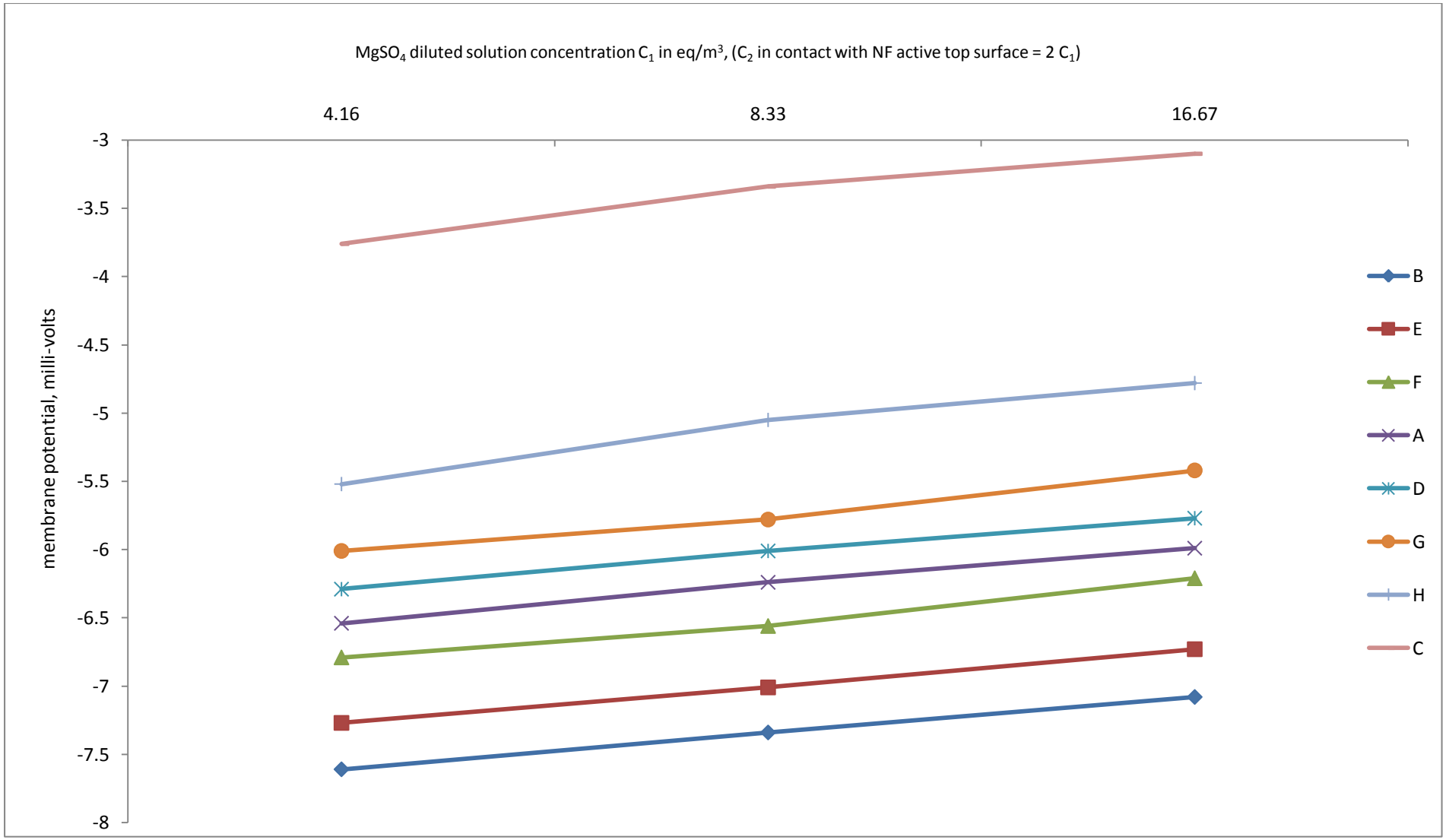

Figure 11.3 Membrane potential of the NF membranes in $MgSO_4$ solution.

6.2.2 in NaCl solution:

The membrane potentials in NaCl solution of all NF membranes under study are listed in Table 11.3 below and represented in Figure 11.4.

NaCl, C_1 in eq/m^3	75	150	300
NF	NF membrane potential in milli-volts		
A	-0.82	-0.80	-0.73
B	-1.06	-1.01	-0.99
C	-0.26	-0.24	-0.23
D	-0.74	-0.70	-0.65
E	-0.95	-0.91	-0.87
F	-1.08	-1.02	-1.0
G	-0.60	-0.57	-0.53
H	-0.52	-0.51	-0.49

Table 11.3 Membrane potential of the NF membranes in NaCl

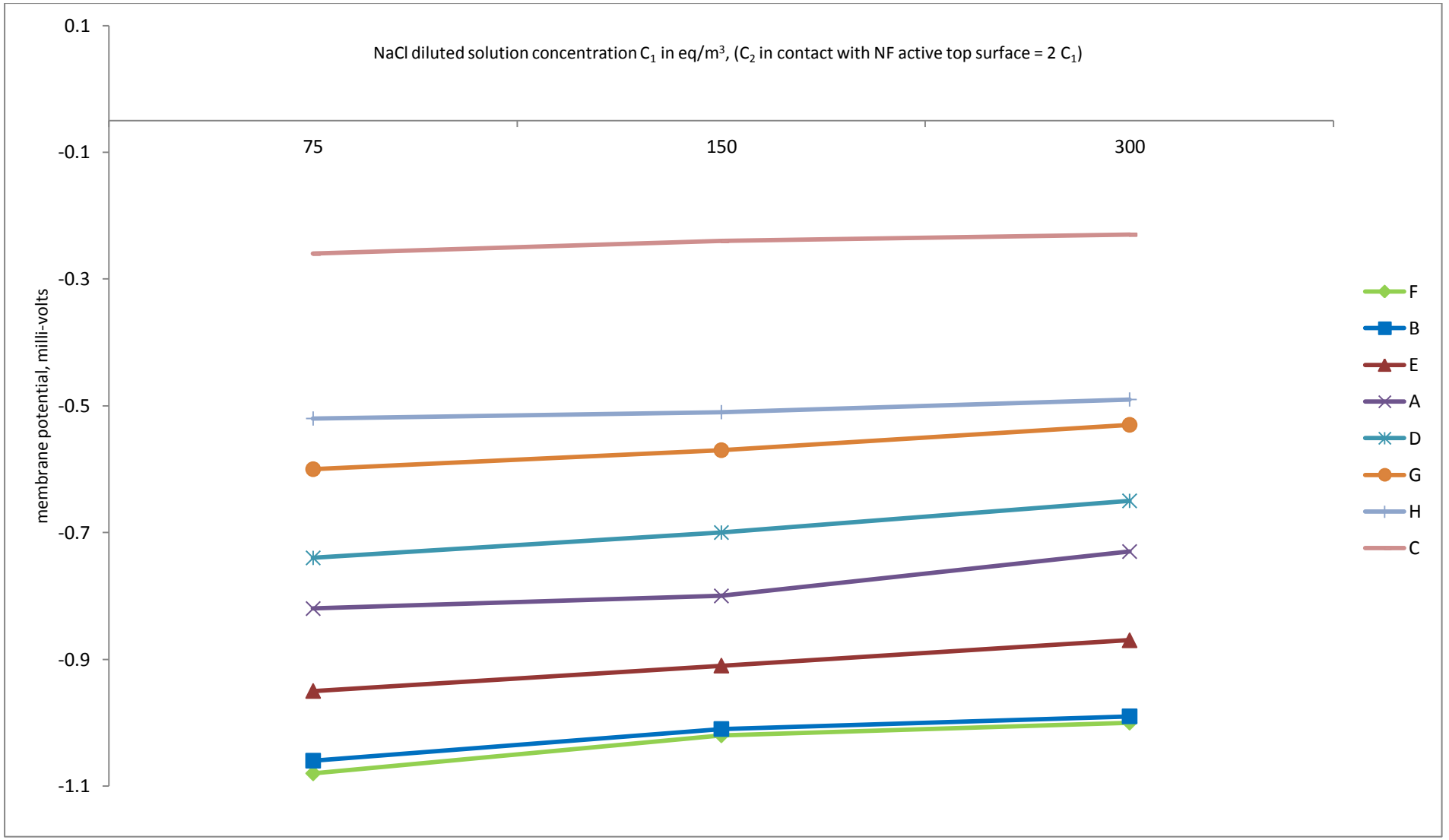

Figure 11.4 Membrane potential of NF membranes in NaCl solution

The measured NF membrane potential is plotted against the solution concentration of $MgSO_4$ in Figure 11.3 and for NaCl in Figure 11.4. All tested NF membranes display negative potential of electrolyte flow through NF membranes.

The behaviour of the membrane potential as a function of solution concentration is almost identical for all NF membranes. As the electrolyte concentration increases membrane potential decreases. This will take place till it reach a state of what is known as point of zero charge (PZC) [169] or it may be refer to as the iso-electrical point (IEP) [128], where, in both cases (PZC or IEP), the membrane is uncharged.

The IEP will take place when the solute concentration is much greater than the membrane charge density ($C \gg X$), therefore the Donnan term E_{DON} (Eq 11.1) of membrane potential equation reaches zero. Or, more accurately, its numerical value into E_m equation is very low that it can be neglected. Therefore, the effect of the membrane charge (X) is almost eliminated when the salt concentration is high enough, where it is expected that the membrane is uncharged [129,168,169]. Therefore, control of ion transport through NF membrane is expected to be controlled mainly by the size of pores.

Although, the exact (IEP) of each NF membrane has not been evaluated as the chosen solution concentrations of both NaCl and $MgSO_4$ is to simulate seawater salts contents.

In this scenario, it is obvious that NF membrane has low net charge in high concentrated environment.

It appears also, that the membrane potential of the NF membranes is much greater in $MgSO_4$ solution in comparison to NaCl solution.

7. NF Charge Density (CD) calculations:

7.1 Equation re-formulation:

The potential difference measured through NF membranes, called the membrane potential, is linked to the membrane charge density by the relation described in section 4.2

$$E_m = E_{DON} + E_{DIF}$$

$$= -\frac{RT}{F}\left[\left(\ln\frac{C_2}{C_1} - \ln\frac{\sqrt{4C_2^2+\emptyset^2X^2}+\emptyset X}{\sqrt{4C_1^2+\emptyset^2X^2}+\emptyset X}\right)+\left((2\alpha-1)\ \ln\frac{\sqrt{4C_2^2+\emptyset^2X^2}+(2\alpha-1)\emptyset X}{\sqrt{4C_1^2+\emptyset^2X^2}+(2\alpha-1)\emptyset X}\right)\right] \text{ (Equation 11.3)}$$

Where, $\emptyset$ is equal to one in TMS model used here [168].

This equation has been solved for each individual NF membrane to calculate:

- The average effective charge density (X) expressed in units of equivalents per meter cube, in $MgSO_4$ and NaCl solutions.
- α (ion diffusion coefficient through NF membrane) as an adjustable parameter that is (> 0.491) for negatively charged membranes [168].

Reformulation of membrane potential equation (Eq 11.3) after substituting constant values of:
R = 8.314 J/mol.K
F = 96487 C/mol
T = 295 K
for a NF membrane is as follows:

$$E_{m,NF} = -0.025\left[\left(0.693 - \ln\frac{\sqrt{4C_2^2+X^2}+X}{\sqrt{4C_1^2+X^2}+X}\right)+\left((2\alpha-1)\ \ln\frac{\sqrt{4C_2^2+X^2}+(2\alpha-1)X}{\sqrt{4C_1^2+X^2}+(2\alpha-1)X}\right)\right]$$

$$\frac{E_{m,NF}}{-0.025} = \left(0.693 - \ln\frac{\sqrt{4C_2^2+X^2}+X}{\sqrt{4C_1^2+X^2}+X}\right)+\left((2\alpha-1)\ \ln\frac{\sqrt{4C_2^2+X^2}+(2\alpha-1)X}{\sqrt{4C_1^2+X^2}+(2\alpha-1)X}\right)$$

$$\frac{E_{m,NF}}{-0.025} - 0.693 = (2\alpha - 1)\ \ln\frac{\sqrt{4C_2^2+X^2} + (2\alpha-1)X}{\sqrt{4C_1^2+X^2} + (2\alpha-1)X} - \ln\frac{\sqrt{4C_2^2+X^2} + X}{\sqrt{4C_1^2+X^2} + X}$$

By re-arranging membrane potential equation, its final form written as:

$$\ln\frac{\sqrt{4C_2^2+X^2} + X}{\sqrt{4C_1^2+X^2} + X} + \frac{E_{m,NF}}{-0.025} - 0.693 = (2\alpha - 1)\ \ln\frac{\sqrt{4C_2^2+X^2} + (2\alpha-1)\,X}{\sqrt{4C_1^2+X^2} + (2\alpha-1)\,X} \qquad (Eq\ 11.4)$$

In the above equation (Eq 11.4), the known and unknown variables are as listed in the following table:

Parameters	Left Hand Side $\left(\ln\frac{\sqrt{4C_2^2+X^2}+X}{\sqrt{4C_1^2+X^2}+X} + \frac{E_{m,NF}}{-0.025} - 0.693\right)$	Right Hand Side $\left((2\alpha-1)\ \ln\frac{\sqrt{4C_2^2+X^2}+(2\alpha-1)X}{\sqrt{4C_1^2+X^2}+(2\alpha-1)X}\right)$
Known	• E_m (measured NF membrane potential) • solution concentrations C_1 and C_2	• solution concentrations C_1 and C_2
Unknown (to be calculated)	• NF effective charge density (X)	• NF effective charge density (X) • adjustable parameter α, where ($\alpha > 0.491$)

Table 11.4 Known and unknown parameters of membrane potential equation (Eq 11.4)

7.2 Calculations method:

The scheme is as follows:

1. Equation 11.4 left hand side LHS: $\left[\ln\frac{\sqrt{4C_2^2+X^2}+X}{\sqrt{4C_1^2+X^2}+X}+\frac{E_{m,NF}}{-0.025}-0.693\right]$

   is to be solved first for *X* (membrane charge density) at different known values of:

   - Solution concentration (C_1) with the concentration ratio $C_2/C_1 = 2$, and
   - The corresponding measured membrane potential E_m.

2. Simultaneously, the right hand side RHS: $\left[(2\alpha-1)\ \ln\frac{\sqrt{4C_2^2+X^2}+(2\alpha-1)\,X}{\sqrt{4C_1^2+X^2}+(2\alpha-1)\,X}\right]$

   is to be solved for both *X* and α (the adjustable parameter) for a best fit obtained by taking $\alpha > 0.491$ [168].

   The fit is based on the line diagrams of Figures 11.3 and 11.4 of the membrane potential measurements of the NF membranes.

3. Obtaining the optimum *X* and α values through a trial and error method applied for various values. Until an optimum numerical values are obtained for least possible error between LHS and RHS of E_m equation of less than 10%. In other words, the numerical error value of LHS and RHS of equation 11.4, is in order of less than (10% at the most) as difference between both sides of E_m equation.

4. Finally, membrane charge density (*X*) can be obtained by the utilisation of solving E_m equation (Eq. 11.4) according to the sequences of mathematical scheme illustrated in next section.

7.3 NF membrane average charge density calculations procedure:

The exact same calculations procedure and method have been applied to all NF membranes in either $MgSO_4$ or NaCl solution. For the purpose of demonstration, NF B membrane average charge density (in $MgSO_4$ solution) calculations procedure is detailed in here as an example, as follows:

1. The equation to solve for NF surface charge density is (eq 11.4):

$$\ln\frac{\sqrt{4C_2^2+X^2}+X}{\sqrt{4C_1^2+X^2}+X}+\frac{E_{m,NF}}{-0.025}-0.693 = (2\alpha-1)\ln\frac{\sqrt{4C_2^2+X^2}+(2\alpha-1)X}{\sqrt{4C_1^2+X^2}+(2\alpha-1)X}$$

2. With the consideration of membrane potential experimental results linearization (as shown in Figures 11.3 and 11.4). Taking the three data points to represent the line to solve E_m equation (11.4) for charge density calculation as boundary conditions.

3. Data for membrane "B" potential measurements at $MgSO_4$ solution:

- 1st set of data at C_1 = 16.67 eq/m^3, hence C_2 = 33.34 eq/m^3, measured E_m = - 7.08 mV,

Fitting those data into the equation (11.4) as follow:

$$\ln\frac{\sqrt{4446.2+X^2}+X}{\sqrt{1111.5+X^2}+X}+\frac{-7.08\,x\,10^{-3}}{-0.025}-0.693 = (2\alpha-1)\ln\frac{\sqrt{4446.2+X^2}+(2\alpha-1)X}{\sqrt{1111.5+X^2}+(2\alpha-1)X}$$

Therefore, 1st set of data equation is:

$$\ln\frac{\sqrt{4446.2+X^2}+X}{\sqrt{1111.5+X^2}+X}-0.41 = (2\alpha-1)\ln\frac{\sqrt{4446.2+X^2}+(2\alpha-1)X}{\sqrt{1111.5+X^2}+(2\alpha-1)X}$$

- 2nd set of data at C_1 = 8.33 eq/m^3, hence C_2 = 16.67 eq/m^3, measured E_m = - 7.34 mV,

Fitting those data into equation (11.4) as follow:

$$\ln\frac{\sqrt{1111.5+X^2}+X}{\sqrt{277.5+X^2}+X}+\frac{-7.34\,x\,10^{-3}}{-0.025}-0.693 = (2\alpha-1)\ln\frac{\sqrt{1111.5+X^2}+(2\alpha-1)X}{\sqrt{277.5+X^2}+(2\alpha-1)X}$$

Therefore, 2nd set of data equation is:

$$\ln\frac{\sqrt{1111.5+X^2}+X}{\sqrt{277.5+X^2}+X}-0.399 = (2\alpha-1)\ln\frac{\sqrt{1111.5+X^2}+(2\alpha-1)X}{\sqrt{277.5+X^2}+(2\alpha-1)X}$$

- 3rd set of data at C_1 = 4.16 eq/m^3, hence C_2 = 8.32 eq/m^3, measured E_m = - 7.61 mV,

Fitting those data into equation (11.4) as follow:

$$\ln\frac{\sqrt{277.5+X^2}+X}{\sqrt{69.2+X^2}+X}+\frac{-7.61\,x\,10^{-3}}{-0.025}-0.693\;=\;(2\alpha-1)\;\ln\frac{\sqrt{277.5+X^2}+(2\alpha-1)\,X}{\sqrt{69.2+X^2}+(2\alpha-1)\,X}$$

Therefore, 3rd set of data equation is:

$$\ln\frac{\sqrt{277.5+X^2}+X}{\sqrt{69.2+X^2}+X}-0.389\;=\;(2\alpha-1)\;\ln\frac{\sqrt{277.5+X^2}+(2\alpha-1)\,X}{\sqrt{69.2+X^2}+(2\alpha-1)\,X}$$

4. With three sets of equations best describing the potential measurements curve, a trial and error method is applied through values generation to identify optimum α, and then substituting the proposed value into equations, followed by solving for *X* through an Excel spreadsheet (available in Appendix 4).

5. Then substituting both values of α and *X* into the three equations to check the accuracy of numbers for equations satisfaction to have a minimum error of less than 10%.

For the demonstration example of NF B data at $MgSO_4$, the optimum found value for

α= 0.719, hence the calculated membrane charge density *X* = – 0.628 eq/m^3

For accuracy check, by substituting both values into equations:

For the 1st set of data equation:

$$\ln\frac{\sqrt{4446.2+(-0.628)^2}-0.628}{\sqrt{1111.5+(-0.628)^2}-0.628}-0.41\;=\;(2*0.719-1)\;\ln\frac{\sqrt{4446.2+(-0.628)^2}+(2*0.719-1)*(-0.628)}{\sqrt{1111.5+(-0.628)^2}+(2*0.719-1)*(-0.628)}$$

LHS = 0.2928 and RHS = 0.3054, with minimum error between LHS and RHS of:

= 0.012 (less than 4.1%).

For the 2nd set of data equation:

$$\ln\frac{\sqrt{1111.5+(-0.628)^2}-0.628}{\sqrt{277.5+(-0.628)^2}-0.628}-0.399\;=\;(2*0.719-1)\;\ln\frac{\sqrt{1111.5+(-0.628)^2}+(2*0.719-1)*(-0.628)}{\sqrt{277.5+(-0.628)^2}+(2*0.719-1)*(-0.628)}$$

LHS = 0.3126 and RHS = 0.3070, with minimum error between LHS and RHS of:

= 0.00557 (less than 1.8%).

For the 3rd set of data equation:

$$\ln\frac{\sqrt{277.5+(-0.628)^2}-0.628}{\sqrt{69.2+(-0.628)^2}-0.628}-0.389 = (2*0.719-1)\ln\frac{\sqrt{1111.5+(-0.628)^2}+(2*0.719-1)*(-0.628)}{\sqrt{277.5+(-0.628)^2}+(2*0.719-1)*(-0.628)}$$

LHS = 0.3422 and RHS = 0.3101, with minimum error between LHS and RHS of:

= 0.0321 (less than 9%).

For the rest of the membranes, the same procedure of membrane average charge density (*X*) calculations has been applied. Detailed Excel spreadsheet calculations of the averaged charge density of the NF membranes in NaCl and $MgSO_4$ solutions are provided in Appendix 4.

8. NF charge density results:

Table 11.5 shows the values for membrane volume averaged charge (*X)* as a density in equivalents per meter cube, calculated from the membrane potential equation (Eq 11.4) as a result of the membrane potential measurements, where a membrane separates two electrolyte solutions. The negative sign of NF charge density is in agreement with the kind of material the membranes are fabricated of, as all eight membranes are TFC made by an interfacial polymerisation process (see chapter 6). Therefore, the carboxylic groups (R-COOH) are expected to be de-protonated ($R\text{-}COO^-$) to confer NF membrane a negative charge.

The charge density, of the NF membranes in NaCl electrolyte, is listed on the left column of Table 11.5, with F membrane having the highest charge density of (-0.42 eq/m^3), followed by NF B, E, A, D, G, H and C on the bottom of the list having the lowest calculated charge density of (-0.02 eq/m^3). Table 11.5, lists the charge densities of the NF membranes in the presence of bi-valence ions of $MgSO_4$, were the charge density increases in comparison to NaCl solution. The percentage of charge density increase, for each NF membrane tested here, between NaCl and $MgSO_4$ testing solutions, is shown. This may be explained as the negatively charged sulphate functional groups of the $MgSO_4$ salt cause the membrane to become more negatively charged. However, the order of top three membranes' charge density is not matching the order in NaCl solution with B membrane having the highest charge density of (-0.628 eq/m^3), followed by E then F in $MgSO_4$ solution, while the order in NaCl solution is F, B then E. For the rest of the membranes, they have the same order of charge density in both salt solutions.

Results at NaCl solution		Results at $MgSO_4$ solution		% Increase $\left(\frac{\text{CD in MgSO4} - \text{CD in NaCl}}{\text{CD in NaCl}}\right)$
NF membrane	NF charge density, eq/m^3	NF membrane	NF charge density, eq/m^3	
A	-0.360	A	-0.562	56.1 %
B	-0.411	B	-0.628	52.8 %
C	-0.020	C	-0.071	255.0 %
D	-0.332	D	-0.545	64.1 %
E	-0.404	E	-0.610	51.0 %
F	-0.420	F	-0.584	39.0 %
G	-0.303	G	-0.460	51.8 %
H	-0.165	H	-0.325	97.0 %

Table 11.5 Results of the membrane charge density in NaCl and $MgSO_4$ solutions as calculated from the membrane potential measurements

Although, in general the effect of SO_4^{2-} on NF charge density is noticeable, the degree (percentage) of increase is different from NF to another. This can be explained by considering the effects of the adsorbed SO_4^{2-} ions. As anions (SO_4^{2-}) can approach more closely to hydrophobic surfaces because they are less hydrated than cations (Mg^{2+}). In this process NF surface will acquire a negative electro-kinetic potential due to the presence of anions beyond the plane shear [128]. Thus, the degree of increasing membrane charge density as a result of sulphate adsorption would depend on the hydrophobicity of the membrane surface. Such phenomenon of influencing the NF membrane charge in the presence of multi-valence salt in comparison with (1:1) electrolyte, is in agreement with previous research work as shown in the next table:

Reference work	Tested NF membrane	Zeta potential Results (at pH = 8)
128	NFT50	- 12.5 mV at 1 mM KCl - 18.0 mV at 0.1 mM $CaCl_2$
173	TFCS	- 15.0 mV at 0.01 M NaCl - 16.0 mV at 0.001 M Na_2SO_4 + 0.01 M NaCl

Table 11.6 Example of data extracted from the literature for the effect of bivalence ion on NF potential

9. Discussion:

9.1 General behaviour:

In here, a conventional technique based on TMS of membrane potential measurements in order to yield information on the membrane average charge density has been implemented.
As for the membrane potential, an increase of electrolyte ionic strength leads to reduction of the absolute value of NF potential as shown in Figures 11.3 and 11.4. Such decrease of membrane potential with the increase of solution ionic strength is regarded as the reduction of electrostatic force between the ions or charged molecules and the NF membrane surface [129,169]. The results obtained from the membrane charge density calculations suggest that the magnitude of membrane charge density will be increased by the presence of bi-valence ions in comparison to mono-valence solution. It shows that SO_4^{2-} ions increases the membranes charge. This suggests that sulphate ions are effective in influencing the membrane charge density. This is an important fact for NF membranes characterisation for sulphate rejection applications as a pretreatment to seawater desalination plants (and for offshore oil/gas industry). As NF membranes are required to reject almost all sulphate content in feed water prior to the desalination unit, increasing the NF charge density through the process of NF manufacturing will strengthen the electrostatic force between sulphate ions and the membrane; thus, it would be much easier for the membrane to reject it presenting this in a repel force.
However, such a proposal of increasing NF charge during membrane fabrication in order to enhance sulphate rejection should be optimised in conjunction with other research work relating the effect of NF charge to fouling tendency. The study of the relation between NF charge and fouling is beyond the scope of the present research work. However, it should be emphasised, that recently, it has been reported [178] that, NF negative charge is a desirable membrane property to reduce fouling. On the other hand, in the presence of calcium ions, (which are present in seawater) carboxyl groups of NF surface layer (that causes the negative charge) can enable the formation of calcium bridges between NF surface and organic foulants and, consequently, increase organic fouling [178].

9.2 Analysis:

The main objective of this part of the work is to provide a mechanistic explanation for the contribution of NF charge on its performance to reject sulphate ions presented in seawater. A thorough understanding of the interrelation between NF membrane filtration performance and its charge characteristics is of paramount importance in this research.

The relation between NF sulphate rejection and charge density is shown in Figure 11.5. There is a clear relation of increasing sulphate rejection with increasing the charge density.

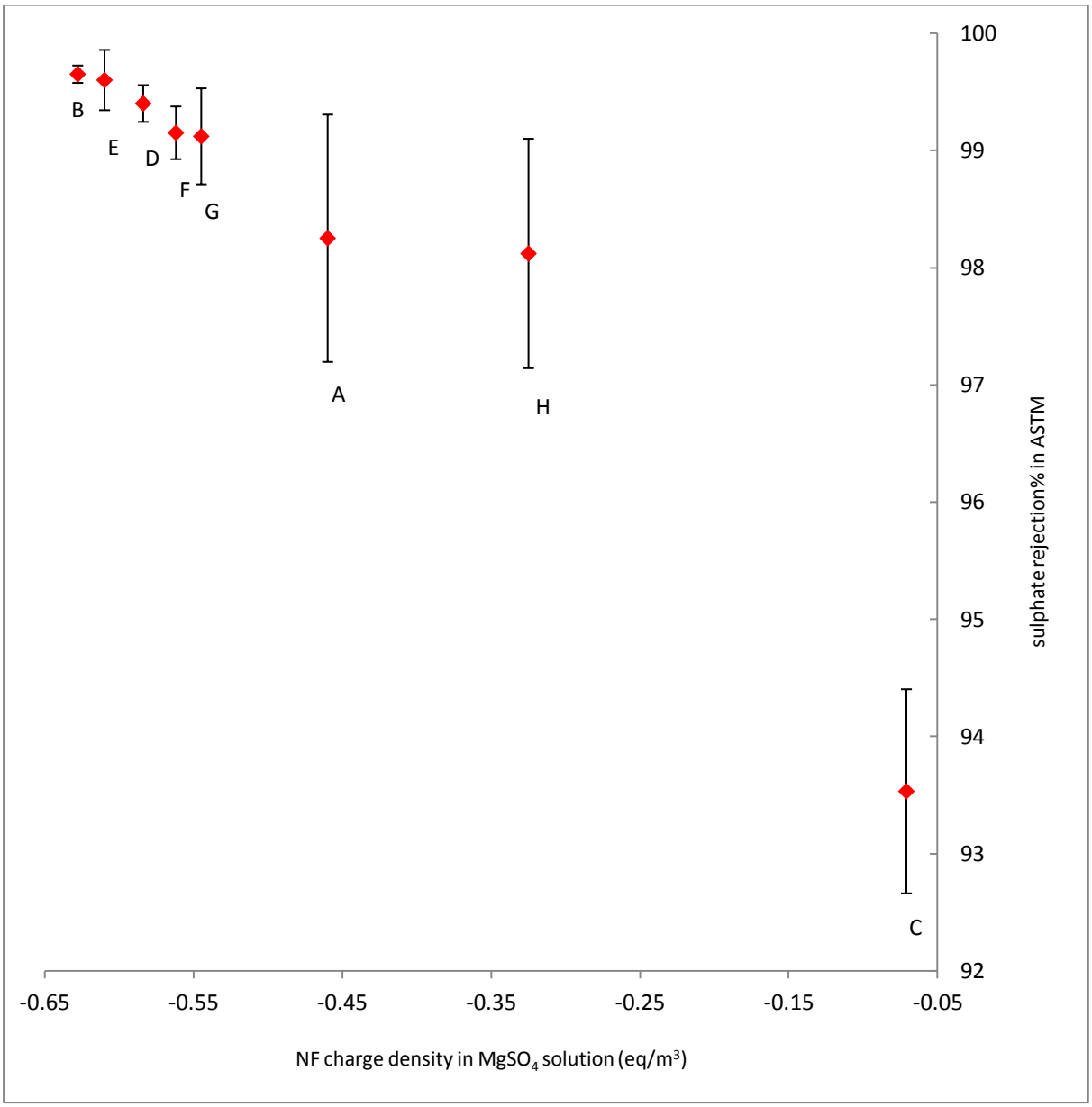

Figure 11.5 NF membranes sulphate rejection percentages and its charge density in ASTM

The main finding of NF charge density results is that nanofiltration performance, more particularly its ability for sulphate rejection is related to its charge density.

A hierarchy list below (Table 11.7), shows NF order from highest to lowest for sulphate rejection ability (according to ASTM experiment) and for their charge density.

Order	NF order in terms of average sulphate rejection% based on ASTM experimental data(1)		NF order in terms of charge density (eq/m^3)			
			in $MgSO_2$ solution		in NaCl solution	
1	**B**	99.65	**B**	- 0.628	**F**	- 0.420
2	**E**	99.60	**E**	- 0.610	**B**	- 0.411
3	**D**	99.40	**F**	- 0.584	**E**	- 0.404
4	**F**	99.15	**A**	- 0.562	**A**	- 0.360
5	**G**	99.12	**D**	- 0.545	**D**	- 0.332
6	**A**	98.25	**G**	- 0.460	**G**	- 0.303
7	**H**	98.12	**H**	- 0.325	**H**	- 0.165
8	**C**	93.50	**C**	- 0.071	**C**	- 0.020

Table 11.7 NF membranes order in terms of: sulphate rejection in ASTM and charge density (note; NF sulphate rejection order is the same in simulated seawater experiment). (1) for ASTM data, please refer to table 7.9

As the data in Table 11.7 implies, the order of NF charge density in both solutions and its sulphate rejection ability order is not much different. However, an in-depth analysis is required for better understanding.

Out of the eight membranes, only NF H and C – on the bottom of the list – are in the same order for both sulphate rejection and charge density in NaCl or $MgSO_4$ solutions. In addition, NF B and E on the top of the list are in the same order (1^{st} and 2^{nd}) in terms of sulphate rejection and charge density in $MgSO_4$, but not the case in NaCl solution, where they are 2^{nd} and 3^{rd} respectively. While, the rest of the membranes (A, D, F and G) are not in a direct relevance of ordering according to their charge density (whether in NaCl or $MgSO_4$ solutions) to match sulphate rejection order.

For NF B and E having high hydrophobic surfaces compared to the rest of membranes under study (check chapter 9), therefore, results in more interactions and absorption between the SO_4^{2-} molecules and the negatively charged membrane. In which explains more negative charge density membrane.

NF F; although it carries the highest charge density at NaCl test, moreover, sulphate presence in $MgSO_4$ generates a higher charge, nevertheless, this much of increase is of less order compared to NF B and E (check Table 11.7). This may be caused by the surface state of NF F membrane being the smoothest in comparison to the rest of the membranes tested here.

NF C; this particular membrane is designed mainly for high rejection of natural organic loading materials. Its charge density is the lowest among the rest of the membranes, as well as its sulphate rejection ability. The low (lack) of negative charge may cause the membrane to be "looser" than when the membrane (hence, pores) are charged. Therefore, its sulphate rejection ability will depend mainly on the size of the pores. Expanding this explanation, NF rejection is due to both size exclusion and co-ion electrostatic repulsion (known as charge exclusion). Indeed, when dealing with organic matters present in seawater, pore size exclusion is more important in the rejection of uncharged molecules, than membrane charge. This fact justifies its low surface charge density as such application does not require surface charge for rejection. NF A, D, G and H; all have the same charge density order (4^{th} to 7^{th}) in NaCl and $MgSO_4$ solutions. With sulphate rejection order of D, G, A and H being 3^{rd}, 5^{th}, 6^{th} and 7^{th} respectively. However, it appears that along with NF charge density, the other parameters of porosity factor and surface morphology (hydrophilicity, wettability, surface free energy and surface roughness) all together, could be correlated in order to explain NF performance and how they contribute to sulphate rejection and permeate flux. This explanation is provided in main discussion chapter 12.

10. Conclusions:

In this part of the experimental work, the electric field generated when either NaCl or $MgSO_4$ electrolytes is in contact with stationary charged NF membrane creating potential difference across the membrane has been measured. As a result of membrane potential measurements, calculations of the averaged charge density of the eight membranes under investigation have been produced. Concerning NF charge density in such environments simulating seawater salt content, where ionisation of membrane active surface polymer material will cause a negative charge. The charge density of NF is not constant and is directly related to the working

solution chemistry as it imposes insight on membrane charge. Predictably, for actual seawater applications, location (site) feed water chemistry and its ionic strength would be a key factor to affect the quantity of NF charge density. Overall, it has been shown that, the negatively charged sulphate functional groups of $MgSO_4$ cause the membrane to become more negatively charged in comparison to its charge density in NaCl solution.

Individually, each NF membrane exhibited different interaction between SO_4^{2-} molecules and its surface. For more hydrophobic membranes, such as NF C, interactions between the SO_4^{2-} molecules and the negatively charged membrane surface result in significant SO_4^{2-} adsorption and more negative charge in comparison to its charge in NaCl solution. For smoother membranes, as the case for NF F, although SO_4^{2-} molecules will increase membrane charge density, however, such increase is limited due to low availability of interaction area. Accordingly, NF charge at monovalent electrolyte as the case in NaCl may contribute to the membrane polymer type and fabrication. While in multivalent electrolyte as $MgSO_4$, the charge depends on membrane surface status either being rough or smooth, along with polymer type.

This important approach to change the membrane charge in presence of sulphate is of great benefit for consideration in membrane quest for optimum NF application for sulphate rejection from seawater.

It is obvious that SO_4^{2-} rejection is more hindered as a result of NF negative charge density than bi-valent hardness cations Mg^{2+}. As both sulphate molecules and NF are negatively charged, thus it will be repulsed by the membrane surface and to satisfy the electro-neutrality condition, an equivalent number of magnesium is retained which results in $MgSO_4$ salt retention. Such factor of electro-neutrality has been referred by previous study [128].

Over the eight NF membranes tested here, the slight variation of sulphate rejection does depend (relatively) on membrane negative charge.

To sum up (to this end), as seawater is characterised by having high content of salts, in such working solution NF membrane acquire negative charge. Certainly, the existence of negative charge on the NF will exhibit its effects on membrane performance for sulphate rejection. Although, the charge density magnitude is low as shown here, there contribution to sulphate rejection is importance for seawater desalination along with other NF features such as porosity and surface nature. Detailed analysis to correlate NF filtration performance in terms of water flux and sulphate rejection with all measured characters through the experimental phases of this work is provided in next chapter (overall discussion – chapter 12).

Chapter 12: OVERALL DISCUSSION

1. NF for sulphate removal:

This research study has demonstrated that the use of NF membranes is a reliable technique for sulphate ions rejection.

Such a substantial reduction in SO_4^{2-} content, confirms the use of NF membranes as a pretreatment for desalination plants and also for offshore oil/gas industry as a sulphate scale prevention technique. It guarantees a sulphate rejection near to 99% (as shown in this study) providing an opportunity for seawater desalination plants operating on such type of feed water to not suffer from sulphate scaling. As a result, it could be expected that NF usage would reduce energy consumption, increase recovery, and reduce running cost as a result of operating the plant with higher recovery ratio (as shown in the case study of this chapter – section 6).

To provide a scale-up between laboratory results to be translated to the field, a study [110], demonstrates that two or three parallel measurements are sufficient to greatly improve the reliability of test cell results, (the term reliability here in the sense of minimal scale-up error) as long as there is enough distance (> 400 mm) between the sample locations on the same sheet. An average scale-up error between test cell measurements and the average filtration performance properties of a large membrane area for three NF membranes was found to be from 2.1 – 10% [110]. Moreover, recently [182], for NF-desalination it has been shown that the dead-end filtration testing protocol to assess NF performance would provide important information for scale-up from laboratory to pilot-plant tests, such as membrane selection, optimum operating parameters and mechanism analysis [182].

The experimental protocol of the current research work measured flux and rejection in a laboratory environment using dead-end filtration, by testing six parallel samples taken from different parts of the membrane sheet apart by (> 400 mm). Also, all the tested NF membranes, were supplied by manufacturers, are available in the market for commercial sale, i.e. material found in modules not membrane material used for laboratory tests. As the difference between the membrane material used for laboratory tests and the material found in commercial modules (due to differences between production batches) may be responsible for scale-up errors.

Hence, it is considered that the data obtained in this research is representative of the tested commercial NF membranes for scale-up purposes.

2. NF performance:

An approximate characterisation for NF based on the use of manufacturer specification data cannot give results which are in satisfactory agreement with those obtained by a full analysis based on laboratory experimentation under uniform conditions.
In order to critically characterise and evaluate the optimum potential use of nanofiltration as pretreatment for seawater desalination plants in terms of sulphate rejection for sulphate scale prevention, eight commercially available membranes for the target process have been studied. All membranes are of TFC made via the process of interfacial polymerisation and are typical nanofiltration membranes for water treatment applications to reduce hardness and remove organics, colour, bacteria, and other impurities from a raw water supply.
The eight tested nanofiltration membranes have shown variation in their characteristics and these variations affect the membrane performance, more particularly, the permeate flux.

Figure 12.1 represents the position of the NF membranes in terms of permeate flux and sulphate rejection that arise from the experimental work of this research following the standard ASTM test procedure [42], (for detailed results refer to Figure 7.4 and Table 7.9).

Figure 12.1 shows the average values together with the scatter expressed as two standard deviation (as detailed in chapter 7 and Appendix 2).

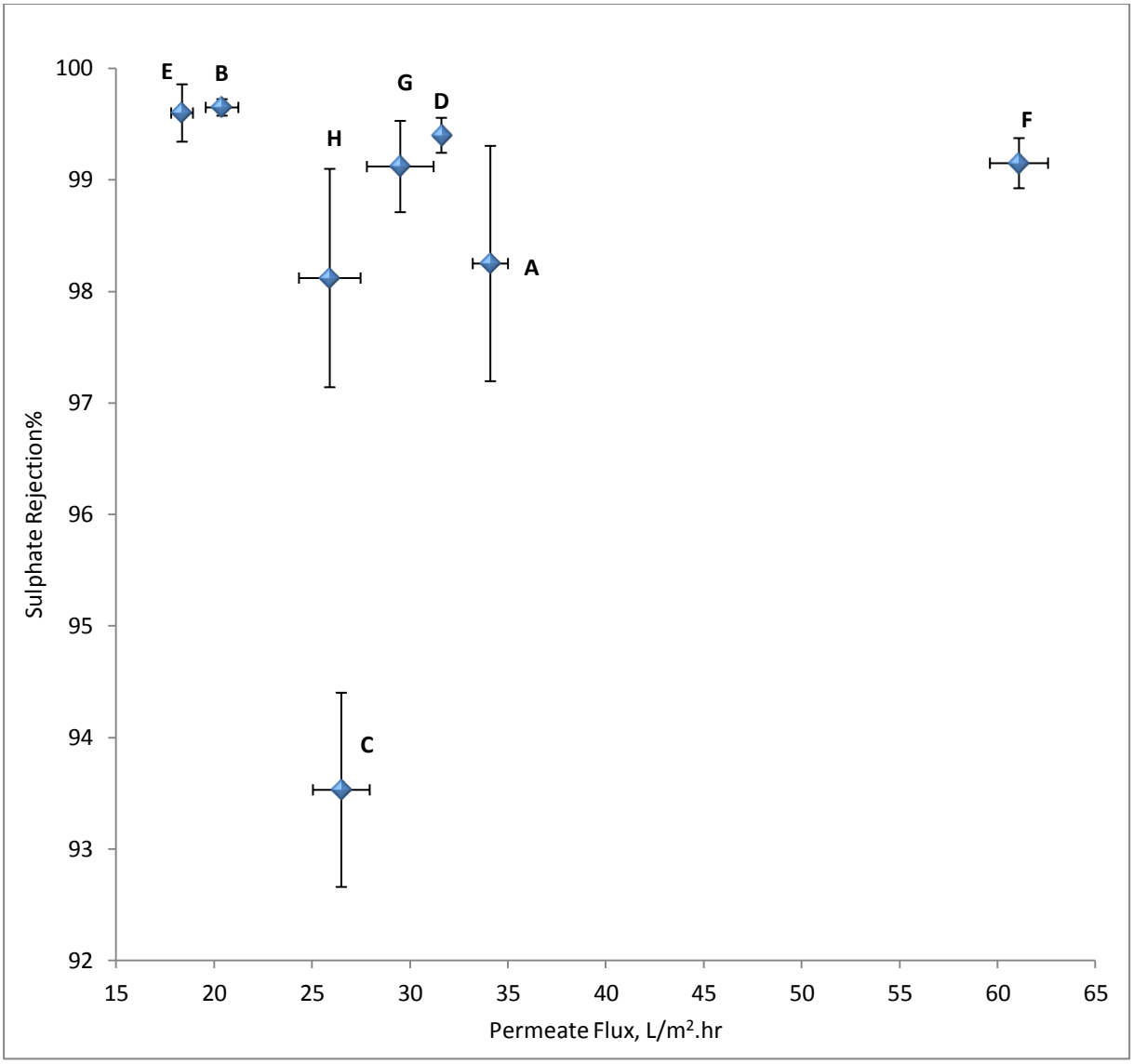

Figure 12.1 The filtration performance of the NF membranes in ASTM testing conditions

The work has confirmed the high sulphate rejection capabilities of currently available NF membranes with sulphate rejection of >98% obtainable from seven membranes under standard ASTM testing conditions and simulated seawater environment.

By comparing the various membranes under an identical testing protocol, the work has, however, revealed, differences in permeate flux between the different membranes. Such comparative information is important to designers of NF equipment and is not available (or hard to realise) from data obtainable from the different membrane manufacturers/suppliers.

The influence of important operational variables, temperature and pressure, has been evaluated:

- Increases in either temperature (between 19 – 40 °C) or pressure (between 9 – 25 bar) results in a continuous rate of increase of permeate flow,
- The influence of increasing feed water temperature and/or pressure was less clear-cut on the sulphate rejection of the NF membranes. Although with the possible trend towards increase sulphate rejection at higher temperature and pressure.

Nevertheless, optimum operating conditions – pressure and temperature – are to be selected based on the inlet feed water quality in addition to NF membrane manufacturer recommendations.

One critical finding in regard NF performance, relates to a general perception (more particularly in seawater desalination community), that a membrane with a high water permeability also has a higher salt permeability compared to a membrane with lower water permeability. However, the results shown here are not in full agreement with such perception. Taking NF F and A as an example, having the following measured filtration performance in the ASTM test:

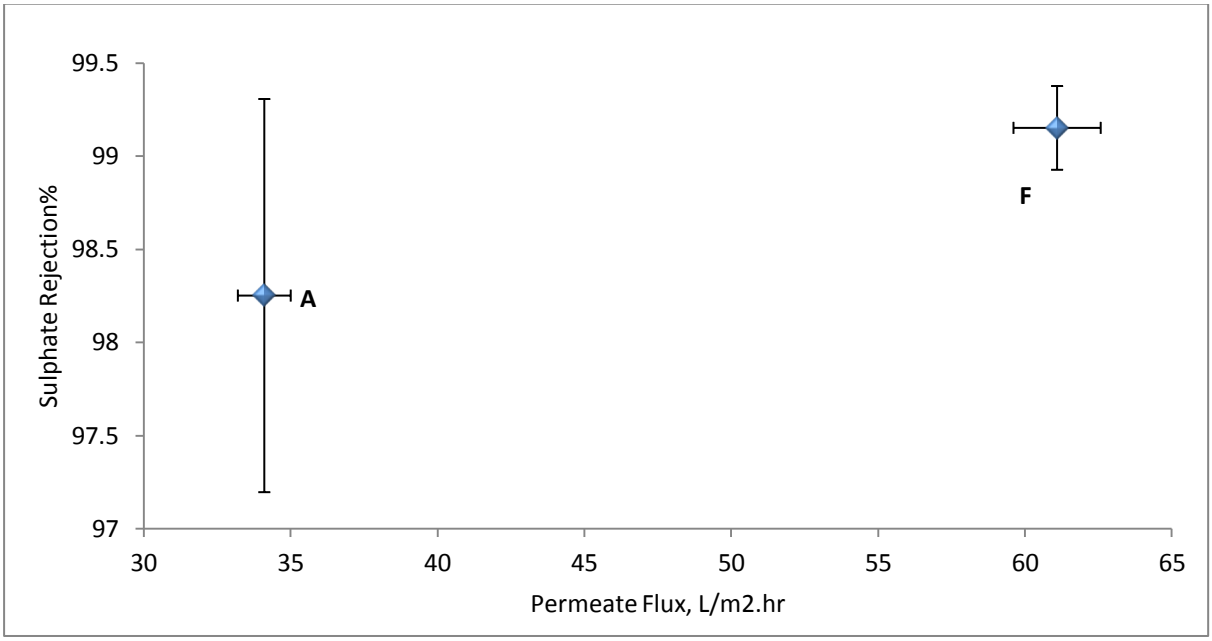

Figure 12.2 The filtration performance of NF A and F membranes in ASTM

As shown in Figure 12.2, NF F membrane has higher water permeability in comparison to NF A, while both membranes almost attain similar sulphate rejection. This is to emphasise the need to check the validity of such generalising perceptions on a critical scientific basis, to validate its relevance for a target application.

3. NF characterisation:

Membrane characterisation is essential in choosing a suitable membrane for a process. To obtain more insight into the performance of the commercial membranes and to validate the limited information supplied by the manufacturers, the objective of this part of the research was to investigate the correlation between NF characteristics and filtration performance.

It appears that, NF sulphate rejection performance is complex and is dependent on a number of events and factors related to the membrane active surface layer features. Accordingly, this research work was targeted to provide a description of the sulphate separation mechanism justifying the correlations in between all factors that control NF performance. That is, it can be explained by a combination of the membrane properties characterisation. Membrane properties, which are crucial to explain NF performance, are:

1. Pore size, indicated by porosity factor calculations.
2. Surface morphology:
    - Hydrophobicity, indicated by contact angle measurements leading to surface free energy calculations.
    - Surface roughness, indicated by AFM analysis.
3. Membrane charge, indicated by membrane potential measurements leading to charge density quantification.

In terms of the above filtration performance/membrane characterisation exercise, the following sub-division becomes clear.

Membrane with (relatively) low sulphate rejection and moderate permeate flux, as the case of NF C membrane. This particular membrane is designed for high rejection of natural organic materials and moderate rejection of total hardness. However, it has been included in this research work to widen the knowledge of specialised NF characteristics. NF C membrane has been characterised with the lowest charge density, most rough surface, most hydrophobic, moderate porosity factor and moderate surface free energy.

The second group includes the remaining seven NF membranes (A, B, D, E, F,G and H) having a sulphate rejection ability over 98%. However, they differ in terms of permeate flux. To fully understand the differences in NF performance, the following discussion has been produced on the basis of the research findings.

- **Correlation between membrane characteristics and membrane filtration performance, for the second group (A, B, D, E, F, G and H):**

Porosity factor:

The aim of the porosity factor calculations was to investigate the contribution of NF pores opening on its filtration performance. Results (in Chapter 8) show that an increase in pore size, due to conformational changes of the cross-linked membrane polymer structure, increases water permeability. The surface porosity gives a good idea about the void volume of membrane that the fluid may pass through it.

For sulphate rejection, it is important to consider the roles of sieving (size exclusion) and electrostatic interactions for the negatively charged sulphate molecules having a hydrated radius = 0.29 nm [93]. It has been acknowledged in the literature, that pore size alone does not govern the efficiency of NF membrane in separation process in water treatment [88].

NF membranes E, B, H and G have porosity factors of 0.22, 0.24, 0.27 and 0.29 nm respectively. Therefore, sulphate rejection is strongly dependent on size exclusion, as pore size is smaller than the size of hydrated sulphate. While the remaining three membranes of the group, NF F, A and D have porosity factors of 0.43, 0.31 and 0.3 nm respectively, therefore sulphate rejection will depend on charge repulsion between molecules and membrane surface, as pore size is larger than the hydrated sulphate.
This indicates that if hydrated sulphate molecules are larger than the NF membrane pore therefore it will experience size exclusion. As opposed to a scenario where molecules are smaller than pores, hence repulsive forces influence rejection. Also, it can be concluded that diffusive transport mechanism becomes more important than convective transport when the NF pore radius is smaller than the hydrated radius of sulphate.

For H_2O transport, over a range of NF membranes, a NF membrane with highest porosity factor produces the highest permeates flux. NF membrane flux is related to the porosity factor in a way that the smaller the porosity factor, the lower the flux is and vice versa (Figure 8.1). This has been explained as; smaller porosity factor indicate that the NF membrane surface structure is more impermeable with narrower pores, thus lower flow rates are expected. At high porosity factor corresponds to a relatively wide pores opening, thus water mass transfer through the membrane surface is very likely to permeate.

Hydrophilicity:

The contact angle measurement provides valuable information about the hydrophilicity of the membrane surface. The contact angle results (in Chapter 9) revealed a relation between NF permeate flux and its hydrophilicity/hydrophobicity. That explains the differences in permeability among the tested NF membranes. High hydrophilic NF membrane surface (indicated by low contact angle), provides more wettability to water molecules. Hence, the ionic interaction between water molecules and the negatively charged NF surface increases. Therefore, NF flux increases in comparison with less hydrophilic membrane.
Usually the analysis of NF hydrophilicity is based on the contact angle of de-ionized water [101]. However, in the current research, results showed that the presence of salts influences the ionic interaction between water molecules and the negatively charged NF surface, indicated by the slight improvement in NF hydrophilicity, which has been explained in Chapter 9. Moreover, during charge density studies, it has been shown that the hydrophilic nature of the NF membranes influences its charge. The membranes initially have a negative charge in NaCl electrolyte. In $MgSO_4$, the membranes become slightly more negative due to hydrophobic interactions between the sulphate and the membrane surface.

NF solid surface free energy and its constituents were calculated from contact angles of simulated seawater solution, diiodomethane and ethylene-glycol. The differences in the surface free energy (and its constituents) exhibited by the NF membranes could be attributed to the polymer concentrations of the surface active thin film composite, as it has been reported in the literature that such concentration have a high influence on the membranes' surface free energy properties [143]. As the NF active-surface, polymer-concentration decreases, this results in decreasing electron acceptor functionality and increasing electron donor functionality, hence the NF membrane surface becomes more hydrophilic represented by low contact angle and high surface free energy. Consequently, the ionic interactions between H_2O molecules and NF membrane surface increases as well as wettability, explaining the increase in permeate flux over the range of NF membranes under study.

Over the tested membranes, it has been shown that an increase in NF permeate flux is associated with a drop in contact angle (i.e. more hydrophilic, hence wettable), (Figure 9.7), an increase in electron donor functionality and a decrease in electron acceptor functionality (Figure 9.9).

Surface roughness:

To further study the morphology of the NF membranes, AFM surface analysis was conducted. Results obtained from AFM characterisation for the surface topographies facilitate the quantitative of average surface roughness of the wet membranes as a key physical parameter.

It has been shown that the surface roughness is an important structural property of NF membranes that influences its performance.

The theoretical description is that, at low surface roughness, more predominant local mass transfer is occurring through flow channels which has been reported to control water permeation flux, in comparison to higher surface roughness [154].

In the current research study, the flux correlated well with the surface roughness in a way that with an increase in the surface roughness, the flux decreases. However, trends in surface roughness did not correlate with the measured sulphate rejection. The highest surface roughness value was measured for NF E membrane having the lowest flux among the other membranes. The roughness of the different membranes generally decreases in the sequence of increasing the corresponding flux. Of the eight membranes analysed by AFM, the F membrane (that produced highest flux among all the membranes) was characterised as having the smoothest surface. The *Ra* value for the F membrane was smaller than those for the other membranes (Figure 10.4). This observation is further supported by the 3D image of the NF F surface, (Figure 10.5) which shows smaller measured height than are seen in the images for the other membrane surfaces.

Charge density:

In this work, the charge of the commercial nanofiltration membranes under investigation has been calculated by means of measurements of membrane potential. The main finding of the NF charge density results is that nanofiltration performance, more particularly its ability for sulphate rejection, is generally related to its charge density. The narrow observed differences in the sulphate rejection (98.0 – 99.7 %) of the NF membranes have been attributed to the NF charge density (Figure 11.5). Although, all tested NF membranes have developed a similar trend of membrane potential curves (shown in Figures 11.3, 11.4), nonetheless, the following aspects have been observed.

- The negatively charged sulphate ion causes the membranes to become more negatively charged in comparison to their charge in NaCl solution.

- For NF B, E and F membranes, the order of the magnitude of the membrane potential, hence, the order of charge density is different from NaCl to $MgSO_4$ solutions. In NaCl solution, the order is: F, B then E, having charge density of (- 0.420, -0.411, -0.404 in eq/m^3) respectively. In $MgSO_4$ solution, NF B membrane followed by E then F, having charge density of (-0.628, -0.610, -0.584 in eq/m^3) respectively.

- For NF A, D, G, H and C membranes, the same order of both membrane potential and charge density from highest to lowest in NaCl or $MgSO_4$ solutions is the same with only difference being in charge density percentage increase from NaCl to $MgSO_4$ solution.

It can be concluded that the negative charge depends upon the degree of de-protonation of the NF active surface polymer material ($R\text{-}COOH \rightarrow R\text{-}COO^- + H^+$) and water chemistry (including ionic strength) of the working solution as a key factor to affect the quantity of membrane charge density.

This imposes the need to critically relate NF charge density to its performance for a better understanding of NF characterisation for seawater sulphate rejection applications. The following figure shows the relation between NF charge density and its normalised flux to porosity factor.

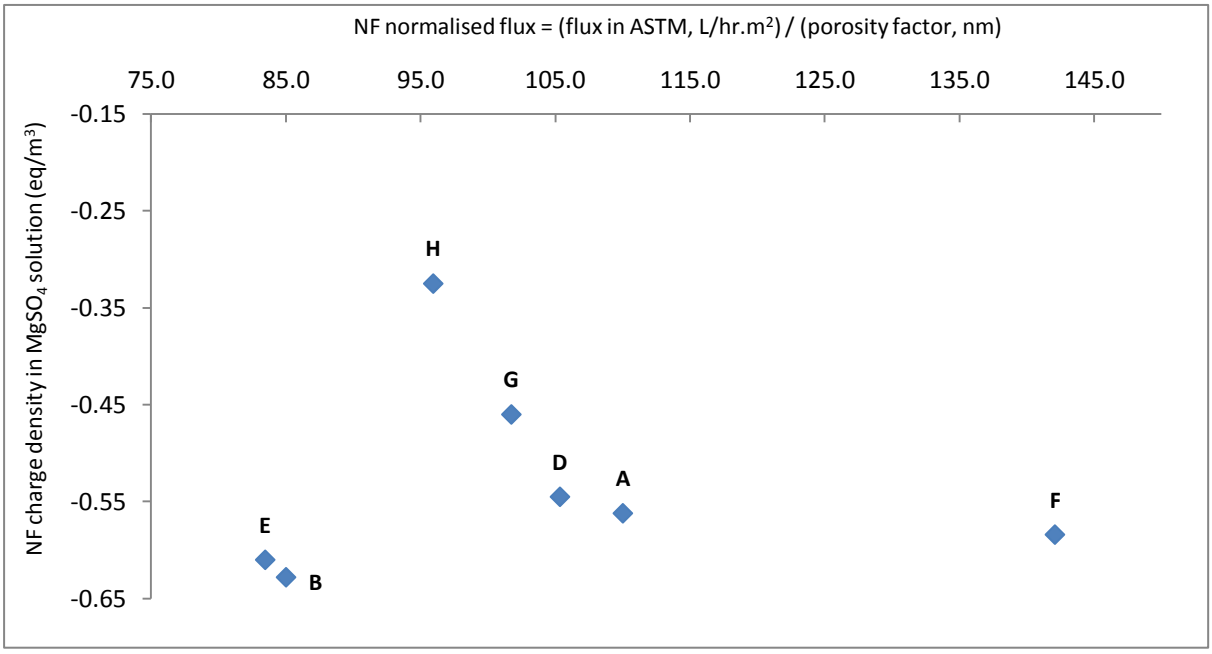

Figure 12.3 Normalised flux to porosity and CD of the NF membranes

Although the difference in the charge density of the tested NF membranes in $MgSO_4$ solution range from (-0.628 to -0.325 eq/m^3), nevertheless, there is not much discrepancy between the sulphate ion separation of the membranes as all seven membranes (shown in Figure 12.3) had sulphate retentions exceeding 98%. Thus, it is apparent that charge density of the NF membranes alone, is not enough to discriminate on the basis of charge between the sulphate rejections of the tested membranes. This can be explained by considering a combination of both separation mechanisms of electrostatic repulsion and by size exclusion.

As discussed earlier, NF F, A and D having a porosity factor larger than the size of hydrated sulphate molecule, therefore, sulphate retention is mostly caused by repulsion due to the NF negative charge. For the rest of the membranes of the same group, NF G, H, B and E the retention of sulphate is mainly caused by size exclusion due to the NF pore size being smaller than sulphate hydrated size.

This is to emphasise the role of NF negative charge for sulphate molecules rejection for membranes having a pore size larger than the size of sulphate hydrated molecule. In such case, sulphate separation is based on the charge repulsion mechanism as a result of the electrostatic interactions between ions and membrane negative charge.

Overall

Over the seven membranes of the same group, the sulphate rejection is relatively constant; nonetheless they show variations in permeate flux. The differences in filtration performance have been explained in relation to NF membrane surface hydrophilicity, roughness, charge and porosity as all play a significant role in the transport of H_2O and $(SO_4)^{2-}$ molecules through the membrane. Permeate (water) flux is determined by the morphology of the NF active surface layer, which in turn depends on its hydrophilicity, roughness and pore size. For sulphate ion rejection, both sieving and electrostatic interactions are responsible for its separation. A conclusion can be drawn in regard the filtration mechanism which separate $(SO_4)^{2-}$ is that diffusion is more controlling the separation when the size of hydrated sulphate (sulphate and the surrounding water) is larger than NF pore size. Also at high membrane negative charge as sulphate will encounter electro-migration. At these occasions less sulphate can enter the membrane pores and is unable to be transported by convection.

It is believed that the approach adopted in this research study leads to a more appropriate selection of NF membrane properties that can result in improved performance for the desalination plant. The data provided here for the tested membranes, resulting from NF characterisation, facilitates the critical evaluation of membrane features and is believed to offer a proper tool for carefully choosing membranes to suit the target usage for sulphate rejection in seawater desalination practices and offshore oil/gas application. Over a range of NF membranes for the target application, the membrane to be characterised with the largest pore size, hydrophilic, smooth and high negatively charge is favourable in terms of filtration performance.

To fully understand the differences in the performance of the seven NF membranes, of the same group, the following envelope (Table 12.1) has been produced from the data collected in this research.

SURFACE MORPHOLOGY PARAMETERS			
Hydrophilicity/Hydrophobicity nature indicated by Contact Angle	Hydrophobic (> 45^0)	Moderate ($43^0 – 32^0$)	Hydrophilic (< 32^0)
AFM – Avg. surface roughness, R_a , nm	Rough (> 8)	Moderate (8 – 4)	Smooth (< 4)

CHARGE DENSITY in $MgSO_4$ solution, eq/m^3 ([- 0.325] – [- 0.628])			
	B **E** Z1	**A** **D** **G** **H** Z2	**F** Z3
	Small (< 0.25)	Moderate (0.25 – 0.39)	Large (≥ 0.4)
	POROSITY FACTOR, nm		

Common features:

1. All are of thin film composite type of commercial NF membranes in spiral wound configuration
2. The SO_4^{2-} rejection of the seven membranes is (> 98%)

Table 12.1 Characterisation envelope for the second group of NF membranes under investigation for sulphate rejection applications (NF permeate flux increases from Z1 – Z2 – Z3)

As shown, this envelope is divided into three zones (Z: 1 – 3). The sulphate rejection of the NF membranes is almost identical over (98%), with the consideration of the statistical standard deviation. However, the position of the membranes is based on correlating permeate flux to the other membrane characteristics.

- NF **B** and **E**, fall in zone 1, having the lowest permeate flux in comparison with the rest of the membranes. Characterised by small pores, hydrophobic surface and high roughness.
- NF **A, D, G** and **H**, having moderate permeate flux fall in zone 2, characterised by moderate: surface roughness, hydrophilicity and pore size.
- NF **F**, falls in zone 3, having substantially the highest permeate flux of almost double that of the membranes in zone 2, characterised by smooth hydrophilic surface and large pores.

Membrane characterisation properties which have been analysed by porosity factor calculation, contact angle measurements, AFM and charge density have been able to explain the differences between the different membranes studied. The contact angle measurements identifies the hydrophilicity nature of the active surface layer of the NF membranes, and indicates that membranes having more hydrophilic surface produces more permeate flux. AFM measurements confirm that membranes with low average surface roughness value corresponds to a higher permeate flux. Finally membrane potential measurements leading to charge density calculations show (Chapter 11) that sulphate rejection is generally related to its charge density.

Results analysis showed one membrane (NF F), that stands out in terms of highest permeate flux with high sulphate rejection (>99%), has been characterised by; large pore size (0.43 nm, as porosity factor), hydrophilic nature (31.9^{o} as a contact angle and a total surface free energy of 46.98 mJ/m^2), smooth surface (average surface roughness, Ra = 3.267 nm) and high charge density (-0.584 eq/m^3). Such a membrane, with high water permeability in comparison to other membranes of the same category and target application, facilitates a low feed pressure and thus a low energy to operate at a given flux and less number of serial elements in a stage (number of elements per vessel).

4. Long term NF operation on seawater

The basic rational for this research study is that accurate comparison of characteristics parameters for various NF membranes with one another, that is only valid and reliable when the measurements have been made on virgin membranes using the same measuring techniques and have been performed by the same method. In this regard NF characteristics parameters determination has been carried out on virgin membrane. It should be recognised that all the findings (and related discussions) in the present thesis relate to the filtration performance of clean membranes. In practice, of course, there is a tendency for membrane to become fouled. Nevertheless, consideration of the behaviour of membranes under fouling conditions should be founded on a knowledge and understanding of characteristics and behaviour of clean membranes.

In order to understand the performance over long term operation of high sulphate rejection NF elements on seawater, consideration of the operational experience at the Umm-Lujj NF-RO plant (Saudi Arabia, started in 2000) is useful. For plant assessment, please refer to Chapter 4, section 1.2, of this thesis. The NF unit consisted of 27 housings in parallel, each with six 8-in diameter Osmonics-DK8040 membrane elements, totalling 162 elements. The unit operated at 65 percent permeate recovery, initially operating at a high permeate flux, 43 L/hr.m^2, which required 25 bar feed pressure at 33°C. The feed pH was 6.0, which resulted in (>98%) sulphate rejection (based on feed concentrations). Conventional pretreatment was used, resulting in a Silt Density Index (SDI) of less than 3.5 in the NF feed. However, the fouling rate of the NF elements was too high, which resulted in frequent element cleanings. At each cleaning the sulphate rejection (and that of all other hardness ions) decreased [25,26]. To decrease the fouling rate, permeate flux was lowered to 20 L/hr.m^2, at 30°C, pH 6.1, and 65 percent recovery, that required 14 bar (gauge) feed pressure, at which time the fouling rate was low. No element cleaning was performed for one year. Sulphate rejection based on feed concentration was 91%. After one year of operation at pH 6.1, permeate recovery increased to 85 percent, the feed gauge pressure was 18 bar, and rejections at 28°C was 79% for sulphate. After a three month, stop necessitated by pretreatment problems, rejections declined to 62% for sulphate. When pH was increased to 8.1, rejections decreased to 28–35%. In addition, the required feed gauge pressure to achieve 21 L/hr. m^2 permeate flux was 17 bar at 20°C and 11 bar at 38°C [34]. Both operations indicated that membrane fouling increased salt passage.

Thus, when a high sulphate rejection is desired, it is crucial to optimise NF selection to reduce NF element fouling.

Interestingly though, a study [66], on three commercially available membranes, two nanofiltration membranes: NF270 and NF90 and a low-pressure reverse osmosis membrane BW30, undertook fouling tests. That involved measuring de-ionized (DI) water flux for the three membranes for 90 min before and after filtrating a sample water having organic compounds of total organic carbon (TOC = 136.4 mg/L) for 20 min at 5.5 bar.

The DI water flux for the second run was lower than the first run indicating fouling of the membranes. BW30 permeate flux shows the most reduction among tested membranes, however it produced the highest quality organic rejection permeate. NF270 showed the least reduction in permeate flux as a result of fouling.

These findings were rationalised in terms of membrane characters, obtained from the literature, summarised below:

Membrane	Rej % (2000 ppm NaCl)	Contact angle in DI	RMS roughness (nm)
NF 270	80	42.7	9.0
NF 90	90 – 96	54.6	129.5
BW 30	99.4	60.8	60.8

It was assumed by the authors [66] that there was a correlation between the NaCl rejection and pore size. On this basis, NF270 is assumed to have the largest pore size. According to the reported contact angle and RMS roughness in the above table, NF270 also has the smoothest and most hydrophilic surface.

Other work has also found a lower surface roughness is a desirable characteristic in NF application in seawater softening if less fouling is a key performance objective [25].

Understandably, over the tested NF membranes presented in this thesis, NF F membrane that has been characterised with the largest porosity factor, smoothest and most hydrophilic surface, in comparison to the other membranes, is expected to be less vulnerable to fouling. In addition, for a practical application the choice of membrane will depend on the water quality requirements for the particular beneficial use being considered. Further the degree of membrane fouling during operation will affect the frequency of membrane cleaning.

Recently, a study [184], examined an ultrafiltration–nanofiltration (UF: HF1500 – NF: ESNA3-4040) integrated membrane system operated for 500 hours to examine the performance of the NF membrane in seawater desalination pretreatment. Chemical cleaning

was carried out when the NF permeation flux declined over 10% after 280 hours during the long run. Chemical cleaning was performed using 2.0 wt.% citric acid and 0.1 wt.% NaOH in sequence for 30 min at atmospheric pressure and temperature. The chemical cleaning procedure and agents were chosen according to the protocol proposed by the manufacturer.

The rejection of sulphate, TDS and TOC by the NF membrane as well as the permeation flux after 30 and 470 hours is reported as follows:

	NF feed water	NF permeate after 30 hours	NF permeate after 470 hours
SO_4^{2-}, mg/L	2310	24	30
TDS, mg/L	33,760	25,500	25,810
TOC, mg/L	0.94	0.06	0.09
Permeate flow rate, m/s	0.035	0.035	0.035
Feed pressure, MPa	2.03	2.05	2.06

As a result of NF chemical cleaning after 280 hours, the long term operation reveals that, at a constant permeate flux, a slight increase in applied feed water pressure enables the NF to maintain its filtration performance.

In summary, based on other research works [25,26,34,66,184], for long term NF operation on seawater to be capable of maintaining its specific ion rejection properties. Optimum NF membrane characteristics have been identified and membrane cleaning protocol.

5. Relevance to choice of NF membrane as pretreatment for desalination plant:

A major conclusion from the present research is that NF membranes had a high ability to reject sulphate. This property would reflect in the performance of a desalination plant which received feed from NF (see next section – case study). Hence, the particular NF membrane which is to be implemented to pretreat seawater prior to sending it to either membrane or thermal desalination system, requires optimum membrane selection. As for complex waters like seawater, it is important to select the optimum membrane for hybrid system design.

- For thermal plants, NF pretreatment should achieve high degree of sulphate ions rejection to meet the requirements of optimum sulphate rejection and high permeate flux. Membranes, such as NF F tested here, are expected to be the optimum selection because of the high flux combined with 99% sulphate rejection. Such membrane of large pore size, smooth hydrophilic surface and high charge density is favourable to meet the requirements.

- While, for RO plants, due to the strict water quality requirements to be met by every pretreatment process in order to prolong membrane life and prevent its fouling, a combination of NF targeting divalent ions rejection and NF of high rejection to organic compounds (such as NF C, characterised with the low charge density, rough surface, hydrophobic, moderate porosity), should be employed for a hybrid operation to treat feed water for stable performance.

6. Analysis of NF pretreatment for MSF – Case Study:

The objective of this part is to analyse the concept of the potential usage benefit of NF as a pretreatment for MSF desalination plants from a practical point of view.

The current research work has revealed that NF implementation, for reducing seawater sulphate content to prevent calcium sulphate scale in desalination plant before feeding it into the unit (SWRO or thermal), is feasible and reliable as NF can reject up to 99% of sulphate ions present in seawater.

➢ Comparison of basic energy consumption of RO and MSF:

From a technical perspective, it is worth considering the following:

1. The current available single pass seawater reverse osmosis (SWRO) elements in the market are capable to reach 45% recovery. Where, NF-RO configurations are limited to maximum of 35% (for more details please see chapter 4, section 1.2).

2. The specific power consumption for SWRO has improved from 15 kWh/m^3 in 1980 to 4.0 kWh/m^3 in 2012. This has been associated with plant size improvement from 1 to 132 MGD over the same period.

3. While for thermal plants (MSF in particular), although the plant size has increased from 0.06 MGD (Duba plant in 1968 – west cost of KSA) to 24 MGD (Ras-ALkhair in 2013 – east cost of KSA), plants specific energy consumption is limited (in best operational scenario) to 232.6 kJ/kg since then.

For better understanding of the differences of the quoted numbers for SWRO specific power consumption of 4.0 kWh/m^3 and for MSF specific energy consumption of 232.6 kJ/kg, the following calculations are made to convert the units for suitable comparison.

SWRO plant specific power consumption = 4.0 kWh/m^3

Where, 1 kW = 1 kJ/s for 1 hr $\rightarrow$ 1 kWh = 3600 kJ

i.e. the 4.0 kWh/m^3 = 4 x 3600 kJ/m^3 = 4 x 3600/1000 kJ/kg

= 14.4 kJ/kg (as electrical energy)

from the 2nd law of thermodynamics;

1 J (as an electrical energy) = 3 J (as thermal energy), considering power plant efficiency is 30% then:

→ 14.4 kJ/kg x 3 = 43.2 kJ/kg (as thermal energy)

In comparison to MSF specific energy consumption = 232.6 kJ/kg

This calculation shows that the current energy consumption of MSF units to desalinate 1 kg of pure water from seawater is practically more than five times greater than the SWRO, e.g. Jeddah-4 MSF plant – west cost KSA – is running at a performance ratio of 7.5 equivalent to specific energy consumption = 310 kJ/kg.

A way in which NF pretreatment can be effective in reducing somewhat the gap, in terms of energy consumption, between the two most implemented technologies in seawater desalination (SWRO and MSF) is discussed below.

For MSF plant the energy consumption is usually expressed in terms of the performance ratio, usually denoted by the symbol PR. It can be regarded as a measure of the plant effectiveness, and defined in terms of the following ratios [8]:

$$Specific\ energy\ requirement = \frac{energy\ consumption}{unit\ mass\ of\ product\ water}\ , i.e.\ kJ/kg$$

$$Or\ the\ inverse\ form, PR = \frac{kg\ of\ product\ water}{2325\ kJ\ of\ energy\ supplied}\ , i.e. \frac{kg}{2325\ kJ}$$

(Note; the 2325 kJ is the latent heat of the saturated heating steam condensed in the brine heater with no condensate under-cooling [180]).

From thermodynamics analysis of MSF technology, where the performance ratio (often called specific energy consumption, in kJ/kg) can be defined by the following equation [6]:

$$PR = \frac{constant}{\left[\partial T_L + \frac{\Delta T}{N}\right]}$$

Where;

∂T_L= is the stage driving temperature difference

ΔT = total plant seawater/brine temperature range

N = total number of the stages

This formula can be approximated simply, with reasonable accuracy [8], to:

$$PR = \frac{\Delta T_{FR}}{\Delta T_{BH}} x\ constant$$

Where;

ΔT_{FR}= flash range = top brine temperature – bottom brine temperature

ΔT_{BH}= brine temperature rise across the brine heater

This shows clearly the relation between the plant performance and the available flash range.

Therefore, increasing the performance ratio (hence, lowering the specific energy consumption) can be achieved by increasing the flash range across the stages, hence increasing the available temperature range (or decreasing the temperature gradient across the brine heater). Here, the first option is considered.

- **Case study:**

To illustrate the above argument, relating to the use of NF pretreatment to MSF plant to facilitate increases in top brine temperature (TBT), a recent conceptual design study is presented and discussed next.

Increasing the flash range, by increasing the TBT above the imposed conventional figure of 112 ^{0}C, which has been based on the traditional strategy to avoid precipitation of calcium sulphate, can be achieved by removing the sulphate from the feed water through the approach of introducing NF as a reliable technique for pre-treatment.

The following proposed fundamental informative data (Table 12.2), based on Shoaiba Phase-2 of 10 MFS units of dual purpose plant (Saudi Arabia), lists the actual (current) operational and a proposed alternative mode of operation involving NF pretreatment.

Note; other critical data and important modifications – such as the pretreatment of the NF membranes and other operational considerations in case of NF failure are not listed in the table, as the purpose of this demonstration is to show the validity and the thermodynamic/economical benefits of utilising NF.

PARAMETER	Actual design	Proposed design [57]	% of change
Scale control strategy	High Temperature Additives (HTA)	NF pretreatment	
Top Brine Temp. TBT, ^{0}C	110	135	≅ 23 % increase
Bottom Brine Temp. BBT, ^{0}C	40	40	
Flash range	70	95	≅ 36 % increase
Performance Ratio, kg/2325 kJ	9.0	15	≅ 60 % increase
Specific thermal energy consumption, kJ/kg	258.4	155	≅ 40 % decrease
Unit production, m^3/hr	1,896	1,896	
Brine heater:			
Surface area, m^2	6578	2110	≅ 70 % decrease
Steam flow, t/hr	221.6	142	≅ 35 % decrease
Steam temperature, ^{0}C	117	143	≅ 20 % increase
Heat rejection No. of stages	3	3	
Heat recovery			
No. of stages	18	30	≅ 60 % increase
Stage surface area, m^2	6348	3244	≅ 50 % decrease
Plant flow rates, m^3/hr:			
CW to heat reject	12,458	11,600	≅ 6 % decrease
Make up	4425	2903	≅ 35 % decrease
Brine recycle	17,120	12,893	≅ 25 % decrease
Brine blow down	2529	1007	≅ 60 % decrease

Table 12.2 Main design and operational parameters of MSF distiller with and without NF as a scale control strategy

- **Further considerations and comments:**

1) The proposal is based on introducing NF as a pretreatment to the MSF units is a re-design concept. As shown for the number of heat recovery section stages, it must increase from the current 18 to 30 stages to fulfil the requirement of achieving higher brine heater inlet temperature. In other words, NF retrofitting to an existing thermal plant is not worth doing due to inability to increase the number of heat recovery stages to satisfy the increase in TBT as well as the needed plant modifications e.g. incorporating a decarbonator to remove the large amount of liberated carbon dioxide. This is to emphasise that the present proposal is a substantial change from previous attempt to introduce NF to an existing MSF unit (Layyah plant evaluation – chapter 4, section 1.2).

2) One critical advantage of increasing the TBT is, that this will reflect on the flash range which will increase from 70 ^{0}C (over 21 stages) to 95 ^{0}C (over 33 stages); therefore, the inter-stage temperature difference will drop from 3.3 to 2.9 ^{0}C.
   This will indeed, reduce the brine heater temperature rise.

3) It is of paramount importance to include, in the plant design,
   I. a by-pass system that will be activated in the event of NF-pretreatment system failure,
   II. and an automatic HTA (high temperature additive) ready supply to the brine recycle stream along with automatic signal to the brine heater steam inlet valve to throttle and to increase the de-super heater spray flow rate.

4) This new conceptual design yields considerable benefits of reducing the specific thermal energy consumption (important in an energy conscious world) by 40% as shown in Table 12.2, but it is expected to be at the expense of increasing the capital cost.

The cost of introducing NF to thermal distillation plant, on the overall capital costs (CAPEX) and operational costs (OPEX) is not well established [181]. As so many factors are to be considered, it has been suggested as an area for future research direction in this thesis. However, the subsequent discussion is an attempt to emphasise the impact of reducing the specific thermal energy consumption on the overall cost by increasing the TBT as a result of utilising NF as a pretreatment for sulphate rejection.

The original design of Shoaiba phase two dual purpose plant consists of 10 evaporators each producing 45,454 m³/d (12 MGD) built in 2001. The overall cost is 2.661 $/m³ with a breakdown as (0.834 capital cost, 1.064 energy cost, 0.435 chemicals cost, 0.106 O&M cost and 0.221 depreciation cost).

The conceptual design of NF implementation ahead of the MSF as a pre-treatment strategy, certainly will incur an increase in the initial capital cost of the pretreatment of the MSF. The salient features acquired by the implementation of the NF with the unequivocal saving in fuel, chemicals and plant dimensions would outweigh the increase in the additional cost in the pretreatment (as shown in Figure 12.4).

Considering the economical parameters used in estimating unit production cost involved: plant capital cost (according to current MSF desalination market price for a MSF unit producing 45,454 m³/d), plant life 25 years with 95% plant availability, depreciation 8.2 % of investment, labour cost at 1.5% of investment, maintenance cost at 2% of investment, electricity price at $0.05 /kWh (Saudi tariff). In addition to NF pretreatment at 90% recovery and 15% replacement per year estimated at 13.6 US cents/m^3 [52].

Moreover, increasing the TBT will require:

I. Supply of steam to the brine heater at higher temperature, nevertheless, the pumping power required to pump all the main streams will reduce (e.g. brine recycle by 25%) as a result of reducing the flow rates (as shown in Table 12.2).
II. The need for thicker brine heater shell. However, by utilising the new materials of super duplex stainless steel for the evaporator shell the brine heater surface area can be reduced by 70%, and the amount of steam supply will also reduced by 35% (as shown in Table 12.2), affecting the running (operational) cost.

Since the energy cost represents the highest cost component in seawater desalination of about 35% of the water cost. The cost breakdown in comparison of the original and proposed design with the predicted 40% reduction in the specific thermal energy consumption is substantial that will reflect on the other cost components (as shown next).

With this said, an estimation of the overall cost for the NF-MSF (in a cogeneration of power and water (dual purpose) station – in Saudi Arabia, where fuel is relatively inexpensive) is 1.996 $/m³ with a breakdown as (1.001 capital cost, 0.639 energy cost, 0.136 NF cost, 0.055 O&M cost and 0.166 depreciation cost)

A comparison of the cost components between the actual and proposed design is shown in Figure 12.4

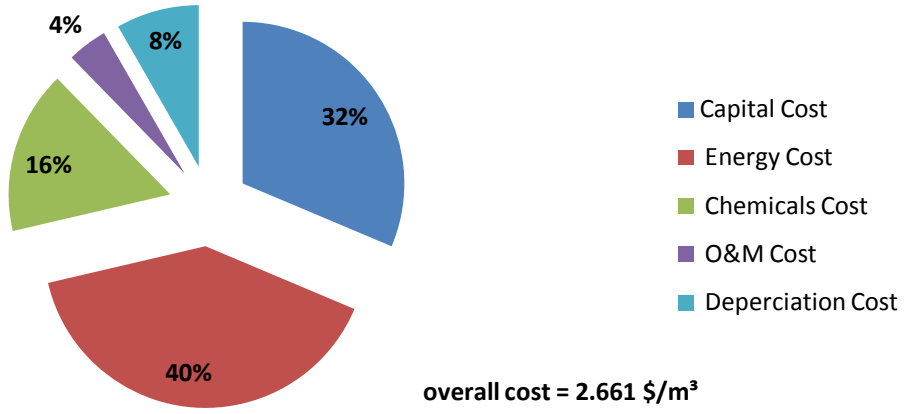

Cost breakdown of 45,454 m³/d MSF unit operating at 110 ^{0}C with high temperature additives as scale control strategy, with specific thermal energy consumption of 258.4 kJ/kg

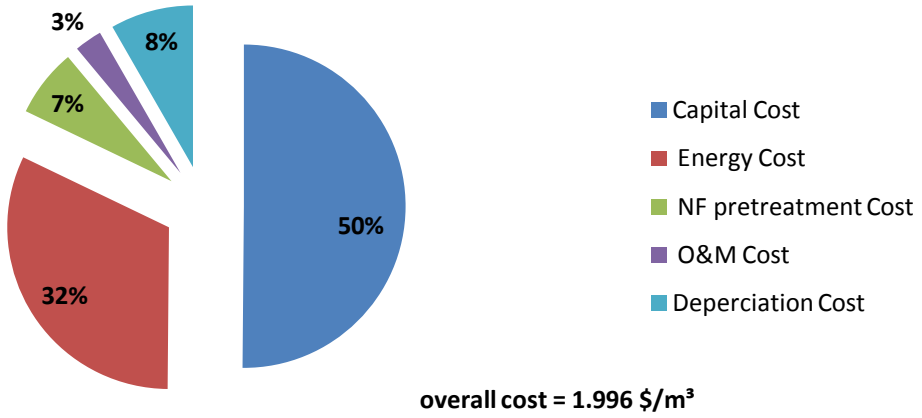

Cost breakdown of 45,454 m³/d MSF unit operating at 135 ^{0}C with NF pretreatment as scale control strategy, with specific thermal energy consumption of 155 kJ/kg

Figure 12.4 Cost comparisons between actual and proposed design

Although the contribution of the capital cost to the overall cost has increased by 20%, nevertheless, the cost breakdown indicated that the energy cost has reduced by about 40% which is reflected on the other cost components. Therefore, the overall cost has been reduced from 2.661 $/m³ to 1.996 $/m³, equivalent to 25% savings.

This illustration, demonstrates the benefit obtainable from the conceptual design of NF – MSF involving an increase in the TBT from 110 ^{0}C to 135 ^{0}C – as a result of sulphate removal from feed water – with improved energy efficiency of the MSF by 40%.

The relevance of conceptual studies, as exemplified by the one above is as follows. In the summer of 2013, daily production of desalinated water in Saudi Arabia peaked at 7 million m^3 of which 5.32 m^3 (i.e. 76%) was produced by MSF dual purpose plants. In order to cope with the future water demands and for the target of sustainable development, the authorities are committed to MSF for the next 25 – 50 years. Improving MSF performance ratio, from the present value, by the use of NF pretreatment based on membrane optimum selection (provided in this research work), hence increasing the TBT, will incur saving of fuel (oil barrel per day), as a result of reducing the specific thermal energy, that will have a considerable impact on the national economy.

Chapter 13: OVERALL CONCLUSIONS

- The difficulties, of assessing the potential of specific NF membranes for practical application using data available from the manufacturers, have been addressed. The value of evaluating commercially available membranes in identical testing exercises has been demonstrated. Thus, in this work, the filtration performance (sulphate rejection and water flux) of eight commercially available nanofiltration membranes has been evaluated by means of a common testing procedure (ASTM [42]) that facilitates a sensible means of comparison between different membranes.

- The testing has included effects of temperature and pressure to extend the usefulness of comparing the performance.

- For the experiment in ($NaCl + MgSO_4$) solution, results have yielded similar and relative performances as those measured in the ASTM solution and have thereby demonstrated the ability of separating sulphate ions in complex multi-ion solution.

- The research has involved an investigations of a number of membrane characteristics in order to correlate the findings from the filtration properties to membrane structure characteristics of:

  I. Pore size, via porosity factor calculations.

  II. Hydrophilicity/hydrophobicity surface nature, via contact angle measurements and surface free energy calculations.

  III. Surface roughness measurements, via AFM studies.

  IV. Membrane charge density, via membrane potential measurements.

- NF characteristics (summarised in Table 12.1) have yielded a good correlation between filtration performance and membrane characteristics.

- The research has shown, through characterisation under consistently uniform testing conditions and environment, that although seven of the tested membranes (A, B, D, E, F, G and H) can achieve sulphate rejection of (> 98%), they exhibit performance variations in terms of permeate flux, which have been explained in relation to membrane properties and features.

- One membrane (NF F), that stands out in terms of highest permeate flux and high sulphate rejection, has been characterised by; large pore size (0.43 nm – as porosity factor), hydrophilic nature (31.9^{o} as a contact angle and a total surface free energy of 46.98 mJ/m^2), smooth surface (average surface roughness, Ra = 3.267 nm) and high charge density (-0.584 eq/m^3). Such a membrane, with high water permeability in comparison to other membranes of the same category and target application, facilitates:

    1. A low feed pressure and thus a low energy to operate at a given flux.

    2. Less number of serial elements in a stage (number of elements per vessel). This particular point is of considerable benefit to NF selection for the offshore oil/gas application, minimising the space and weight requirements, hence, reducing the capital cost for platform area required for installation.

- The provided information for the criteria of optimum membrane selection based on these characteristic parameters that represent optimum product quality and quantity (as well as time dependent process such as fouling and scaling) confirms that NF pretreatment is technically attractive for seawater desalination in the view of sulphate removal, which will guaranty an important role on the process performance.

- MSF-NF case study demonstrates the thermodynamic/economical benefits of utilising NF pretreatment, summarised in Table 12.2 and Figure 12.4.

Suggested future research directions:

The work presented in this thesis would be further developed by the following suggestions:

- **NF characterisation for sulphate rejection applications:**

1. The exact pore features (shape) of NF membranes are still debatable. Although several methods are available, new techniques are required to achieve a more accurate determination of pore size, radius, dimensions and shape. Using positron annihilation spectroscopy could be a good choice.

2. Utilising a sulphate functional tip during AFM studies would yield information on the forces associated with NF sulphate rejection.

3. Extension of the research to assess NF membrane performance and characteristics for the effect of organic fouling (presented in seawater) in order to identify optimum NF properties (porosity, hydrophilicity, surface roughness and charge) which make the membrane less vulnerable to fouling and also are capable of maintaining its sulphate ion rejection.

- **NF usage as a pretreatment to desalination for sulphate removal**:

1. A critical investigation is needed to analyse the economics of reducing the cost from MSF as a result of increasing the plant performance ratio by the use of NF as pretreatment, in comparison to the capital and operational costs.

2. A full study is required to be carried out to idealise the pretreatment ahead of the NF membranes to investigate their operation without the addition of anti-scalent (or at very reduced dosing rate).

3. For NF system design, because of the varied rejection between mono and divalent ions, a research study on the effect of concentration polarisation (CP) degree on NF water recovery is needed by investigating the relationship between CP, salt rejection and water recovery in order to maintain a long-run stable performance.

1. IDA Desalination Year Book 2013-2014, Media Analytics Ltd, Oxford, 2013.
2. C. Sommariva, "New IDA president seeks sustainability", Desalination and Water Reuse, 21 (2012) 10 – 11
3. T. Pankratz, "Water Desalination Report", 48: (21) May 2012 and (38,39) October 2012
4. A. AL-Alshaikh, "Seawater Desalination in Saudi Arabia: An Overview", presentation at 2010 Asia-Pacific Conference on Desalination & Water Reclamation, China, June 23, 2010.
5. A. Cipollina, G. Micale, L. Rizzuti, "Seawater Desalination – Conventional and Renewable Energy Processes", Springer-Verlag, Berlin Heidelberg, 2009
6. T. Hodgkiess, "Desalination Technology", lectures notes, University of Glasgow, 2009.
7. R. Clayton, "Desalination for Water Supply – Review of Current Knowledge", foundation of water research, UK, 2006.
8. A. Porteous, "Desalination Technology – Development and Practice", Applied Science Publishers Ltd, N. Ireland, 1983.
9. C. Fritzmann, J. Löwenberg, T. Wintgens, T. Melin, "State-of-the-art of reverse osmosis desalination", Desalination, 216 (2007) 1–76
10. Global Water Intelligence (GWI/IDA DesalData), Market profile and desalination markets, GWI website, http://www.desaldata.com/.
11. N. Ghaffour, T. Missimer, G. Amy, "Technical review and evaluation of the economics of water desalination: Current and future challenges for better water supply sustainability", Desalination 309 (2013) 197–207
12. R. Huehmer, J. Gomez, J. Curl, "Cost modelling of Desalination systems", International Desalination Association World Congress, Perth, Australia, September 4-9, 2011, IDAWC/PER11-302
13. L. Awerbuch, "Nanofiltration: the Great Potential in Reducing Cost of Desalination", International Desalination Association World Congress, Gran Canarias, Spain. 21-26 October 2007, SP05-227
14. I. Karagiannis, P. Soldatos, "Water desalination cost literature: review and assessment", Desalination, 223 (2008) 448–456
15. A. Khawajia, I. Kutubkhanaha, J. Wie, "Advances in seawater desalination technologies", Desalination, 221 (2008) 47–69
16. M. Al-Ahmad, F. Abdul Aleem, "Scale formation and fouling problems effect on the performance of MSF and RO desalination plants in Saudi Arabia", Desalination, 93 (1993) 287-3 10

17. P. Dydo, M. Turek, J. Ciba, "Scaling analysis of nanofiltration systems fed with saturated calcium sulfate solutions in the presence of carbonate ions", Desalination, 159 (2003) 245-251
18. M. A1-Shammiri, M. Ahmed, M. A1-Rageeb, "Nanofiltration and calcium sulfate limitation for top brine temperature in Gulf desalination plants", Desalination, 167 (2004) 335-346
19. P. Schausbergera, G. Mustafab, G. Leslieb, A. Friedla, "Scaling prediction based on thermodynamic equilibrium calculation — scopes and limitations", Desalination, 244 (2009) 31–47
20. Q. Huang, W. Ma, "A model of estimating scaling potential in reverse osmosis and nanofiltration systems", Desalination, 288 (2012) 40–46
21. H. Hömig, "Seawater and Seawater Distillation", pg.68., Fichtner-Handbook, 1978
22. N. Li, A. Fane, W. Winston Ho, T. Matsuura, "Advanced Membrane Technology and Applications", Hoboken, New Jersey, John Wiley & Sons Inc., 2008
23. A. Mnif, M. Ben Sik Ali, B. Hamrouni, "Effect of some physical and chemical parameters on fluoride removal by nanofiltration", Ionics, 16 (2010) 245–253
24. P. Eriksson, "Nanofiltration Extend the range of membrane filtration", American institute of chemical engineers, New York, 1986
25. P. Eriksson, U. Bharwada, Q. Niu, R. Reddy, P.R. Dontula, Y. Tayalia "Nanofiltration for Seawater Softening: An Emerging and Economically Viable Process", IDA journal – Desalination and Water Reuse, 2 (Fourth Quarter 2010) 26 – 33
26. A. Farooque, "Research efforts by SWCC SWDRI towards the development of nanofiltration pretreatment for seawater desalination", Presented at 2009 IDA World Congress, UAE, REF: IDAWC/DB09-061
27. J. Tomaschke, "Membrane preparation, interfacial composite membranes, in: Encyclopedia of Separation Science", Academic Press, Oxford, 2000
28. A. Ahmad, B. Ooi, A. Mohammad, J. Choudhury, "Development of a highly hydrophilic nanofiltration membrane for desalination and water treatment", Desalination, 168 (2004) 215-221
29. W. Lau, A. Ismail, N. Misdan, M. Kassim, "A recent progress in thin film composite membrane: A review" Desalination, 287 (2012) 190–199
30. S. Subramanian, R. Seeram "New directions in nanofiltration applications — Are nano-fibers the right materials as membranes in desalination?", Desalination, 308, (2013) 198–208

31. C. Zhao, J. Xue, F. Ran, S. Sun, "Modification of polyethersulfone membranes – A review of methods", Progress in Materials Science, 58 (2013) 76–150
32. S. Kaur, S. Sundarrajan, D. Rana, T.Matsuura, S. Ramakrishna, "Influence of electrospun fiber size on the separation efficiency of thin film nanofiltration composite membrane", Journal of Membrane Science, 392 (2012) 101–111
33. R. Weber, H. Chmiel, V. Mavrov, "Characteristics and application of new ceramic nanofiltration membranes", Desalination, 157 (2003) 113 – 125
34. A. Abdullatef, A. Farooque, G. Al-Otaibi, N. Kither, S. Al-Khames, "Optimum nanofiltration membrane arrangements in seawater pretreatment - part-1", Paper presented at IDA World Congress – Spain, 2007 under Ref: MP07 – 163
35. AWWA Manual, "Reverse Osmosis and Nanofiltration", American Water Works Association, 1999
36. M. Bader, "Sulphate removal technologies for oil fields seawater injection operations", Journal of Petroleum Science and Engineering, 55 (2007) 93 – 110
37. W. van der Meer, C. Aeijelts Averink, J. van Dijk, "Mathematical model of nanofiltration systems", Desalination, 105 (1995) 25-31.
38. W. R. Bowen, W.A. Mohammad, "A theoretical basis for specifying nanofiltration membranes -dye/salt/water streams", Desalination, 117 (1998) 257-264.
39. J. Schaep, B. Van der Bruggen, C. Vandecasteele, D. Wilms, "Influence of ion size and charge in nanofiltration". Separation and Purification Technology, 14 (1998) 155–162.
40. S. Deon, A. Escoda, P. Fievet, "A transport model considering charge adsorption inside pores to describe salts rejection by nanofiltration membranes", Chemical Engineering Science, 66 (2011) 2823–2832
41. L. Malaeb, G. Ayoub, "Reverse osmosis technology for water treatment: State of the art review", Desalination, 267 (2011) 1–8
42. Standard Test Method for Operating Characteristics of Reverse Osmosis and Nanofiltration Devices1, ASTM procedure, Designation: D 4194 – 03 (Reapproved 2008)
43. A. Hassan, *et al*, "A new approach to membrane and thermal seawater desalination processes using nanofiltration membranes", Desalination, 118 (1998) 35-51
44. M. Al-Sofi, A. Hassan, G. Mustafa, A. Dalvi, M. Kither, "NANOFILTRATION AS MEANS OF ACHIEVING HIGHER TBT OF ≥120°C in MSF", Desalination, 118 (1998) 123-129.
45. A. Hassan, *et al*, "A DEMONSTRATION PLANT BASED ON THE NEW NF-SWRO PROCESS", Desalination, 131 (2000) 157-171

46. A. Hassan, "DEVELOPMENT OF A NOVEL NF- SEAWATER DESALINATION - PROCESS AND REVIEW OF APPLICATION FROM PILOT PLANT TO COMMERCIAL PRODUCTION PLANT STAGES-1" Paper presentation at the 4th International Water Conference in Arab Countries, Lebanon, 2004
47. O. Hamed, "Overview of hybrid desalination systems — current status and future prospects", Desalination, 186 (2005) 207–214
48. P. Eriksson, M. Kyburz, W. Pergande, "NF membrane characteristics and evaluation for sea water processing applications", Desalination, 184 (2005) 281–294
49. O. Hamed, M. Al-Ghannam,K. Al-Shail' T. Goto, Y. Taniguchi, M. Hirai' T. Kannari, K. Maekawa, "DEVELOPMENT OF TRI-HYBRID NF/RO/MED DESALINATION SYSTEM", Paper presented at Arwadex Conference held in Riyadh during 21-23 January 2007.
50. L. Awerbuch, "Integrated Upgrading of Thermal Processes and Nanofiltration Experience of SEWA", IDA journal – Desalination & Water Reuse, (May-June 2007), 18-28
51. A. Llansana, E. Ferrero, V. Ayala,J. Malfeito, "Characterization of Nanofiltration Membranes and Their Evaluation for RO Desalination Pre-Treatment", International Desalination Association IDA World Congress, Spain, 2007, REF: IDAWC/MP07-089
52. A. Abdullatef, A. Farooque, G. Al-Otaibi, N. Kither, "SIGNIFICANT IMPROVEMENTS IN NF SEAWATER PRETREATMENT UP TO 90% RECOVERY WITH 40% REDUCTION IN NF PRODUCTION COST" Paper presented at WSTA 9th Gulf Water Conference held in Muscat, Oman on 22-25 March 2010.
53. O. Hamed, *et al*, "Successful operation of MED/TVC Desalination process at TBT of 125 ^{0}C without scaling", Paper presented at SWCC 6th acquired experience symposium, 2011
54. C. Kurth, R. Burk, J. Green, "UTILIZING NANOTECHNOLOGY TO ENHANCE RO MEMBRANE PERFORMANCE FOR SEAWATER DESALINATION", International Desalination Association IDA World Congress, Australia, 2011, REF: IDAWC/PER11-323
55. A. Helal, A. Al-Jafri, A. Al-Yafeai, "Enhancement of existing MSF plant productivity through design modification and change of operating conditions", Desalination, 307 (2012) 76–86
56. A. Hassan, "Time to upgrade Carlsbad SWRO design to NF-SWRO Hybrid", IDA journal – Desalination and Water Reuse, (May-June 2012) 17 – 21

57. N. Nada, "Bridging the Gap between MSF and RO", Presentation at KAUST – Water Desalination and Reuse Center, 2nd Thermal workshop, 12-13 March 2013
58. A. Hassan, *et al*, "CONVERSION AND OPERATION OF THE COMMERCIAL UMM LUJJ SWRO PLANT FROM A SINGLE SWRO DESALINATION PROCESS TO THE NEW DUAL NF-SWRO DESALINATION PROCESS", International Desalination Association IDA World Congress, Bahrain, 2002
59. P. Eriksson, "Evaluation of Nanofiltration as Pretreatment to Reverse Osmosis in Seawater Desalination", International Desalination Association IDA World Congress, Singapore, 2005, REF: SP05-004
60. A. Mohammad, N. Ali, A. Ahmad, N. Hilal, "Optimized nanofiltration membranes relevance to economic assessment and process performance", Desalination, 165 (2004) 243-250
61. A. Mohammada, N. Hilal, H. Al-Zoubib, N.A. Darwish, N. Alia, "Modelling the effects of nanofiltration membrane properties on system cost assessment for desalination applications", Desalination, 206 (2007) 215–225
62. M. Bader, "Sulphate scale problems in oil fields water injection operations", Desalination 201 (2006) 100–105
63. M. Bader, "Nanofiltration for oil-fields water injection operations: analysis of concentration polarization", Desalination 201 (2006) 106 –113
64. M. Bader, "Nanofiltration for oil-fields water injection operations: analysis of osmotic pressure and scale tendency", Desalination 201 (2006) 114–120
65. M. Bader, "Innovative technologies to solve oil fields water injection sulphate problems", Desalination 201 (2006) 121–129
66. S. Mondal, S. Wickramasinghe, "Produced water treatment by nanofiltration and reverse osmosis membranes", Journal of Membrane Science, 322 (2008) 162–170
67. D. Williams, "Turning water into oil: desalination: A process to enhance world oil resources", International Desalination Association World Congress, Perth, Australia, September 4-9, 2011, IDAWC/PER11-134
68. B. Su, F. Liu, X. Gao, F. Yi, C. Gao, "Study on seawater nanofiltration softening technology for offshore oilfield water flooding", International Desalination Association World Congress, Perth, Australia, September 4-9, 2011, IDAWC/PER11-321
69. L. Henthorne, M. Hartman, "Desalination in the oil industry - perfecting enhanced oil recovery using optimized water quality", International Desalination Association World Congress, Perth, Australia, September 4-9, 2011, IDAWC/PER11-368

70. B. Su, M. Dou, X. Gao, Y. Shang, C. Gao, "Study on seawater nanofiltration softening technology for offshore oilfield water and polymer flooding", Desalination, 297 (2012) 30–37
71. T. Pankratz, "Water Desalination Report", 49 (24), (July 2013) 1 – 4
72. T. Pankratz, "Water Desalination Report", 49 (1), (January 2013) pg.3
73. R.S. SILVER, "Desalination – The Distant Future", Desalination, 68 (1988) 1-10
74. W. R. Bowen, A. W. Mohammad, "A theoretical basis for specifying nanofiltration membranes – Dye/salt/water streams", Desalination, 117 (1998) 257 – 264
75. J. Schaep, C. Vandecasteele, A. W. Mohammad, W. R. Bowen, "Modelling the retention of ionic components for different NF", Separation and Purification Technology, 22-23 (2001) 169–179
76. J. Straatsma, G. Bargemana, H.C. van der Horst, J.A. Wesselingh, "Can nanofiltration be fully predicted by a model?", Journal of Membrane Science, 198 (2002) 273–284
77. W. R. Bowen, J. S. Welfoot, "Predictive modelling of nanofiltration: membrane specification and process optimisation", Desalination, 147 (2002) 197-203
78. K. Wesolowska, S. Koter, M. Bodzek, "Modelling of nanofiltration in softening water", Desalination, 163 (2004) 137-151
79. S. Bandini, C. Mazzoni, "Modelling the amphoteric behaviour of polyamide nanofiltration membrane", Desalination, 184 (2005) 327 – 336
80. H. Al-Zoubi, N. Hilal, N.A. Darwish, A.W. Mohammad, "Rejection and modelling of sulphate and potassium salts by nanofiltration membranes: neural network and Spiegler–Kedem model", Desalination, 206 (2007) 42–60
81. A.R. Hassana, N. Alia, N. Abdulla, A.F. Ismail, "A theoretical approach on membrane characterization: the deduction of fine structural details of asymmetric nanofiltration membranes", Desalination, 206 (2007) 107–126
82. F. Fadaei, S. Shirazian, S. Ashrafizadeh, "Mass transfer modeling of ion transport through nanoporous media", Desalination, 281 (2011) 325–333
83. F. Fadaei, V. Hoshyargar, S. Shirazian, S. Ashrafizadeh, "Mass transfer simulation of ion separation by nanofiltration considering electrical and dielectrical effects", Desalination, 284 (2012) 316–323
84. R. Wang, Y. Li, J. Wang, G. You, C. Cai, B. H. Chen, "Modeling the permeate flux and rejection of nanofiltration membrane separation with high concentration uncharged aqueous solutions Desalination 299 (2012) 44–49

85. W. R. Bowen, A. W. Mohammad, N. Hilal, "Characterisation of nanofiltration membranes for predictive purposes - use of salts, uncharged solutes and atomic force microscopy", Journal of Membrane Science, 126 (1997) 91-105.
86. A. E. Yaroshchuk, "Recent progress in the transport characterisation of nanofiltration membranes", Desalination, 149 (2002) 423–428
87. N. Hilal, H. A1-Zoub, N.A. Darwish, A.W. Mohammad, M. Abu Arabi, "A comprehensive review of nanofiltration membranes: Treatment, pretreatment, modelling, and atomic force microscopy", Desalination, 170 (2004) 281-308
88. N. Hilal, H. Al-Zoubi, N.A. Darwish, A.W. Mohammad, "Characterisation of nanofiltration membranes using atomic force microscopy", Desalination, 177 (2005) 187-199.
89. K. Boussua, B. Van der Bruggena, A. Volodinb, C. Van Haesendonckb, J.A. Delcourc, P. Van der Meerend, C. Vandecasteelea, "Characterization of commercial nanofiltration membranes and comparison with self-made polyethersulfone membranes", Desalination, 191 (2006) 245–253
90. K. Boussu, Y. Zhang, J. Cocquyt, P. Van der Meeren, A. Volodin,C. Van Haesendonck, J.A. Martens, B. Van der Bruggen, "Characterization of polymeric nanofiltration membranes for systematic analysis of membrane performance", Journal of Membrane Science, 278 (2006) 418–427
91. J. Brant, K. Johnson, A. Childress, "Characterizing NF and RO membrane surface heterogeneity using chemical force microscopy", Colloids and Surfaces A: Physicochem. Eng. Aspects, 280 (2006) 45–57
92. M. Nilssona, G. Trägårdha, K. Östergren, "Salt and temperature dependent permeability changes of a NF membrane", Desalination, 199 (2006) 39–40
93. A. Hussain, M. Abashar, I. Al-Mutaz, "Influence of ion size on the prediction of nanofiltration membrane systems", Desalination, 214 (2007) 150–166
94. V. K. Gupta, S. Hwang, W. B. Krantz, A. R. Greenberg, "Characterization of nanofiltration and reverse osmosis membrane performance for aqueous salt solutions using irreversible thermodynamics", Desalination, 208 (2007) 1–18
95. K. Boussu, *et al.,* "Physico-Chemical Characterization of Nanofiltration Membranes", ChemPhysChem 2007, 8, 370 – 379
96. S. Lin, S. Sicairos, R. Navarro, "Preparation, Characterization and Salt Rejection of Negatively Charged Polyamide Nanofiltration Membranes", Journal of Mexican Chemical Society, 51 (2007) 129-135

97. C. Harrison, Y. Gouellec, R. Cheng, A. Childress, "Bench-Scale Testing of Nanofiltration for Seawater Desalination", Journal of Environmental Engineering, 133 (2007) 1004 – 1014
98. A.A. Hussain, S.K. Nataraj, M.E.E. Abashar, I.S. Al-Mutaz, T.M. Aminabhavi, "Prediction of physical properties of nanofiltration membranes using experiment and theoretical models", Journal of Membrane Science, 310 (2008) 321–336
99. K. Northcott, S.E. Kentish, J. Best, G. Stevens, "Development of membrane testing protocols for characterisation of RO and NF membranes", Desalination, 236 (2009) 194–201
100. X. Wang, W. Shang, D. Wang, L. Wu, C. Tu, "Characterization and applications of nanofiltration membranes: State of the art", Desalination, 236 (2009) 316 – 326
101. G. Hurwitz, G.R. Guillen, E. Hoek, "Probing polyamide membrane surface charge, zeta potential, wettability, and hydrophilicity with contact angle measurements", Journal of Membrane Science, 349 (2010) 349–357
102. H. Kelewou, A. Lhassani, M. Merzouki, P. Drogui, B. Sellamuthu, "Salts retention by nanofiltration membranes: Physicochemical and hydrodynamic approaches and modelling", Desalination, 277 (2011) 106–112
103. B. Tansel, "Significance of thermodynamic and physical characteristics on permeation of ions during membrane separation: Hydrated radius, hydration free energy and viscous effects" Separation and Purification Technology 86 (2012) 119–126
104. A. Childress, J. Brant, P. Rempala, D. Phipps Jr., P. Kwan, "Evaluation of Membrane Characterization Methods", water research foundation, 2012.
105. S. Deon, A. Escoda, P. Fievet, R. Salut, "Prediction of single salt rejection by NF membranes: An experimental methodology to assess physical parameters from membrane and streaming potentials", Desalination, 315 (2013) 37–45
106. D. Oatley, L. Llenas, N. Aljohani, P. Williams, X. Martínez-Lladó, M. Rovira, J. de Pablo, "Investigation of the dielectric properties of nanofiltration membranes", Desalination, 315 (2013) 100 – 106
107. D.J. Johnson, S.A. Al Malek, B.A.M. Al-Rashdi, N. Hilal, "Atomic force microscopy of nanofiltration membranes: Effect of imaging mode and environment", Journal of Membrane Science, 389 (2012) 486– 498
108. Q. Li, M. Elimelech, "Natural organic matter fouling and chemical cleaning of nanofiltration membranes", Water Science and Technology: Water Supply, 4 (2004) 245–251

109. H.M. Krieg, S.J. Modise, K. Keizer, H.W.J.P. Neomagus, "Salt rejection in nanofiltration for single and binary salt mixtures in view of sulphate removal", Desalination, 171 (2004) 205-215

110. T. Schipolowski, A. Jeowska and G. Wozny, "Reliability of membrane test cell measurements", Desalination, 189 (2006) 71–80

111. A. Abdulgader, G. Troy, S. Al-Ghamd, "Effect of High Feed Temperature on Nanofiltration and RO Membrane Performance", SWCC R&DC, issued as Troubleshooting Technical Report No. 3807/03016 in May 2005

112. L. A. Richards, B. S. Richards, B. Corry, A. I. Schäfer, "Experimental Energy Barriers to Anions Transporting through Nanofiltration Membranes", Environmental Science and Technology, 47 (2013) 1968−1976

113. W. T. Hanbury, "Trends In Desalination Technology", 2005, Portland Ltd., U.K.

114. J. Stawikowska, A. Livingston, "New Developments in the Physio-chemical Characterisation of OSN Membranes, in: Proceedings of 'Third International Conference on Organic Solvent Nanofiltration', 13–15 September, Imperial College London, UK, 2010

115. J. Pellegrino, "Filtration and ultrafiltration equipment and techniques", NIST, (2007) 1–13

116. R. Vacassy, C. Combe, V. Thoraval, L. Cot, "Synthesis and characterisation of microporous zirconia powders: application in nanofilters and nanofiltration characteristics", Journal of Membrane Science, 132 (1997) 109–118

117. J.A. Otero, O. Mazarrasa, J. Villasante, V. Silva, P. Prádanos, J.I. Calvo, A. Hernández, "Three independent ways to obtain information on pore size distributions of nanofiltration membranes", Journal of Membrane Science, 309 (2008) 17-27

118. C. Bellona, J.E. Drewes, P. Xu, G. Amy, "Factors affecting the rejection of organic solutes during NF/RO treatment—a literature review", Water Research, 38 (2004) 2795–2809

119. C.T. Cleveland, T.F. Seacord, A.K. Zander, "Standardized membrane pore size characterization by polyethylene glycol rejection", Journal of Environmental Engineering, 128 (2002) 399–407

120. K. Kosutie, B. Kunst, "Removal of organics from aqueous solutions by commercial RO and NF membranes of characterized porosities", Desalination, 142 (2002) 47-56

121. Y. Kiso, Y. Sugiura, K. Kitao, K. Nishimura, "Effects of hydrophobicity and molecular size on rejection of aromatic pesticides with nanofiltration membranes", Journal of Membrane Science, 192 (2001) 1-10

122. M.D. Afonso, N.M. de Pinho, "Transport of $MgSO_4$, $MgCl_2$, and Na_2SO_4 across an amphoteric nanofiltration membrane", Journal of Membrane Science, 179 (2000) 137-154

123. A.V.R. Reddy, J.J. Trivedi, C.V. Devmurari, D.J. Mohan, P. Singh, A.P. Rao, S.V. Joshi, P.K. Ghosh, "Fouling resistant membranes in desalination and water recovery", Desalination, 183 (2005) 301–306

124. K. Košutić, I. Novak, L. Sipos, B. Kunst, "Removal of sulfates and other inorganics from potable water by nanofiltration membranes of characterized porosity", Separation and Purification Technology, 37 (2004) 177–185

125. M.S. Oak, T. Kobayashi, H.Y. Wang, T. Fukaya, N. Fujii, "pH effect on molecular size exclusion of polyacrylonitrile ultrafiltration membranes having carboxylic acid groups", Journal of Membrane Science, 123 (1997) 185–195

126. V. Silva, P. Prádanos, L. Palacio, A. Hernández, "Alternative pore hindrance factors: What one should be used for nanofiltration modelization?", Desalination, 245 (2009) 606–613

127. K. Tung, Y. Jean, D. Nanda, K. Lee, W. Hung, C. Lo, J. Lai, "Characterization of multilayer nanofiltration membranes using positron annihilation spectroscopy", Journal of Membrane Science, 343 (2009) 147–156

128. M. Teixeira, M. Rosa, M. Nystrom, "The role of membrane charge on nanofiltration performance", Journal of Membrane Science, 265 (2005) 160–166

129. A. Childress, M. Elimelech, "Relating Nanofiltration Membrane Performance to Membrane Charge (Electrokinetic) Characteristics", Environmental Science and Technology, 34 (2000) 3710-3716

130. A. Marmur, "Equilibrium contact angles: theory and measurement", Colloid and Surfaces A: Physicochemical and Engineering Aspects, 116 (1996) 55–61.

131. E. Vrijenhoek, S. Hongb, M. Elimelech, "Influence of membrane surface properties on initial rate of colloidal fouling of reverse osmosis and nanofiltration membranes", Journal of Membrane Science 188 (2001) 115–128

132. K.L. Mittal, "Contact Angle, Wettability and Adhesion", The Netherlands, VSP BV, 1993

133. A. W. Neumann, R. J. Good, "Techniques of Measuring Contact Angles", Berlin, Springer, 1979

134. D.Y. Kwok, A.W. Neumann, "Contact angle measurement and contact angle interpretation", Advances in Colloid and Interface Science, 81 (1999) 167-249

135. A.F. Stalder, G. Kulik, D. Sage, L. Barbieri, P. Hoffmann, "A snake-based approach to accurate determination of both contact points and contact angles", Colloids and Surfaces A: Physicochemical and Engineering Aspects, 286 (2006) 92–103

136. M. Żenkiewicz, "Methods for the calculation of surface free energy of solids", Journal of Achievements in Materials and Manufacturing Engineering, 24 (2007) 137–145

137. D. Li, A.W. Neumann, "Equation of state for interfacial tensions of solid-liquid systems", Advances in Colloid and Interface Science, 39 (1992) 299-345.

138. C.J. Van Oss, R.J. Good, M.K. Chaudhury, "The role of van der Waals forces and hydrogen bonds in "hydrophobic interactions" between biopolymers and low energy surfaces", Journal of Colloid and Interface Science, 111 (1986) 378-390

139. C.J. van Oss, "Interfacial Forces in Aqueous Media", Marcel Dekker, New York, 1994

140. Q. Li, X. Pan, Z. Qu, X. Zhao, Y. Jin, H. Dai, B. Yang, X. Wang, "Understanding the dependence of contact angles of commercially RO membranes on external conditions and surface features", Desalination 309 (2013) 38–45

141. M.A. Butkus, D. Grasso, "Impact of aqueous electrolytes on interfacial energy", Journal of Colloid Interface Science, 200 (1998) 172–181

142. J. Cowie, V. Arrighi, "Polymers: Chemistry and Physics of Modern Materials", 3rd ed., CRC Press, 2008

143. B. Stefan, B. Marius, B. Lidia, "INFLUENCE OF POLYMER CONCENTRATION ON THE PERMEATION PROPERTIES OF NANOFILTRATION MEMBRANES", TEHNOMUS - New Technologies and Products in Machine Manufacturing, 18 (2011) 227-232.

144. W. Zhang, B. Hallstrom, "Membrane Characterization Using the Contact Angle Technique", Desalination, 79 (1990) 1–12

145. P. Eaton, P. West, "Atomic Force Microscopy", New York, Oxford University Press, 2010.

146. K.C. Khulbe, C.Y. Feng, T. Matsuura, "Synthetic Polymeric Membranes Characterization by Atomic Force Microscopy", Berlin, Springer, 2008.

147. D.F. Stamatialis, C.R. Dias, M. Norberta de Pinho, J. Membr., "Atomic force microscopy of dense and asymmetric cellulose-based membranes", Journal of Membrane Science, 160 (1999) 235-242.

148. K. C. Khulbe, T. Matsuura, "Characterization of synthetic membranes by Raman spectroscopy, electron spin resonance, and atomic force microscopy; a review", Polymer, 41 (2000) 1917–1935.

149. W. R. Bowen, T.A. Doneva, "Atomic force microscopy studies of nanofiltration membranes: surface morphology, pore size distribution and adhesion", Desalination, 129 (2000) 163-172.

150. P.C.Y. Wong, Y. N. Kwon, C.S. Criddle, "Use of atomic force microscopy and fractal geometry to characterize the roughness of nano-, micro-, and ultrafiltration membranes", Journal of Membrane Science, 340 (2009) 117–132.

151. W.R. Bowen, A.W. Mohammad, "Characterization and prediction of nanofiltration membrane performance - a general assessment", Chemical Engineering Research and Design, 76 (1998) 885- 893.

152. W. R. Bowen, J. S. Welfoot, "Modelling the performance of membrane nanofiltration - critical assessment and model development", Chemical Engineering Science, 57 (2002) 1121-1137.

153. A.W. Mohammad, N. Hilal, M.N. Abu Seman, "Interfacially polymerised nanofiltration membranes: atomic force microscopy and salt rejection studies", Journal of Applied Polymer Science, 96 (2005) 605–612.

154. N. Hilal, A.W. Mohammad, B. Atkin, N.A. Darwish, "Using atomic force microscopy towards improvement in nanofiltration membranes properties for desalination pretreatment: a review", Desalination, 157 (2003) 137-144.

155. JPK NanoWizard® II – AFM user manual 3.1, 10/2007.

156. K. Boussu, B. Van der Bruggen, A. Volodin, J. Snauwaert, C. Van Haesendonck, C. Vandecasteele, "Roughness and hydrophobicity studies of nanofiltration membranes using different modes of AFM", Journal of Colloid and Interface Science, 286 (2005) 632-638.

157. J. Peltonen, M. Jarn, S. Areva, M. Linden, J.B. Rosenholm, "Topographical parameters for specifying a three-dimensional surface", Langmuir, 20 (2004) 9428–9431.

158. J. Stawikowska, A.G. Livingston, "Nanoprobe imaging molecular scale pores in polymeric membranes", Journal of Membrane Science, 413–414 (2012) 1–16.

159. J. Stawikowska, A. G. Livingston, "Assessment of atomic force microscopy for characterisation of nanofiltration membranes", Journal of Membrane Science, 425–426 (2013) 58–70.

160. R.S. McLean, M. Doyle, B.B. Sauer, “High-resolution imaging of ionic domains and crystal morphology in ionomers using AFM techniques”, Macromolecules, 33 (2000) 6541–6550.

161. S. Singh, K. Khulbe, T. Matsuura, P. Ramamurthy, “Membrane characterization by solute transport and atomic force microscopy", Journal of Membrane Science, 142 (1998) 111-127.

162. M.M. Pendergast, E.M.V. Hoek, “A review of water treatment membrane nanotechnologies”, Energy & Environmental Science, 4 (2011) 1946–1971

163. L. Perry, O. Coronell, “Reliable, bench-top measurements of charge density in the active layers of thin-film composite and nanocomposite membranes using quartz crystal microbalance technology”, Journal of Membrane Science, 429 (2013) 23–33

164. J.M.M. Peeters, M.H.V. Mulder , H. Strathmann, “Streaming potential measurements as a characterization method for NF”, Colloids and Surfaces; A: Physicochemical and Engineering Aspects, 150 (1999) 247–259

165. P. Fievet, B. Aoubizab, A. Szymczyka, J. Pagettia, “Membrane potential in charged porous membranes”, Journal of Membrane Science, 160 (1999) 267 – 275

166. P. Fievet, A. Szymczyk, B. Aoubiza, J. Pagetti, “Evaluation of three methods for the characterisation of the membrane–solution interface: streaming potential, membrane potential and electrolyte conductivity inside pores”, Journal of Membrane Science, 168 (2000) 87–100

167. A. Yaroshchuk, A. Makovetskiy, Y. Boikob, E. Galinker “Non-steady-state membrane potential: theory and measurements by a novel technique to determine the ion transport numbers in active layers of NF”, Journal of Membrane Science, 172 (2000) 203–221

168. J. Schaep, C. Vandecasteele, “Evaluating the charge of nanofiltration membranes”, Journal of Membrane Science, 188 (2001) 129–136

169. J. Tay, J. Liu, D. Sun, “Effect of solution physico-chemistry on the charge property of nanofiltration membranes”, Water Research, 36 (2002) 585–598

170. M. Afonso, “Surface charge on loose nanofiltration membranes”, Desalination, 191 (2006) 262–272

171. A. Tiraferri, M. Elimelech, “Direct quantification of negatively charged functional groups on membrane surfaces”, Journal of Membrane Science, 389 (2012) 499–508

172. W.R. Bowen, X. Cao, “Electrokinetic effects in membrane pores and the determination of the zeta potential”, Journal of Membrane Science, 140 (1998) 267–273

173. A. Childress, M. Elimelech, “Effect of solution chemistry on the surface charge of polymeric reverse osmosis and nanofiltration membranes”, Journal of Membrane Science, 119 (1996) 253-268

174. M. Afonso, G. Hagmeyer, R. Gimbel, “Streaming potential measurements to assess the variation of nanofiltration membranes surface charge with the concentration of salt solutions”, Separation and Purification Technology, 22-23 (2001) 529 541

175. M. Ariza, J. Benavente, “Streaming potential along the surface of polysulfone membranes: a comparative study between two different experimental systems and determination of electrokinetic and adsorption parameters”, Journal of Membrane Science 190 (2001) 119–132

176. T. Xu, Y. Fu, X. Wang, “Membrane potential model for an asymmetrical nanofiltration membrane — consideration of non-continuous concentration at the interface”, Desalination, 171 (2004) 155–165

177. W. Shang, X. Wang, Y. Yu, ”Theoretical calculation on the membrane potential of charged porous membranes in 1-1, 1-2, 2-1 and 2-2 electrolyte solutions”, Journal of Membrane Science, 285 (2006) 362–375

178. Y. Mo, A. Tiraferri, N. Yin Yip, A. Adout, X. Huang, M. Elimelech, “Improved Antifouling Properties of Polyamide Nanofiltration Membranes by Reducing the Density of Surface Carboxyl Groups”, Environmental Science and Technology, 46 (2012) 13253−13261

179. S. Mondal, C. Hsiao, S. Wickramasinghe, “Nanofiltration/reverse osmosis for treatment of coproduced waters”, Environmental Progress, 27 (2008) 173–179

180. W. Hanbury, “Distillation Processes for Seawater desalination”, A Set of Course Notes written for A workshop at ARWATEX, June 2005

181. T. Mezher, H. Fath, Z. Abbas, A. Khaled, “Techno-economic assessment and environmental impacts of desalination technologies”, Desalination, 266 (2011) 263–273

182. J. Luo, Y. Wan, “Desalination of effluents with highly concentrated salt by nanofiltration: From laboratory to pilot-plant”, Desalination, 315 (2013) 91-99

183. R. Sharma, S. Chellam, “Temperature Effects on the Morphology of Porous Thin Film Composite Nanofiltration Membranes”, Environmental Science and Technology, 13 (2005) 5022–5030

184. Y. Song, B. Su, X. Gao, C. Gao, “The performance of polyamide nanofiltration membrane for long-term operation in an integrated membrane seawater pretreatment system”, Desalination, 296 (2012) 30–36

APPENDICES

APPENDIX 1

Sulphate content determination of nanofiltration membrane permeate during ASTM experiments (illustrated in chapter 7 – section 2.5.2.1) through conversion of using the conductivity reading calibration graphs produced from a series of standard solutions made up using magnesium sulphate salt $MgSO_4$.

Solution concentration: mg $MgSO_4$ per one litter of distilled water	X-axis: (SO_4^{2-}) content, ppm	Y-axis (Conductivity reading in µs/cm)
2000	1596	2190
1500	1197	1688
1000	798	1233
750	598.5	1138
500	399	702
375	299.2	478
200	159.6	292
187.5	149.6	268
100	79.8	171
93.75	74.8	131.4
50	39.9	95.7
46.875	37.4	87
23.4	18.6	50.8
20	15.9	40
11.75	9.3	28.3
10	7.9	23.1
5.859	4.6	12.3
5	4	12.3
2.9295	2.3	8.3
1.46475	1.1	5.3
1	0.8	4.2
0	0	2

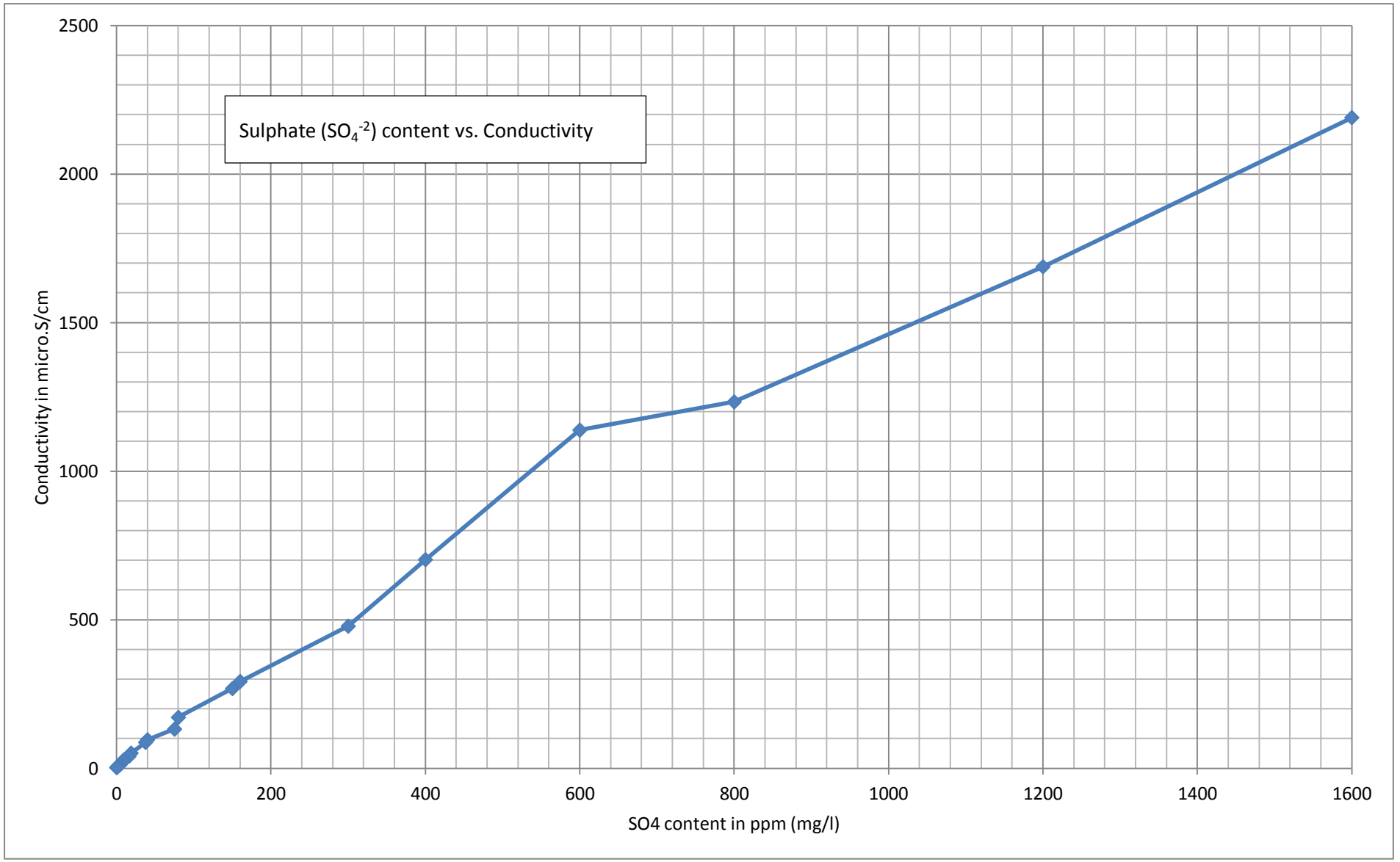
Sulphate (SO_4^{-2}) content vs. Conductivity
Conductivity in micro.S/cm
SO4 content in ppm (mg/l)
2500
2000
1500
1000
500
0
0
200
400
600
800
1000
1200
1400
1600

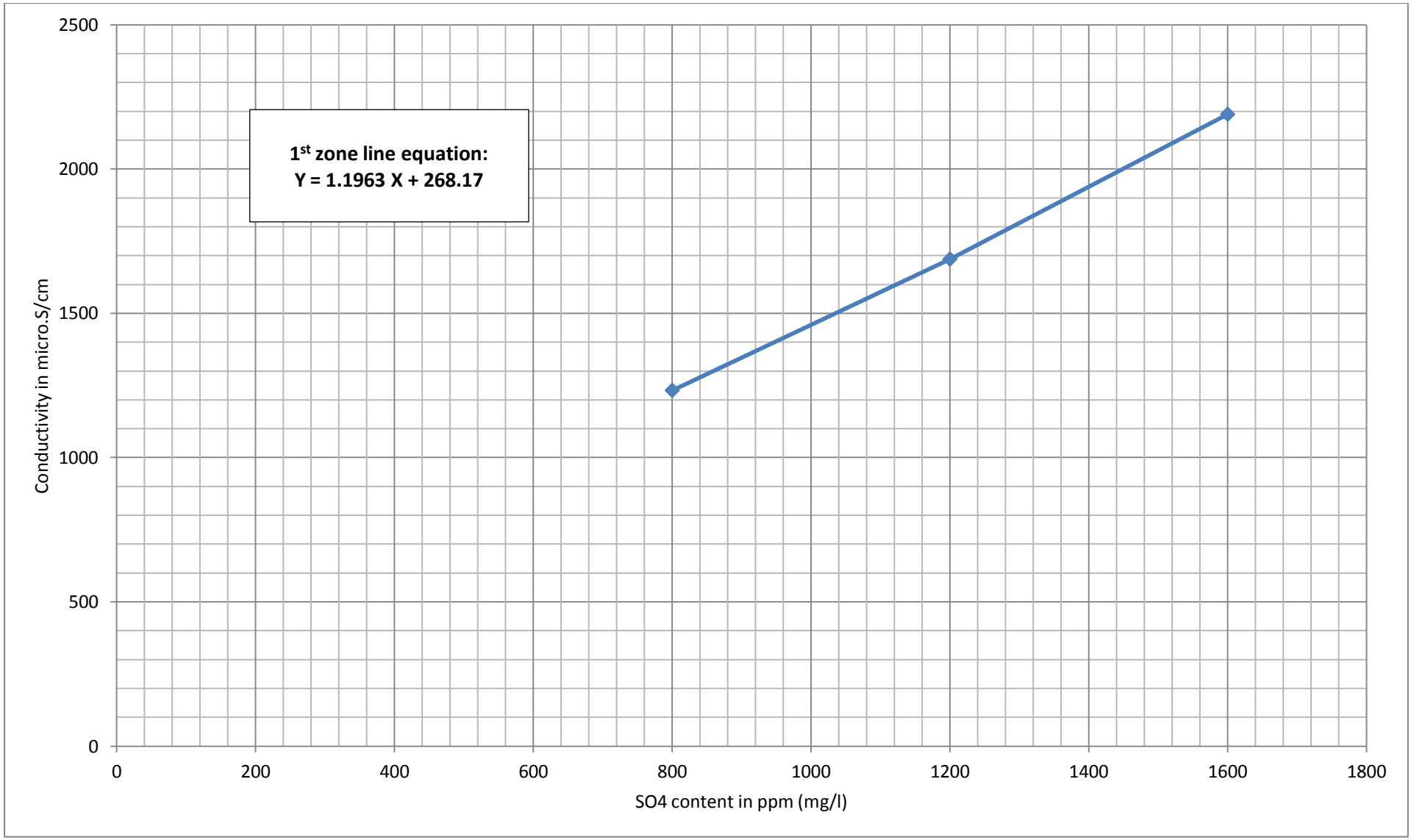
1st zone line equation:
Y = 1.1963 X + 268.17
Conductivity in micro.S/cm
SO4 content in ppm (mg/l)
0
500
1000
1500
2000
2500
0
200
400
600
800
1000
1200
1400
1600
1800

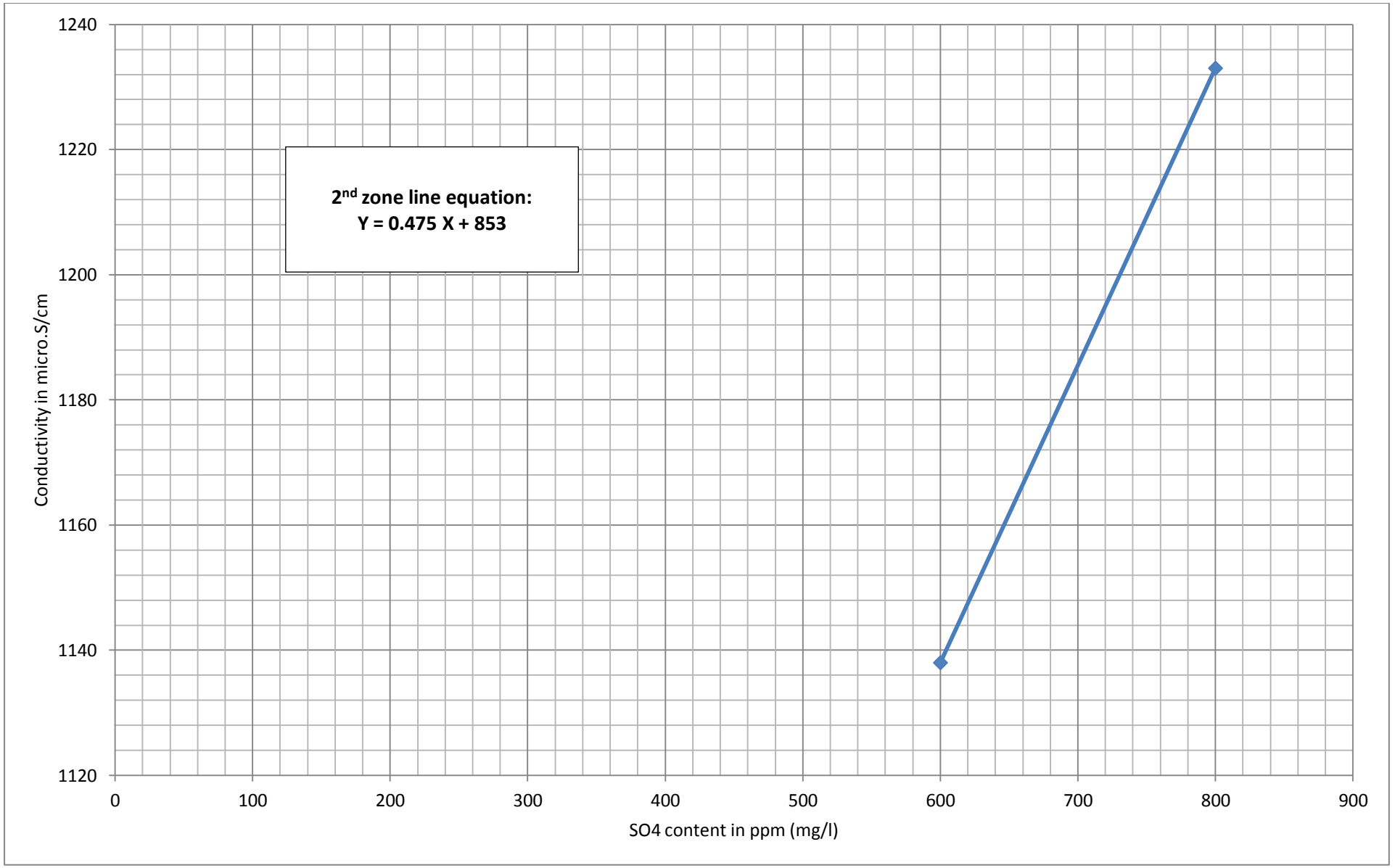
2nd zone line equation:
Y = 0.475 X + 853
Conductivity in micro.S/cm
SO4 content in ppm (mg/l)
1240
1220
1200
1180
1160
1140
1120
0
100
200
300
400
500
600
700
800
900

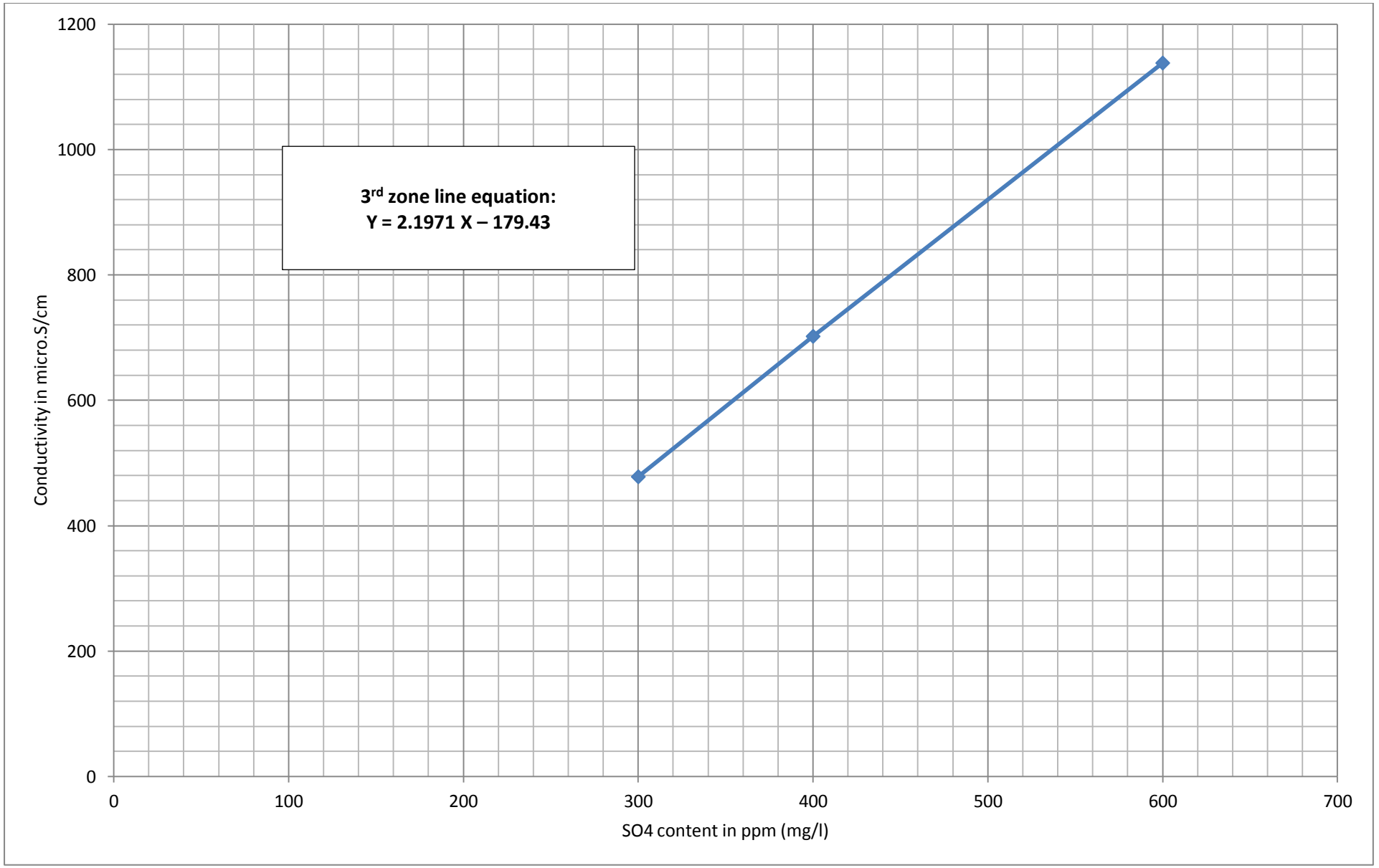
3rd zone line equation:
Y = 2.1971 X – 179.43
Conductivity in micro.S/cm
SO4 content in ppm (mg/l)
0
200
400
600
800
1000
1200
0
100
200
300
400
500
600
700

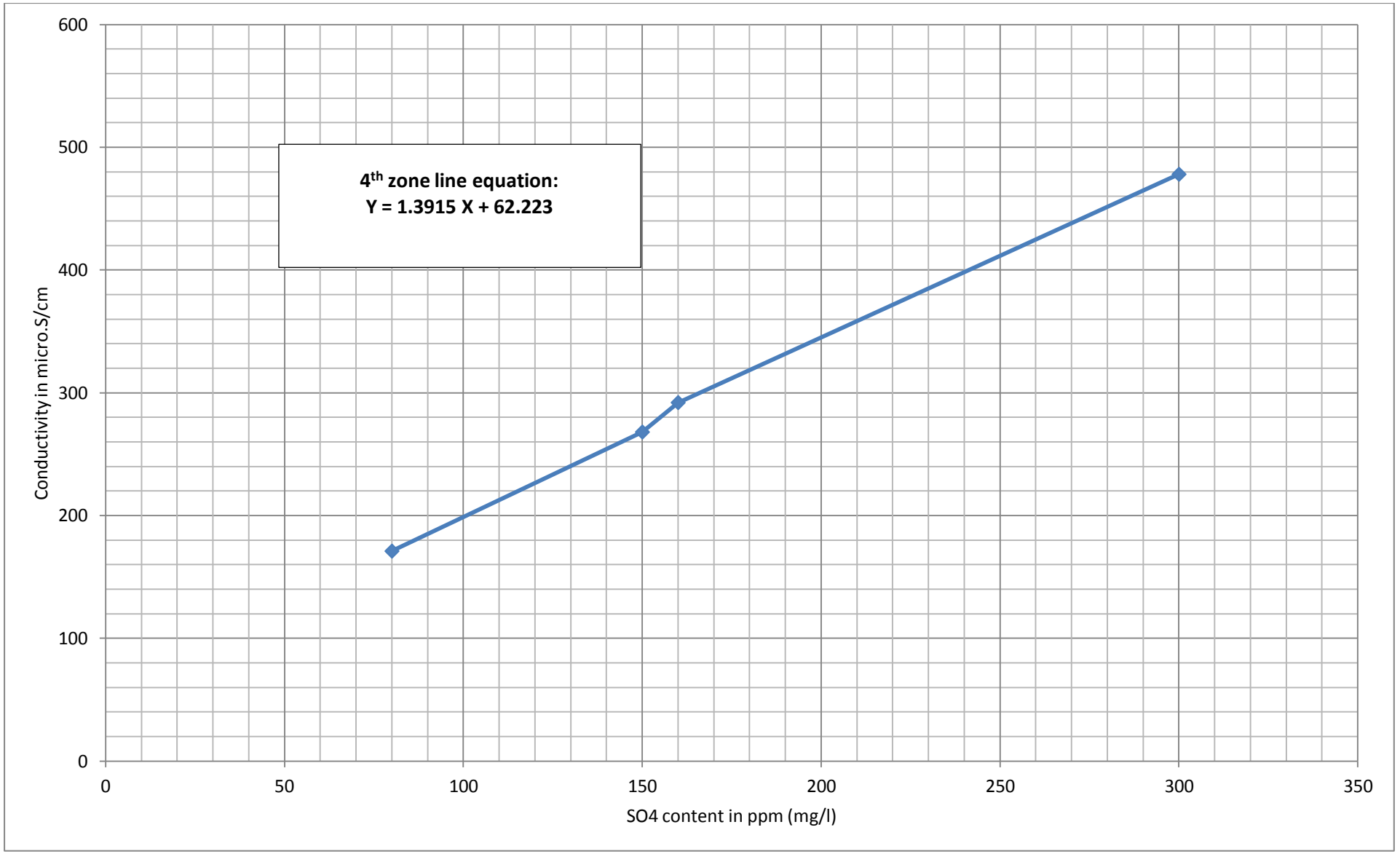
4th zone line equation:
Y = 1.3915 X + 62.223
Conductivity in micro.S/cm
SO4 content in ppm (mg/l)
0
100
200
300
400
500
600
0
50
100
150
200
250
300
350

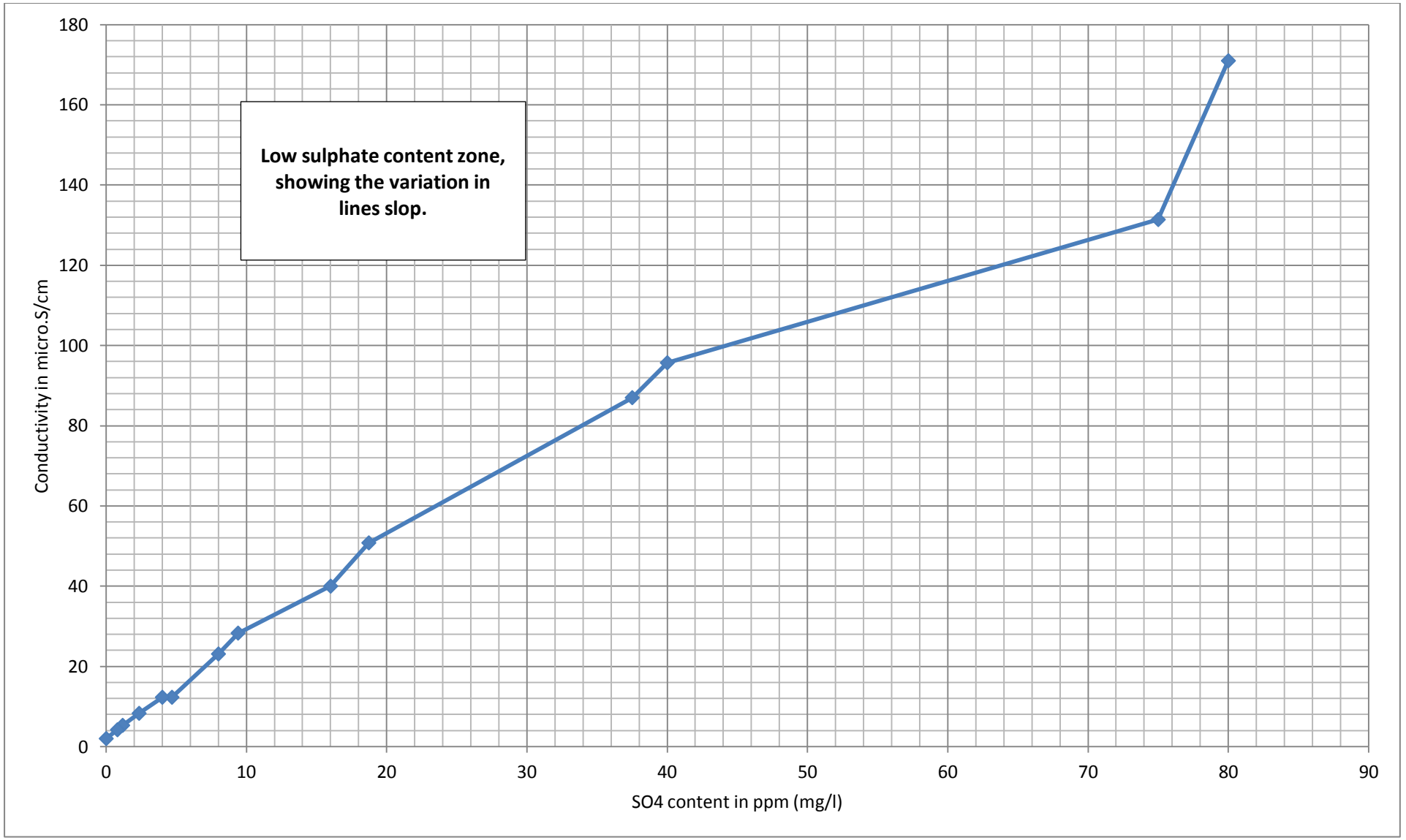
Low sulphate content zone, showing the variation in lines slop.
Conductivity in micro.S/cm
SO4 content in ppm (mg/l)
0
20
40
60
80
100
120
140
160
180
0
10
20
30
40
50
60
70
80
90

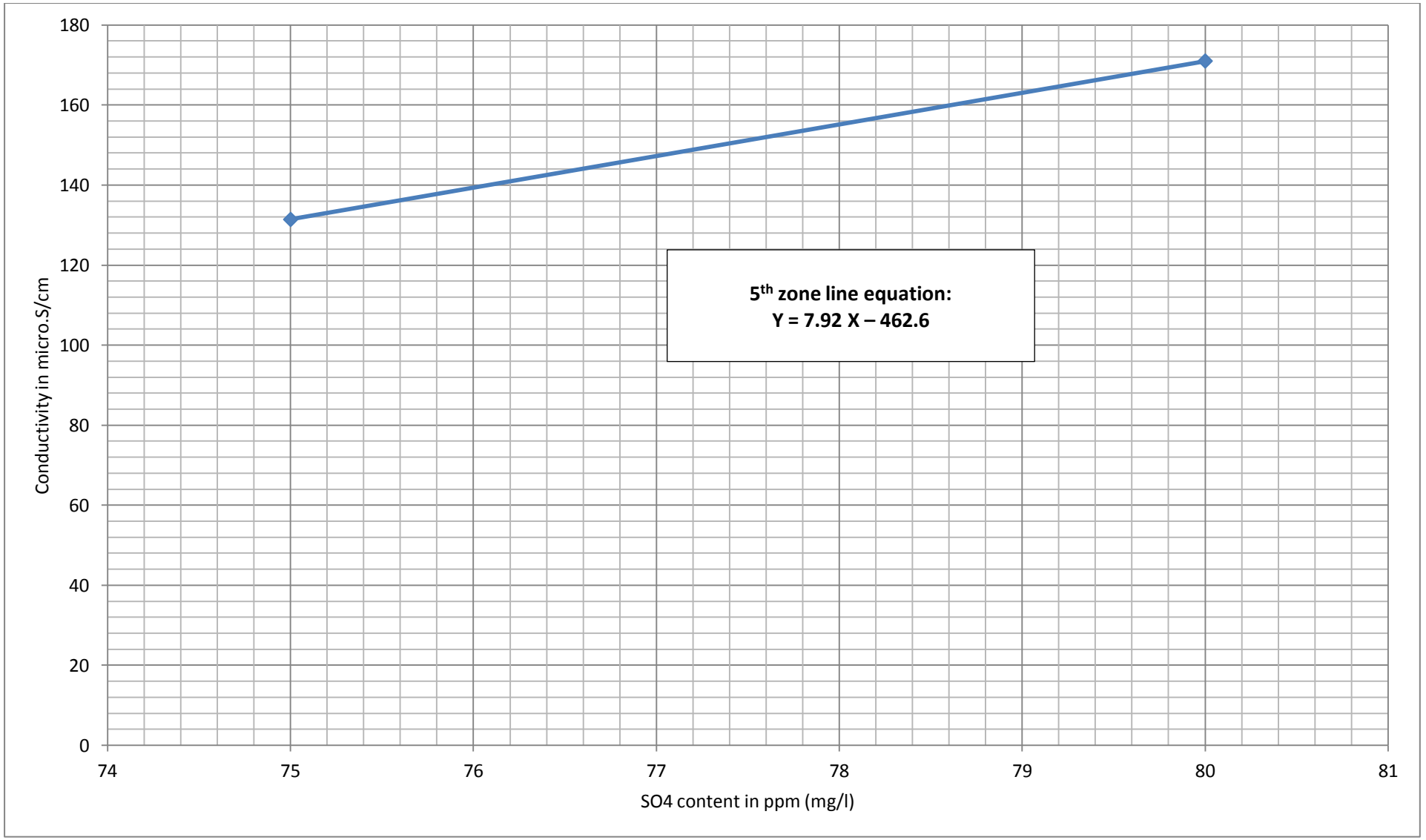
180
160
140
120
100
80
60
40
20
0
Conductivity in micro.S/cm
74
75
76
77
78
79
80
81
SO4 content in ppm (mg/l)
5th zone line equation:
Y = 7.92 X – 462.6

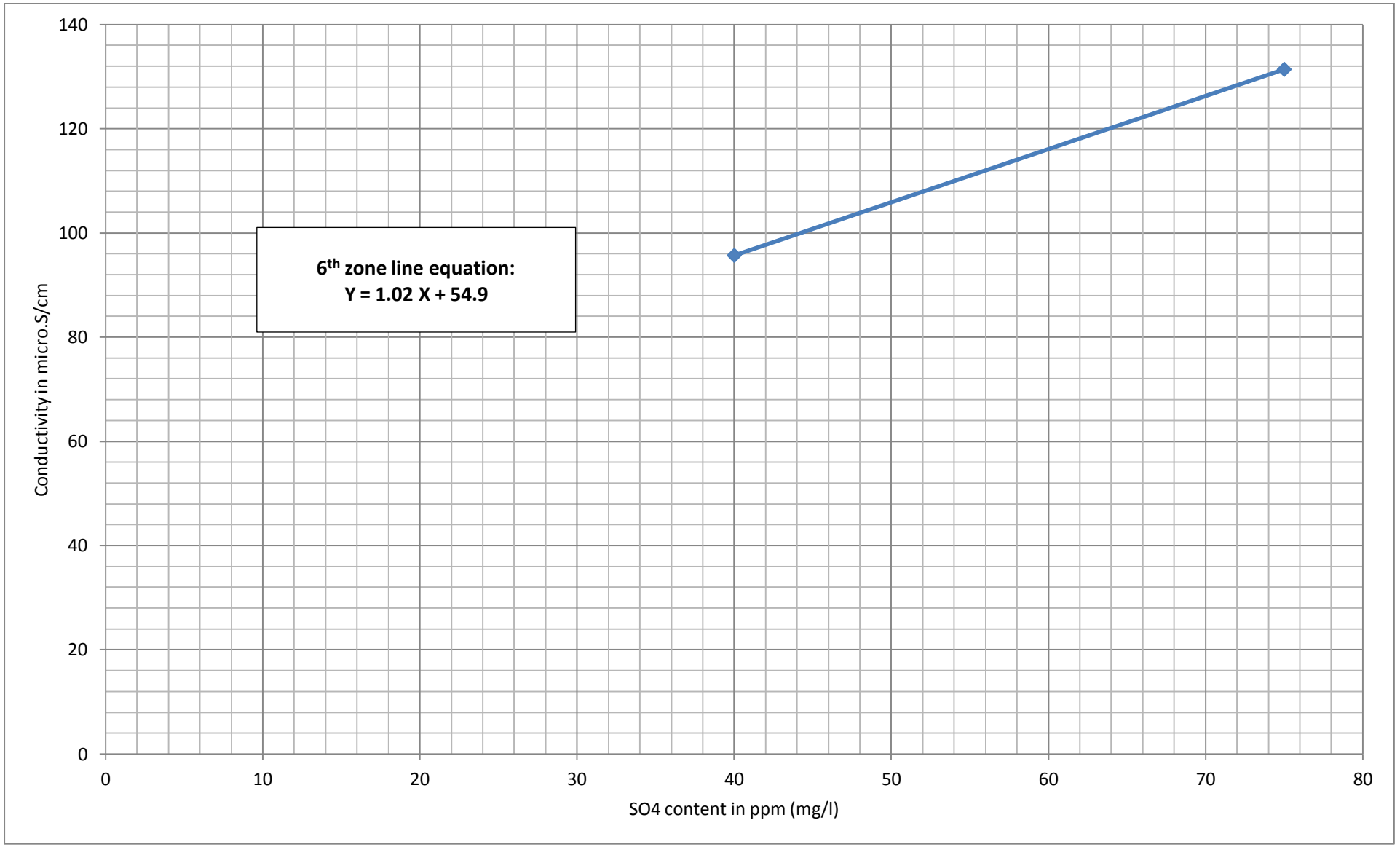
6th zone line equation:
Y = 1.02 X + 54.9
Conductivity in micro.S/cm
SO4 content in ppm (mg/l)
0
20
40
60
80
100
120
140
0
10
20
30
40
50
60
70
80

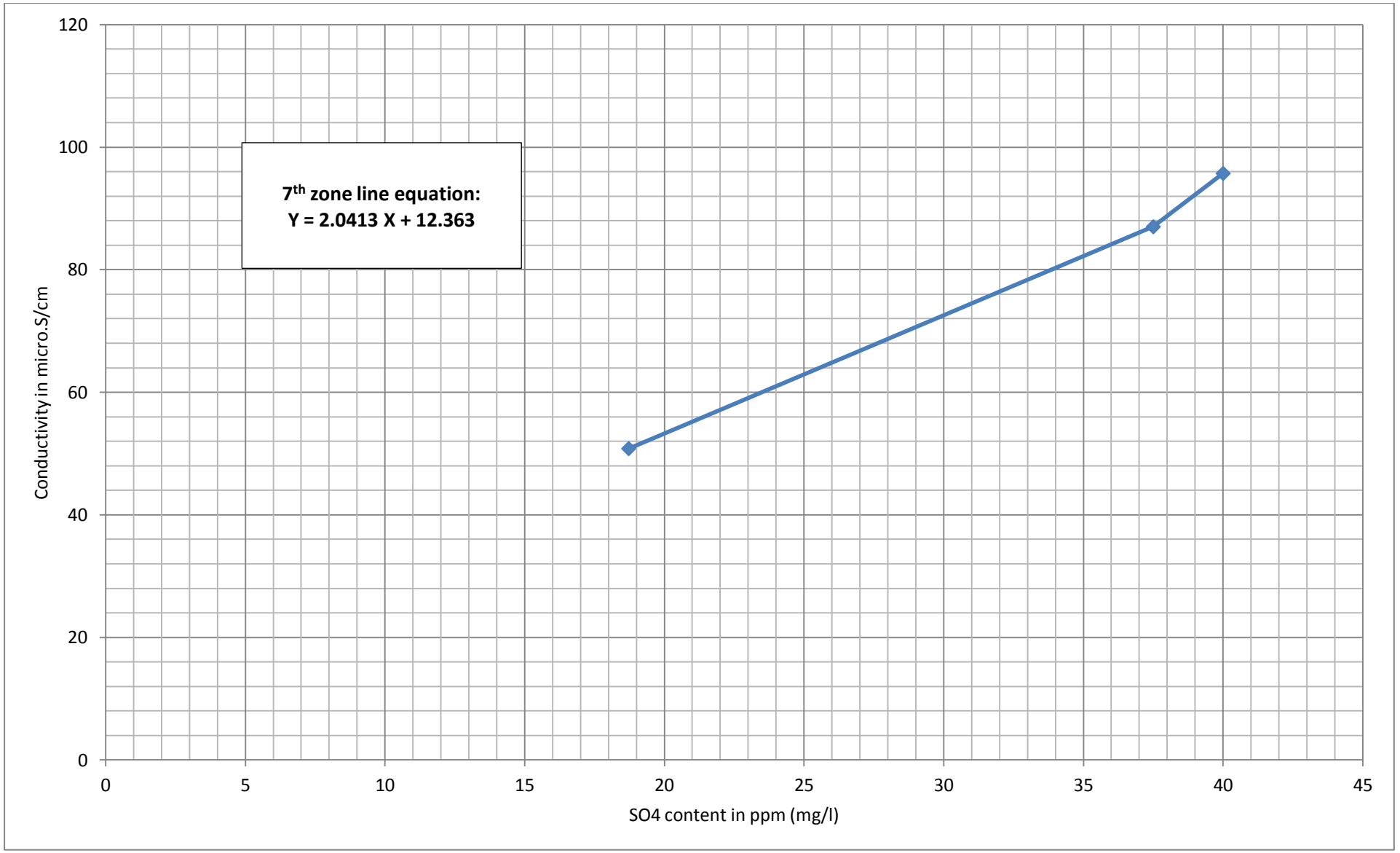
7th zone line equation:
Y = 2.0413 X + 12.363
Conductivity in micro.S/cm
SO4 content in ppm (mg/l)
0
20
40
60
80
100
120
0
5
10
15
20
25
30
35
40
45

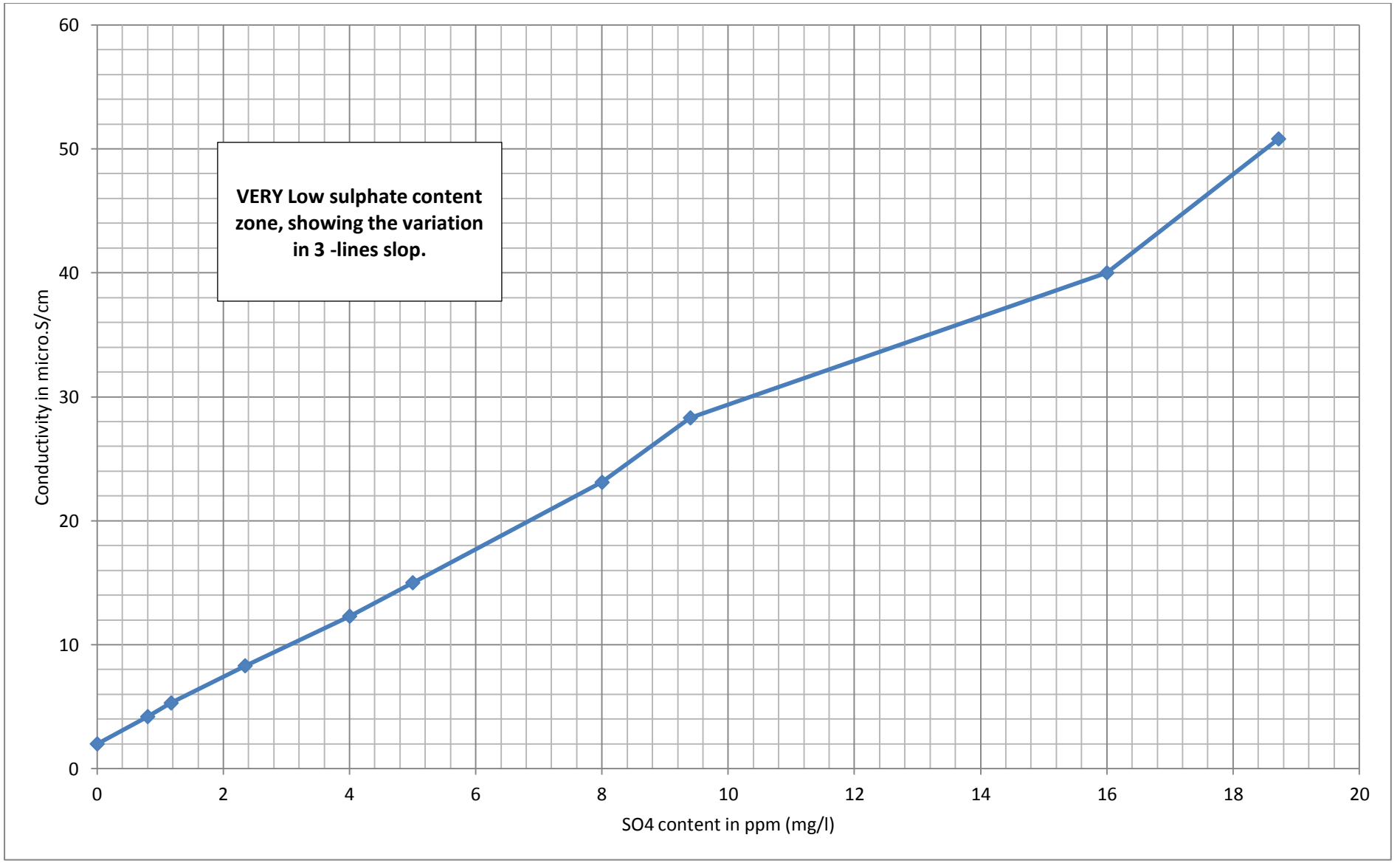
VERY Low sulphate content zone, showing the variation in 3 -lines slop.
Conductivity in micro.S/cm
SO4 content in ppm (mg/l)
0
10
20
30
40
50
60
0
2
4
6
8
10
12
14
16
18
20

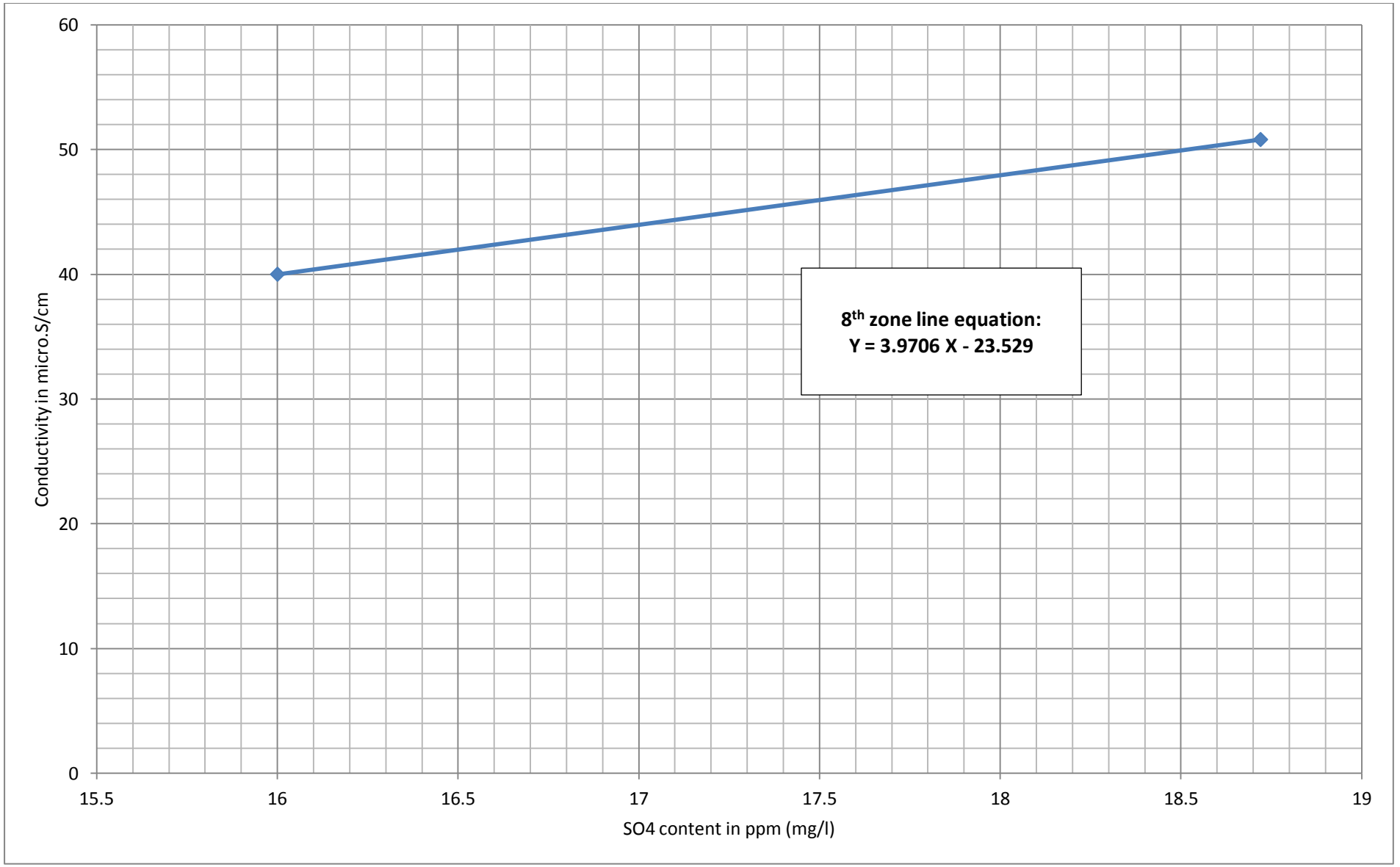
60
50
40
30
20
10
0
Conductivity in micro.S/cm
15.5
16
16.5
17
17.5
18
18.5
19
SO4 content in ppm (mg/l)
8th zone line equation:
Y = 3.9706 X - 23.529

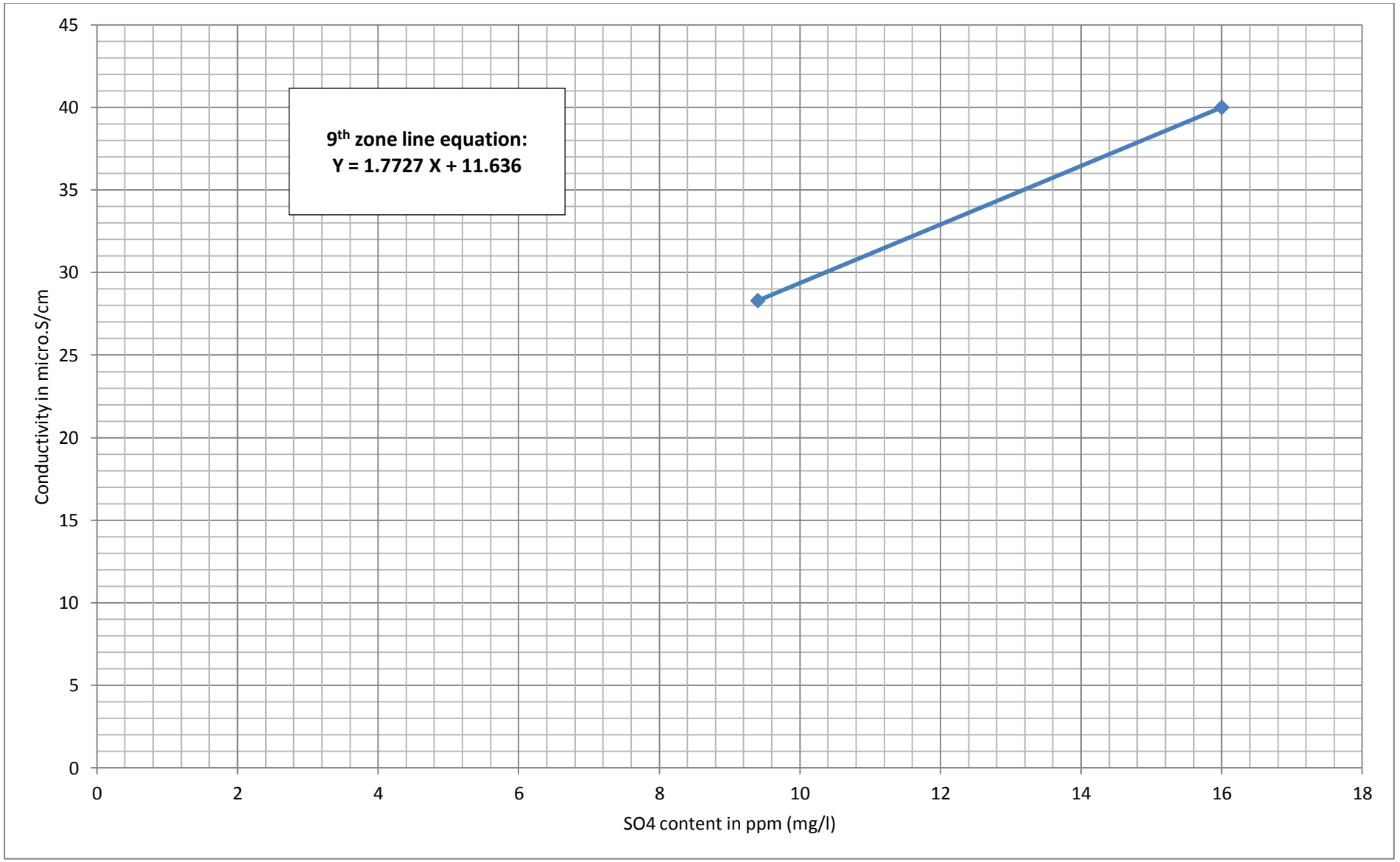
9th zone line equation:
Y = 1.7727 X + 11.636
Conductivity in micro.S/cm
SO4 content in ppm (mg/l)
0
5
10
15
20
25
30
35
40
45
0
2
4
6
8
10
12
14
16
18

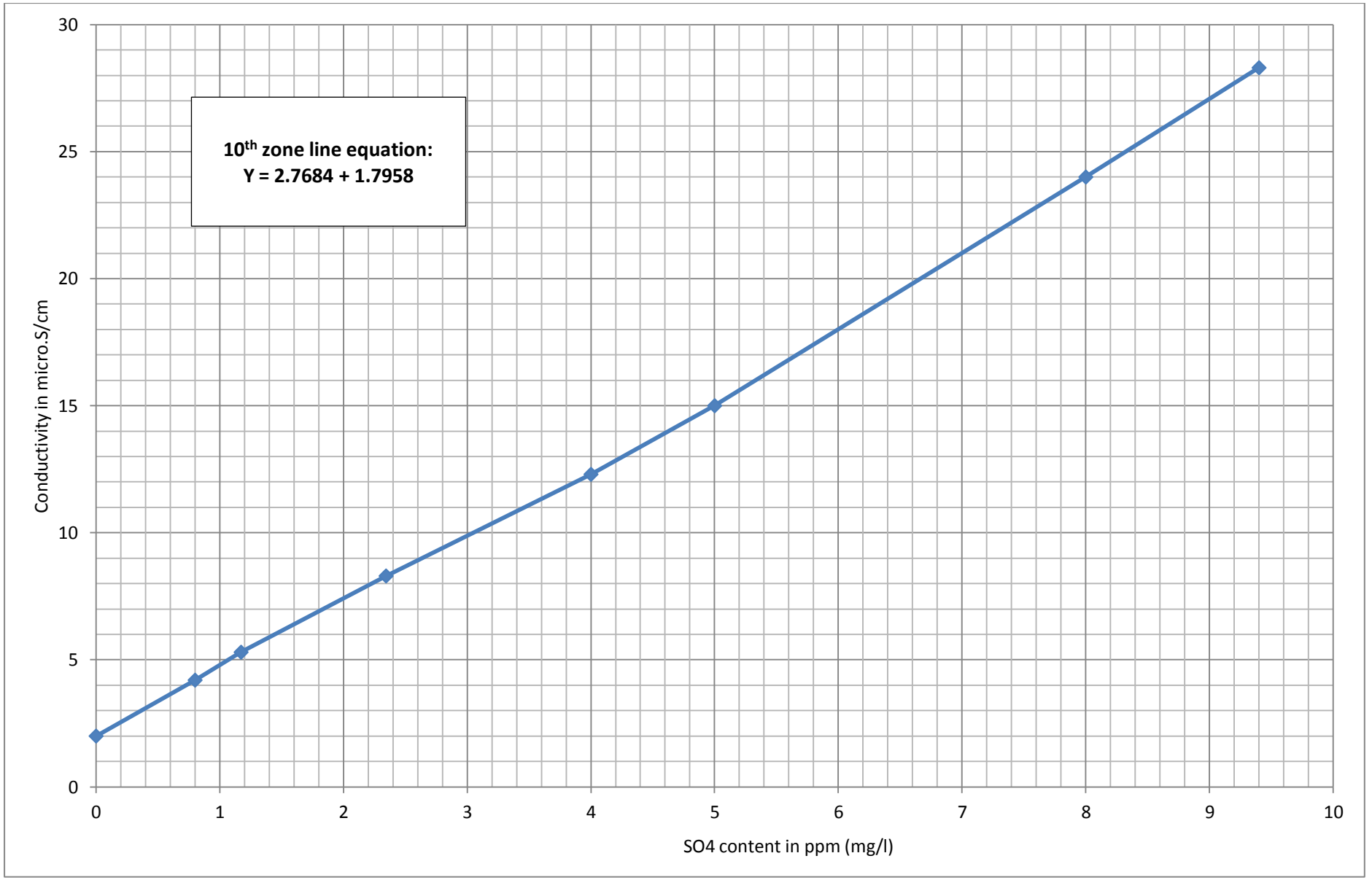
10th zone line equation:
Y = 2.7684 + 1.7958
Conductivity in micro.S/cm
SO4 content in ppm (mg/l)
0
5
10
15
20
25
30
0
1
2
3
4
5
6
7
8
9
10

Equations of Permeate Conductivity reading conversion to sulphate content

Y – axis = conductivity, µs/cm X – axis = sulphate content (SO_4^{2-}) in ppm

sulphate range in ppm	conductivity range in micro.S/cm	line equation
1596 – 798	2190 – 1233	Y = 1.1963 X + 268.17
798 – 598.5	1233 – 1138	Y = 0.475 X + 853
598.5 – 299.2	1138 – 478	Y = 2.1971 X – 179.43
299.2 – 79.8	478 – 171	Y = 1.3915 X + 62.223
79.8 – 74.8	171 – 131.4	Y = 7.92 X – 462.6
74.8 – 39.9	131.4 – 95.7	Y = 1.02 X + 54.9
39.9 – 18.6	95.7 – 50.8	Y = 2.0413 X + 12.363
18.6 – 15.9	50.8 – 40	Y = 3.9706 X - 23.529
15.9 – 9.3	40 – 28.3	Y = 1.7727 X + 11.636
9.3 – 0	28.3 – 2	Y = 2.7684 + 1.7958

A	reading	C1	C2	C3	C4	C5	C6	AVG		
	1	34.10	33.40	34.10	34.08	34.10	34.82	34.10		
FLUX	2	33.80	34.10	33.45	34.10	34.10	35.05	34.10		
	3	33.37	34.88	34.20	34.00	34.10	34.10	34.10		
								34.10		
									READINGS STND.DEV.	0.4592
		C1	C2	C3	C4	C5	C6	AVG		
REJ	1	98.80	98.14	98.14	98.14	98.14	97.48	98.14		
	2	98.41	98.33	97.88	98.23	98.32	98.75	98.32		
	3	98.32	96.66	98.88	98.34	98.57	98.97	98.29		
								98.25		
									READINGS STND.DEV.	0.5383

B	reading	C1	C2	C3	C4	C5	C6	AVG		
	1	20.30	20.07	20.44	20.61	20.33	20.83	20.43		
FLUX	2	20.33	20.12	21.04	20.58	20.40	19.93	20.40		
	3	20.30	20.55	20.38	20.90	19.18	20.85	20.36		
								20.40		
									READINGS STND.DEV.	0.4252
		C1	C2	C3	C4	C5	C6	AVG		
REJ	1	99.66	99.64	99.64	99.66	99.66	99.64	99.65		
	2	99.65	99.68	99.61	99.64	99.65	99.67	99.65		
	3	99.66	99.68	99.68	99.68	99.52	99.68	99.65		
								99.65		
									READINGS STND.DEV.	0.0377

C	reading	C1	C2	C3	C4	C5	C6	AVG		
	1	26.51	26.45	26.48	26.48	26.45	26.51	26.48		
FLUX	2	26.50	26.54	28.21	26.45	26.45	24.55	26.45		
	3	26.50	25.48	27.05	26.71	26.07	27.49	26.55		
								26.49		
									READINGS STND.DEV.	0.7393
		C1	C2	C3	C4	C5	C6	AVG		
REJ	1	93.42	93.50	93.50	93.50	93.60	93.48	93.50		
	2	93.44	93.50	93.52	93.30	93.60	93.64	93.50		
	3	93.60	92.33	93.60	93.60	93.60	94.87	93.60		
								93.53		
									READINGS STND.DEV.	0.4443

D	reading	C1	C2	C3	C4	C5	C6	AVG		
	1	31.54	31.70	31.60	31.54	31.60	31.62	31.60		
FLUX	2	31.54	31.72	31.60	31.55	31.60	31.59	31.60		
	3	31.54	31.72	31.59	31.54	31.60	31.61	31.60		
								31.60		
									READINGS STND.DEV.	0.0594
		C1	C2	C3	C4	C5	C6	AVG		
REJ	1	99.38	99.42	99.40	99.38	99.40	99.40	99.40		
	2	99.40	99.38	99.41	99.40	99.44	99.25	99.38		
	3	99.44	99.20	99.40	99.38	99.60	99.44	99.42		
								99.40		
									READINGS STND.DEV.	0.0801

E	reading	C1	C2	C3	C4	C5	C6	AVG		
	1	18.25	18.31	18.29	18.30	18.30	18.35	18.30		
FLUX	2	17.95	18.55	18.55	18.44	18.50	19.01	18.50		
	3	17.66	18.52	18.55	18.41	18.55	18.11	18.30		
								18.36		
									READINGS STND.DEV.	0.2836
		C1	C2	C3	C4	C5	C6	AVG		
REJ	1	99.68	99.68	99.68	99.68	99.68	99.68	99.68		
	2	99.64	99.25	99.68	99.60	99.68	99.27	99.52		
	3	99.60	99.54	99.65	99.64	99.60	99.57	99.60		
								99.60		
									READINGS STND.DEV.	0.1312

F	reading	C1	C2	C3	C4	C5	C6	AVG		
	1	61.11	61.05	61.07	60.97	61.10	61.18	61.08		
FLUX	2	61.10	61.07	61.07	58.88	62.00	61.70	60.97		
	3	61.10	62.23	61.61	59.74	61.11	61.59	61.23		
								61.09		
									READINGS STND.DEV.	0.7574
		C1	C2	C3	C4	C5	C6	AVG		
REJ	1	99.16	99.16	99.14	99.19	99.16	99.15	99.16		
	2	99.15	99.16	99.16	99.16	99.20	99.19	99.17		
	3	99.20	99.20	98.70	99.20	99.20	99.22	99.12		
								99.15		
									READINGS STND.DEV.	0.1147

G	reading	C1	C2	C3	C4	C5	C6	AVG		
	1	29.50	29.52	29.77	30.07	27.56	29.98	29.40		
FLUX	2	29.55	31.18	29.90	29.78	28.70	28.31	29.57		
	3	29.55	30.74	29.70	29.94	28.50	28.75	29.53		
								29.50		
									READINGS STND.DEV.	0.8693
		C1	C2	C3	C4	C5	C6	AVG		
REJ	1	99.20	99.18	99.20	99.20	99.20	98.56	99.09		
	2	99.20	99.20	99.20	98.77	99.15	99.20	99.12		
	3	99.20	99.20	98.70	99.20	99.20	99.34	99.14		
								99.12		
									READINGS STND.DEV.	0.2089

H	reading	C1	C2	C3	C4	C5	C6	AVG		
	1	26.00	25.41	26.01	26.01	26.01	26.62	26.01		
FLUX	2	26.01	23.70	25.90	25.11	26.02	26.74	25.58		
	3	26.00	24.68	26.10	27.11	25.90	26.87	26.11		
								25.90		
									READINGS STND.DEV.	0.8024
		C1	C2	C3	C4	C5	C6	AVG		
REJ	1	98.10	97.58	98.20	98.12	98.14	98.70	98.14		
	2	98.22	98.02	98.05	98.77	96.47	98.77	98.05		
	3	98.16	98.12	98.12	98.16	98.20	98.20	98.16		
								98.12		
									READINGS STND.DEV.	0.4996

Appendix 3: SURFACE FREE ENERGY CALCULATIONS

NF B membrane:

Contact angle measurements for NF B membrane are; 50.2°, 36.1° and 31.8° in seawater, diiodomethane and ethylene-glycol respectively.

6. $\gamma_{NF}^{LW} = \left(\frac{25.4\,(1+\cos\theta_{D,NF})}{7.127}\right)^2 = \left(\frac{25.4\,(1+\cos 36.1)}{7.127}\right)^2 = 41.52\ mJ/m^2$

7. $\gamma_{NF}^{p+} = \left(\frac{24\,(1+\cos\theta_{EG,NF}) - \sqrt{29\,\gamma_{NF}^{LW}}}{1.38} - \frac{36.4\,(1+\cos\theta_{sw,NF}) - \sqrt{21.8\,\gamma_{NF}^{LW}}}{5.05} \Big/ 3.96 \right)^2 =$

$$\left(\frac{24\,(1+\cos 31.8) - \sqrt{29*(41.52)}}{1.38} - \frac{36.4\,(1+\cos 50.2) - \sqrt{21.8(41.52)}}{5.05} \Big/ 3.96 \right)^2 = 0.086\ mJ/m^2$$

8. $\gamma_{NF}^{p-} = \left(\frac{36.4\,(1+\cos\theta_{sw,NF}) - \sqrt{21.8\,\gamma_{NF}^{LW}}}{5.05} - \sqrt{\gamma_{NF}^{p+}} \right)^2$

$$= \left(\frac{36.4\,(1+\cos 50.2) - \sqrt{21.8*(41.52)}}{5.05} - \sqrt{0.086} \right)^2 = 31.04\ mJ/m^2$$

9. $\gamma_{NF}^{p} = 2\sqrt{\gamma_{NF}^{p-}}\sqrt{\gamma_{NF}^{p+}} = 2\sqrt{31.04}\sqrt{0.086} = 3.27\ mJ/m^2$

10. $\gamma_{NF} = \gamma_{NF}^{LW} + \gamma_{NF}^{p} = 41.52 + 3.27 = 44.79\ mJ/m^2$

NF C membrane:

Contact angle measurements for NF C membrane are; 38.0°, 33.5° and 26.0° in seawater, diiodomethane and ethylene-glycol respectively.

1. $\gamma_{NF}^{LW} = \left(\frac{25.4\,(1+\cos\theta_{D,NF})}{7.127}\right)^2 = \left(\frac{25.4\,(1+\cos 33.5)}{7.127}\right)^2 = 42.71\ mJ/m^2$

2. $\gamma_{NF}^{p+} = \left(\frac{24\,(1+\cos\theta_{EG,NF}) - \sqrt{29\,\gamma_{NF}^{LW}}}{1.38} - \frac{36.4\,(1+\cos\theta_{sw,NF}) - \sqrt{21.8\,\gamma_{NF}^{LW}}}{5.05} \Big/ 3.96\right)^2 =$

$$\left(\frac{24\,(1+\cos 26) - \sqrt{29*(42.71)}}{1.38} - \frac{36.4\,(1+\cos 38) - \sqrt{21.8(42.71)}}{5.05} \Big/ 3.96\right)^2 = 0.028\ mJ/m^2$$

3. $\gamma_{NF}^{p-} = \left(\frac{36.4\,(1+\cos\theta_{sw,NF}) - \sqrt{21.8\,\gamma_{NF}^{LW}}}{5.05} - \sqrt{\gamma_{NF}^{p+}}\right)^2$

$$= \left(\frac{36.4\,(1+\cos 38) - \sqrt{21.8*(42.71)}}{5.05} - \sqrt{0.028}\right)^2 = 44.56\ mJ/m^2$$

4. $\gamma_{NF}^{p} = 2\sqrt{\gamma_{NF}^{p-}}\sqrt{\gamma_{NF}^{p+}} = 2\sqrt{44.56}\sqrt{0.028} = 2.26\ mJ/m^2$

5. $\gamma_{NF} = \gamma_{NF}^{LW} + \gamma_{NF}^{p} = 42.71 + 2.26 = 44.98\ mJ/m^2$

NF D membrane:

Contact angle measurements for NF D membrane are; 34.0°, 29.3° and 23.2° in seawater, diiodomethane and ethylene-glycol respectively.

1. $\gamma_{NF}^{LW} = \left(\frac{25.4\,(1+\cos\theta_{D,NF})}{7.127}\right)^2 = \left(\frac{25.4\,(1+\cos 29.3)}{7.127}\right)^2 = 44.51\ mJ/m^2$

2. $\gamma_{NF}^{p+} = \left(\frac{24\,(1+\cos\theta_{EG,NF}) - \sqrt{29\,\gamma_{NF}^{LW}}}{1.38} - \frac{36.4\,(1+\cos\theta_{sw,NF}) - \sqrt{21.8\,\gamma_{NF}^{LW}}}{5.05} \Big/ 3.96\right)^2 =$

$$\left(\frac{24\,(1+\cos 23.2) - \sqrt{29*(44.51)}}{1.38} - \frac{36.4\,(1+\cos 34) - \sqrt{21.8(44.51)}}{5.05} \Big/ 3.96\right)^2 = 0.006\ mJ/m^2$$

3. $\gamma_{NF}^{p-} = \left(\frac{36.4\,(1+\cos\theta_{sw,NF}) - \sqrt{21.8\,\gamma_{NF}^{LW}}}{5.05} - \sqrt{\gamma_{NF}^{p+}}\right)^2$

$$= \left(\frac{36.4\,(1+\cos 34) - \sqrt{21.8*(44.51)}}{5.05} - \sqrt{0.006}\right)^2 = 48.06\ mJ/m^2$$

4. $\gamma_{NF}^{p} = 2\sqrt{\gamma_{NF}^{p-}}\sqrt{\gamma_{NF}^{p+}} = 2\sqrt{48.06}\sqrt{0.006} = 1.13\ mJ/m^2$

5. $\gamma_{NF} = \gamma_{NF}^{LW} + \gamma_{NF}^{p} = 44.51 + 1.13 = 45.65\ mJ/m^2$

NF E membrane:

Contact angle measurements for NF E membrane are; 53.6°, 39.9° and 32.3° in seawater, diiodomethane and ethylene-glycol respectively.

1. $\gamma_{NF}^{LW} = \left(\frac{25.4\ (1+\cos\theta_{D,NF})}{7.127}\right)^2 = \left(\frac{25.4\ (1+\cos 39.9)}{7.127}\right)^2 = 39.66\ mJ/m^2$

2. $\gamma_{NF}^{p+} = \left(\frac{24\ (1+\cos\theta_{EG,NF}) - \sqrt{29\ \gamma_{NF}^{LW}}}{1.38} - \frac{36.4\ (1+\cos\theta_{sw,NF}) - \sqrt{21.8\ \gamma_{NF}^{LW}}}{5.05} \Big/ 3.96\right)^2 =$

$$\left(\frac{24\ (1+\cos 32.3) - \sqrt{29*(39.66)}}{1.38} - \frac{36.4\ (1+\cos 53.6) - \sqrt{21.8(39.66)}}{5.05} \Big/ 3.96\right)^2 = 0.218\ mJ/m^2$$

3. $\gamma_{NF}^{p-} = \left(\frac{36.4\ (1+\cos\theta_{sw,NF}) - \sqrt{21.8\ \gamma_{NF}^{LW}}}{5.05} - \sqrt{\gamma_{NF}^{p+}}\right)^2$

$$= \left(\frac{36.4\ (1+\cos 53.6) - \sqrt{21.8*(39.66)}}{5.05} - \sqrt{0.218}\right)^2 = 26.99\ mJ/m^2$$

4. $\gamma_{NF}^{p} = 2\sqrt{\gamma_{NF}^{p-}}\sqrt{\gamma_{NF}^{p+}} = 2\sqrt{26.99}\sqrt{0.218} = 4.85\ mJ/m^2$

5. $\gamma_{NF} = \gamma_{NF}^{LW} + \gamma_{NF}^{p} = 39.66 + 4.85 = 44.52\ mJ/m^2$

NF F membrane:

Contact angle measurements for NF F membrane are; 31.3°, 25.7° and 18.9° in seawater, diiodomethane and ethylene-glycol respectively.

1. $\gamma_{NF}^{LW} = \left(\frac{25.4\,(1+\cos\theta_{D,NF})}{7.127}\right)^2 = \left(\frac{25.4\,(1+\cos 25.7)}{7.127}\right)^2 = 45.90\ mJ/m^2$

2. $\gamma_{NF}^{p+} = \left(\frac{24\,(1+\cos\theta_{EG,NF}) - \sqrt{29\,\gamma_{NF}^{LW}}}{1.38} - \frac{36.4\,(1+\cos\theta_{sw,NF}) - \sqrt{21.8\,\gamma_{NF}^{LW}}}{5.05} \Big/ 3.96\right)^2 =$

$$\left(\frac{24\,(1+\cos 18.9) - \sqrt{29*(45.9)}}{1.38} - \frac{36.4\,(1+\cos 31.3) - \sqrt{21.8(45.9)}}{5.05} \Big/ 3.96\right)^2 = 0.005\ mJ/m^2$$

3. $\gamma_{NF}^{p-} = \left(\frac{36.4\,(1+\cos\theta_{sw,NF}) - \sqrt{21.8\,\gamma_{NF}^{LW}}}{5.05} - \sqrt{\gamma_{NF}^{p+}}\right)^2$

$$= \left(\frac{36.4\,(1+\cos 31.3) - \sqrt{21.8*(45.9)}}{5.05} - \sqrt{0.005}\right)^2 = 49.37\ mJ/m^2$$

4. $\gamma_{NF}^{p} = 2\sqrt{\gamma_{NF}^{p-}}\sqrt{\gamma_{NF}^{p+}} = 2\sqrt{49.37}\sqrt{0.005} = 1.07\ mJ/m^2$

5. $\gamma_{NF} = \gamma_{NF}^{LW} + \gamma_{NF}^{p} = 45.90 + 1.07 = 46.97\ mJ/m^2$

NF G membrane:

Contact angle measurements for NF G membrane are; 37.0°, 32.2° and 25.6° in seawater, diiodomethane and ethylene-glycol respectively.

1. $\gamma_{NF}^{LW} = \left(\frac{25.4\,(1+\cos\theta_{D,NF})}{7.127}\right)^2 = \left(\frac{25.4\,(1+\cos 32.2)}{7.127}\right)^2 = 43.29\ mJ/m^2$

2. $\gamma_{NF}^{p+} = \left(\frac{24\,(1+\cos\theta_{EG,NF}) - \sqrt{29\,\gamma_{NF}^{LW}}}{1.38} - \frac{36.4\,(1+\cos\theta_{sw,NF}) - \sqrt{21.8\,\gamma_{NF}^{LW}}}{5.05} \Big/ 3.96\right)^2 =$

$$\left(\frac{24\,(1+\cos 25.6) - \sqrt{29*(43.29)}}{1.38} - \frac{36.4\,(1+\cos 37) - \sqrt{21.8(43.29)}}{5.05} \Big/ 3.96\right)^2 = 0.017\ mJ/m^2$$

3. $\gamma_{NF}^{p-} = \left(\frac{36.4\,(1+\cos\theta_{sw,NF}) - \sqrt{21.8\,\gamma_{NF}^{LW}}}{5.05} - \sqrt{\gamma_{NF}^{p+}}\right)^2$

$$= \left(\frac{36.4\,(1+\cos 37) - \sqrt{21.8*(43.29)}}{5.05} - \sqrt{0.017}\right)^2 = 45.57\ mJ/m^2$$

4. $\gamma_{NF}^{p} = 2\sqrt{\gamma_{NF}^{p-}}\sqrt{\gamma_{NF}^{p+}} = 2\sqrt{45.57}\sqrt{0.017} = 1.76\ mJ/m^2$

5. $\gamma_{NF} = \gamma_{NF}^{LW} + \gamma_{NF}^{p} = 43.29 + 1.76 = 45.06\ mJ/m^2$

NF H membrane:

Contact angle measurements for NF H membrane are; 42.1°, 34.6° and 28.1° in seawater, diiodomethane and ethylene-glycol respectively.

1. $\gamma_{NF}^{LW} = \left(\frac{25.4\,(1+\cos\theta_{D,NF})}{7.127}\right)^2 = \left(\frac{25.4\,(1+\cos 34.6)}{7.127}\right)^2 = 42.22\ mJ/m^2$

2. $\gamma_{NF}^{p+} = \left(\frac{24\,(1+\cos\theta_{EG,NF}) - \sqrt{29\,\gamma_{NF}^{LW}}}{1.38} - \frac{36.4\,(1+\cos\theta_{sw,NF}) - \sqrt{21.8\,\gamma_{NF}^{LW}}}{5.05} \Big/ 3.96\right)^2 =$

$$\left(\frac{24\,(1+\cos 28.1) - \sqrt{29*(42.22)}}{1.38} - \frac{36.4\,(1+\cos 42.1) - \sqrt{21.8(42.22)}}{5.05} \Big/ 3.96\right)^2 = 0.043\ mJ/m^2$$

3. $\gamma_{NF}^{p-} = \left(\frac{36.4\,(1+\cos\theta_{sw,NF}) - \sqrt{21.8\,\gamma_{NF}^{LW}}}{5.05} - \sqrt{\gamma_{NF}^{p+}}\right)^2$

$$= \left(\frac{36.4\,(1+\cos 42.1) - \sqrt{21.8*(42.22)}}{5.05} - \sqrt{0.043}\right)^2 = 40.19\ mJ/m^2$$

4. $\gamma_{NF}^{p} = 2\sqrt{\gamma_{NF}^{p-}}\sqrt{\gamma_{NF}^{p+}} = 2\sqrt{40.19}\sqrt{0.043} = 2.65\ mJ/m^2$

5. $\gamma_{NF} = \gamma_{NF}^{LW} + \gamma_{NF}^{p} = 42.22 + 2.65 = 44.87\ mJ/m^2$

Appendix 4.1: Excel spreadsheet for NF averaged charge density calculations in NaCl from equation 11.4

NaCl

LEFT HAND SIDE = $\ln\frac{\sqrt{4C_2^2+X^2}+X}{\sqrt{4C_1^2+X^2}+X}+\frac{E_{m,NF}}{-0.025}-0.693$

RIGHT HAND SIDE = $(2\alpha-1)\ln\frac{\sqrt{4C_2^2+X^2}+(2\alpha-1)X}{\sqrt{4C_1^2+X^2}+(2\alpha-1)X}$

C1	C2	Em	NF	CHARGE	ALPHA	$\frac{E_{m,NF}}{-0.025}-0.693$	$\sqrt{4C_2^2+X^2}+X$	$\sqrt{4C_1^2+X^2}+X$	$\ln\frac{\sqrt{4C_2^2+X^2}+X}{\sqrt{4C_1^2+X^2}+X}$	LHS	$\sqrt{4C_2^2+X^2}+(2\alpha-1)X$	$\sqrt{4C_1^2+X^2}+(2\alpha-1)X$	RHS	RHS - LHS	% ERROR
300	600	-1	F	-0.42	0.53	-0.653	1199.58	599.580	0.6935	0.04050	1199.974874	599.97495	0.04159	0.00109	2.6
150	300	-1.02	F	-0.42	0.53	-0.6522	599.58	299.580	0.6938	0.04165	599.974947	299.97509	0.04159	0.00006	0.1
75	150	-1.08	F	-0.42	0.53	-0.6498	299.58	149.581	0.6945	0.04475	299.975094	149.97539	0.04159	0.00315	7.0
300	600	-0.99	B	-0.411	0.529	-0.6534	1199.59	599.589	0.6935	0.04009	1199.976232	599.9763	0.04020	0.00011	0.3
150	300	-1.01	B	-0.411	0.529	-0.6526	599.59	299.589	0.6938	0.04123	599.9763028	299.97644	0.04020	0.00103	2.5
75	150	-1.06	B	-0.411	0.529	-0.6506	299.59	149.590	0.6945	0.04392	299.9764435	149.97673	0.04021	0.00371	8.4
300	600	-0.87	E	-0.404	0.526	-0.6582	1199.60	599.596	0.6935	0.03528	1199.97906	599.97913	0.03604		0.0
150	300	-0.91	E	-0.404	0.526	-0.6566	599.60	299.596	0.6938	0.03722	599.979128	299.97926	0.03605	0.00118	3.2
75	150	-0.95	E	-0.404	0.526	-0.655	299.60	149.597	0.6945	0.03949	299.979264	149.97954	0.03605	0.00345	8.7
300	600	-0.73	A	-0.36	0.522	-0.6638	1199.64	599.640	0.6934	0.02965	1199.984214	599.98427	0.03050	0.00085	2.8
150	300	-0.8	A	-0.36	0.522	-0.661	599.64	299.640	0.6937	0.03275	599.984268	299.98438	0.03050	0.00225	6.9
75	150	-0.82	A	-0.36	0.522	-0.6602	299.64	149.640	0.6943	0.03415	299.984376	149.98459	0.03050	0.00365	10.7
300	600	-0.65	D	-0.332	0.52	-0.667	1199.67	599.668	0.6934	0.02642	1199.986766	599.98681	0.02773	0.00130	4.7
150	300	-0.7	D	-0.332	0.52	-0.665	599.67	299.668	0.6937	0.02870	599.9868119	299.9869	0.02773	0.00097	3.4
75	150	-0.74	D	-0.332	0.52	-0.6634	299.67	149.668	0.6943	0.03085	299.9869037	149.98709	0.02773	0.00313	10.1

300	600	-0.53	G	-0.303	0.517	-0.6718	1199.70	599.697	0.6934	0.02160	1199.989736	599.98977	0.02357	0.00197	8.3
150	300	-0.57	G	-0.303	0.517	-0.6702	599.70	299.697	0.6937	0.02345	599.9897745	299.98985	0.02357	0.00012	0.5
75	150	-0.6	G	-0.303	0.517	-0.669	299.70	149.697	0.6942	0.02516	299.989851	149.99	0.02357	0.00159	6.3
300	600	-0.49	H	-0.165	0.514	-0.6734	1199.84	599.835	0.6933	0.01988	1199.995391	599.9954	0.01941	0.00048	2.4
150	300	-0.51	H	-0.165	0.514	-0.6726	599.84	299.835	0.6934	0.02082	599.9954027	299.99543	0.01941	0.00141	6.8
75	150	-0.52	H	-0.165	0.514	-0.6722	299.84	149.835	0.6937	0.02150	299.9954254	149.99547	0.01941	0.00209	9.7
300	600	-0.23	C	-0.02	0.507	-0.6838	1199.98	599.980	0.6932	0.00936	1199.99972	599.99972	0.00970	0.00034	3.5
150	300	-0.24	C	-0.02	0.507	-0.6834	599.98	299.980	0.6932	0.00978	599.9997203	299.99972	0.00970	0.00008	0.8
75	150	-0.26	C	-0.02	0.507	-0.6826	299.98	149.980	0.6932	0.01061	299.9997207	149.99972	0.00970	0.00091	8.6

Appendix 4.2: Excel spreadsheet for NF averaged charge density calculations in $MgSO_4$ from equation 11.4

MgSO4

LEFT HAND SIDE = $\ln\frac{\sqrt{4C_2^2+X^2}+X}{\sqrt{4C_1^2+X^2}+X}+\frac{E_{m,NF}}{-0.025}-0.693$

RIGHT HAND SIDE = $(2\alpha-1)\ln\frac{\sqrt{4C_2^2+X^2}+(2\alpha-1)X}{\sqrt{4C_1^2+X^2}+(2\alpha-1)X}$

C1	C2	Em	NF	CHARGE	ALPHA	$\frac{E_{m,NF}}{-0.025}-0.693$	$\sqrt{4C_2^2+X^2}+X$	$\sqrt{4C_1^2+X^2}+X$	$\ln\frac{\sqrt{4C_2^2+X^2}+X}{\sqrt{4C_1^2+X^2}+X}$	LHS	$\sqrt{4C_2^2+X^2}+(2\alpha-1)X$	$\sqrt{4C_1^2+X^2}+(2\alpha-1)X$	RHS	RHS - LHS	% ERROR
16.67	33.34	-7.08	B	-0.628	0.719	-0.410	66.055	32.718	0.703	0.2928	66.408	33.071	0.3054	0.01259	4.1
8.33	16.66	-7.34	B	-0.628	0.719	-0.399	32.698	16.044	0.712	0.3126	33.051	16.397	0.3070	0.00557	1.8
4.16	8.32	-7.61	B	-0.628	0.719	-0.389	16.024	7.716	0.731	0.3422	16.377	8.069	0.3101	0.03217	9.4
16.67	33.34	-6.73	E	-0.61	0.711	-0.424	66.073	32.736	0.702	0.2785	66.425	33.088	0.2941	0.01560	5.6
8.33	16.66	-7.01	E	-0.61	0.711	-0.413	32.716	16.061	0.711	0.2988	33.068	16.414	0.2956	0.00326	1.1
4.16	8.32	-7.27	E	-0.61	0.711	-0.402	16.041	7.732	0.730	0.3275	16.394	8.085	0.2983	0.02924	8.9
16.67	33.34	-6.21	F	-0.584	0.697	-0.445	66.099	32.761	0.702	0.2573	66.452	33.115	0.2744	0.01712	6.7
8.33	16.66	-6.56	F	-0.584	0.697	-0.431	32.741	16.086	0.711	0.2801	33.095	16.440	0.2757	0.00440	1.6
4.16	8.32	-6.79	F	-0.584	0.697	-0.421	16.066	7.756	0.728	0.3068	16.420	8.110	0.2779	0.02888	9.4
16.67	33.34	-5.99	A	-0.562	0.691	-0.453	66.120	32.783	0.702	0.2482	66.468	33.130	0.2660	0.01780	7.2
8.33	16.66	-6.24	A	-0.562	0.691	-0.443	32.763	16.107	0.710	0.2666	33.110	16.455	0.2671	0.00049	0.2
4.16	8.32	-6.54	A	-0.562	0.691	-0.431	16.087	7.777	0.727	0.2955	16.435	8.124	0.2691	0.02634	8.9
16.67	33.34	-5.77	D	-0.545	0.683	-0.462	66.137	32.799	0.701	0.2391	66.483	33.145	0.2548	0.01563	6.5
8.33	16.66	-6.01	D	-0.545	0.683	-0.453	32.779	16.124	0.709	0.2569	33.125	16.469	0.2558	0.00114	0.4
4.16	8.32	-6.29	D	-0.545	0.683	-0.441	16.104	7.793	0.726	0.2845	16.449	8.138	0.2576	0.02690	9.5

16.67	33.34	-5.42	G	-0.46	0.672	-0.476	66.222	32.883	0.700	0.2238	66.523	33.185	0.2392	0.01539	6.4
8.33	16.66	-5.78	G	-0.46	0.672	-0.462	32.863	16.206	0.707	0.2451	33.165	16.508	0.2400	0.00516	2.1
4.16	8.32	-6.01	G	-0.46	0.672	-0.453	16.186	7.873	0.721	0.2682	16.488	8.174	0.2461	0.02207	8.2
16.67	33.34	-4.78	H	-0.325	0.655	-0.502	66.356	33.017	0.698	0.1962	66.580	33.241	0.2053	0.00908	4.6
8.33	16.66	-5.05	H	-0.325	0.655	-0.491	32.997	16.338	0.703	0.2119	33.221	16.562	0.2158	0.00387	1.8
4.16	8.32	-5.52	H	-0.325	0.655	-0.472	16.318	8.001	0.713	0.2405	16.542	8.226	0.2166	0.02388	9.9
16.67	33.34	-3.1	C	-0.071	0.599	-0.569	66.609	33.269	0.694	0.1252	66.666	33.326	0.1373	0.01207	9.6
8.33	16.66	-3.34	C	-0.071	0.599	-0.559	33.249	16.589	0.695	0.1359	33.306	16.646	0.1373	0.00145	1.1
4.16	8.32	-3.76	C	-0.071	0.599	-0.543	16.569	8.249	0.697	0.1548	16.626	8.306	0.1473	0.00751	4.9